

(17.82) and (17.85) and rewrite the integral over k as

$$d^3k = dk^3 d^2k_\perp = pdz \cdot \pi dp_\perp^2. \quad (17.94)$$

Then the cross section can be expressed as

$$\begin{aligned} \sigma &= \int \frac{pdzdp_\perp^2}{16\pi^2(1-z)p} \left[\frac{1}{2} \sum |\mathcal{M}|^2 \right] \frac{(1-z)^2}{p_\perp^4} \frac{z}{(1+v_X)2zp2E_X} \int d\Pi_Y |\mathcal{M}_{\gamma X}|^2 \\ &= \int \frac{dzdp_\perp^2}{16\pi^2(1-z)} \left[\frac{1}{2} \sum |\mathcal{M}|^2 \right] \frac{z(1-z)^2}{p_\perp^4} \cdot \sigma(\gamma X \rightarrow Y). \end{aligned} \quad (17.95)$$

Finally, insert the spin-averaged electron emission vertex (17.92), to obtain

$$\begin{aligned} \sigma &= \int \frac{dzdp_\perp^2}{16\pi^2} \frac{z(1-z)}{p_\perp^4} \frac{2e^2p_\perp^2}{z(1-z)} \left[\frac{1 + (1-z)^2}{z} \right] \cdot \sigma(\gamma X \rightarrow Y) \\ &= \int_0^1 dz \int \frac{dp_\perp^2}{p_\perp^2} \frac{\alpha}{2\pi} \left[\frac{1 + (1-z)^2}{z} \right] \cdot \sigma(\gamma X \rightarrow Y). \end{aligned} \quad (17.96)$$

The integral over p_\perp^2 runs from momentum transfers of order s down to the electron mass m^2 , which cuts off the singularity. Thus, our final result is

$$\sigma(e^- X \rightarrow e^- Y) = \int_0^1 dz \frac{\alpha}{2\pi} \log \frac{s}{m^2} \left[\frac{1 + (1-z)^2}{z} \right] \cdot \sigma(\gamma X \rightarrow Y). \quad (17.97)$$

The cross section on the right-hand side is computed for a real, transversely polarized photon of momentum zp . The factor $\log(s/m^2)$ represents the mass singularity. This formula is the Weizsäcker-Williams *equivalent photon approximation*, which we encountered earlier in Problems 5.5 and 6.2.

Formula (17.97) takes on a new significance when it is juxtaposed with the QCD predictions of the previous two sections. This QED formula has just the same form as a parton model expression, with the Weizsäcker-Williams distribution function

$$f_\gamma(z) = \frac{\alpha}{2\pi} \log \frac{s}{m^2} \left[\frac{1 + (1-z)^2}{z} \right] \quad (17.98)$$

playing the role of the probability to find a photon of longitudinal fraction z in the incident electron.

The Electron Distribution

The first diagram of Fig. 17.5, with an emitted photon and a virtual electron, can be treated in the same way. The analogue of (17.93) is

$$\sigma = \frac{1}{(1+v_X)2p2E_X} \int \frac{d^3q}{(2\pi)^3} \frac{1}{2q^0} \int d\Pi_Y \left[\frac{1}{2} \sum |\mathcal{M}|^2 \right] \left(\frac{1}{k^2} \right)^2 |\mathcal{M}_{e^- X}|^2.$$

Following the steps that led to (17.97), we find

$$\begin{aligned}
 \sigma(e^- X \rightarrow \gamma Y) &= \int \frac{dz dp_\perp^2}{16\pi^2 z} \left[\frac{1}{2} \sum |\mathcal{M}|^2 \right] \frac{z^2}{p_\perp^4} \cdot (1-z) \sigma(e^- X \rightarrow Y) \\
 &= \int \frac{dz dp_\perp^2}{16\pi^2} \frac{z(1-z)}{p_\perp^4} \frac{2e^2 p_\perp^2}{z(1-z)} \left[\frac{1 + (1-z)^2}{z} \right] \cdot \sigma(e^- X \rightarrow Y) \\
 &= \int_0^1 dz \int \frac{dp_\perp^2}{p_\perp^2} \frac{\alpha}{2\pi} \left[\frac{1 + (1-z)^2}{z} \right] \cdot \sigma(e^- X \rightarrow Y), \quad (17.99)
 \end{aligned}$$

where the intermediate electron carries a longitudinal fraction $(1-z)$.

It is tempting substitute $x = (1-z)$ and interpret the factor multiplying the cross section under the integral in (17.99) as the parton distribution for finding an electron parton in the electron. This would give

$$f_e^{(1)}(x) = \frac{\alpha}{2\pi} \log \frac{s}{m^2} \left[\frac{1+x^2}{1-x} \right]. \quad (17.100)$$

However, this expression is not adequate. Most obviously, it does not take into account the processes without radiation, in which the electron remains an electron at the full energy. This is easily remedied by considering (17.100) as the order- α correction to the most naive expectation,

$$f_e^{(0)}(x) = \delta(1-x), \quad (17.101)$$

in which we consider the electron to contain only an electron at the full energy. Unfortunately, the sum of (17.101) and (17.100) still does not give an adequate description of the electron distribution, for two reasons. First, Eq. (17.100) diverges near $x = 1$, and we need a prescription for treating this singularity. Second, while Eq. (17.100) takes into account the virtual electrons moved to longitudinal fraction x from $x = 1$ by radiation, it does not take into account the concomitant loss of electrons from the delta function peak at $x = 1$.

The divergence of (17.100) at $x = 1$ corresponds to the emission of soft photons. We saw in Section 6.5 that the emission of soft photons does not affect the rate of a QED reaction. Order by order in α , one finds that infrared-divergent positive contributions to the total rate from the emission of soft photons are balanced by negative contributions from diagrams with soft virtual photons. In the present example, the negative contribution must decrease the weight of the process in which no photon is emitted. Thus, to order α , the parton distribution for electrons in the electron should have the form

$$f_e(x) = \delta(1-x) + \frac{\alpha}{2\pi} \log \frac{s}{m^2} \left(\frac{1+x^2}{(1-x)} - A\delta(1-x) \right). \quad (17.102)$$

The coefficient A results from diagrams with virtual photons that we have not computed. However, the effect of these diagrams is easy to understand; they subtract from the delta function the probability that has been moved

to lower x by radiation, so that the integral over the full term of order α is zero. Another way of expressing this criterion is that A is determined by the condition that the electron contain exactly one electron parton,

$$\int_0^1 dx f_e(x) = 1. \quad (17.103)$$

(This equation will be modified below, when we include pair-creation processes.)

It is not so clear how to integrate over the singular denominator in (17.100) to determine A explicitly. It is conventional to define a distribution that can be integrated by subtracting a delta function from the singular term. Define the distribution

$$\frac{1}{(1-x)_+} \quad (17.104)$$

to agree with the function $1/(1-x)$ for all values of x less than 1, and to have a singularity at $x = 1$ such that the integral of this distribution with any smooth function $f(x)$ gives

$$\int_0^1 dx \frac{f(x)}{(1-x)_+} = \int_0^1 dx \frac{f(x) - f(1)}{(1-x)}. \quad (17.105)$$

Less formally,

$$\frac{1}{(1-x)_+} = \lim_{\epsilon \rightarrow 0} \left[\frac{1}{(1-x)} \theta(1-x-\epsilon) - \delta(1-x) \int_0^{1-\epsilon} dx' \frac{1}{(1-x')} \right]. \quad (17.106)$$

The more formal definition (17.105) is often easier to use in practice.

Using this definition, we can bring a piece of the delta function into the singular term of (17.102) by changing the denominator $(1-x)$ to $(1-x)_+$. Then, to normalize (17.102), we need the integral

$$\int_0^1 dx \frac{1+x^2}{(1-x)_+} = \int_0^1 dx \frac{x^2-1}{(1-x)} = -\frac{3}{2}.$$

Our final form of the electron distribution, to order α , is

$$f_e(x) = \delta(1-x) + \frac{\alpha}{2\pi} \log \frac{s}{m^2} \left[\frac{1+x^2}{(1-x)_+} + \frac{3}{2} \delta(1-x) \right]. \quad (17.107)$$

This distribution is now properly normalized, but it is still highly singular near $x = 1$. Thus, we should expect higher-order corrections to the electron distribution function to be important in this region. We must, then, think about how to treat the emission of many collinear photons.

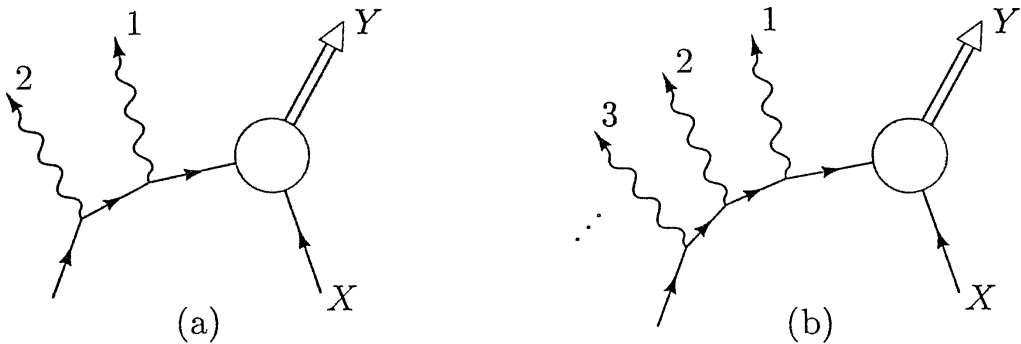


Figure 17.17. Higher-order diagrams with collinear photon emission: (a) two collinear photons; (b) many collinear photons.

Multiple Splittings

In fact, it is not difficult to extend the analysis we have just completed to account for emission of many collinear photons. Consider the process shown in Fig. 17.17(a), in which photon 1 is radiated with a transverse momentum $p_{1\perp}$ and photon 2 with a transverse momentum $p_{2\perp}$. The emission of photon 2 can be computed just as we did above. If $p_{2\perp} \ll p_{1\perp}$, the first virtual electron is very close to mass shell compared to $p_{1\perp}^2$ and so we can ignore its virtuality in computing the emission of the photon 1. The double photon emission gives a contribution of order

$$\left(\frac{\alpha}{2\pi}\right)^2 \int \frac{dp_{1\perp}^2}{m^2} \int \frac{dp_{2\perp}^2}{m^2} = \frac{1}{2} \left(\frac{\alpha}{2\pi}\right)^2 \log^2 \frac{s}{m^2}.$$

In the opposite limit, $p_{2\perp} \gg p_{1\perp}$, there is no denominator of order $p_{1\perp}^2$, and so we do not find a double logarithm. Only in the case $p_{2\perp} \ll p_{1\perp}$ can the contribution of order α^2 compete with the contribution of order α .

This argument extends to the emission of arbitrarily many collinear photons, Fig. 17.17(b). The region of integration over the photon phase space corresponding to the ordering

$$p_{1\perp} \gg p_{2\perp} \gg p_{3\perp} \gg \dots \quad (17.108)$$

gives a contribution that contains the factor

$$\frac{1}{n!} \left(\frac{\alpha}{2\pi}\right)^n \log^n \frac{s}{m^2}. \quad (17.109)$$

If the photon transverse momenta are ordered in any other way, the contribution from that region contains at least one less power of the large logarithm at the same order in α . If condition (17.108) holds, the virtual electron momenta are increasingly off-mass-shell as one proceeds from the outside of the diagram toward the hard collision. In this case, the electron momenta are said to be *strongly ordered*.

This set of conclusions has an interesting physical interpretation. Since the intermediate electrons are increasingly virtual as we go into the diagram, it is natural to interpret them as components of the physical electron when this particle is analyzed at successively smaller distance scales. The intermediate electron with $k^2 \sim p_\perp^2$ may be thought of as a constituent of the electron made visible when the wavefunction of the physical electron is probed with a resolution $\Delta r \sim (p_\perp)^{-1}$. In this picture, the electron seen at one resolution can be resolved at a finer scale into a more virtual electron and a number of photons.

From either the perspective of computing Feynman diagrams or the grander perspective of the electron structure, it is useful to imagine the splitting of the electron into a virtual electron plus photons to be a continuous evolution process as a function of the transverse momentum of the electron constituent. To describe this process mathematically, we introduce an explicit p_\perp dependence of the electron and photon distribution functions. We define the functions $f_\gamma(x, Q)$ and $f_e(x, Q)$ to give the probabilities of finding a photon or an electron of longitudinal fraction x in the physical electron, taking into account collinear photon emissions with transverse momenta $p_\perp < Q$. If Q is slightly increased to $Q + \Delta Q$, we must take into account the possibility that an electron constituent in $f_e(x, Q)$ will radiate a photon with $Q < p_\perp < Q + \Delta Q$. The differential probability for an electron to split off a photon that carries away a fraction z of its energy is

$$\frac{\alpha}{2\pi} \frac{dp_\perp^2}{p_\perp^2} \frac{1 + (1-z)^2}{z}. \quad (17.110)$$

The new photon distribution can therefore be computed as follows:

$$\begin{aligned} f_\gamma(x, Q + \Delta Q) &= f_\gamma(x, Q) + \int_0^1 dx' \int_0^1 dz \left[\frac{\alpha}{2\pi} \frac{\Delta Q^2}{Q^2} \frac{1 + (1-z)^2}{z} \right] f_e(x', p_\perp) \delta(x - zx') \\ &= f_\gamma(x, Q) + \frac{\Delta Q}{Q} \int_x^1 \frac{dz}{z} \left[\frac{\alpha}{\pi} \frac{1 + (1-z)^2}{z} \right] f_e\left(\frac{x}{z}, p_\perp\right). \end{aligned} \quad (17.111)$$

Passing to a continuous evolution, we find that the function $f_\gamma(x, Q)$ is determined by the integral-differential equation

$$\frac{d}{d \log Q} f_\gamma(x, Q) = \int_x^1 \frac{dz}{z} \left[\frac{\alpha}{\pi} \frac{1 + (1-z)^2}{z} \right] f_e\left(\frac{x}{z}, Q\right). \quad (17.112)$$

Similarly, the distribution of component electrons in the physical electron will evolve with Q , reflecting the appearance of electrons at lower values of x due to photon radiation, and the disappearance of these electrons at higher x . The term in brackets in Eq. (17.107) gives a correct accounting of both effects

for the radiation of a single photon. Thus, the electron distribution evolves according to

$$\frac{d}{d \log Q} f_e(x, Q) = \int_x^1 \frac{dz}{z} \left[\frac{\alpha}{\pi} \left(\frac{1+z^2}{(1-z)_+} + \frac{3}{2} \delta(1-z) \right) \right] f_e\left(\frac{x}{z}, Q\right). \quad (17.113)$$

By integrating these integral-differential equations using appropriate initial conditions, we sum all of the logarithmically enhanced terms of the form (17.109). The initial conditions should be fixed at a point that will reproduce the correct denominator of the logarithms in Eqs. (17.98) and (17.107). Thus, we should set

$$f_e(x, Q) = \delta(1-x), \quad f_\gamma(x, Q) = 0, \quad (17.114)$$

at $Q^2 \sim m^2$.

The resulting distribution functions can be used to compute the cross sections for electron hard scattering from an arbitrary target. Then Eqs. (17.97) and (17.99) should be replaced by

$$\begin{aligned} \sigma(e^- X \rightarrow e^- + n\gamma + Y) &= \int_0^1 dx f_\gamma(x, Q) \sigma(\gamma X \rightarrow Y), \\ \sigma(e^- X \rightarrow n\gamma + Y) &= \int_0^1 dx f_e(x, Q) \sigma(e^- X \rightarrow Y), \end{aligned} \quad (17.115)$$

where the cross sections under the integrals are computed for a photon or electron carrying a fraction x of the original electron momentum, the functions $f_\gamma(x, Q)$, $f_e(x, Q)$ are the solutions to Eqs. (17.112) and (17.113), and the momentum Q is chosen as a characteristic momentum transfer of the γX or $e^- X$ subprocess.

Photon Splitting to Pairs

The evolution equations for $f_\gamma(x)$ and $f_e(x)$ need one more modification before they can be considered complete. As written, these equations account for the radiation of photons by electrons to all orders. However, they omit another process that is of the same order in α : the splitting of a photon into an electron-positron pair. We must include this process in our evolution equations, because the process shown in Fig. 17.18, for example, has the same logarithmic enhancement as that shown in Fig. 17.17(a).

We can compute the effects of photon splitting in the same way that we computed with effects of photon radiation. The basic kinematics of the process is very similar, as shown in Fig. 17.19; the only difference is that the photon is now in the initial state, while the final state consists of an almost collinear electron-positron pair. We need to work out the analogue of Eq. (17.92) for this process.

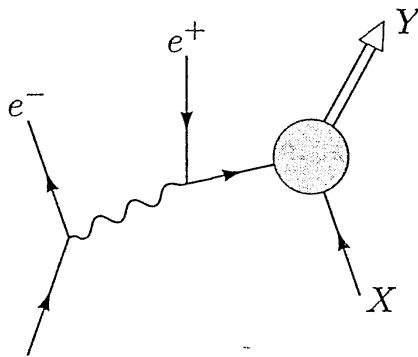


Figure 17.18. A process that involves e^+e^- pair creation enhanced by a collinear mass singularity.

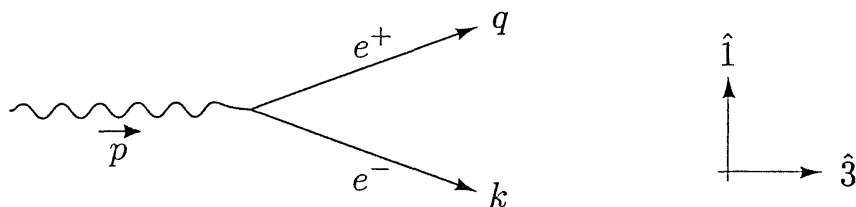


Figure 17.19. Kinematics of the vertex for photon conversion to a collinear electron-positron pair.

Consider the case in which the outgoing electron is left-handed. Then the outgoing positron must be right-handed, by helicity conservation; its spin wavefunction will contain a left-handed spinor. Let us take the electron momentum to be k , given by Eq. (17.82), and the positron momentum to be q . Then the vertex gives a matrix element

$$i\mathcal{M} = -ie\bar{u}_L(k)\gamma_5 v_L(q)\epsilon_T^\mu(p), \quad (17.116)$$

where the photon polarization vector can be either left- or right-handed. When we insert the explicit forms for the massless spinors, we obtain

$$i\mathcal{M} = ie\sqrt{2(1-z)p}\sqrt{2zp}\xi^\dagger(k)\sigma^i\xi(q)\cdot\epsilon_T^i(p),$$

where the electron and positron spinors are given, to order p_\perp , by

$$\xi(q) = \begin{pmatrix} -p_\perp/2zp \\ 1 \end{pmatrix}, \quad \xi(k) = \begin{pmatrix} p_\perp/2(1-z)p \\ 1 \end{pmatrix}.$$

The polarization vectors for the photon are

$$\epsilon_L^i(p) = \frac{1}{\sqrt{2}}(1, -i, 0), \quad \epsilon_R^i(p) = \frac{1}{\sqrt{2}}(1, i, 0).$$

Dotting these vectors into σ^i , we find for the polarized matrix elements

$$i\mathcal{M}(\gamma_L \rightarrow e_L^- e_R^+) = -ie\frac{\sqrt{2z(1-z)}}{z}p_\perp,$$

and

$$i\mathcal{M}(\gamma_R \rightarrow e_L^- e_R^+) = +ie \frac{\sqrt{2z(1-z)}}{(1-z)} p_\perp.$$

Again, the matrix elements are unchanged if all helicities are flipped. Thus the squared matrix element, averaged over initial photon polarizations, is

$$\frac{1}{2} \sum_{\text{pols.}} |\mathcal{M}|^2 = \frac{2e^2 p_\perp^2}{z(1-z)} [z^2 + (1-z)^2], \quad (17.117)$$

where z is the momentum fraction carried by the positron. The first term in the brackets comes from processes in which the spin of the positron is parallel to the spin of the photon; the second term comes from processes where the electron spin is parallel to the photon spin.

The squared matrix element (17.117) generates an evolution of constituent photons into electrons and positrons. The form of the evolution equation is similar to (17.113), but with the photon distribution on the right-hand side, and with the expression in parentheses replaced by

$$(z^2 + (1-z)^2). \quad (17.118)$$

When we create an electron-positron pair, we must remove a photon; this requires a negative term in the evolution equation for the photon distribution (17.112) that contains a delta function multiplying the normalization of (17.118):

$$\int_0^1 dz (z^2 + (1-z)^2) = \frac{2}{3}. \quad (17.119)$$

Evolution Equations for QED

Including the effects of pair creation, we find the complete evolution equations for electron, positron, and photon distributions in QED. These equations, originally derived by Gribov and Lipatov, sum the leading logarithms from collinear singularities to all orders in α . The evolution equations take the form

$$\begin{aligned} \frac{d}{d \log Q} f_\gamma(x, Q) &= \frac{\alpha}{\pi} \int_x^1 \frac{dz}{z} \left\{ P_{\gamma \leftarrow e}(z) \left[f_e\left(\frac{x}{z}, Q\right) + f_{\bar{e}}\left(\frac{x}{z}, Q\right) \right] \right. \\ &\quad \left. + P_{\gamma \leftarrow \gamma}(z) f_\gamma\left(\frac{x}{z}, Q\right) \right\}, \\ \frac{d}{d \log Q} f_e(x, Q) &= \frac{\alpha}{\pi} \int_x^1 \frac{dz}{z} \left\{ P_{e \leftarrow e}(z) f_e\left(\frac{x}{z}, Q\right) + P_{e \leftarrow \gamma}(z) f_\gamma\left(\frac{x}{z}, Q\right) \right\}, \\ \frac{d}{d \log Q} f_{\bar{e}}(x, Q) &= \frac{\alpha}{\pi} \int_x^1 \frac{dz}{z} \left\{ P_{e \leftarrow \bar{e}}(z) f_{\bar{e}}\left(\frac{x}{z}, Q\right) + P_{e \leftarrow \gamma}(z) f_\gamma\left(\frac{x}{z}, Q\right) \right\}. \end{aligned} \quad (17.120)$$

The *splitting functions* $P_{i \leftarrow j}(z)$ are given by

$$\begin{aligned} P_{e \leftarrow e}(z) &= \frac{1+z^2}{(1-z)_+} + \frac{3}{2}\delta(1-z), \\ P_{\gamma \leftarrow e}(z) &= \frac{1+(1-z)^2}{z}, \\ P_{e \leftarrow \gamma}(z) &= z^2 + (1-z)^2, \\ P_{\gamma \leftarrow \gamma}(z) &= -\frac{2}{3}\delta(1-z). \end{aligned} \quad (17.121)$$

To obtain the distribution functions for an electron relevant to a given momentum transfer Q , we should integrate these equations with the initial conditions

$$f_e(x, Q) = \delta(1-x), \quad f_{\bar{e}}(x, Q) = 0, \quad f_{\gamma}(x, Q) = 0, \quad (17.122)$$

at $Q = m$. With different initial conditions, the same equations give the distribution functions for a physical positron or photon. The solutions to these equations are used as in Eq. (17.115) to compute cross sections involving processes induced by electrons, positrons, or photons that involve large momentum transfer.

The evolution equations (17.120) are constructed in such a way as to conserve electron number and longitudinal momentum. Thus, the basic sum rules (17.36) and (17.39) satisfied by the parton distributions of hadrons also apply to the QED distribution functions. Specifically, the distribution functions of the electron contain one net electron constituent,

$$\int_0^1 dx [f_e(x, Q) - f_{\bar{e}}(x, Q)] = 1, \quad (17.123)$$

and account for the total momentum of the physical electron,

$$\int_0^1 dx x [f_e(x, Q) + f_{\bar{e}}(x, Q) + f_{\gamma}(x, Q)] = 1. \quad (17.124)$$

It is an instructive exercise to verify explicitly, using Eq. (17.120), that the values of these integrals do not depend on Q .

The Altarelli-Parisi Equations

If we encounter mass singularities in QED associated with collinear photon emission, we must also encounter mass singularities in QCD associated with collinear gluon and quark emission. If we compute the corrections of order α_s to the leading-order parton cross sections discussed in Sections 17.3 and 17.4, using massless quarks and gluons, we will find that these correction terms

diverge when we integrate over the collinear configurations. Thus the parton-model expressions, at least in their simplest form, break down already at the next-to-leading order in α_s .

However, assuming that the singularities of QCD are no worse than those of QED, the considerations of the previous section tell us how to treat these singular terms. In QED, we found it natural to include the large corrections associated with the mass singularities in the parton distributions rather than in the hard-scattering cross sections. Viewed in this way, the singular terms supply the kernel of an evolution equation for the parton distributions as a function of the logarithm of the momentum scale. Hard scattering with a momentum transfer Q probes the electron at a distance of order Q^{-1} . When the electron wavefunction is resolved to very small scales, it appears as a constituent electron, carrying only a fraction of the total longitudinal momentum, plus a number of constituent photons and electron-positron pairs. Any one of these constituents that carries a substantial fraction of the total electron momentum can initiate a hard-scattering process.

Precisely the same logic applies to the calculation of QCD cross sections. The contributions from the region of collinear gluon or quark emission should be associated with the parton distribution functions rather than with the hard-scattering cross sections. If we make this association, we find that the parton distributions are no longer independent of the momentum Q that characterizes the hard-scattering process; rather, they now evolve logarithmically with Q . For example, the basic equation (17.30) for deep-inelastic scattering will become

$$\frac{d^2\sigma}{dxdy}(e^- p \rightarrow e^- X) = \left(\sum_f f_f(x, Q) Q_f^2 \right) \cdot \frac{2\pi\alpha^2 s}{Q^4} [1 + (1-y)^2], \quad (17.125)$$

and so Bjorken scaling will be violated. Since this violation takes place only on a logarithmic scale in Q^2 , it will be a subtle effect, and *approximate* Bjorken scaling will still be a prediction of QCD. But the violation of Bjorken scaling is inevitable, since QCD is a quantum field theory with degrees of freedom at all momentum scales. As we probe the proton wavefunction at increasingly short distances, we excite the high-momentum degrees of freedom and resolve the wavefunction into an increasing number of quarks, antiquarks, and gluons.

The evolution of the QED parton distributions, governed by Eq. (17.120), is characterized by the parameter α/π , so the parton distributions change by $\sim 1\%$ as Q is changed by a factor of 10. In QCD, the corresponding factor governing the rate of evolution should be $\alpha_s(Q)/\pi$. Thus, when Q is very small, the evolution is rapid and contributions of higher order in perturbation theory are important. Ultimately, the initial conditions for the evolution are determined by the form of the proton wavefunction at large distance scales, which cannot be calculated using Feynman diagrams. On the other hand, when Q is large, well above 1 GeV in practice, the evolution becomes slow and is dominated by the leading order in perturbation theory. In that case,

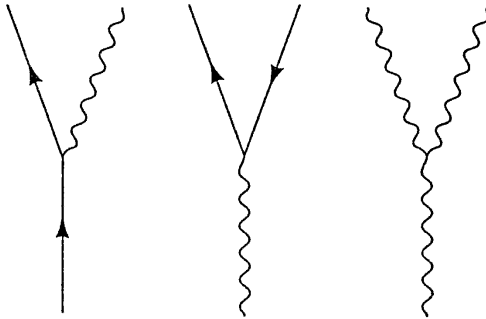


Figure 17.20. The three vertices that contribute to parton evolution in QCD.

QCD perturbation theory makes precise predictions for the form of the evolution of the parton distributions, and these predictions can be tested against experiment.

To derive the evolution equations of parton distributions in QCD we can use the same techniques and logic that we used above for QED. There is a subtlety, that the reduction of the gluon propagator to transverse polarization states in the limit $q^2 \rightarrow 0$, Eq. (17.81), cannot be proved so simply as in QED. However, the result is correct also in the non-Abelian case.* Once this technical point is resolved, the kinematics of collinear emission is exactly the same as in QED. Thus we find evolution equations of the same form as in QED, modified only by the replacement of α by α_s , the insertion of appropriate color factors, and the accounting of the effects of the three-gluon vertex.

Collinear emission processes in QCD involve the three vertices shown in Fig. 17.20. Of these, the first two have the same Lorentz structure as those shown in Figs. 17.16 and 17.19. The only difference, aside from the strength of the coupling constant, comes in the color indices. We will treat color just as we treated spin in the preceding analysis: We average over initial colors, and sum over final colors. Then the first vertex of Fig. 17.20, representing the splitting of a quark into a quark and a gluon, receives the color factor

$$\frac{1}{3} \text{tr}[t^a t^a] = C_2(r) = \frac{4}{3}. \quad (17.126)$$

The second vertex, representing the splitting of a gluon into a quark-antiquark pair, receives the factor

$$\frac{1}{8} \text{tr}[t^a t^a] = \frac{1}{2}. \quad (17.127)$$

The third vertex in Fig. 17.20 represents the splitting of a gluon to two gluons, an effect that is new to the non-Abelian case. It is straightforward to compute the contribution of this vertex to the evolution equations by taking the matrix elements of the vertex between transverse gluon states of definite helicity. This calculation is the subject of Problem 17.4.

*See, for example, J. Collins and D. Soper, in A. Mueller, *Quantum Chromodynamics* (World Scientific, Singapore, 1991).

By accounting for all of these effects, we can modify the QED evolution equations (17.120) into the correct set of evolution equations for parton distributions in QCD. These are known as the *Altarelli-Parisi equations*. They describe the coupled evolution of parton distributions $f_f(x, Q)$, $f_{\bar{f}}(x, Q)$ for each flavor of quark and antiquark that can be treated as massless at the scale Q , together with the parton distribution of gluons, $f_g(x, Q)$. Explicitly,

$$\begin{aligned} \frac{d}{d \log Q} f_g(x, Q) &= \frac{\alpha_s(Q^2)}{\pi} \int_x^1 \frac{dz}{z} \left\{ P_{g \leftarrow q}(z) \sum_f [f_f(\frac{x}{z}, Q) + f_{\bar{f}}(\frac{x}{z}, Q)] \right. \\ &\quad \left. + P_{g \leftarrow g}(z) f_g(\frac{x}{z}, Q) \right\}, \\ \frac{d}{d \log Q} f_f(x, Q) &= \frac{\alpha_s(Q^2)}{\pi} \int_x^1 \frac{dz}{z} \left\{ P_{q \leftarrow q}(z) f_f(\frac{x}{z}, Q) + P_{q \leftarrow g}(z) f_g(\frac{x}{z}, Q) \right\}, \\ \frac{d}{d \log Q} f_{\bar{f}}(x, Q) &= \frac{\alpha_s(Q^2)}{\pi} \int_x^1 \frac{dz}{z} \left\{ P_{q \leftarrow \bar{q}}(z) f_{\bar{f}}(\frac{x}{z}, Q) + P_{q \leftarrow g}(z) f_g(\frac{x}{z}, Q) \right\}. \end{aligned} \quad (17.128)$$

The first three splitting functions can be taken from Eqs. (17.121), multiplied by the color factors computed in Eqs. (17.126) and (17.127):

$$\begin{aligned} P_{q \leftarrow q}(z) &= \frac{4}{3} \left[\frac{1+z^2}{(1-z)_+} + \frac{3}{2} \delta(1-z) \right], \\ P_{g \leftarrow q}(z) &= \frac{4}{3} \left[\frac{1+(1-z)^2}{z} \right], \\ P_{q \leftarrow g}(z) &= \frac{1}{2} [z^2 + (1-z)^2]. \end{aligned} \quad (17.129)$$

The fourth splitting function requires also the computation of Problem 17.4; the result is

$$P_{g \leftarrow g}(z) = 6 \left[\frac{(1-z)}{z} + \frac{z}{(1-z)_+} + z(1-z) + \left(\frac{11}{12} - \frac{n_f}{18} \right) \delta(1-z) \right]. \quad (17.130)$$

The final term in this expression, which is proportional to n_f , the number of light quark flavors, is the subtraction term associated with gluon splitting into $q\bar{q}$ pairs. The Altarelli-Parisi equations describe the evolution of parton distributions for any hadron, or any hadronic constituent, up to corrections of order α_s that are not enhanced by large logarithms.

Our derivation of the Altarelli-Parisi equations respects the conservation laws of QCD for quark numbers and longitudinal momentum. Thus, the equations must respect the parton-model sum rules (17.36) and (17.39). As in the QED case, it is instructive to verify explicitly that these integrals are independent of Q .

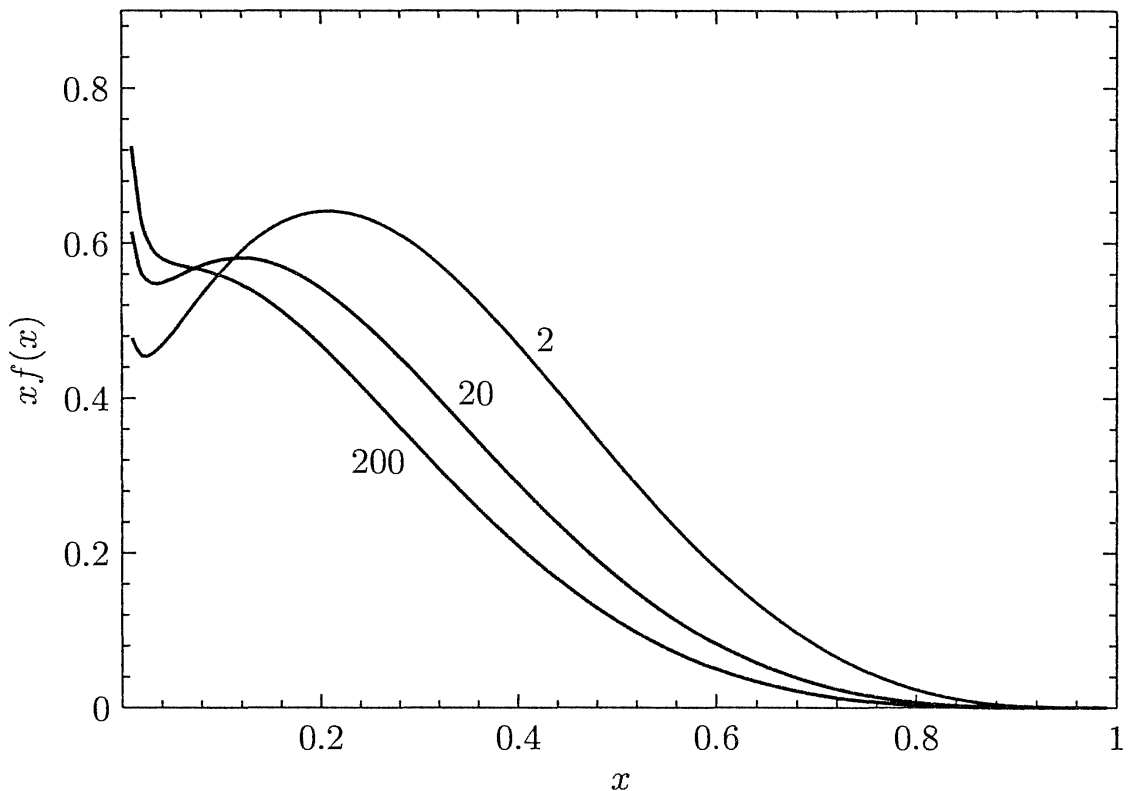


Figure 17.21. The u quark parton distribution function $xf_u(x, Q)$ at $Q = 2, 20$, and 200 GeV, showing the effects of parton evolution according the Altarelli-Parisi equations. These curves are taken from the CTEQ fit to deep inelastic scattering data described in Fig. 17.6.

In QED, we could use the evolution equations to explicitly compute the structure function of the electron. In QCD, this is no longer possible, because the initial conditions required to integrate the equations are determined by the strong-coupling region of QCD and so are not known *a priori*. However, one can determine the initial conditions of the proton structure experimentally, by measuring the cross section for deep inelastic scattering at a given value of Q^2 . One can then predict the structure functions, and thus the deep inelastic cross sections, at higher values of Q^2 . There is one subtlety in this analysis: The gluon distribution is not directly measured in deep inelastic scattering, but it does enter the evolution equation for the quark distributions. Thus, some of the information on the Q^2 dependence of deep inelastic scattering simply goes into determining the gluon distribution. However, the gluon distribution is absolutely normalized by the momentum sum rule (17.39), so the evolution equations have predictive power even if this distribution must be fit from the data.

The Altarelli-Parisi equations predict a characteristic form for the evolution of parton distribution functions, shown in Fig. 17.21. Partons at high x tend to radiate and drop down to lower values of x . Meanwhile, new partons are formed at low x as products of this radiation. Thus, the parton distributions decrease at large x and increase much more rapidly at small x as Q^2 increases. We can picture the proton as having more and more constituents,

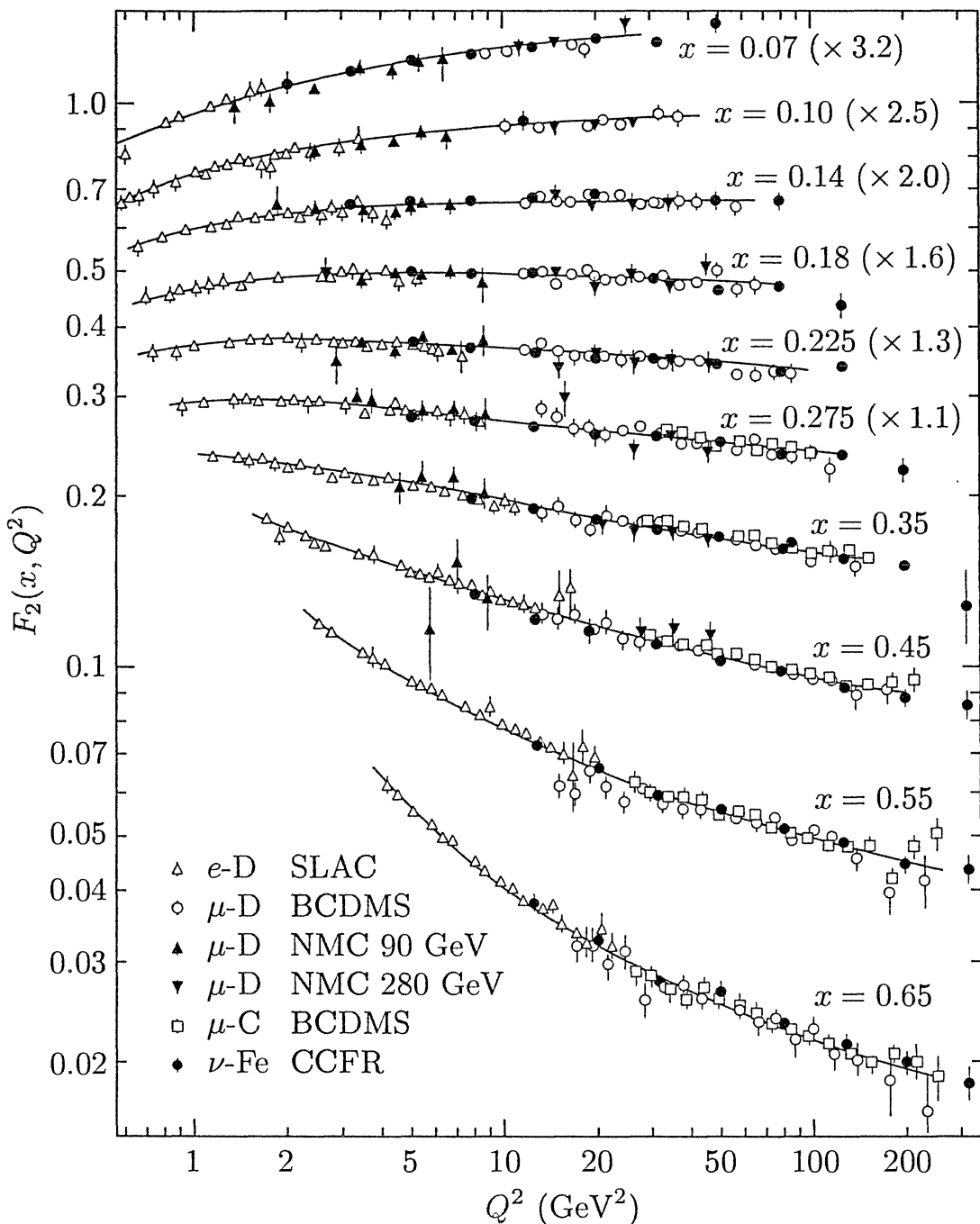


Figure 17.22. Dependence on Q^2 of the combination of quark distribution functions $F_2 = \sum_f x Q_f^2 f_f(x, Q^2)$ measured in deep inelastic electron-proton scattering. The various curves show the variation of F_2 for fixed values of x , and the comparison of this variation to a model evolved with the Altarelli-Parisi equations. The upper six data sets have been multiplied by the indicated factors to separate them on the plot. The data were compiled by M. Virchaux and R. Voss for the Particle Data Group, *Phys. Rev. D50*, 1173 (1994), Fig. 32.2. The complete references to the original experiments are given there.

which share its total momentum, as its wavefunction is probed on finer and finer distance scales.

Figure 17.22 shows the evolution of the combination of distribution functions that is measured in deep inelastic scattering, as a function of Q^2 . We see the characteristic decrease of the distribution functions at large x and the increase at small x . The data are compared to a model evolved according to the Altarelli-Parisi equations; this model apparently describes the data quite well.

17.6 Measurements of α_s

Before concluding our introductory survey of QCD, we should summarize the quantitative verification of the theory. We discussed precision tests of QED in Section 6.3, bringing together various measurements of the coupling α ; the best determinations agree to eight significant figures. Since QCD perturbation theory works only for hard-scattering processes, with uncertainties due to soft processes that are difficult to estimate, this theory has not been tested to such extreme accuracy. Nevertheless, it is interesting to bring together the best available determinations of α_s , to see how well they agree.

In order to compare values of α_s , it is necessary to express these using a common set of conventions. First, one must set the renormalization scale; a useful choice is the mass of the neutral weak boson Z^0 : $m_Z = 91.19$ GeV. Second, one must fix the renormalization scheme that defines the QCD coupling constant at this scale. It has become conventional to use as a standard the bare coupling after regularization by modified minimal subtraction, Eq. (11.77). The resulting standard coupling constant is called $\alpha_{s\overline{\text{MS}}}(m_Z^2)$.

Measurements of α_s from a number of types of experiments are summarized in Table 17.1. In Section 17.2 we saw that one can obtain a value of α_s from the measurement of the total cross section for e^+e^- annihilation to hadrons or, equivalently, the ratio R of the number of observed hadronic and leptonic events. An independent measurement of α_s can be obtained from the fraction of e^+e^- annihilation events with three-jet final states or, equivalently, from the transverse momentum distribution of produced hadrons relative to the jet axis. A number of measurements of this type are collected and averaged under the heading ‘Event shapes’. A similar measurement of α_s is obtained from the measurement of the transverse momentum spectrum of W bosons produced from quark-antiquark annihilation at high-energy $p\bar{p}$ colliders. The gluon radiative correction to the vertex in deep inelastic neutrino scattering can also be used to extract α_s . The rate of Bjorken scaling violation in deep inelastic scattering is controlled by α_s , and so this effect provides another α_s measurement. The decays of the lightest $b\bar{b}$ bound state Υ and the $c\bar{c}$ bound state ψ are governed by QCD and yield a measurement of α_s . Finally, the spectrum of $c\bar{c}$ and $b\bar{b}$ bound states can be computed numerically in terms of the QCD coupling constant, and the comparison with experiment gives a determination of α_s .

Table 17.1. Values of $\alpha_s(m_Z)$ Obtained from QCD Experiments

Process:	$\alpha_s(m_Z)$	Q (GeV)
Deep inelastic scattering	0.118 (6)	1.7
R in τ lepton decay	0.123 (4)	1.8
ψ , Υ spectroscopy	0.110 (6)	2.3
Transverse momentum of W production	0.121 (24)	4.
Deep inelastic scattering (evolution)	0.112 (4)	5.
Event shapes in e^+e^- annihilation	0.121 (6)	5.8,9.1
Rate for ψ , Υ decay	0.108 (10)	9.5
R in e^+e^- annihilation (20–65 GeV)	0.124 (21)	35.
R in Z^0 decay	0.124 (7)	91.2

The values of $\alpha_s(m_Z)$ displayed in this table are obtained by fitting experimental results to the theoretical expressions given by perturbative QCD using minimal subtraction. The values of α_s have been evolved to $Q = m_Z$ using the renormalization group equation. R refers to the ratio of cross sections or partial widths to hadrons versus leptons. The numbers in parentheses are the standard errors in the last displayed digits. The column labelled ‘ Q ’ gives an idea of the value of Q at which the measurement was made. (Typically, these measurements average over a range of Q , and that averaging is taken into account in the quoted values of α_s .) This table is based on the results compiled by I. Hinchliffe in his article for the Particle Data Group, *Phys. Rev. D50*, 1297 (1994). This article contains a full set of references and a discussion of the sources of uncertainty in these determinations.

The table shows the values of α_s extracted from each of these measurements, expressed in terms of the value in the reference conventions, $\alpha_{s\overline{\text{MS}}}(m_Z^2)$. We see that several of the experiments determine α_s to an accuracy of 5%, and that the various determinations are consistent with one another at this level. In Fig. 17.23, we have plotted the original values of α_s represented in Table 17.1, before conversion to a common scale, versus the momentum scale Q at which each was obtained. This comparison gives a striking direct verification of the running of α_s .

At the beginning of this chapter, we wrote down a candidate for the fundamental theory of strong interactions using only a few simple principles: the existence of quarks and the identification of their quantum numbers, and the idea that the theory of the quark interactions should be an asymptotically free gauge theory. It is remarkable that these simple considerations have led us to a description of strong interactions that is quantitatively correct for a broad range of phenomena in the hard-scattering regime where asymptotic freedom can be used as a tool for calculation.

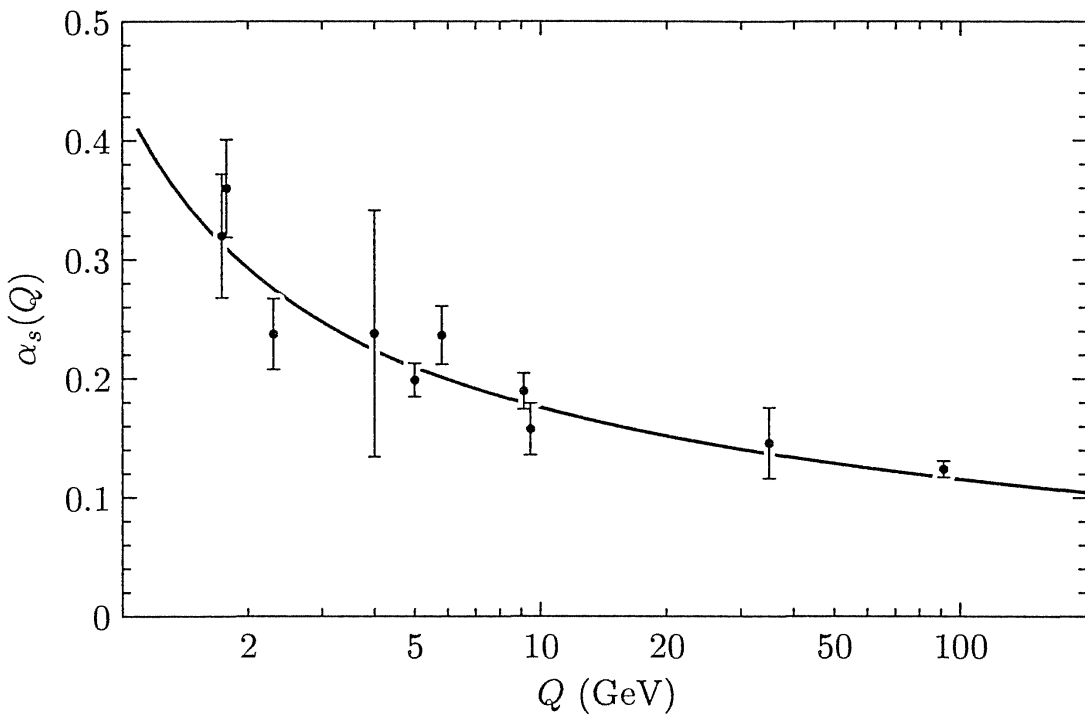


Figure 17.23. Measurements of α_s , plotted against the momentum scale Q at which the measurement was made. This figure was constructed by evolving the values of $\alpha_s(m_Z)$ listed in Table 17.1 back to the values of Q indicated in the table. The value for e^+e^- event shapes has been split into two points corresponding to experiments at the TRISTAN and LEP accelerators. These values are compared to the theoretical expectation from the renormalization group evolution with the initial condition $\alpha_s(m_Z) = 0.117$.

Problems

17.1 Two-loop renormalization group relations.

- (a) In higher orders of perturbation theory, the expression for the QCD β function will be a series

$$\beta(g) = -\frac{b_0}{(4\pi)^2} g^3 - \frac{b_1}{(4\pi)^4} g^5 - \frac{b_2}{(4\pi)^6} g^7 + \dots$$

Integrate the renormalization group equation and show that the running coupling constant is now given by

$$\alpha_s(Q^2) = \frac{4\pi}{b_0} \left[\frac{1}{\log(Q^2/\Lambda^2)} - \frac{b_1}{b_0^2} \frac{\log \log(Q^2/\Lambda^2)}{(\log(Q^2/\Lambda^2))^2} + \dots \right],$$

where the omitted terms decrease as $(\log(Q^2/\Lambda^2))^{-2}$.

- (b) Combine this formula with the perturbation series for the e^+e^- annihilation cross section:

$$\sigma(e^+e^- \rightarrow \text{hadrons}) = \sigma_0 \cdot \left(3 \sum_f Q_f^2 \right) \cdot \left[1 + \frac{\alpha_s}{\pi} + a_2 \left(\frac{\alpha_s}{\pi} \right)^2 + \mathcal{O}(\alpha_s^3) \right].$$

The coefficient a_2 depends on the details of the renormalization conditions defining α_s . Show that the leading two terms in the asymptotic behavior of $\sigma(s)$ for large s depend only on b_0 and b_1 and are independent of a_2 and b_2 . Thus the first *two* coefficients of the QCD β function are independent of the renormalization prescription.

17.2 A direct test of the spin of the gluon. In this problem, we compare the predictions of QCD with those of a model in which the interaction of quarks is mediated by a scalar boson. Let the coupling of the scalar gluon to quarks be given by

$$\delta\mathcal{L} = gS\bar{q}q,$$

and define $\alpha_g = g^2/4\pi$.

- (a) Using the technique described in parts (b) and (c) of the Final Project of Part I, compute the cross section for $e^+e^- \rightarrow q\bar{q}S$ to the leading order of perturbation theory. This cross section depends on the energies of the q , \bar{q} , and S , which we represent as fractions x_1 , x_2 , x_3 of the electron beam energy, as in Eq. (17.18). Show that

$$\frac{d^2\sigma}{dx_1dx_2}(e^+e^- \rightarrow q\bar{q}S) = \frac{4\pi\alpha^2 Q_q^2}{3s} \cdot \frac{\alpha_g}{4\pi} \frac{x_3^2}{(1-x_q)(1-x_{\bar{q}})}.$$

- (b) In practice, it is very difficult to tell quarks from gluons experimentally, since both particles appear as jets of hadrons. Therefore, let x_a be the largest of x_1 , x_2 , x_3 , let x_b be the second largest, and let x_c be the smallest. Sum over the various possibilities to derive an expression for $d^2\sigma/dx_a dx_b$, both in QCD, using Eq. (17.18), and in the scalar gluon model. Show that these models can be distinguished by their distributions in the x_a, x_b plane.

17.3 Quark-gluon and gluon-gluon scattering.

- (a) Compute the differential cross section

$$\frac{d\sigma}{d\hat{t}}(q\bar{q} \rightarrow gg)$$

for quark-antiquark annihilation in QCD to the leading order in α_s . This is most easily done by computing the amplitudes between states of definite quark and gluon helicity. Ignore all masses. Use explicit polarization vectors and spinors, for example,

$$\epsilon^\mu = \frac{1}{\sqrt{2}}(0, 1, i, 0)$$

for a right-handed gluon moving in the $+\hat{3}$ direction. You need only consider transversely polarized gluons. By helicity conservation, only the initial states $q_L\bar{q}_R$ and $q_R\bar{q}_L$ can contribute; by parity, these two states give identical cross sections. Thus it is necessary only to compute the amplitudes for the three processes

$$q_L\bar{q}_R \rightarrow g_R g_R,$$

$$q_L\bar{q}_R \rightarrow g_R g_L,$$

$$q_L\bar{q}_R \rightarrow g_L g_L.$$

In fact, by CP invariance, the first and third processes have equal cross sections. After computing the amplitudes, square them and combine them properly with

color factors to construct the various helicity cross sections. Finally, combine these to form the total cross section averaged over initial spins and colors.

- (b) Compute the differential cross section

$$\frac{d\sigma}{d\hat{t}}(gg \rightarrow gg)$$

for gluon-gluon scattering. There are 16 possible combinations of helicities, but many of them are related to each other by parity and crossing symmetry. All 16 can be built up from the three amplitudes for

$$\begin{aligned} gRgR &\rightarrow gRgR, \\ gRgR &\rightarrow gRgL, \\ gRgR &\rightarrow gLgL. \end{aligned}$$

Show that the last two of these amplitudes vanish. The first can be dramatically simplified using the Jacobi identity. When the smoke clears, only three of the 16 polarized gluon scattering cross sections are nonzero. Combine these to compute the spin- and color-averaged differential cross section.

17.4 The gluon splitting function. Compute the gluon splitting function (17.130) for the Altarelli-Parisi equations. To carry out this computation, first compute the matrix elements of the three-gluon vertex shown in Fig. 17.20 between gluon states of definite helicity. Combine these to derive the splitting function in the region $x < 1$. Then fix the singularity of the splitting function at $x = 1$ to give this function the correct overall normalization.

17.5 Photoproduction of heavy quarks. Consider the process of heavy quark pair photoproduction, $\gamma + p \rightarrow Q\bar{Q} + X$, for a heavy quark of mass M and electric charge Q . If M is large enough, any diagram contributing to this process must involve a large momentum transfer; thus a perturbative QCD analysis should apply. This idea applies in practice already for the production of c quark pairs. Work out the cross section to the leading order in QCD. Choose the parton subprocess that gives the leading contribution to this reaction, and write the parton-model expression for the cross section. You will need to compute the relevant subprocess cross section, but this can be taken directly from one of the QED calculations in Chapter 5. Then use this result to write an expression for the cross section for γ -proton scattering.

17.6 Behavior of parton distribution functions at small x . It is possible to solve the Altarelli-Parisi equations analytically for very small x , using some physically motivated approximations. This discussion is based on a paper of Ralston.[†]

- (a) Show that the Q^2 dependence of the right-hand side of the A-P equations can be expressed by rewriting the equations as differential equations in

$$\xi = \log \log \left(\frac{Q^2}{\Lambda^2} \right),$$

where Λ is the value of Q^2 at which $\alpha_s(Q^2)$, evolved with the leading-order β function, formally goes to infinity.

[†]J. P. Ralston, *Phys. Lett.* **172B**, 430 (1986).

- (b) Since the branching functions to gluons are singular as z^{-1} as $z \rightarrow 0$, it is reasonable to guess that the gluon distribution function will blow up approximately as x^{-1} as $x \rightarrow 0$. The resulting distribution

$$dx f_g(x) \sim \frac{dx}{x}$$

is approximately scale invariant, and so its form should be roughly preserved by the A-P equations. Let us, then, make the following two approximations: (1) the terms involving the gluon distribution completely dominate the right-hand sides of the A-P equations; and (2) the function

$$\tilde{g}(x, Q^2) = x f_g(x, Q^2)$$

is a slowly varying function of x . Using these approximations, and the limit $x \rightarrow 0$, show that the A-P equation for $f_g(x)$ can be converted to the following differential equation:

$$\frac{\partial^2}{\partial w \partial \xi} \tilde{g}(x, \xi) = \frac{12}{b_0} \tilde{g}(x, \xi),$$

where $w = \log(1/x)$ and $b = (11 - \frac{2}{3}n_f)$. Show that if $w\xi \gg 1$, this equation has the approximate solution

$$\tilde{g} = K(Q^2) \cdot \exp\left(\left[\frac{48}{b_0} w(\xi - \xi_0)\right]^{1/2}\right),$$

where $K(Q^2)$ is an initial condition.

- (c) The quark distribution at very small x is mainly created by branching of gluons. Using the approximations of part (b), show that, for any flavor of quark, the right-hand side of the A-P equation for $f_q(x)$ can be approximately integrated to yield an equation for $\tilde{q}(x) = x f_q(x)$:

$$\frac{\partial}{\partial \xi} \tilde{q}(x, \xi) = \frac{2}{3b_0} \tilde{g}(x, \xi).$$

Show, again using $w\xi \gg 1$, that this equation has as its integral

$$\tilde{q} = \left(\frac{\xi - \xi_0}{27b_0 w}\right)^{1/2} K(Q^2) \cdot \exp\left(\left[\frac{48}{b_0} w(\xi - \xi_0)\right]^{1/2}\right).$$

- (d) Ralston suggested that the initial condition

$$K(Q^2) = 50.36(\exp(\xi - \xi_0) - 0.957) \cdot \exp\left[-7.597(\xi - \xi_0)^{1/2}\right],$$

with $Q_0^2 = 5 \text{ GeV}^2$, $\Lambda = 0.2 \text{ GeV}$, and $n_f = 5$, gave a reasonable fit to the known properties of parton distributions, extrapolated into the small x region. Use this function and the results above to sketch the behavior of the quark and gluon distributions at small x and large Q^2 .

Operator Products and Effective Vertices

Our analysis of QCD in Chapter 17 was founded on the principle of asymptotic freedom, which told us that strong interaction processes with large momentum transfer might reliably be treated in weak-coupling perturbation theory. So far, however, we have made little use in QCD of the more powerful tools of the renormalization group. In this chapter, we will work out some implications of the Callan-Symanzik equation in QCD. We will see that asymptotically free theories have their own characteristic scaling behavior, with corrections in the form of anomalous powers of logarithms of the momentum scale. Though these corrections are generally weaker than those in the scalar field theories studied in Chapter 13, they nevertheless have important qualitative effects on the strong interactions.

We begin by considering the scaling law for mass terms in QCD, taking over directly the formalism that we used to describe the mass term of ϕ^4 theory in Sections 12.4 and 12.5. Other applications, however, require a more powerful theoretical tool, the *operator product expansion*. Section 18.3 introduces a general description of products of operators in quantum field theory and explains how such operator products are constrained by the Callan-Symanzik equation. The last two sections use this tool to develop a new viewpoint toward deep inelastic scattering and other hard processes in QCD.

18.1 Renormalization of the Quark Mass Parameter

Up to this point, we have always assumed that quark masses are small enough that they can be ignored in high-energy processes. This is not always an adequate assumption even for the light quarks u, d, s ; for the heavier quarks c, b, t , the masses can have very important effects. However, since isolated quarks do not exist, it is not possible to define the mass of a quark unambiguously. In the discussion to follow, we will consider the quark mass to be a parameter of QCD perturbation theory, defined by a renormalization prescription at some renormalization scale M .

Because we define the quark mass as we would a coupling constant, by a renormalization convention, we should expect that this parameter will run according to a renormalization group evolution, so that different values of the

mass parameter apply to different processes. We say that our original prescription leads to an *effective* quark mass, which depends on the momentum scale at which it is evaluated. In this section, we will work out the leading dependence of this effective mass on the momentum scale.

The basic formalism for effective mass terms was set out in Section 12.5. To add a mass term to the QCD Lagrangian, we must first define the mass operator $(\bar{q}q)$ by a renormalization prescription at a scale M . Then we can define the quark mass by adding to the Lagrangian the term

$$\Delta\mathcal{L}_m = -m(\bar{q}q)_M. \quad (18.1)$$

In this discussion, we will assume that the quark mass m is small enough that we need only keep terms of leading order in m . We will also assume, for simplicity, that we have such a mass term for only one quark flavor.

In the zero-mass limit, Green's functions of the operator $(\bar{q}q)$ with quark fields,

$$\begin{aligned} G^{(n,k)}(x_1, \dots, x_n, y_1, \dots, y_n, z_1, \dots, z_k) \\ = \langle q(x_1) \cdots q(x_n) \bar{q}(y_1) \cdots \bar{q}(y_n) \bar{q}q(z_1) \cdots \bar{q}q(z_k) \rangle, \end{aligned} \quad (18.2)$$

obey the Callan-Symanzik equation

$$\left[M \frac{\partial}{\partial M} + \beta \frac{\partial}{\partial g} + 2n\gamma + k\gamma_{\bar{q}q} \right] G^{(n,k)}(\{x_i\}, \{y_i\}, \{z_j\}, g, M) = 0, \quad (18.3)$$

where γ is the anomalous dimension of the quark field and $\gamma_{\bar{q}q}$ is the anomalous dimension of the operator $\bar{q}q$. If we include the mass terms in the Lagrangian according to (18.1), the Green's function of n quark fields and n antiquark fields satisfies

$$\left[M \frac{\partial}{\partial M} + \beta \frac{\partial}{\partial g} + 2n\gamma + \gamma_{\bar{q}q} m \frac{\partial}{\partial m} \right] G^{(n)}(\{x_i\}, \{y_i\}, g, m, M) = 0. \quad (18.4)$$

The derivative with respect to m counts the number of times the mass operator is used. In Section 12.5, we traded the variable m , with the dimensions of mass, for a dimensionless variable. However, in QCD, it is just as convenient to consider the dimensionful parameter m as a coupling constant. The solution of the Callan-Symanzik equation will then contain a running mass parameter $\bar{m}(Q)$, which depends on a typical momentum Q of the Green's function. This parameter is defined as the solution to a renormalization group equation analogous to Eq. (12.126). For this case, the equation is

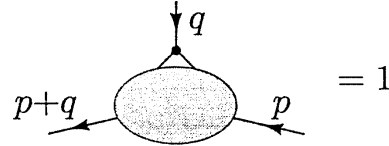
$$\frac{d}{d \log(Q/M)} \bar{m} = \gamma_{\bar{q}q}(\bar{g}) \cdot \bar{m}, \quad (18.5)$$

with the initial condition

$$\bar{m}(M) = m. \quad (18.6)$$

The quantity $\bar{m}(Q)$ is the *effective mass*, which should be used to compute the mass effects on quark production or scattering processes with the momentum transfer Q .

To compute $\bar{m}(Q)$ explicitly, we need to work out the anomalous dimension of the mass operator $\gamma_{\bar{q}q}$. This can be done as explained in Section 12.4. We define the normalization of the operator explicitly by the prescription that the vertex function of $(\bar{q}q)$ between renormalized quark fields should satisfy



(18.7)

for $p^2 = q^2 = (p+q)^2 = -M^2$. To preserve (18.7), we will need a counterterm vertex $\delta_{\bar{q}q}$ with the structure of the operator insertion. Then, as in Eq. (12.112), the anomalous dimension is given to one-loop order by

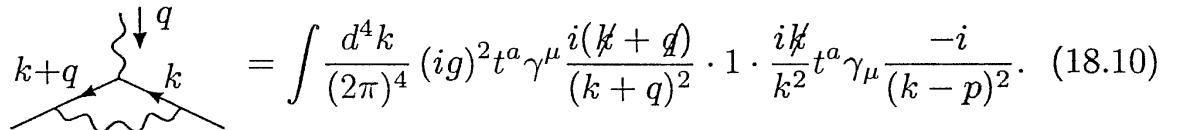
$$\gamma_{\bar{q}q} = M \frac{\partial}{\partial M} (-\delta_{\bar{q}q} + \delta_2), \quad (18.8)$$

where δ_2 is the counterterm for the quark field strength renormalization, defined in Fig. 16.8. Correlation functions of the gauge-invariant operator $(\bar{q}q)$ are gauge invariant, and so the various terms in the Callan-Symanzik equation for this function must sum to a gauge-invariant result. Since the leading coefficient of $\beta(g)$ is independent of the gauge and of other conventions, it follows from (18.3) that the leading coefficient of $\gamma_{\bar{q}q}$ is also convention independent. The counterterms δ_2 and $\delta_{\bar{q}q}$ both depend on the gauge. This argument shows that the gauge dependence must cancel in (18.8). In the calculation to follow, and in the other anomalous dimension calculations in this chapter, we will work consistently in Feynman-'t Hooft gauge.

We have already computed the divergent part of the counterterm δ_2 in Feynman-'t Hooft gauge in Section 16.4. Evaluating the group-theory factor in the result (16.77) for QCD, we find

$$\delta_2 = \frac{4}{3} \frac{g^2}{(4\pi)^2} \frac{\Gamma(2-\frac{d}{2})}{(M^2)^{2-d/2}}. \quad (18.9)$$

To compute $\delta_{\bar{q}q}$, we must work out the one-loop correction to the vertex (18.7). This is given by the diagram



(18.10)

In the expression for this diagram, the factor 1 represents the $\bar{q}q$ operator insertion. In the corresponding diagram for the renormalization of the quark number current $j^\nu = \bar{q}\gamma^\nu q$, this factor would be replaced by γ^ν . Since we need only the divergent part of the vertex renormalization (18.10), we can

approximate the integrand by its value for large k . Then this diagram becomes

$$\begin{aligned}
 \text{Diagram: } & \sim \int \frac{d^4 k}{(2\pi)^4} (ig)^2 t^a \gamma^\mu \frac{i k}{k^2} \cdot 1 \cdot \frac{i k}{k^2} t^a \gamma_\mu \frac{-i}{k^2} \\
 & \sim -i \frac{4}{3} g^2 \int \frac{d^4 k}{(2\pi)^4} \frac{d \cdot k^2}{(k^2)^3} \\
 & \sim \frac{4}{3} g^2 \cdot 4 \cdot \frac{1}{(4\pi)^2} \Gamma(2 - \frac{d}{2}).
 \end{aligned} \tag{18.11}$$

To preserve the normalization condition (18.7), we must add the counterterm

$$\delta_{\bar{q}q} = -4 \cdot \frac{4}{3} \frac{g^2}{(4\pi)^2} \frac{\Gamma(2 - \frac{d}{2})}{(M^2)^{2-d/2}}. \tag{18.12}$$

Assembling (18.8), (18.9), and (18.12), we find

$$\gamma_{\bar{q}q} = -8 \frac{g^2}{(4\pi)^2}. \tag{18.13}$$

As we have noted in the previous paragraph, the anomalous dimension γ_j of the quark number current can be found by a very similar calculation. This will give a good check on our formalism, since, as we have argued above Eq. (12.110), a conserved current is unambiguously normalized by its integral, the conserved charge, and so must have zero anomalous dimension. If we substitute γ^ν for 1 in (18.10) and use the same set of approximations to reduce the integral, we find in the numerator the Dirac matrix structure

$$\begin{aligned}
 \gamma^\mu k^\nu k^\lambda \gamma_\mu &= \frac{1}{d} k^2 \gamma^\mu \gamma^\lambda \gamma^\nu \gamma_\lambda \gamma_\mu \\
 &= \frac{1}{4} (-2)^2 k^2 \gamma^\nu.
 \end{aligned} \tag{18.14}$$

Then, instead of (18.12), we need the counterterm

$$\delta_j = -\frac{4}{3} \frac{g^2}{(4\pi)^2} \frac{\Gamma(2 - \frac{d}{2})}{(M^2)^{2-d/2}}. \tag{18.15}$$

Combining this result with (18.9), we find

$$\gamma_j = 0, \tag{18.16}$$

in accord with our general arguments.

If we replace the gamma function in (18.11) by an explicit factor of $\log(\Lambda^2/Q^2)$, and then subtract the divergence using the counterterm (18.12), we find that the vertex diagram behaves as

$$\text{Diagram: } = \frac{4}{3} \cdot 4 \frac{g^2}{(4\pi)^2} \log \frac{M^2}{Q^2}. \tag{18.17}$$

This diagram gives an enhancement at small external momenta. Some of this enhancement is associated with the (gauge-dependent) rescaling of the external quark fields; relation (18.8) tells us how to extract the piece of this

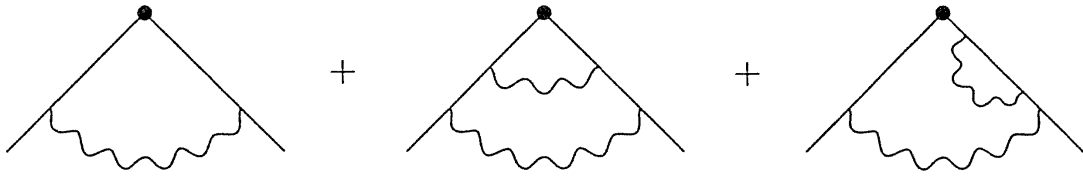


Figure 18.1. Diagrams giving the leading logarithmic contributions to the momentum dependence of the quark effective mass.

logarithm associated with the gauge-invariant enhancement of the effective mass. Thus, to order α_s ,

$$\bar{m}(Q) = m \cdot \left(1 + 8 \frac{g^2}{(4\pi)^2} \log \frac{M^2}{Q^2} \right). \quad (18.18)$$

To compute the momentum dependence of the effective mass more accurately, we must take two more features of the calculation into account. First, the quantity $(\alpha_s \log(M^2/Q^2))$ may become of order 1, and, in this case, we must take into account all leading logarithmic terms of the form $(\alpha_s \log(M^2/Q^2))^n$. Contributions of this type come from all the diagrams shown in Fig. 18.1. Second, the coupling constant α_s is itself a function of the momentum scale, giving a further enhancement to contributions from small Q . Both of these effects are properly accounted by solving the renormalization group equation (18.5). To the leading order in g^2 , this equation takes the explicit form

$$\frac{d}{d \log(Q/M)} \bar{m} = -8 \frac{\bar{g}^2}{(4\pi)^2} m = -2 \frac{\alpha_s(Q^2)}{\pi} \bar{m}. \quad (18.19)$$

Inserting the solution of the renormalization group equation for \bar{g} in the form (17.17), we find

$$\frac{d}{d \log(Q/M)} \bar{m} = -\frac{8}{b_0 \log(Q^2/\Lambda^2)} \bar{m}, \quad (18.20)$$

where b_0 is the first coefficient of the QCD β function and Λ is now the QCD scale parameter defined in (17.16). The integral of this equation, satisfying the initial condition (18.6), is

$$\bar{m}(Q^2) = \left(\frac{\log(M^2/\Lambda^2)}{\log(Q^2/\Lambda^2)} \right)^{4/b_0} m. \quad (18.21)$$

Recall that $b_0 = 11 - \frac{2}{3}n_f$ in QCD. Another way to express (18.21) is by writing

$$\bar{m}(Q^2) = \left(\frac{\alpha_s(Q^2)}{\alpha_s(M^2)} \right)^{4/b_0} m. \quad (18.22)$$

Just as an illustration, take $n_f = 4$ and $\Lambda = 150$ MeV; then the effective masses of the light quarks increase by about a factor 2 from $Q = 100$ GeV to $Q = 1$ GeV.

The method we have just used for computing the QCD enhancement of the quark mass operator applies equally well to the matrix elements of any other gauge-invariant operator. We conclude this section by recapitulating the conclusions of the argument in their more general form.

Let $\mathcal{O}(x)$ be any gauge-invariant operator in QCD. As we saw for the mass term, the one-loop corrections to the matrix elements of this operator may contain enhancement or suppression terms proportional to $\alpha_s \log(M^2/Q^2)$, where Q is the momentum scale of a QCD process mediated by $\mathcal{O}(x)$ and M is the renormalization scale used to define the operator normalization. The part of these one-loop corrections specifically associated with the operator normalization is given by the anomalous dimension $\gamma_{\mathcal{O}}$. For an operator containing n quark or antiquark fields and k gluon fields,

$$\gamma_{\mathcal{O}} = M \frac{\partial}{\partial M} \left(-\delta_{\mathcal{O}} + \frac{n}{2} \delta_2 + \frac{k}{2} \delta_3 \right), \quad (18.23)$$

where $\delta_{\mathcal{O}}$ is the counterterm needed to preserve the operator normalization condition and δ_2 and δ_3 are the counterterms for the quark and gluon field strength renormalization defined in Fig. 16.8. From (18.23), we can derive the explicit one-loop expression for $\gamma_{\mathcal{O}}$ in the form

$$\gamma_{\mathcal{O}} = -a_{\mathcal{O}} \frac{g^2}{(4\pi)^2}. \quad (18.24)$$

Using this result, we can solve the renormalization group equation for the coefficient of $\mathcal{O}(x)$ and find the QCD renormalization factor

$$\left(\frac{\log(M^2/\Lambda^2)}{\log(Q^2/\Lambda^2)} \right)^{a_{\mathcal{O}}/2b_0}, \quad (18.25)$$

where b_0 is the first coefficient of the QCD β function,

$$b_0 = 11 - \frac{2}{3}n_f. \quad (18.26)$$

The QCD renormalization (18.25) is an enhancement at small momenta if $a_{\mathcal{O}} > 0$.

In the remainder of this chapter, we will present further examples of this enhancement or suppression by QCD logarithms. In many cases, we will see that these factors lead to striking and nontrivial physical effects.

18.2 QCD Renormalization of the Weak Interaction

Our next example of the appearance of QCD enhancement factors occurs in the theory of the weak interactions of hadrons. In Section 17.3, we introduced the weak interaction coupling of quarks and leptons, which we described by an effective Lagrangian. For our analysis here, we will need to know a few more details of the structure of the weak interactions, so we begin this section by presenting these facts. The complete structure of the weak interactions of quarks and leptons will be discussed systematically in Chapter 20.

As we discussed in Section 17.3, the weak interactions among quarks and leptons are described by an effective Lagrangian resulting from the exchange of a virtual W vector boson. In (17.31), we wrote the effective vertex that couples quarks to leptons:

$$\Delta\mathcal{L} = \frac{g^2}{2m_W^2} \bar{l}\gamma^\mu \frac{(1-\gamma^5)}{2} \nu \bar{u}\gamma_\mu \frac{(1-\gamma^5)}{2} d + \text{h.c.} \quad (18.27)$$

In this chapter, we will mainly be concerned with the effects of this interaction for momentum scales much larger than 1 GeV. Thus, we will ignore quark masses. All fermion fields that appear in the weak-interaction vertices are multiplied by the left-handed projector $\frac{1}{2}(1 - \gamma^5)$. In the rest of this section, we will not write this projector explicitly; rather, we will denote the projection by a subscript L . We will also introduce the Fermi constant, given by (17.32). Then (18.27) can be rewritten as

$$\Delta\mathcal{L} = \frac{4G_F}{\sqrt{2}} (\bar{l}_L \gamma^\mu \nu_L) (\bar{u}_L \gamma_\mu d_L) + \text{h.c.} \quad (18.28)$$

There is an analogous vertex that represents W exchange between pairs of quarks; this has the form

$$\Delta\mathcal{L} = \frac{4G_F}{\sqrt{2}} (\bar{d}_L \gamma^\mu u_L) (\bar{u}_L \gamma_\mu d_L) + \text{h.c.} \quad (18.29)$$

However, for the discussion of this chapter, we will need to write a modified, and less approximate, expression. When we discuss the theory of weak interactions in detail in Chapter 20, we will learn that the charge $+2/3$ quarks (u, c, t) couple to the charge $-1/3$ quarks (d, s, b) through the weak interactions via a unitary rotation. Thus, for example, u couples to the combination

$$\cos \theta_c d + \sin \theta_c s, \quad (18.30)$$

plus a small admixture of b , which we will ignore in this section. The mixing angle θ_c is called the *Cabibbo angle*. Because of this rotation, the weak interaction effective Lagrangian coupling quarks to quarks actually contains a number of terms, of which a particularly important one is

$$\Delta\mathcal{L} = \frac{4G_F}{\sqrt{2}} \cos \theta_c \sin \theta_c (\bar{d}_L \gamma^\mu u_L) (\bar{u}_L \gamma_\mu s_L). \quad (18.31)$$

This term allows the s quarks to decay through the process $s \rightarrow u\bar{u}d$. Similarly, the rotation of (18.28) produces the effective interaction

$$\Delta\mathcal{L} = \frac{4G_F}{\sqrt{2}} \sin \theta_c (\bar{\ell}_L \gamma^\mu \nu_L) (\bar{u}_L \gamma_\mu s_L), \quad (18.32)$$

which leads to the decay $s \rightarrow u\bar{v}\ell$. These weak interaction processes are referred to as *nonleptonic* and *semileptonic* decay processes, respectively. Similar expressions apply to the other heavy quarks.

Given that (18.31) and (18.32) describe the weak interaction coupling of the s quark at a fundamental level, we now discuss the modification of these couplings by QCD logarithms. We have seen in the previous section that QCD corrections have a profound effect in enhancing the strength of the quark mass term of the underlying Lagrangian. We will now investigate whether the strength of the weak interactions can receive a similar enhancement.

We first consider the semileptonic weak interaction operator (18.32). The leptonic fermion bilinear is not affected by QCD, so the QCD enhancement of this operator is just the same as that of its quark component

$$\bar{u}_L \gamma_\mu s_L. \quad (18.33)$$

However, this operator is a current and so has $\gamma = 0$. In terms of diagrams, the logarithmic enhancement resulting from the diagram shown in Fig. 18.2 is canceled by the quark field-strength renormalization, as we saw already in our discussion of the current vertex in Section 18.1. The left-handed projector $\frac{1}{2}(1 - \gamma^5)$ commutes through the diagram and has no effect on the final result. The same remark applies to the semileptonic weak interaction that links u and d quarks. It implies, for that case, that the normalization of the cross sections for deep inelastic neutrino scattering given in (17.35) is not affected by QCD logarithms.

In the case of nonleptonic weak interactions, however, the effect of QCD is not so simple. Let us first compute the Feynman diagrams that give the leading corrections to the renormalization of the weak interaction vertex (18.31) and then, at a later stage, build up the renormalization group interpretation of these results.

At order α_s , the nonleptonic weak interaction vertex receives corrections from the diagrams shown in Fig. 18.3. Notice that the first diagram is precisely the current renormalization found in the semileptonic case. The second diagram gives the analogous renormalization of the second quark current. In the computation of γ , these two contributions cancel the contributions from the field-strength renormalization of the four quark fields. The remaining four diagrams of Fig. 18.3 are new contributions which contribute potentially large rescaling factors.

We now compute these diagrams, beginning with the third diagram in Fig. 18.3. As in the computation of Section 18.1, we are interested in the logarithmically divergent contribution associated with values of the loop momentum k much larger than the external momenta. The simplest way to extract this

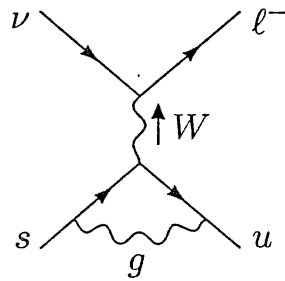


Figure 18.2. QCD correction to the strength of the semileptonic weak interaction vertex.

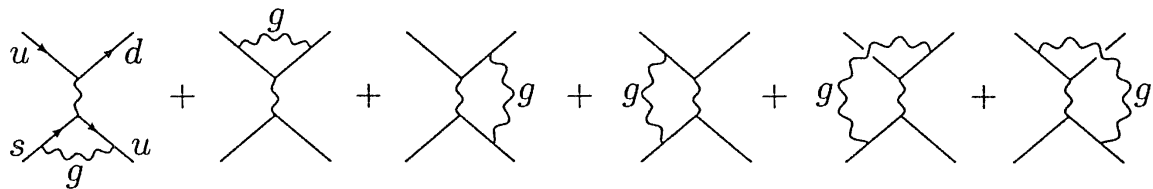


Figure 18.3. QCD corrections to the strength of the nonleptonic weak interaction vertex.

contribution is to compute each diagram in the approximation of zero external momentum. In writing the expression for these diagrams, we will omit the prefactor

$$\frac{4G_F}{\sqrt{2}} \cos \theta_c \sin \theta_c. \quad (18.34)$$

We will retain the quark fields to represent the external states, so that our final expressions will have the form of rescaled operators.

Using this notation, the third diagram in Fig. 18.3 has the value

$$\text{Diagram} = \int \frac{d^4 k}{(2\pi)^4} (ig)^2 \frac{-i}{k^2} \left(\bar{d}_L \gamma^\nu t^a \frac{i k}{k^2} \gamma^\mu u_L \right) \left(\bar{u}_L \gamma_\nu t^a \frac{-i k}{k^2} \gamma_\mu s_L \right). \quad (18.35)$$

Using the symmetry of the k integral, we extract the divergent piece:

$$\begin{aligned} \text{Diagram} &= ig^2 \int \frac{d^4 k}{(2\pi)^4} \frac{k^2/d}{(k^2)^3} \left(\bar{d}_L \gamma^\nu t^a \gamma^\lambda \gamma^\mu u_L \right) \left(\bar{u}_L \gamma_\nu t^a \gamma_\lambda \gamma_\mu s_L \right) \\ &= -\frac{g^2}{4} \frac{\Gamma(2-\frac{d}{2})}{(4\pi)^2} \left(\bar{d}_L \gamma^\nu t^a \gamma^\lambda \gamma^\mu u_L \right) \left(\bar{u}_L \gamma_\nu t^a \gamma_\lambda \gamma_\mu s_L \right). \end{aligned} \quad (18.36)$$

To put the product of quark fields into a more familiar form, we apply the Fierz transformation discussed at the end of Section 3.4. If the color matrices t^a were not present, the product of fermion fields would be exactly the one appearing in (3.82), and we would find

$$(\bar{d}_L \gamma^\nu \gamma^\lambda \gamma^\mu u_L) (\bar{u}_L \gamma_\nu \gamma_\lambda \gamma_\mu s_L) = 16 \bar{d}_L \gamma^\nu u_L \bar{u}_L \gamma_\nu s_L. \quad (18.37)$$

The matrices t^a redirect the color quantum numbers of the quark fields. To clarify this, we need the analogue of identity (3.77) for color. To find this

identity, consider the color invariant

$$(t^a)_{ij}(t^a)_{kl}. \quad (18.38)$$

The indices i, k transform according to the 3 representation of color; the indices j, ℓ transform according to the $\bar{3}$. Thus, (18.38) must be a linear combination of the two possible ways to contract these indices,

$$A\delta_{i\ell}\delta_{kj} + B\delta_{ij}\delta_{k\ell}. \quad (18.39)$$

The constants A and B can be determined by contracting (18.38) and (18.39) with δ_{ij} and with δ_{jk} and adjusting A and B so that the contractions of (18.39) obey the identities

$$\text{tr}t^a_{k\ell} = 0; \quad (t^a t^a)_{i\ell} = \frac{4}{3}. \quad (18.40)$$

This gives the identity

$$(t^a)_{ij}(t^a)_{k\ell} = \frac{1}{2}(\delta_{i\ell}\delta_{kj} - \frac{1}{3}\delta_{ij}\delta_{k\ell}). \quad (18.41)$$

A similar relation holds for the generators of $SU(N)$ in the fundamental representation, with (1/3) replaced by (1/ N) in that case.

Inserting (18.41) into (18.36), we find that the first term of the identity generates a new four-fermion operator,

$$(\bar{d}_{Li}\gamma^\nu\gamma^\lambda\gamma^\mu u_{Lj})(\bar{u}_{Lj}\gamma_\nu\gamma_\lambda\gamma_\mu s_{Li}), \quad (18.42)$$

where i, j are color indices. Applying the Fierz rearrangement in (18.37), and then applying the additional rearrangement (3.79), we can convert this operator to the form

$$16(\bar{d}_{Li}\gamma^\nu u_{Lj})(\bar{u}_{Lj}\gamma_\nu s_{Li}) = 16(\bar{u}_{Lj}\gamma^\nu u_{Lj})(\bar{d}_{Li}\gamma_\nu s_{Li}). \quad (18.43)$$

The minus sign in (3.79) is compensated by a minus sign from interchanging the order of fermion fields. The final result is a product of color-singlet quark currents; however, the fields in these currents are associated differently from the original operator.

The final result of our evaluation of this diagram is

$$\text{Diagram} = -4g^2 \frac{\Gamma(2-\frac{d}{2})}{(4\pi)^2} \left[\frac{1}{2}\bar{u}_L\gamma^\mu u_L \bar{d}_L\gamma_\mu s_L - \frac{1}{6}\bar{d}_L\gamma^\mu u_L \bar{u}_L\gamma_\mu s_L \right]. \quad (18.44)$$

The fourth diagram of Fig. 18.3 gives precisely the same contribution.

The evaluation of the last two diagrams in Fig. 18.3 is quite similar. The fifth diagram gives

$$\begin{aligned} \text{Diagram} &= \int \frac{d^4 k}{(2\pi)^4} (ig)^2 \frac{-i}{k^2} \left(\bar{d}_L\gamma^\nu t^a \frac{ik}{k^2} \gamma^\mu u_L \right) \left(\bar{u}_L\gamma_\mu t^a \frac{ik}{k^2} \gamma_\nu t^a s_L \right) \\ &= -ig^2 \int \frac{d^4 k}{(2\pi)^4} \frac{k^2/d}{(k^2)^3} (\bar{d}_L\gamma^\nu t^a \gamma^\lambda \gamma^\mu u_L) (\bar{u}_L\gamma_\mu t^a \gamma_\lambda \gamma_\nu s_L) \\ &= +\frac{g^2}{4} \frac{\Gamma(2-\frac{d}{2})}{(4\pi)^2} (\bar{d}_L\gamma^\nu t^a \gamma^\lambda \gamma^\mu u_L) (\bar{u}_L\gamma_\mu t^a \gamma_\lambda \gamma_\nu s_L). \end{aligned} \quad (18.45)$$

The four-fermion operator can be simplified as follows, by the use of the Fierz identity (3.79):

$$\begin{aligned} (\bar{d}_L \gamma^\nu \gamma^\lambda \gamma^\mu u_L) (\bar{u}_L \gamma_\mu \gamma_\lambda \gamma_\nu s_L) &= +(\bar{d}_L \gamma^\nu \gamma^\lambda \gamma^\mu \gamma_\lambda \gamma_\nu s_L) (\bar{u}_L \gamma_\mu u_L) \\ &= +(-2)^2 (\bar{d}_L \gamma^\mu s_L) (\bar{u}_L \gamma_\mu u_L) \\ &= 4(\bar{d}_L \gamma^\mu u_L) (\bar{u}_L \gamma_\mu s_L). \end{aligned} \quad (18.46)$$

Again, we must reduce the product of color matrices using identity (18.41), and, again, the first term of this identity will require an additional Fierz transformation. The final result is

$$\text{Diagram} = +g^2 \frac{\Gamma(2-\frac{d}{2})}{(4\pi)^2} \left[\frac{1}{2} \bar{u}_L \gamma^\mu u_L \bar{d}_L \gamma_\mu s_L - \frac{1}{6} \bar{d}_L \gamma^\mu u_L \bar{u}_L \gamma_\mu s_L \right]. \quad (18.47)$$

The last diagram in Fig. 18.3 gives an identical contribution. The sum of the contributions from these four diagrams is

$$-3g^2 \frac{\Gamma(2-\frac{d}{2})}{(4\pi)^2} \left[\bar{u}_L \gamma^\mu u_L \bar{d}_L \gamma_\mu s_L - \frac{1}{3} \bar{d}_L \gamma^\mu u_L \bar{u}_L \gamma_\mu s_L \right]. \quad (18.48)$$

The extraction of the ultraviolet-divergent pieces of the diagrams of Fig. 18.3 is part of our formal prescription for computing the Callan-Symanzik γ function of the weak interaction vertex. However, it is useful to pause at this point and ask about the physical significance of this divergence. The diagrams of Fig. 18.3 would not be divergent if we computed them in the underlying theory with W bosons. In writing the weak interaction as an effective local vertex, we approximated the W boson propagator by a constant, assuming that the momentum k that it carried was much less than m_W :

$$\frac{1}{k^2 - m_W^2} \rightarrow \frac{-1}{m_W^2}. \quad (18.49)$$

The approximation we used to compute the QCD corrections to the effective vertex is valid only in the region of integration where $k^2 \ll m_W^2$. Outside this region we must use the full W propagator; this introduces an extra factor of k^2 in the denominator and makes the integral converge. Thus, in a direct calculation of the QCD correction, the ultraviolet-divergent terms in the evaluation of Fig. 18.3 would be replaced by logarithms cut off at m_W . The lower limit of the logarithm is set by the external momenta. In the decay of a K meson—the lightest hadron containing the s quark—these are of order m_K . Thus the correction given in (18.48) should be evaluated by replacing

$$g^2 \frac{\Gamma(2-\frac{d}{2})}{(4\pi)^2} \rightarrow \frac{\alpha_s}{4\pi} \log \frac{m_W^2}{m_K^2}. \quad (18.50)$$

With this interpretation, we can rewrite (18.48) as the order- α_s correction to the leading-order weak interaction vertex. The effect of this correction is

the rescaling and modification of the weak interaction operator:

$$\bar{d}_L \gamma^\mu u_L \bar{u}_L \gamma_\mu s_L \rightarrow \left(1 + \frac{\alpha_s}{4\pi} \log \frac{m_W^2}{m_K^2}\right) \bar{d}_L \gamma^\mu u_L \bar{u}_L \gamma_\mu s_L - 3 \left(\frac{\alpha_s}{4\pi} \log \frac{m_W^2}{m_K^2}\right) \bar{u}_L \gamma^\mu u_L \bar{d}_L \gamma_\mu s_L. \quad (18.51)$$

Notice that the QCD corrections not only rescale the normalization of the original operator but also introduce a new operator with a different structure. This calculation makes concrete the idea introduced in Section 12.4 that the diagrams that change the normalization of local operators may also mix together different operators with the same dimension and quantum numbers.

Since the value of the logarithm in (18.50) is about 10, the size of the leading QCD correction is of order 1 and so higher-order corrections are important. To sum the leading logarithmic corrections, we return to the renormalization group analysis. For clarity, define

$$\mathcal{O}^1 = \bar{d}_L \gamma^\mu u_L \bar{u}_L \gamma_\mu s_L; \quad \mathcal{O}^2 = \bar{u}_L \gamma^\mu u_L \bar{d}_L \gamma_\mu s_L. \quad (18.52)$$

We will use the subscript 0 to denote bare operators and the subscript M to denote operators obeying renormalization conditions at the scale M . From the diagrams of Fig. 18.3, we have found that the operator whose matrix elements have the quark structure of \mathcal{O}^1 , properly normalized at the scale M , is given by

$$\mathcal{O}_M^1 = \mathcal{O}_0^1 + \delta^{11} \mathcal{O}_0^1 + \delta^{12} \mathcal{O}_0^2, \quad (18.53)$$

where the δ^{ij} are counterterms,

$$\delta^{11} = -\frac{g^2}{(4\pi)^2} \frac{\Gamma(2-\frac{d}{2})}{M^2}; \quad \delta^{12} = +3 \frac{g^2}{(4\pi)^2} \frac{\Gamma(2-\frac{d}{2})}{M^2}. \quad (18.54)$$

A reciprocal calculation gives \mathcal{O}_M^2 in terms of bare operators:

$$\mathcal{O}_M^2 = \mathcal{O}_0^2 + \delta^{21} \mathcal{O}_0^1 + \delta^{22} \mathcal{O}_0^2, \quad (18.55)$$

with

$$\delta^{21} = \delta^{12}, \quad \delta^{22} = \delta^{11}.$$

Then, in the manner than we discussed in Eq. (12.109), the operator rescaling of \mathcal{O}^1 and \mathcal{O}^2 is described in the Callan-Symanzik equation by a matrix γ^{ij} linking the two operators. Expanding this equation to first order in g^2 , we see that this matrix is given to one-loop order by

$$\gamma^{ij} = M \frac{\partial}{\partial M} [-\delta^{ij}]. \quad (18.56)$$

Thus we find

$$\gamma = \frac{g^2}{(4\pi)^2} \begin{pmatrix} -2 & 6 \\ 6 & -2 \end{pmatrix}, \quad (18.57)$$

acting on the space of operators $\mathcal{O}^1, \mathcal{O}^2$.

The simplest way to deduce the physical effects of the rescaling described by (18.57) is to diagonalize this matrix and thus find a new basis of operators that are rescaled without mixing. For the matrix (18.57), the eigenoperators are easily seen to be

$$\begin{aligned}\mathcal{O}^{1/2} &= \frac{1}{2} [\bar{d}_L \gamma^\mu u_L \bar{u}_L \gamma_\mu s_L - \bar{u}_L \gamma^\mu u_L \bar{d}_L \gamma_\mu s_L], \\ \mathcal{O}^{3/2} &= \frac{1}{2} [\bar{d}_L \gamma^\mu u_L \bar{u}_L \gamma_\mu s_L + \bar{u}_L \gamma^\mu u_L \bar{d}_L \gamma_\mu s_L].\end{aligned}\quad (18.58)$$

The superscripts on these operators are their isospin quantum numbers. The operator $\mathcal{O}^{1/2}$ is antisymmetric under the interchange of the labels \bar{d} and \bar{u} ; thus, these two isospin-1/2 fields are combined to total isospin zero, and so the whole operator is isospin-1/2. This operator can mediate decays of the K meson that change the isospin by 1/2 unit, such as $K^0 \rightarrow \pi^+ \pi^-$, but not processes that change the isospin by 3/2, such as $K^+ \rightarrow \pi^+ \pi^0$. Experimentally, processes of the former type occur almost a thousand times faster (an observation called the $\Delta I = 1/2$ rule). Thus, it is interesting that the hard QCD corrections already make a distinction between these operators.

From the eigenvalues of (18.57), we obtain the Callan-Symanzik γ functions of the eigenoperators (18.58):

$$\gamma_{1/2} = -8 \frac{g^2}{(4\pi)^2}; \quad \gamma_{3/2} = +4 \frac{g^2}{(4\pi)^2}. \quad (18.59)$$

According to Eqs. (18.24) and (18.25), this implies that the operator $\mathcal{O}^{1/2}$ receives an enhancement from hard QCD logarithms, while the operator $\mathcal{O}^{3/2}$ receives a suppression. More explicitly, we can write the operator that appears in the original nonleptonic weak interaction vertex (18.31) as

$$[\bar{d}_L \gamma^\mu u_L \bar{u}_L \gamma_\mu s_L] \Big|_{m_W} = [\mathcal{O}^{1/2}] \Big|_{m_W} + [\mathcal{O}^{3/2}] \Big|_{m_W}. \quad (18.60)$$

As above, the subscript refers to the mass scale at which the operator is normalized. We now account for the QCD logarithms associated with evaluating the matrix element of this operator at a lower momentum scale, m_K , by replacing the operators on the right-hand side of (18.60) with operators renormalized at m_K , with the rescaling factor (18.25). This gives

$$\begin{aligned}[\bar{d}_L \gamma^\mu u_L \bar{u}_L \gamma_\mu s_L] \Big|_{m_W} &= \left(\frac{\log(m_W^2/\Lambda^2)}{\log(m_K^2/\Lambda^2)} \right)^{4/b_0} [\mathcal{O}^{1/2}] \Big|_{m_K} \\ &\quad + \left(\frac{\log(m_W^2/\Lambda^2)}{\log(m_K^2/\Lambda^2)} \right)^{-2/b_0} [\mathcal{O}^{3/2}] \Big|_{m_K},\end{aligned}\quad (18.61)$$

where, again, $b_0 = 11 - \frac{2}{3}n_f$. This equation shows that, unlike the case of semileptonic weak interactions, the overall normalization of the effective Lagrangian for nonleptonic weak interactions is changed by QCD logarithms. In addition, the quark structure of the effective Lagrangian is altered.

Quantitatively, taking $n_f = 4$ and $\Lambda = 150$ MeV as an illustration, we find

$$[\bar{d}_L \gamma^\mu u_L \bar{u}_L \gamma_\mu s_L] \Big|_{m_W} = 2.1 [\mathcal{O}^{1/2}] \Big|_{m_K} + 0.7 [\mathcal{O}^{3/2}] \Big|_{m_K}. \quad (18.62)$$

Thus, the QCD logarithmic corrections from m_W to m_K give the $\Delta I = 1/2$ part of the effective vertex an enhancement of about a factor of 3.* The observed $\Delta I = 1/2$ rule in K decays requires a factor of 20 enhancement. However, part of this is expected to arise from the ratio of the matrix elements of the operators $\mathcal{O}_{m_K}^{1/2}$ and $\mathcal{O}_{m_K}^{3/2}$ between physical hadron states, which are determined by the soft, nonperturbative part of QCD dynamics.

18.3 The Operator Product Expansion

One way to describe the development of the previous section is to say that we studied an interaction that was fundamentally a product of currents by replacing this product of operators with a single local operator. We then derived the physical consequences of the original, composite, interaction by working out the QCD rescaling of this operator. The procedure of replacing a product of operators with a single effective vertex is useful in many contexts in quantum field theory. Thus, in this section, we will pause from our study of QCD to write out the general formalism governing this procedure.

Let us abstract the situation described in the previous section as follows: Consider a quantum field theory process that includes two operators \mathcal{O}_1 , \mathcal{O}_2 separated by a small distance x , together with other fields $\phi(y_i)$ located much farther away, or together with external physical states. In the example above, the two operators are the quark currents that appear in the weak interaction vertex, and their separation x is a distance of order m_W^{-1} , the range of the W propagator. The external states, which contain K and π mesons, can be described by operators that create and destroy these particles. The amplitude for K decay by the weak interactions, or any more general process of this class, can then be extracted from the Green's function

$$G_{12}(x; y_1, \dots, y_m) = \langle \mathcal{O}_1(x) \mathcal{O}_2(0) \phi(y_1) \dots \phi(y_m) \rangle, \quad (18.63)$$

considered in the limit $x \rightarrow 0$, with the y_i fixed away from the origin. Here and in the following discussion, products of operators will be considered to be time-ordered, just as we would find by writing the product of fields under the functional integral.

The product of operators $\mathcal{O}_1(x) \mathcal{O}_2(0)$ can potentially create the most general local disturbance in the vicinity of the point 0. However, any such disturbance can be described as the effect of a local operator placed at 0. This

*M. K. Gaillard and B. W. Lee, *Phys. Rev. Lett.* **33**, 108 (1974); G. Altarelli and L. Maiani, *Phys. Lett.* **52B**, 351 (1974).

local operator must have the global symmetry quantum numbers of the product of $\mathcal{O}_1 \mathcal{O}_2$, but it is otherwise unrestricted. It is useful to write this operator as a linear combination of operators from a standard basis. The coefficients in this linear combination can depend on the separation x . Typically, products of operators in quantum field theory are singular, so it is likely that some of the coefficients will have singularities as $x \rightarrow 0$. Combining these observations, Wilson proposed that the effects of the operator product could be computed by replacing the product of operators in (18.63) with a linear combination of local operators,

$$\mathcal{O}_1(x) \mathcal{O}_2(0) \rightarrow \sum_n C_{12}^n(x) \mathcal{O}_n(0), \quad (18.64)$$

where the coefficients $C_{12}^n(x)$ are c-number functions. This *operator product expansion* (OPE) will depend only on the operators \mathcal{O}_1 , \mathcal{O}_2 , and their separation and will be independent of the identity and location of the other fields appearing in the Green's function.

The expansion (18.64) implies that the Green's function (18.63) can be expanded for small x as follows:

$$G_{12}(x; y_1, \dots, y_m) = \sum_n C_{12}^n(x) G_n(y_1, \dots, y_m), \quad (18.65)$$

where

$$G_n(y_1, \dots, y_m) = \langle \mathcal{O}_n(0) \phi(y_1) \dots \phi(y_m) \rangle, \quad (18.66)$$

and all of the dependence on x is now carried by the OPE coefficient functions. In the example of the previous section, the final amplitudes depended in a rather involved way on the small separation of the two operators, through the dependence of the coefficients in (18.61) on m_W . From the viewpoint of the operator product expansion, this dependence is carried by the coefficient functions and is determined for all matrix elements when these are computed.

In Sections 18.1 and 18.2, we used the renormalization group to compute the enhancement or suppression factors for operator matrix elements. Thus it is natural to expect that the form of the operator product coefficients is also determined by the renormalization group. We will now work out this relation. To begin, we rewrite the expansion (18.64) more precisely. The operators that appear in this relation must be defined at some renormalization scale M . Then the operator product expansion reads:

$$[\mathcal{O}_1(x)]_M [\mathcal{O}_2(0)]_M = \sum_n C_{12}^n(x; M) [\mathcal{O}_n(0)]_M. \quad (18.67)$$

Note that the coefficient functions can depend on M , since they must absorb the M -dependent operator rescalings. If we use the left-hand side of (18.67) to compute (18.63), this function obeys the Callan-Symanzik equation

$$\left[M \frac{\partial}{\partial M} + \beta \frac{\partial}{\partial g} + m\gamma + \gamma_1 + \gamma_2 \right] G_{12}(x; y_1, \dots, y_m; M) = 0. \quad (18.68)$$

Similarly, with the operator \mathcal{O}_n normalized at M , the Green's function (18.66) obeys

$$\left[M \frac{\partial}{\partial M} + \beta \frac{\partial}{\partial g} + m\gamma + \gamma_n \right] G_n(y_1, \dots, y_m; M) = 0. \quad (18.69)$$

By applying (18.68) to the right-hand side of (18.65), we see that these relations are consistent only if the OPE coefficient functions obey the Callan-Symanzik equation

$$\left[M \frac{\partial}{\partial M} + \beta \frac{\partial}{\partial g} + \gamma_1 + \gamma_2 - \gamma_n \right] C_{12}^n(x; M) = 0. \quad (18.70)$$

We now solve this equation by our standard methods. First, let us apply dimensional analysis. If the operators $\mathcal{O}_1, \mathcal{O}_2, \mathcal{O}_n$ have dimensions d_1, d_2, d_n , the coefficient function $C_{12}^n(x)$ must have the dimensions of $(\text{mass})^{d_1+d_2-d_n}$. Thus,

$$C_{12}^n(x) = \left(\frac{1}{|x|} \right)^{d_1+d_2-d_n} \tilde{C}(xM), \quad (18.71)$$

where $\tilde{C}(xM)$ is a dimensionless function. This function is determined from (18.70) according to the method of Section 12.3. Thus,

$$C_{12}^n(x) = \left(\frac{1}{|x|} \right)^{d_1+d_2-d_n} c(\bar{g}(1/x)) \exp \left[\int_{1/x}^M d \log M' (\gamma_n - \gamma_1 - \gamma_2) \right], \quad (18.72)$$

with $c(\bar{g})$ a dimensionless function of the running coupling constant at the separation scale $1/x$.

At a fixed point of the renormalization group, the γ functions would take definite values $\gamma_{j*} = \gamma_j(g_*)$. Then, the solution (18.72) can be evaluated as

$$C_{12}^n(x) = \left(\frac{1}{|x|} \right)^{d_1+d_2-d_n} c(g_*) \exp \left[\log(xM) (\gamma_{n*} - \gamma_{1*} - \gamma_{2*}) \right]. \quad (18.73)$$

Thus, in this case,

$$C_{12}^n(x) \sim \left(\frac{1}{|x|} \right)^{d_1^* + d_2^* - d_n^*}, \quad (18.74)$$

where

$$d_j^* = d_j + \gamma_j(g_*) \quad (18.75)$$

is the true scaling dimension of the operator \mathcal{O}_j at the fixed point.

For the case of an asymptotically free theory, the scaling relation is complicated in the way that we worked out in Section 18.1. In the leading order of perturbation theory, the three γ functions take the form (18.24). Then the solution of (18.72) takes the form

$$C_{12}^n(x) \sim \left(\frac{1}{|x|} \right)^{d_1+d_2-d_n} \left(\frac{\log(1/|x|^2 \Lambda^2)}{\log(M^2/\Lambda^2)} \right)^{(a_n - a_1 - a_2)/2b_0}. \quad (18.76)$$

In the example of Section 18.2, the original operators were currents with dimension 3 and $\gamma = 0$, at separation m_W^{-1} , and the final local operators had dimension 6. Thus, (18.76) does properly reproduce the dependence of (18.61) on m_W . Notice that the renormalization group dependence is less complicated for a product of currents, which have a fixed normalization independent of scale. This special case occurs often in applications of the operator product expansion.

We have written Eq. (18.70) without taking account of operator mixing. However, as we have already seen, operator mixing is often an essential part of the applications of the OPE. It is straightforward to include this effect by rewriting the analysis that leads to (18.70) using matrix-valued γ functions. For example, with operator mixing, the Callan-Symanzik equation for G_n will be modified to

$$\left[\delta_{np} \left(M \frac{\partial}{\partial M} + \beta \frac{\partial}{\partial g} + m\gamma \right) + \gamma_{np} \right] G_p(y_1, \dots, y_m; M) = 0. \quad (18.77)$$

With these changes, (18.70) becomes

$$\begin{aligned} \left[M \frac{\partial}{\partial M} + \beta \frac{\partial}{\partial g} \right] C_{12}{}^n(x; M) + \gamma_{1k} C_{k2}{}^n(x; M) \\ + \gamma_{2k} C_{1k}{}^n(x; M) - \gamma_{kn} C_{12}{}^k(x; M) = 0. \end{aligned} \quad (18.78)$$

Notice that the first two γ matrices act on the OPE coefficient from the left, while the third acts from the right. In the case of a product of currents, the first two γ matrices vanish and (18.78) simplifies to

$$\left[M \frac{\partial}{\partial M} + \beta \frac{\partial}{\partial g} \right] C_{12}{}^n(x; M) - C_{12}{}^k(x; M) \gamma_{kn} = 0. \quad (18.79)$$

This equation will play an important role in the analysis of Section 18.5.

18.4 Operator Analysis of e^+e^- Annihilation

It is not difficult to imagine that there is a connection between matrix elements in which currents are placed at short distances from one another and matrix elements in which currents deliver a hard momentum transfer. Thus we might expect that the idea of the operator product expansion will give us a new viewpoint from which to understand the theory of hard-scattering processes in QCD. In this section and the next, we will work out the relation of the operator product expansion to the perturbative QCD analysis of Chapter 17.

We begin by discussing the total cross section for e^+e^- annihilation to hadrons. Below Eq. (17.9), we argued that this total cross section could be computed in QCD perturbation theory, using a value of α_s corresponding to the scale of the total center of mass energy. However, this argument was a purely intuitive one, with many logical jumps. In this section, we will give a more rigorous argument to the same conclusion.

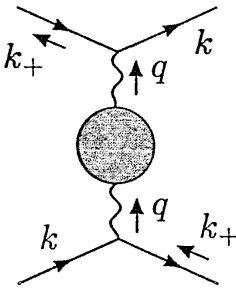


Figure 18.4. Diagrams whose imaginary part yields the total cross section for $e^+e^- \rightarrow \text{hadrons}$.

In order to invoke the operator product expansion, we must write the total cross section for e^+e^- annihilation to hadrons as the matrix element of a product of currents. To do this, we use the optical theorem to relate the total e^+e^- scattering cross section to the forward scattering amplitude for $e^+e^- \rightarrow e^+e^-$. Ignoring the mass of the electron, we see from Eq. (7.49) that

$$\sigma(e^+e^-) = \frac{1}{2s} \text{Im } \mathcal{M}(e^+e^- \rightarrow e^+e^-). \quad (18.80)$$

To compute the cross section for $e^+e^- \rightarrow \text{hadrons}$, we consider in the computation of the imaginary part only the contributions from hadronic intermediate states. To leading order in α , but to all orders in the strong interactions, these contributions come from considering only diagrams of the form of Fig. 18.4, and taking the imaginary part of the hadronic contributions to the vacuum polarization.

The value of the diagrams shown in Fig. 18.4 is

$$i\mathcal{M} = (-ie)^2 \bar{u}(k) \gamma_\mu v(k_+) \frac{-i}{s} (i\Pi_h^{\mu\nu}(q)) \frac{-i}{s} \bar{v}(k_+) \gamma_\nu u(k), \quad (18.81)$$

where $s = q^2$ and $\Pi_h^{\mu\nu}(q)$ is the hadronic part of the vacuum polarization. By the Ward identity, this can be written

$$\Pi_h^{\mu\nu}(q) = (q^2 g^{\mu\nu} - q^\mu q^\nu) \Pi_h(q^2). \quad (18.82)$$

The $q^\mu q^\nu$ terms give zero when contracted with the external electron currents, so only the $g^{\mu\nu}$ term survives. To evaluate the electron spinor part of (18.81), we use the fact that, in this forward scattering amplitude, the initial and final momenta and spins are set equal. Then, averaging over the initial spin gives

$$\begin{aligned} \frac{1}{2} \cdot \frac{1}{2} \sum_{\text{spins}} \bar{u}(k) \gamma^\mu v(k_+) \bar{v}(k_+) \gamma_\mu u(k) &= \frac{1}{4} \text{tr} [\not{k} \gamma^\mu \not{k}_+ \gamma_\mu] \\ &= \frac{1}{4} \cdot (-2) \cdot 4(k \cdot k_+) \\ &= -s. \end{aligned} \quad (18.83)$$

Thus, we find

$$\sigma(e^+e^- \rightarrow \text{hadrons}) = -\frac{4\pi\alpha}{s} \text{Im } \Pi_h(s). \quad (18.84)$$

To check this result, we can look back to the one-loop value of Π in QED (7.91), or to the imaginary part of this expression given in Eq. (7.92):

$$\text{Im } \Pi(s + i\epsilon) = -\frac{\alpha}{3} \sqrt{1 - \frac{4m^2}{s}} \left(1 + \frac{2m^2}{s}\right). \quad (18.85)$$

Combining (18.85) with (18.84), we obtain the correct leading-order cross section for production of a new heavy lepton in e^+e^- annihilation,

$$\sigma(e^+e^- \rightarrow L^+L^-) = \frac{4\pi\alpha^2}{3s} \sqrt{1 - \frac{4m^2}{s}} \left(1 + \frac{2m^2}{s}\right). \quad (18.86)$$

If we multiply (18.86) by a factor of 3 for color and sum over quark flavors with the squares of the quark charges, we obtain the leading-order prediction of QCD.

Now that we have relation (18.84), we complete the connection we wished to prove by noting that the hadronic vacuum polarization is simply a matrix element of a product of currents. Let J^μ be the electromagnetic current of quarks,

$$J^\mu = \sum_f Q_f \bar{q}_f \gamma^\mu q_f. \quad (18.87)$$

Then

$$i\Pi_h^{\mu\nu}(q) = -e^2 \int d^4x e^{iq\cdot x} \langle 0 | T\{J^\mu(x)J^\nu(0)\} | 0 \rangle. \quad (18.88)$$

In the limit in which the point x approaches 0, we can reduce the product of currents by applying the operator product expansion. Since we will be taking the vacuum expectation value of the product, we need only list the contribution from operators that are gauge-invariant Lorentz scalars. Thus,

$$J_\mu(x)J_\nu(0) \sim C_{\mu\nu}^{-1}(x) \cdot 1 + C_{\mu\nu}^{\bar{q}q}(x) \bar{q}q(0) + C_{\mu\nu}^{F^2}(x) (F_{\alpha\beta}^a)^2(0) + \dots \quad (18.89)$$

Note that we have included the operator 1 on the right-hand side, and the next possible operators in QCD have dimension 3 and 4, respectively. Since the operator $\bar{q}q$ violates chiral symmetry, its coefficient function must have an explicit factor of the quark mass. Thus, by dimensional analysis,

$$C_{\mu\nu}^{-1} \sim x^{-6}, \quad C_{\mu\nu}^{\bar{q}q} \sim mx^{-2}, \quad C_{\mu\nu}^{F^2} \sim x^{-2}, \quad (18.90)$$

and the higher terms in the series are less singular as $x \rightarrow 0$.

To compute $\Pi_h^{\mu\nu}(q)$, we need the Fourier transform of the product of currents. Assuming that this Fourier transform is indeed dominated by the limit of short distances, we can compute it by Fourier-transforming the individual OPE coefficients. Since the currents are conserved, the individual terms in the OPE must give zero when dotted with q^μ . Thus the transformed OPE takes

the form

$$\begin{aligned} -e^2 \int d^4x e^{iq \cdot x} J^\mu(x) J^\nu(0) \\ = -ie^2 (q^2 g^{\mu\nu} - q^\mu q^\nu) [c^1(q^2) \cdot 1 + c^{\bar{q}q}(q^2) \cdot m\bar{q}q + c^{F^2}(q^2) \cdot (F_{\alpha\beta}^a)^2 + \dots], \end{aligned} \quad (18.91)$$

where the c^i are Lorentz-invariant c-number functions of q^2 , and the factor of i at the beginning of the second line is inserted as a convenient convention. By dimensional analysis, we find

$$c^1 \sim (q^2)^0, \quad c^{\bar{q}q} \sim (q^2)^{-2}, \quad c^{F^2} \sim (q^2)^{-2}, \quad (18.92)$$

and the higher terms are more irrelevant for large q .

The OPE coefficients $c^i(q^2)$ can be computed from Feynman diagrams. As shown in Fig. 18.5, the coefficient of the operator 1 is the sum of diagrams with no external legs other than the current insertions. The leading QCD diagram is just the simple vacuum polarization diagram, multiplied by the color factor 3 and the sum of the squares of the quark charges. Combining these factors with Eq. (7.91), we have

$$c^1(q^2) = -\left(3 \sum_f Q_f^2\right) \cdot \frac{\alpha}{3\pi} \log(-q^2). \quad (18.93)$$

The corrections to this result are of order $\alpha_s(q^2)$. The higher coefficient functions are extracted from diagrams with more external legs. For example, the coefficient function of $(F_{\alpha\beta}^a)^2$ is determined by diagrams with two external gluon legs.

Still assuming that the Fourier transform of the product of currents can be computed from the OPE for the region of large timelike q^2 , we can complete our evaluation of the cross section for $e^+e^- \rightarrow \text{hadrons}$ by taking the vacuum expectation value of (18.91), extracting the imaginary parts of the coefficient functions, and substituting the result into (18.84). We find

$$\begin{aligned} \sigma(e^+e^- \rightarrow \text{hadrons}) = \frac{4\pi\alpha^2}{s} & [\text{Im } c^1(q^2) + \text{Im } c^{\bar{q}q}(q^2) \langle 0 | m\bar{q}q | 0 \rangle \\ & + \text{Im } c^{F^2}(q^2) \langle 0 | (F_{\alpha\beta}^a)^2 | 0 \rangle + \dots]. \end{aligned} \quad (18.94)$$

The first term of this series is just the result of summing perturbative QCD diagrams for the e^+e^- total cross section. The additional terms give corrections to this result which depend on soft hadronic matrix elements, but these corrections are explicitly suppressed at high energy by factors $(q^2)^{-2}$. (Incidentally, this expansion, which applies equally well in the absence of QCD interactions, explains why (18.86) contains no term of order s^{-2} when expanded for large s .) If we insert the leading-order expression (18.93) into (18.94), we obtain the familiar result

$$\sigma(e^+e^- \rightarrow \text{hadrons}) = \frac{4\pi\alpha^2}{s} \sum_f Q_f^2. \quad (18.95)$$

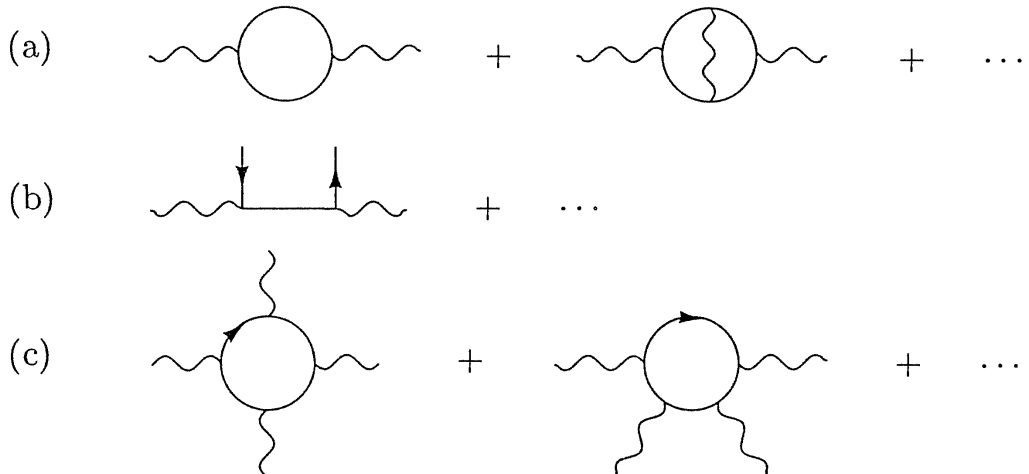


Figure 18.5. Feynman diagrams contributing the operator product coefficient, in the expansion of the product of currents, for the operator (a) 1; (b) $\bar{q}q$; (c) $(F_{\alpha\beta}^a)^2$.

Our result (18.94) is pleasing, but the logic that led us to it was not correct. To compute the e^+e^- total cross section, we must compute $\Pi_h(q^2)$ in the region of large *timelike* momentum q , where the expectation value of the product of currents is dominated by intermediate states of high energy, involving large numbers of physical hadrons. Thus we need $\Pi_h(q^2)$ in precisely the region where it is not dominated by short-distance perturbations of the quark and gluon fields. To compute the product of currents from the short-distance expansion, we choose kinematic conditions such that the intermediate states that enter the computation of the product of currents are far off-shell, so that they cannot propagate far from the converging points x and 0. This condition is satisfied at large *spacelike* momentum, or, equivalently, at small spacelike separation. However, it seems at first sight that a computation in this region is useless for determination of the e^+e^- cross section.

Fortunately, there is a wonderful trick for relating the values of a quantum field theory amplitude in two well-separated kinematic regions. This trick, called the method of *dispersion relations*, makes use of the general analytic properties of the amplitude. Since (18.88) is the Fourier transform of a two-point correlation function, we know from the analysis of Section 7.1 that $\Pi_h(q^2)$ possesses a Källén-Lehmann spectral representation. Thus, $\Pi_h(q^2)$ is an analytic function of q^2 with a branch cut on the positive q^2 axis and no other singularities in the complex q^2 plane. This analytic structure is shown in Fig. 18.6. The discontinuity of $\Pi_h(q^2)$ across the branch cut is $(2i)$ times the imaginary part of Π_h and so is directly related to the total e^+e^- annihilation cross section.

With this additional knowledge about $\Pi_h(q^2)$, we can argue as follows. Let $q^2 = -Q_0^2$ be a value sufficiently far into the spacelike region of q that the Fourier transform of the product of currents can be computed from the

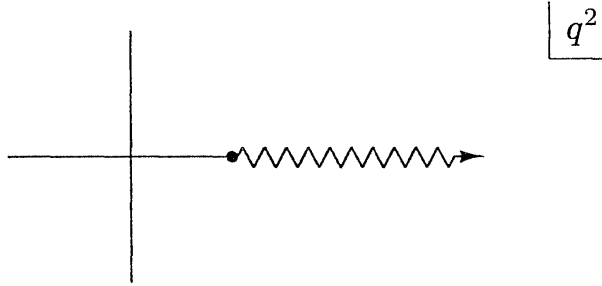


Figure 18.6. Analytic singularities of $\Pi_h(q^2)$ in the complex q^2 plane.

operator product expansion. Now consider the integral

$$I_n = -4\pi\alpha \oint \frac{dq^2}{2\pi i} \frac{1}{(q^2 + Q_0^2)^{n+1}} \Pi_h(q^2), \quad (18.96)$$

for $n \geq 1$, evaluated on a contour encircling $q^2 = -Q_0^2$. If we contract the contour onto the pole, we find

$$I_n = \frac{1}{n!} \frac{d^n}{d(q^2)^n} \Pi_h \Big|_{q^2 = -Q_0^2}, \quad (18.97)$$

which can be computed by evaluating Π_h from the the operator product relation (18.91),

$$\Pi_h(q^2) = -e^2 [c^1(q^2) + c^{\bar{q}q}(q^2) \langle 0 | m\bar{q}q | 0 \rangle + c^{F^2}(q^2) \langle 0 | (F_{\alpha\beta}^a)^2 | 0 \rangle + \dots]. \quad (18.98)$$

On the other hand, we can evaluate the integral by distorting the contour to the form of Fig. 18.7. Since none of the coefficient functions grow faster than $(q^2)^0$ times logarithms as $q^2 \rightarrow \infty$, the contour at infinity can be neglected for $n \geq 1$. The piece of the contour that wraps around the branch cut gives

$$\begin{aligned} I_n &= -4\pi\alpha \int \frac{dq^2}{2\pi i} \frac{1}{(q^2 + Q_0^2)^n} \text{Disc } \Pi_h(q^2) \\ &= -4\pi\alpha \int \frac{dq^2}{2\pi} \frac{1}{(q^2 + Q_0^2)^{n+1}} \frac{1}{i} 2i \text{Im } \Pi_h(q^2) \\ &= \frac{1}{\pi} \int_0^\infty ds \frac{s}{(s + Q_0^2)^{n+1}} \sigma(s). \end{aligned} \quad (18.99)$$

This is an integral over the total cross section for $e^+e^- \rightarrow \text{hadrons}$. By equating (18.97) and (18.99), we obtain a series of integral relations between the OPE coefficients, evaluated in QCD perturbation theory, and the observable cross section. These relations, which were first constructed by Novikov, Shifman, Voloshin, Vainshtein, and Zakharov, are known as the *ITEP sum rules*.[†]

[†]The theory of these sum rules is reviewed in V. A. Novikov, L. B. Okun, M. A. Shifman, A. I. Vainshtein, M. B. Voloshin, and V. I. Zakharov, *Phys. Repts.* **41**, 1 (1978).

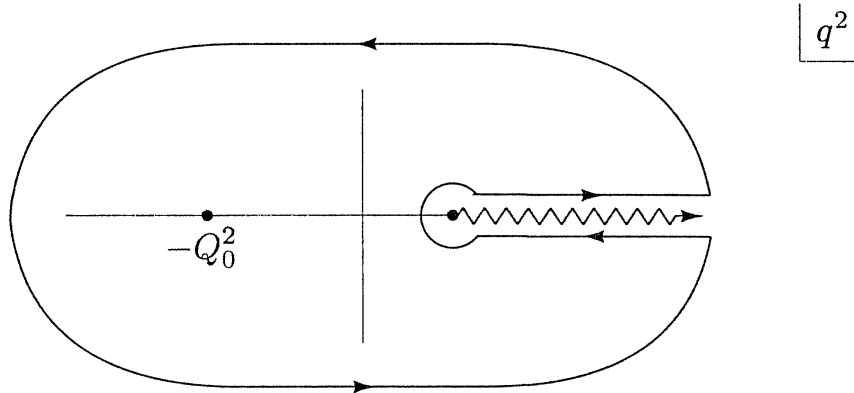


Figure 18.7. Contour of integration involved in the derivation of the ITEP sum rules for $\sigma(e^+e^- \rightarrow \text{hadrons})$.

Evaluating the sum rules with only the leading QCD expression for $c^1(q^2)$, we find

$$\int_0^\infty ds \frac{s}{(s + Q_0^2)^{n+1}} \sigma(s) = \frac{4\pi\alpha^2}{n(Q_0^2)^n} \sum_f Q_f^2 + \mathcal{O}(\alpha_s(Q_0^2)) + \mathcal{O}((Q_0^2)^{-2}). \quad (18.100)$$

The leading-order relation is consistent with the lowest-order cross section given in Eq. (18.95). The corrections come from higher orders of QCD perturbation theory, with α_s taken at the scale Q_0^2 , and from the higher operator terms in the OPE.

If the correction terms in (18.100) converged to zero uniformly in n , we could invert the sum rules and derive from them our result (18.94). However, the true situation is more subtle. Because the derivatives in (18.97) emphasize terms with stronger q^2 variation, the correction terms in the ITEP sum rules are more and more important as n increases. Thus the most important deviations of the cross section from the prediction of QCD perturbation theory are oscillations about this prediction, which average out in the sum rules for low n . The comparison of theory and experiment is shown in Fig. 18.8. At large s , (18.94) is quite accurate. As s becomes smaller, however, the oscillations grow in size. Eventually, they come to dominate the total cross section as the resonances associated with quark-antiquark bound states.

18.5 Operator Analysis of Deep Inelastic Scattering

We now apply the operator product expansion to another example of a QCD hard-scattering process, deep inelastic electron scattering. In Chapter 17 we found that the predictions of QCD for deep inelastic scattering are precise but also intricate in structure. At a first level, QCD implies that deep inelastic scattering is described by the parton model, in which the incident electron scatters from quarks and antiquarks that carry fractions of the total momentum of the proton. These fractions are determined by parton distribution

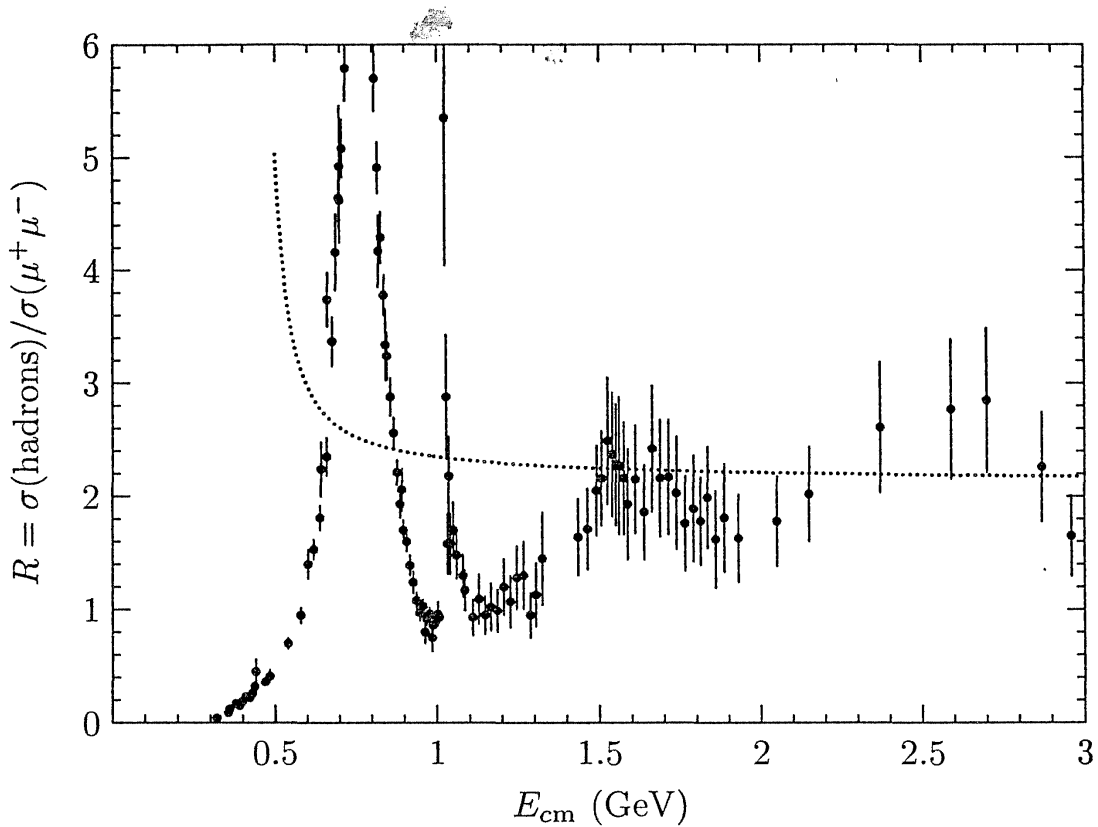


Figure 18.8. Experimental measurements of the total cross section for the reaction $e^+e^- \rightarrow \text{hadrons}$ at energies below 3 GeV, compared to the prediction of perturbative QCD for 3 quark flavors. The data are taken from the compilation of M. Swartz, *Phys. Rev. D* (to appear). Complete references to the various results are given there.

functions, which reflect the form of the proton wavefunction and are determined by soft QCD dynamics. However, we saw in Section 17.5 that effects of QCD perturbation theory cause the parton distributions to change their form as a function of the momentum transfer Q^2 . We will now show that much of this picture can be reconstructed from our new viewpoint, using the operator product expansion.

In the previous section, we derived the OPE relations for the e^+e^- annihilation cross section in three steps. First, we used the optical theorem to relate this cross section to a matrix element of a product of currents. Second, we applied the operator product expansion to the product of currents. Unfortunately, this expansion could be used only in an unphysical kinematic region. However, in the third step, we used the method of dispersion relations to connect this unphysical result to an integral over the cross section we wished to predict. In our discussion of deep inelastic scattering, we will go through these same three steps. To obtain our final result, we will need to add a fourth step, involving QCD operator rescaling.

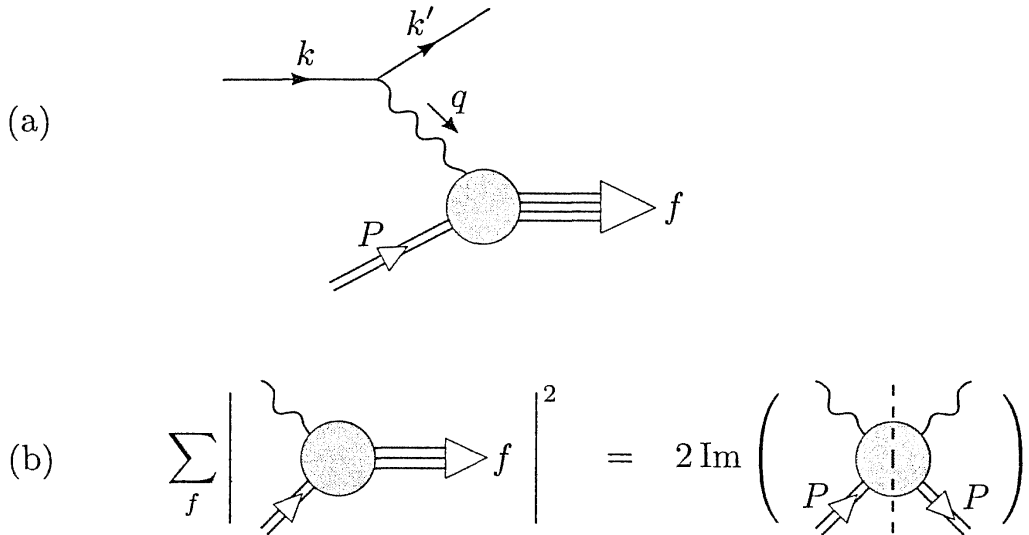


Figure 18.9. Computation of the cross section for deep inelastic electron scattering: (a) general structure of the amplitudes; (b) application of the optical theorem.

Kinematics of Deep Inelastic Scattering

We begin by writing a general expression for the deep inelastic scattering cross section. The matrix element for deep inelastic electron scattering to a final state f is computed as shown in Fig. 18.9(a):

$$i\mathcal{M}(ep \rightarrow ef) = (-ie)\bar{u}(k')\gamma_\mu u(k) \frac{-i}{q^2}(ie) \int d^4x e^{iq \cdot x} \langle f | J^\mu(x) | P \rangle, \quad (18.101)$$

where $J^\mu(x)$ is the quark electromagnetic current (18.87). The core of this expression is the hadronic matrix element of the current between the proton and some high-energy hadronic state. This matrix element must be squared and summed over possible final states. That sum can be computed, using the optical theorem, by relating it to the forward matrix element of two currents in the proton state, as shown in Fig. 18.9(b). Define

$$W^{\mu\nu} = i \int d^4x e^{iq \cdot x} \langle P | T \{ J^\mu(x) J^\nu(0) \} | P \rangle, \quad (18.102)$$

averaged over the spin of the proton. This object is known as the *forward Compton amplitude*, since if it is evaluated at $q^2 = 0$ and contracted with physical polarization vectors, it gives the forward amplitude for photon-proton scattering:

$$i\mathcal{M}(\gamma p \rightarrow \gamma p) = (ie)^2 \epsilon_\mu^*(q) \epsilon_\nu(q) (-iW^{\mu\nu}(P, q)). \quad (18.103)$$

However, in the following discussion we will need to analyze (18.102) for general spacelike q and for general polarization states.

The optical theorem for Compton scattering from a proton is

$$2 \operatorname{Im} \mathcal{M}(\gamma p \rightarrow \gamma p) = \sum_f \int d\Pi_f |\mathcal{M}(\gamma p \rightarrow f)|^2. \quad (18.104)$$

In the generalization given in (7.49), this result extends to the more general situation in which the initial and final photon polarizations can differ arbitrarily. Transcribing (18.104) to $W^{\mu\nu}$, we find

$$2 \operatorname{Im} W^{\mu\nu}(P, q) = \sum_f \int d\Pi_f \langle P | J^\mu(-q) | f \rangle \langle f | J^\nu(q) | P \rangle, \quad (18.105)$$

where $J^\mu(q)$ is the Fourier transform of the current.

We can now compute the deep inelastic cross section in terms of $W^{\mu\nu}$, using (18.105) to represent the square of the last factor. The cross section should be averaged over initial and summed over final electron spins. Thus,

$$\begin{aligned} \sigma(ep \rightarrow eX) &= \frac{1}{2s} \int \frac{d^3 k'}{(2\pi)^3} \frac{1}{2k'} e^4 \frac{1}{2} \sum_{\text{spins}} [\bar{u}(k) \gamma_\mu u(k') \bar{u}(k') \gamma_\nu u(k)] \\ &\quad \cdot \left(\frac{1}{Q^2}\right)^2 \cdot 2 \operatorname{Im} W^{\mu\nu}(P, q). \end{aligned} \quad (18.106)$$

The electron spinor product can be evaluated as

$$\begin{aligned} \frac{1}{2} \sum_{\text{spins}} [\bar{u}(k) \gamma_\mu u(k') \bar{u}(k') \gamma_\nu u(k)] &= \frac{1}{2} \operatorname{tr} [\not{k} \gamma_\mu \not{k}' \gamma_\nu] \\ &= 2(k_\mu k'_\nu + k_\nu k'_\mu - g_{\mu\nu} k \cdot k'). \end{aligned} \quad (18.107)$$

It is useful to convert the integral over the final electron momentum k' and scattering angle θ to an integral over the dimensionless variables x and y that we introduced in Section 17.3. These variables are given in terms of the initial and final electron energies k and k' by

$$x = \frac{Q^2}{2P \cdot q} = \frac{2kk'(1 - \cos\theta)}{2m(k - k')}, \quad y = \frac{2P \cdot q}{2P \cdot k} = \frac{k - k'}{k}. \quad (18.108)$$

Then

$$\left| \frac{\partial(x, y)}{\partial(k', \cos\theta)} \right| = \frac{2k'}{2m(k - k')} = \frac{2k'}{ys}, \quad (18.109)$$

and so

$$\int \frac{d^3 k'}{(2\pi)^3} \frac{1}{2k'} = \int \frac{2\pi dk' k' d\cos\theta}{(2\pi)^3 \cdot 2} = \int dx dy \frac{ys}{(4\pi)^2}. \quad (18.110)$$

Using (18.107) and (18.110) to simplify (18.106), we find

$$\frac{d^2\sigma}{dxdy}(ep \rightarrow eX) = \frac{2\alpha^2 y}{(Q^2)^2} (k_\mu k'_\nu + k_\nu k'_\mu - g_{\mu\nu} k \cdot k') \operatorname{Im} W^{\mu\nu}(P, q). \quad (18.111)$$

To go further, we need to know something about the structure of $W^{\mu\nu}$. In the previous section, we used current conservation to write the matrix element of currents in terms of a single scalar function $\Pi_h(q^2)$, as in Eq. (18.82). In

the case of the forward Compton amplitude, the Ward identity again requires

$$q_\mu W^{\mu\nu} = q_\nu W^{\mu\nu} = 0, \quad (18.112)$$

but now there are two possible tensors built from P and q that satisfy these constraints. Thus the forward Compton amplitude is written as an expression involving two scalar form factors:

$$W^{\mu\nu} = \left(-g^{\mu\nu} + \frac{q^\mu q^\nu}{q^2} \right) W_1 + \left(P^\mu - q^\mu \frac{P \cdot q}{q^2} \right) \left(P^\nu - q^\nu \frac{P \cdot q}{q^2} \right) W_2. \quad (18.113)$$

The scalar functions W_1, W_2 depend on the two invariants of the problem, $(P \cdot q)$ and q^2 , or, alternatively, x and Q^2 . If we insert (18.113) into (18.111) and use the fact that dotting q^μ with the lepton tensor gives zero, we find

$$\begin{aligned} \frac{d^2\sigma}{dxdy}(ep \rightarrow eX) &= \frac{2\alpha^2 y}{(Q^2)^2} [2k \cdot P k' \cdot P \operatorname{Im} W_2 + 2k \cdot k' \operatorname{Im} W_1] \\ &= \frac{\alpha^2 y}{Q^4} [s^2(1-y) \operatorname{Im} W_2 + 2xys \operatorname{Im} W_1]. \end{aligned} \quad (18.114)$$

Expression (18.114) is completely general and makes no assumptions about the nature of the strong interactions. It is also rather formal. However, we can easily get an idea of the relation of this formula to our earlier analysis by evaluating $W^{\mu\nu}$ in the parton model and working out the parton expressions for W_1 and W_2 . In the parton model, we replace the proton matrix element in (18.102) by a sum of quark matrix elements, weighted with the parton distribution functions. Thus,

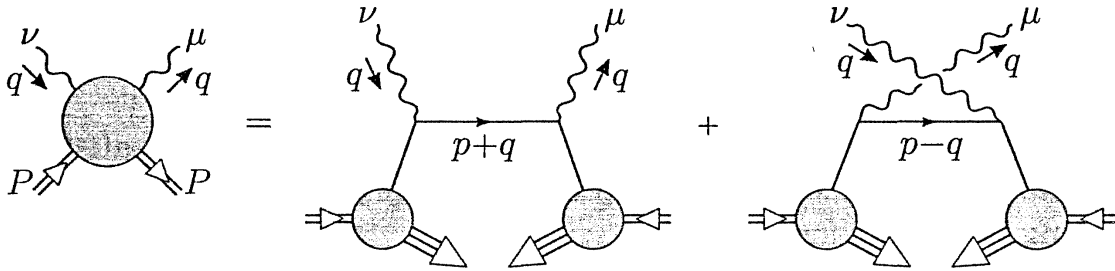
$$W^{\mu\nu} \approx i \int d^4x e^{iq \cdot x} \int_0^1 d\xi \sum_f f_f(\xi) \cdot \frac{1}{\xi} \langle q_f(p) | T \{ J^\mu(x) J^\nu(0) \} | q_f(p) \rangle \Big|_{p=\xi P}. \quad (18.115)$$

The factor $(1/\xi)$ in front of the matrix element gives the proper normalization of the proton state in terms of the quark states. The simplest way to understand this factor is to note that the kinematic prefactor $(1/2s)$ in (18.106) and in other expressions involving an initial-state proton becomes $(1/2\xi s)$, under the ξ integral, in the parton model.

We now evaluate the matrix element in (18.115) using noninteracting fermions. There are two Feynman diagrams, shown in Fig. 18.10. The first diagram on the right in Fig. 18.10 has the value

$$i \int_0^1 d\xi \sum_f f_f(\xi) \frac{1}{\xi} Q_f^2 \bar{u}(p) \gamma^\mu \frac{i(p + q)}{(p + q)^2 + i\epsilon} \gamma^\nu u(p); \quad (18.116)$$

the second diagram gives a contribution identical to this one after the interchange of q, μ with $(-q), \nu$. To evaluate (18.116), we average over the quark

Figure 18.10. Evaluation of $W^{\mu\nu}$ in the parton model.

spin to find

$$\begin{aligned}
 & \int_0^1 d\xi \sum_f f_f(\xi) \frac{1}{\xi} \cdot \frac{1}{2} \text{tr} [\not{p} \gamma^\mu (\not{p} + \not{q}) \gamma^\nu] \frac{-1}{2p \cdot q + q^2 + i\epsilon} \\
 &= \int_0^1 d\xi \sum_f f_f(\xi) \frac{1}{\xi} \cdot 2(p^\mu (p+q)^\nu + p^\nu (p+q)^\mu - g^{\mu\nu} p \cdot (p+q)) \\
 & \quad \cdot \frac{-1}{2\xi P \cdot q - Q^2 + i\epsilon}. \tag{18.117}
 \end{aligned}$$

The imaginary part of this expression, which we need to evaluate (18.114), comes from the last factor in (18.117):

$$\text{Im} \left(\frac{-1}{2\xi P \cdot q - Q^2 + i\epsilon} \right) = \pi \delta(2\xi P \cdot q - Q^2) = \frac{\pi}{ys} \delta(\xi - x). \tag{18.118}$$

In the second diagram of Fig. 18.10, the two factors in the denominator have a relative + sign, so this diagram has no imaginary part in the physical region for deep inelastic scattering. Thus, we find that in the parton model,

$$\text{Im } W^{\mu\nu} = \sum_f Q_f^2 f_f(x) \frac{1}{x} \frac{\pi}{ys} (4x^2 P^\mu P^\nu + 2x(P^\mu q^\nu + P^\nu q^\mu) - g^{\mu\nu} x y s). \tag{18.119}$$

By adding and subtracting terms proportional to $q^\mu q^\nu$, we can see that this expression is of the form (18.113), with

$$\text{Im } W_1 = \pi \sum_f Q_f^2 f_f(x), \quad \text{Im } W_2 = \frac{4\pi}{ys} \sum_f Q_f^2 x f_f(x). \tag{18.120}$$

The parton model expressions for W_1 and W_2 obey the relation

$$\text{Im } W_1 = \frac{ys}{4x} \text{Im } W_2. \tag{18.121}$$

This is another form of the Callan-Gross relation, since the substitution of (18.121) into (18.114) gives

$$\frac{d^2\sigma}{dxdy} (ep \rightarrow eX) = \frac{\alpha^2 y s^2}{2Q^4} [1 + (1-y)^2] \text{Im } W_2, \tag{18.122}$$

with the y dependence characteristic of free fermions, as in Eq. (17.125). Finally, substituting from (18.120) for the imaginary part of W_2 , we recover this parton model expression precisely:

$$\frac{d^2\sigma}{dxdy}(ep \rightarrow eX) = \frac{2\pi\alpha^2 s}{Q^4} \left(\sum_f Q_f^2 x f_f(x) \right) [1 + (1 - y)^2]. \quad (18.123)$$

This equation will give us a reference point for comparison with more general expressions that we will derive as we continue our analysis.

Expansion of the Operator Product

Since the forward Compton amplitude is a matrix element of a product of currents, an alternative strategy for calculating $W^{\mu\nu}$ is to expand this product as a series of local operators. Like the parton model evaluation, this method makes use of asymptotic freedom. However, in this case, the assumption is applied more directly. The computation of the operator product coefficients will take place explicitly at a small distance of order $1/Q$, and so we can calculate these coefficients in a perturbation theory whose coupling constant is $\alpha_s(Q^2)$.

In the previous section, we computed the coefficients of operators that contribute to the vacuum expectation value of the product of currents by considering the various ways of contracting the quark fields in the product. Here, we should note that the operator 1 does not contribute to the Compton scattering amplitude. The leading contributions come from operators that can create and annihilate quarks in the proton wavefunction.

The most important terms in the operator product of two currents J^μ come from products of two quark currents $\bar{q}_f \gamma^\mu q_f$ with quarks of the same flavor. Therefore we will begin by studying the OPE of the individual quark currents. To zeroth order in α_s , the leading terms of the operator product of quark currents are given by

$$\begin{aligned} & \bar{q} \gamma^\mu q(x) \bar{q} \gamma^\nu q(0) \\ &= \bar{q}(x) \gamma^\mu \overbrace{q(x) \bar{q}(0)} \gamma^\nu q(0) + \overbrace{\bar{q}(x) \gamma^\mu q(x) \bar{q}(0)} \gamma^\nu q(0) + \dots, \end{aligned} \quad (18.124)$$

where the contractions should be evaluated as Feynman propagators for the quark fields. The terms with explicit contractions are singular as $x \rightarrow 0$; the remaining terms are nonsingular and thus less important in the short-distance limit. In the OPE of currents with quarks of different flavor, there are no corresponding singular terms; we will argue below that this conclusion is valid even beyond the leading order in α_s .

To evaluate $W^{\mu\nu}$, we must take the Fourier transform of the terms in (18.124), as indicated in (18.102). When we do this, we should remember that the propagators carry not only the Fourier transform momentum q but also whatever momentum is carried in through the quark fields. To take account

of this, it is convenient to represent

$$\int d^4x e^{iq \cdot x} \bar{q}(x) \gamma^\mu \overline{q(x) \bar{q}(0)} \gamma^\nu q(0) = \bar{q} \gamma^\mu \frac{i(i\partial + q)}{(i\partial + q)^2} \gamma^\nu q(0), \quad (18.125)$$

where the derivatives ∂ act to the right on the quark field. Notice that this contribution has the structure of the first diagram on the right in Fig. 18.10. Similarly, the second contraction indicated in (18.124) has the form of the second diagram in Fig. 18.10.

In the short-distance limit, the momentum q will be larger than any external momentum entering the quark fields. Thus we should expand

$$\frac{1}{(i\partial + q)^2} = \frac{-1}{Q^2 - 2iq \cdot \partial + \partial^2} = -\frac{1}{Q^2} \sum_{n=0}^{\infty} \left(\frac{2iq \cdot \partial - \partial^2}{Q^2} \right)^n. \quad (18.126)$$

We will argue below that the terms with ∂^2 in the numerator are unimportant and may be dropped. However, we should retain all powers of the ratio $(2iq \cdot \partial / Q^2)$. This ratio has Q^2 in the denominator and so is formally suppressed in the short-distance limit. However, in the parton model

$$\frac{2iq \cdot \partial}{Q^2} \rightarrow \frac{2q \cdot \xi P}{Q^2} = 1, \quad (18.127)$$

so, eventually, all of these terms must be equally important. We will see how this works in a moment.

The last step required to reduce the operator product (18.124) to a useful form is to reduce the product of Dirac matrices. We know from (18.113) that, after we average over the proton spin, $W^{\mu\nu}$ will be symmetric under the interchange of μ and ν . Thus, it does no harm to symmetrize the OPE. We can then reduce the product of three Dirac matrices to one by using the identity

$$\frac{1}{2} (\gamma^\mu \gamma^\alpha \gamma^\nu + \gamma^\nu \gamma^\alpha \gamma^\mu) = g^{\mu\alpha} \gamma^\nu + \gamma^\mu g^{\alpha\nu} - g^{\mu\nu} \gamma^\alpha, \quad (18.128)$$

which is easily proved from the anticommutation relations. By the use of (18.126) and (18.128), we can rewrite (18.125) as

$$-i\bar{q} \left(\gamma^\mu (i\partial^\nu) + \gamma^\nu (i\partial^\mu) - ig^{\mu\nu} \not{\partial} + \gamma^\mu q^\nu + \gamma^\nu q^\mu - g^{\mu\nu} \not{q} \right) \frac{1}{Q^2} \sum_{n=0}^{\infty} \left(\frac{2iq \cdot \partial}{Q^2} \right)^n q. \quad (18.129)$$

We can remove the term $(i\not{\partial})q$, which vanishes to leading order in α_s , since the quark field obeys the Dirac equation. To compute W_1 and W_2 , we can also drop the terms with explicit factors of q^μ , since these will eventually be organized into the general form (18.113). Then, finally, (18.125) takes the form

$$\begin{aligned} & \int d^4x e^{iq \cdot x} \bar{q}(x) \gamma^\mu q(x) q(0) \gamma^\nu q(0) \\ &= -i\bar{q} (2\gamma^\mu (i\partial^\nu) - g^{\mu\nu} \not{q}) \frac{1}{Q^2} \sum_{n=0}^{\infty} \left(\frac{2iq \cdot \partial}{Q^2} \right)^n q, \end{aligned} \quad (18.130)$$

symmetrized under $\mu \leftrightarrow \nu$.

The second term in (18.124) differs from the first by the interchange of the points x and 0 and the interchange of indices μ and ν . Its Fourier transform is thus given by (18.130) with the replacement $q \rightarrow -q$. The complete operator product therefore contains only terms even in q . All remaining contributions from the singular terms of the operator product contain the operator

$$\bar{q} \gamma^{\mu_1} (i\partial^{\mu_2}) \cdots (i\partial^{\mu_k}) q, \quad (18.131)$$

with an even number of indices, with these indices either identified with μ or ν or contracted with powers of q . To write the relevant terms of the operator product expansion, we will modify this operator in two ways. First, since the operator in (18.131) has n vector indices, it contains components that transform under many different irreducible representations of the Lorentz group. Each component has a different rescaling law under renormalization. However, we will see below that only the component of (18.131) with the highest spin is relevant to our analysis. This component is obtained by totally symmetrizing the indices μ_1, \dots, μ_n and then subtracting terms proportional to $g^{\mu_i \mu_j}$ so that the operator is traceless on all pairs of indices. We will retain only this component when we write out the operator product of currents. Second, the operator (18.131) does not transform simply under gauge transformations. Since the original currents J^μ were invariant to color gauge transformations, the operator product of two currents must be a sum of gauge-invariant operators. We can make (18.131) gauge-invariant by replacing each factor of $(i\partial^\mu)$ with a covariant derivative (iD^μ) . This modification adds only terms proportional to the strong coupling constant g , so it has no effect on our derivation of the operator product coefficients.

Incorporating these changes, let us define a spin- n operator with quarks of flavor f as follows:

$$\mathcal{O}_f^{(n)\mu_1 \cdots \mu_n} = \bar{q}_f \gamma^{\{\mu_1} (iD^{\mu_2}) \cdots (iD^{\mu_n\}}) q_f - \text{traces}, \quad (18.132)$$

with indices symmetrized and with appropriate subtractions. We can use these operators to write a final expression for the most singular part of the OPE of two currents J^μ . The leading terms in this operator product come from (18.130) and the corresponding contraction with $q \leftrightarrow -q$. Extracting the pieces of these expressions that contain the highest spin operators (18.132), we find

$$\begin{aligned} i \int d^4 x e^{iq \cdot x} J^\mu(x) J^\nu(0) \\ = \sum_f Q_f^2 \left[4 \sum_{n=2}^{\infty} \frac{(2q^{\mu_1}) \cdots (2q^{\mu_{n-2}})}{(Q^2)^{n-1}} \mathcal{O}_f^{(n)\mu\nu\mu_1 \cdots \mu_{n-2}} \right. \\ \left. - g^{\mu\nu} \sum_{n=2}^{\infty} \frac{(2q^{\mu_1}) \cdots (2q^{\mu_n})}{(Q^2)^n} \mathcal{O}_f^{(n)\mu_1 \cdots \mu_n} \right] + \dots \end{aligned} \quad (18.133)$$

where the sums over n run over even integers only.

Expression (18.133) has been derived in the leading order in α_s . Higher-order Feynman diagrams will contribute corrections to the coefficient functions of order $\alpha_s(Q^2)$. These corrections will be important only if they are multiplied by large logarithms. If we consider the operators $\mathcal{O}_f^{(n)}$ appearing on the right-hand side to be normalized at the renormalization scale Q , there is no large ratio of momenta available to enhance the QCD corrections to the coefficient functions. Large logarithmic corrections may still arise at a later stage of the calculation, when we compute the matrix elements of the operators $\mathcal{O}_f^{(n)}$.

From the expansion (18.133), it is straightforward to compute an expansion for $W^{\mu\nu}$ by taking its expectation value in the proton state. To carry out this computation, we need to know the proton matrix elements of the operators $\mathcal{O}_f^{(n)}$. Notice that these matrix elements cannot depend on the direction of the momentum q^μ , since that dependence has been isolated in the coefficient functions. This means that only the proton momentum P^μ is available to carry the vector indices of the matrix element. We can therefore write the spin-averaged matrix element of $\mathcal{O}_f^{(n)}$ as

$$\langle P | \mathcal{O}_f^{(n)\mu_1 \dots \mu_n} | P \rangle = A_f^n \cdot 2P^{\mu_1} \dots P^{\mu_n} - \text{traces.} \quad (18.134)$$

The coefficients A_f^n are dimensionless. They are not quite pure numbers, because they depend on the renormalization scale of the operators, but we will treat them as constants in the next few paragraphs.

For the case $n = 1$, the operators $\mathcal{O}_f^{(1)}$ reduce simply to the quark flavor currents $\bar{q}\gamma^\mu q$; in this case the operators are normalized independently of any scale and the coefficients A_f^1 are truly constants. From our general discussion of form factors in Section 6.2, we know that the proton matrix element of a conserved flavor current at zero momentum transfer is given by

$$\langle P | \bar{q}_f \gamma^\mu q_f | P \rangle = \bar{u}(P) \gamma^\mu u(P) F_{f1}(0), \quad (18.135)$$

where $F_{f1}(0)$ is equal to the value of the corresponding conserved charge in the proton state. For the quark currents, this charge is just the number of quarks (minus antiquarks) of flavor f in the state $|P\rangle$, which we will call N_f . Averaging (18.135) over the proton spin, we find

$$\langle P | \bar{q}_f \gamma^\mu q_f | P \rangle = 2P^\mu \cdot N_f. \quad (18.136)$$

Thus, for $n = 1$,

$$A_f^1 = N_f = \begin{cases} 2 & f = u, \\ 1 & f = d. \end{cases} \quad (18.137)$$

Similarly, $\mathcal{O}_f^{(2)}$ is the contribution of the quark flavor f to the energy-momentum tensor of QCD:

$$(T^{\mu\nu})_f = \bar{q}_f \gamma^{\{\mu} (iD^{\nu\}}) q_f. \quad (18.138)$$

Thus, A_f^2 is the fraction of the total energy-momentum of the proton that is carried by the quark flavor f .

When we evaluate the series for $W^{\mu\nu}$ using (18.133) and the expression (18.134) for the operator matrix elements, we find

$$W^{\mu\nu} = \sum_f Q_f^2 \left[8 \sum_n P^\mu P^\nu \frac{(2q \cdot P)^{n-2}}{(Q^2)^{n-1}} A_f^n - 2g^{\mu\nu} \sum_n \frac{(2q \cdot P)^n}{(Q^2)^n} A_f^n \right] + \dots, \quad (18.139)$$

where the sums over n run over even integers from 2 to infinity. In addition to the corrections to the OPE omitted in (18.133), we have also dropped contributions from the trace terms in (18.134). This is quite appropriate: In each of these terms, two factors of the proton momentum $P^\alpha P^\beta$ are replaced by $g^{\alpha\beta} m_p^2$, where $m_p^2 = P^2$ is the proton mass. When the indices are contracted with powers of q , we obtain a term of order

$$m_p^2 Q^2 \ll (2q \cdot P)^2. \quad (18.140)$$

Since $(Q^2/2P \cdot q) = x$, which is held fixed in deep inelastic scattering as Q^2 becomes large, the contribution from the trace terms is suppressed by a factor m_p^2/Q^2 , times powers of x .

In general, an operator of dimension d has a coefficient function in the operator product expansion of currents that has dimension $(\text{mass})^{6-d}$; in the Fourier transform of the OPE, this coefficient function will carry a suppression factor

$$\left(\frac{1}{Q}\right)^{d-2}. \quad (18.141)$$

However, if the operator has spin s , the operator matrix element will contribute s factors of the vector P^μ , so that, in the kinematic region of deep inelastic scattering, the contribution will be of order

$$\left(\frac{2P \cdot q}{Q^2}\right)^s \left(\frac{1}{Q}\right)^{d-s-2}. \quad (18.142)$$

Thus, the relative size of contributions from the OPE to deep inelastic scattering is controlled, not exactly by the dimension of the operator, but rather by the *twist*, defined as

$$t = d - s. \quad (18.143)$$

In our selection of the leading terms in the operator product expansion of currents, we have consistently kept the contribution of leading spin for each dimension or for each power of Q^{-1} in the coefficient. The operators $\mathcal{O}_f^{(n)}$ all have twist $t = 2$, which is the smallest possible value for QCD operators other than the operator 1.

In the operator product of two different flavor currents—for example, $\bar{u}\gamma^\mu u$ and $\bar{d}\gamma^\nu d$ —the leading terms in the OPE have the quark structure $(\bar{u}\Gamma u \bar{d}\Gamma d)$ and thus have twist $t \geq 4$. Thus, to all orders in α_s , the cross terms in the operator product of currents J^μ are suppressed by at least a factor

$(1/Q^2)$ relative to the leading-twist terms presented in (18.133). If we neglect these suppressed terms, the expression for $W^{\mu\nu}$ separates, to all orders, into a sum of contributions

$$W^{\mu\nu} = \sum_f Q_f^2 W_f^{\mu\nu}, \quad (18.144)$$

where $W_f^{\mu\nu}$ is the matrix element of two quark flavor currents $\bar{q}_f \gamma^\mu q_f$.

We can read from (18.139) the following expressions for W_1 and W_2 :

$$\begin{aligned} W_1 &= \sum_f Q_f^2 \sum_n 2 \frac{(2q \cdot P)^n}{(Q^2)^n} A_f^n, \\ W_2 &= \sum_f Q_f^2 \sum_n \frac{8}{Q^2} \frac{(2q \cdot P)^{n-2}}{(Q^2)^{n-2}} A_f^n, \end{aligned} \quad (18.145)$$

where the sum over n in each line runs over even integers from 2 to infinity. Like (18.139), these expressions explicitly separate according to (18.144). It is noteworthy that the series (18.145) satisfy the Callan-Gross relation in the form (18.121), without further parton model input. However, this relation is corrected in order α_s due to the next-order contributions to the operator product coefficients.

Because the leading contributions to the deep inelastic form factors can be written as sums over quark flavors, it is tempting to reverse the logic of Eq. (18.120) and use these equations to define the parton distribution functions. In particular, let us define

$$x f_f^+(x, Q^2) = \frac{ys}{4\pi} \text{Im } W_{2f}(x, Q^2), \quad (18.146)$$

where W_{2f} is the second form factor of $W_f^{\mu\nu}$, defined in (18.144), neglecting terms suppressed by powers of Q^2 . In the parton model evaluation,

$$f_f^+(x) = f_f(x) + f_{\bar{f}}(x). \quad (18.147)$$

From (18.123) and the definition (18.146), we know that $f_f^+(x)$ enters in the correct way into the formula for the deep inelastic scattering cross section. However, parton distribution functions have other important properties, including the normalization conditions (17.36) and (17.39) and the evolution with Q^2 discussed in Section 17.6. We must now see whether we can derive these properties from (18.146) using the operator product expansion.

The Dispersion Integral

The operator product analysis has given us explicit expressions for W_1 and W_2 as a series in inverse powers of Q^2 . In the following discussion, we will concentrate on the analysis of W_2 . We must work out the relation of its series expansion to the observable deep inelastic scattering cross section. As in the discussion of Section 18.4, the OPE analysis naturally takes place in an unphysical kinematic region. To make the operator product expansion, we

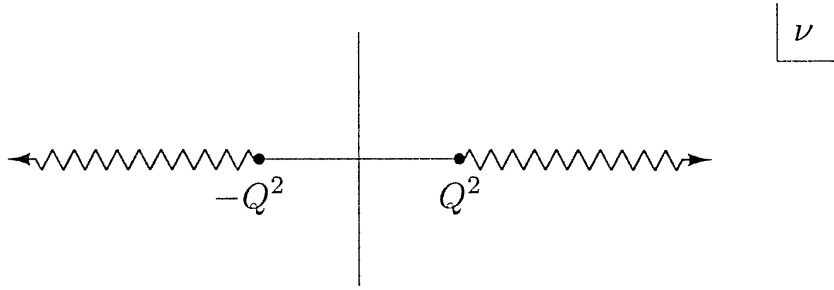


Figure 18.11. Analytic singularities of $W_2(\nu, Q^2)$ in the complex ν plane, for fixed Q^2 .

needed to consider Q^2 to be larger than any other kinematic invariant. However, in the physical region for deep inelastic scattering, $2P \cdot q \geq Q^2$. We need a formula that connects these two distinct regions.

To state this problem more precisely, define

$$\nu = 2P \cdot q = ys; \quad (18.148)$$

in the frame in which the proton is at rest, $\nu = 2m_p q^0$. The form factor W_2 can be viewed as a function of ν and Q^2 . Then, for fixed Q^2 , the OPE gives a series expansion about the point $\nu = 0$, while the physical region for deep inelastic scattering is $\nu \geq Q^2$. Because this region is associated with a physical scattering process, $W_2(\nu, Q^2)$, viewed as an analytic function of ν for fixed Q^2 , will have a branch cut along the real ν axis in this region. The discontinuity across this branch cut will be $(2i)$ times the imaginary part of W_2 , which appears in the expression (18.123) for the deep inelastic cross section. Because expression (18.102) is symmetric under the interchange of (q, μ) and $(-q, \nu)$, W_2 must obey

$$W_2(-\nu, Q^2) = W_2(\nu, Q^2). \quad (18.149)$$

Thus, W_2 must also have a branch cut along the negative real axis, from $\nu = -Q^2$ to $-\infty$. The discontinuity across this cut gives the cross section for the u -channel process in which positive energy comes in through the second current and out through the first. Since $q^2 = -Q^2 < 0$, there is no possible physical t -channel process; thus W_2 has no further singularities in the complex ν plane. The analytic structure of $W_2(\nu, Q^2)$ is shown in Fig. 18.11.

Now consider the contour integral

$$I_n = \int \frac{d\nu}{2\pi i} \frac{1}{\nu^{n-1}} W_2(\nu, Q^2), \quad (18.150)$$

for n even, taken on a small circle surrounding the origin. This integral picks out the coefficient of ν^{n-2} in the series expansion for W_2 . The OPE formula (18.145) gives us the leading contribution to this coefficient for large Q^2 :

$$I_n = \sum_f Q_f^2 \frac{8}{(Q^2)^{n-1}} A_f^n. \quad (18.151)$$

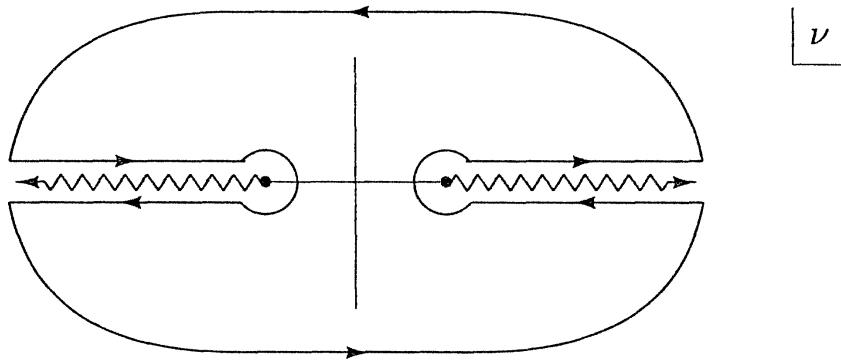


Figure 18.12. Contour of integration involved in the derivation of the moment sum rules for W_2 .

The corrections to this formula are of order $\alpha_s(Q^2)$, from the evaluation of the OPE coefficient functions.

On the other hand, we can also distort the contour as shown in Fig. 18.12 and evaluate it as an integral over the discontinuities of W_2 . By the symmetry (18.149), the two branch cuts give equal contributions. Thus,

$$I_n = 2 \int_{Q^2}^{\infty} \frac{d\nu}{2\pi i} \frac{1}{\nu^{n-1}} (2i) \operatorname{Im} W_2(\nu, Q^2). \quad (18.152)$$

Now change variables to $x = Q^2/\nu$. The integral becomes

$$I_n = \frac{8}{(Q^2)^{n-1}} \int_0^1 dx x^{n-2} \frac{\nu}{4\pi} \operatorname{Im} W_2. \quad (18.153)$$

When we equate (18.151) and (18.153) and relate $\operatorname{Im} W_2$ to the parton distributions $f_f^+(x)$ using (18.146), the relation we have derived splits into a series of sum rules,

$$\int_0^1 dx x^{n-1} f_f^+(x, Q^2) = A_f^n, \quad (18.154)$$

for n even. These relations are known as the *moment sum rules* for the deep inelastic form factors. They relate the x moments of the parton distribution functions, as defined by Eq. (18.146), to the proton matrix elements of twist-2 operators.

Because W_2 is a symmetric function of ν , the moment sum rules apply only for even n . However, in deep inelastic neutrino scattering, there is a third form factor in $W^{\mu\nu}$, associated with the interference term between the vector and axial vector parts of the weak interaction current. In Problem 18.2, we show that this form factor can be used to derive a set of sum rules for odd n :

$$\int_0^1 dx x^{n-1} f_f^-(x, Q^2) = A_f^n, \quad (18.155)$$

where A_f^n is the coefficient of the proton matrix element (18.134) for odd n , and $f_f^-(x)$ is a form factor which, in the parton model, evaluates to

$$f_f^-(x) = f_f(x) - f_{\bar{f}}(x). \quad (18.156)$$

Combining this information with the argument given below (18.136), we can see that the definition of the parton distribution functions from the deep inelastic form factors has the correct normalization. Using (18.137), we find

$$\int_0^1 dx f^-(x) = N_f, \quad (18.157)$$

the (net) number of quarks of flavor f in the proton. Similarly, (18.154) and (18.138) imply

$$\int_0^1 dx x f^+(x) = \langle x \rangle_f, \quad (18.158)$$

where $\langle x \rangle_f$ is the fraction of the total energy-momentum of the proton carried by quarks and antiquarks of flavor f .

Operator Rescaling

If the coefficients A_f^n were truly constants, relations (18.154) and (18.155) would be consistent with parton distribution functions that satisfy Bjorken scaling. However, as we remarked below (18.134), these factors actually depend on Q^2 , since this is the normalization point of the operators in the operator product expansion (18.133). Since this dependence comes only through operator rescaling, it involves only logarithms of Q^2 , and so contributes only a slow violation of Bjorken scaling. We can work out the Q^2 dependence of the parton distribution functions quantitatively by summing the leading logarithmic corrections to the matrix elements of the twist-2 operators.

To account for these corrections, let us first assume (incorrectly, as we will see below) that the twist-2 operators (18.132) are renormalized without operator mixing. Then the leading logarithmic corrections to the matrix element of the operator $\mathcal{O}_f^{(n)}$ would be summed by rescaling the operator normalized at Q to operators normalized at a standard reference point μ , of order 1 GeV. The relation between these conventions would be

$$[\mathcal{O}_f^{(n)}]_Q = \left(\frac{\log(Q^2/\Lambda^2)}{\log(\mu^2/\Lambda^2)} \right)^{a_f^n/2b_0} [\mathcal{O}_f^{(n)}]_\mu, \quad (18.159)$$

where a_f^n is the first coefficient of the γ function of $\mathcal{O}_f^{(n)}$. Then the factors A_f^n would depend on Q^2 according to

$$A_f^n(Q^2) = \left(\frac{\log(Q^2/\Lambda^2)}{\log(\mu^2/\Lambda^2)} \right)^{a_f^n/2b_0} A_f^n(\mu^2). \quad (18.160)$$

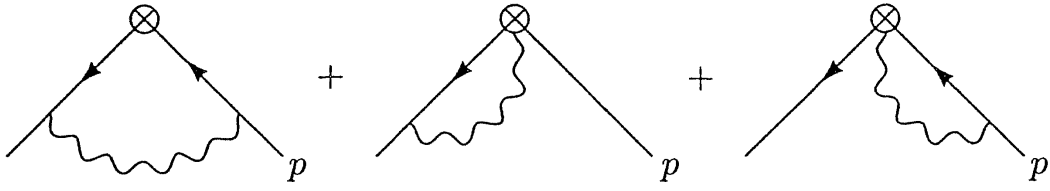


Figure 18.13. Diagrams contributing the anomalous dimension of the quark twist-2 operators.

This equation agrees with the scale dependence of operator product coefficients written in (18.76), for the special case of an operator product of currents, $a_1 = a_2 = 0$. To find the explicit form of the rescaling factor, we must compute a_f^n .

To compute the γ functions of the quark twist-2 operators, we must compute their counterterms for operator rescaling. These are determined by the diagrams shown in Fig. 18.13. It suffices to compute these diagrams with external momentum p entering through the quark line and zero external momentum injected into the operator. Under these conditions, the matrix element of the operator $\mathcal{O}_f^{(n)}$, in leading order, equals

$$\text{Diagram: } \text{a wavy line entering a vertex with a circle containing a cross (operator) and a straight line leaving. The straight line has an arrow pointing down and to the right. The wavy line is labeled 'p' at the vertex.} = \gamma^{\mu_1} p^{\mu_2} \cdots p^{\mu_n}. \quad (18.161)$$

Here and at all later points in the discussion, we will treat the matrix elements of $\mathcal{O}_f^{(n)}$ as though they are symmetrized in the n indices and have all possible traces subtracted. We must now evaluate the diagrams of Fig. 18.13 and collect all terms that rescale this structure.

The first diagram of Fig. 18.13 is quite straightforward to evaluate:

$$\begin{aligned} \text{Diagram: } \text{a wavy line entering a vertex with a circle containing a cross (operator) and a straight line leaving. The straight line has an arrow pointing down and to the right. The wavy line is labeled 'k' at the vertex.} &= \int \frac{d^4 k}{(2\pi)^4} (ig)^2 \gamma^\lambda t^a \frac{i k^\mu}{k^2} \gamma^{\mu_1} k^{\mu_2} \cdots k^{\mu_n} \frac{i k^\nu}{k^2} \gamma_\nu t^a \frac{-i}{(k-p)^2} \\ &= -ig^2 C_2(r) \cdot (-2) \int \frac{d^4 k}{(2\pi)^4} \frac{1}{(k^2)^2 (k-p)^2} k^\mu \gamma^{\mu_1} k^{\mu_2} \cdots k^{\mu_n} k^\nu. \end{aligned} \quad (18.162)$$

We combine denominators using identity (6.40):

$$\frac{1}{(k^2)^2 (k-p)^2} = \int_0^1 dx \frac{2(1-x)}{(k^2 - \Delta)^3}; \quad (18.163)$$

the quantities in the denominator on the right are $k = k - xp$ and $\Delta = -x(1-x)p^2$. We must now shift the integral, substitute $k = k + xp$ in the numerator, and pick out a term proportional to $(n-1)$ powers of p . If this term contains the factor $g^{\mu_i \mu_j}$, we may drop it, since it contributes to the coefficient of an operator of higher twist and since, in any event, it will be removed when we subtract traces. Thus, we must choose carefully which two factors of k we replace with k when we replace the others with (xp) . The

following choices, simplified using the rotational symmetry of the \mathbf{k} integral, do not give useful contributions:

$$\begin{aligned} \mathbf{k}^{\mu_i} \mathbf{k}^{\mu_j} &= \frac{1}{4} \mathbf{k}^2 g^{\mu_i \mu_j}, \\ \not{k} \gamma^{\mu_1} \mathbf{k}^{\mu_j} &\rightarrow \frac{1}{4} \mathbf{k}^2 \gamma^{\mu_j} \gamma^{\mu_1} = \frac{1}{4} \mathbf{k}^2 g^{\mu_1 \mu_j}. \end{aligned} \quad (18.164)$$

In the second line, we have used the symmetry under $\mu_1 \leftrightarrow \mu_j$. The one remaining placement of the factors of \mathbf{k} is

$$\not{k} \gamma^{\mu_1} \not{k} \rightarrow \frac{1}{4} \mathbf{k}^2 \gamma^\nu \gamma^{\mu_1} \gamma_\nu = -\frac{1}{2} \mathbf{k}^2 \gamma^{\mu_1}. \quad (18.165)$$

Thus (18.162) has the value

$$\begin{aligned} \text{Diagram: } &= -ig^2 \frac{4}{3} \int_0^1 dx \cdot 2(1-x) \int \frac{d^4 k}{(2\pi)^4} \frac{\mathbf{k}^2}{(\mathbf{k}^2 - \Delta)^3} \gamma^{\mu_1} (xp^{\mu_2}) \cdots (xp^{\mu_n}) \\ &= -i \frac{8}{3} g^2 \int_0^1 dx (1-x) x^{n-1} \frac{i}{(4\pi)^2} \Gamma(2 - \frac{d}{2}) \gamma^{\mu_1} p^{\mu_2} \cdots p^{\mu_n} \\ &= \frac{4}{3} \frac{2}{n(n+1)} \frac{g^2}{(4\pi)^2} \Gamma(2 - \frac{d}{2}) \gamma^{\mu_1} p^{\mu_2} \cdots p^{\mu_n}. \end{aligned} \quad (18.166)$$

It is not so obvious that there are additional contributions to the rescaling of the operators $\mathcal{O}_f^{(n)}$. Note, however, that the covariant derivatives in (18.132) contain explicit factors of the gauge field,

$$iD^{\mu_j} = i\partial^{\mu_j} - gA^{a\mu_j}t^a, \quad (18.167)$$

and these may be contracted with gauge field vertices on the external legs. These contributions give rise to the second and third diagrams in Figure 18.13. The term in which two factors of $A^{a\mu}$ from (18.167) are contracted with one another is proportional to $G^{\mu_i \mu_j}$ and thus does not contribute to the rescaling of the leading-twist operators.

The contributions we have just described have the form of sums over j , where μ_j is the index of the derivative that includes the contraction. Then the second diagram of Fig. 18.3 is the sum over j of the following integral:

$$\begin{aligned} \text{Diagram: } &= \int \frac{d^4 k}{(2\pi)^4} (ig) \gamma_\lambda t^a \frac{i \not{k}}{k^2} \gamma^{\mu_1} k^{\mu_2} \cdots k^{\mu_{j-1}} \\ &\quad \cdot (-gt^a g^{\lambda \mu_j}) p^{\mu_{j+1}} \cdots p^{\mu_n} \frac{-i}{(k-p)^2} \\ &= ig^2 C_2(r) \int \frac{d^4 k}{(2\pi)^4} \frac{1}{k^2 (k-p)^2} \gamma^{\mu_j} \not{k} \gamma^{\mu_1} k^{\mu_2} \cdots k^{\mu_{j-1}} p^{\mu_{j+1}} \cdots p^{\mu_n}. \end{aligned} \quad (18.168)$$

Since μ_j and μ_1 are symmetrized, we can use (18.128) to rewrite

$$\begin{aligned}\gamma^{\mu_j} k \gamma^{\mu_1} &\rightarrow k^{\mu_j} \gamma^{\mu_1} + \gamma^{\mu_j} k^{\mu_1} - g^{\mu_j \mu_1} k \\ &\rightarrow 2\gamma^{\mu_1} k^{\mu_j},\end{aligned}\quad (18.169)$$

where, in the second line, the symmetrization of indices and subtraction of traces is understood. Now combine denominators. To obtain a term with $(n-1)$ factors of p , we must replace every factor k in the numerator of (18.168) with (xp) . This gives

$$\begin{aligned}\text{Diagram with a wavy line and a circle with a cross} &= ig^2 \frac{4}{3} \int_0^1 dx \int \frac{d^4 k}{(2\pi)^4} \frac{1}{(k^2 - \Delta)^2} 2\gamma^{\mu_1} (xp^{\mu_2}) \cdots (xp^{\mu_j}) p^{\mu_{j+1}} \cdots p^{\mu_n} \\ &= ig^2 \frac{8}{3} \int_0^1 dx x^{j-1} \frac{i}{(4\pi)^2} \Gamma(2 - \frac{d}{2}) \gamma^{\mu_1} p^{\mu_2} \cdots p^{\mu_n} \\ &= -\frac{4}{3} \frac{2}{j} \frac{g^2}{(4\pi)^2} \Gamma(2 - \frac{d}{2}) \gamma^{\mu_1} p^{\mu_2} \cdots p^{\mu_n}.\end{aligned}\quad (18.170)$$

This contribution must be summed over j from 2 to n . The third diagram of Fig. 18.13 makes an equal contribution.

Summing the rescaling factors from the three diagrams of Fig. 18.13, we find for the operator rescaling counterterm of $\mathcal{O}_f^{(n)}$

$$\delta_f = \frac{g^2}{(4\pi)^2} \frac{4}{3} \left[4 \sum_{j=2}^n \frac{1}{j} - \frac{2}{n(n+1)} \right] \frac{\Gamma(2 - \frac{d}{2})}{(M^2)^{2-d/2}}. \quad (18.171)$$

From this result, we can derive the Callan-Symanzik γ function by the use of (18.23) and the field strength renormalization counterterm (18.9). We find

$$\gamma_f^n = \frac{8}{3} \frac{g^2}{(4\pi)^2} \left[1 + 4 \sum_2^n \frac{1}{j} - \frac{2}{n(n+1)} \right]. \quad (18.172)$$

Notice that this expression vanishes for $n = 1$, so that there is no rescaling of A_f^1 , as required by (18.157). For $n > 1$, γ_f^n is positive and so its coefficient a_f^n is negative. This implies that the higher moments of the quark distribution functions are suppressed as Q^2 becomes large.

Operator Mixing

The QCD rescaling of the operators $\mathcal{O}_f^{(n)}$ is still more complicated because QCD contains additional twist-2 operators which can be built from gluon fields. These new operators are mixed with the quark twist-2 operators by the diagrams of Fig. 18.14.

For n even, the diagrams of Fig. 18.14 give the operators $\mathcal{O}_f^{(n)}$ matrix elements in the state of a gluon with momentum p . The tensor structure of

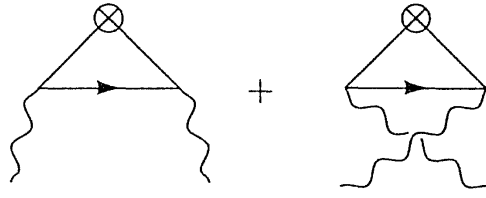


Figure 18.14. Diagrams that produce operator mixing between twist-2 quark and gluon operators.

this matrix element contains the term

$$g^{\alpha\beta} p^{\mu_1} \cdots p^{\mu_n}, \quad (18.173)$$

where α, β are the polarization indices of the external gluons. This structure arises from the operator

$$\mathcal{O}_g^{(n)\mu_1 \cdots \mu_n} = -\frac{1}{2} F^{\{\mu_1 \nu} (iD^{\mu_2}) \cdots (iD^{\mu_{n-1}}) F^{\mu_n\}}_{\nu} - \text{traces}, \quad (18.174)$$

symmetrized on μ_1, \cdots, μ_n , with traces subtracted. These operators have dimension $(n+2)$ and spin n , and thus have twist 2.

The gluon operators (18.174) are relevant only for n even. Using the manipulation

$$F^{\mu_1 \nu} (iD^{\mu_2}) \cdots F^{\mu_n \nu} = i\partial^{\mu_2} (F^{\mu_1 \nu} \cdots F^{\mu_n \nu}) - (iD^{\mu_2}) F^{\mu_1 \nu} \cdots F^{\mu_n \nu}, \quad (18.175)$$

we can transfer the covariant derivatives from one factor of $F^{\mu \nu}$ to the other, giving

$$\mathcal{O}_g^{(n)} = (-1)^n \mathcal{O}_g^{(n)} + \partial^{\mu_1} (\mathcal{O}'). \quad (18.176)$$

Thus, for n odd, the operator $\mathcal{O}_g^{(n)}$ is equal to a total derivative. The matrix elements of a total derivative are proportional to the momentum injected into this operator. Since zero momentum is injected in the calculation of the proton matrix elements of the OPE of currents, the operators $\mathcal{O}_g^{(n)}$ have no effect on the deep inelastic scattering cross section for n odd.

For n even, however, we must take account of the mixing of $\mathcal{O}_g^{(n)}$ with $\mathcal{O}_f^{(n)}$. The computation of the diagrams of Fig. 18.14 is quite similar to the other operator rescaling calculations we have done in this chapter, and so we reserve working out the details for Problem 18.3. We find that the diagrams of Fig. 18.14 contain a structure proportional to (18.173) with the coefficient

$$\frac{2(n^2 + n + 2)}{n(n+1)(n+2)} \frac{g^2}{(4\pi)^2} \Gamma(2 - \frac{d}{2}). \quad (18.177)$$

From this computation, we find that the renormalized twist-2 quark operator, properly normalized at the scale M , is given in terms of bare operators by

$$[\mathcal{O}_f^{(n)}]_M = (1 + \delta_f) [\mathcal{O}_f^{(n)}]_0 + (\delta_g) [\mathcal{O}_g^{(n)}]_0, \quad (18.178)$$

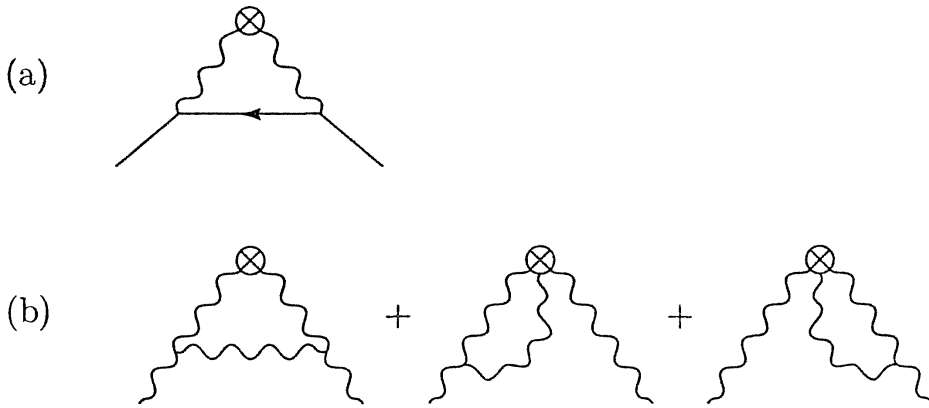


Figure 18.15. Diagrams contributing to the operator rescaling of twist-2 gluon operators: (a) contributions to gluon-quark mixing; (b) contributions to diagonal gluon operator renormalization.

where δ_f is given by (18.171) and

$$\delta_g = -\frac{g^2}{(4\pi)^2} \frac{2(n^2 + n + 2)}{n(n+1)(n+2)} \frac{\Gamma(2 - \frac{d}{2})}{(M^2)^{2-d/2}}. \quad (18.179)$$

This equation gives us two elements of the anomalous dimension matrix of twist-2 operators.

The remaining elements of the γ matrix for twist-2 operators are generated by the diagrams shown in Fig. 18.15. The diagram of Fig. 18.15(a) gives the mixing of $\mathcal{O}_g^{(n)}$ back into $\mathcal{O}_f^{(n)}$. The diagrams of Fig. 18.15(b), combined with the counterterm δ_3 for gluon field strength rescaling, gives the diagonal anomalous dimension. The counterterm δ_3 is given explicitly, in Feynman-'t Hooft gauge, in (16.74). The remainder of this anomalous dimension computation is discussed in Problem 18.3.

To describe the complete anomalous dimension matrix, we begin by considering a strong interaction model with one quark flavor. In this case, there is one twist-two operator $\mathcal{O}_f^{(n)}$ which mixes with $\mathcal{O}_g^{(n)}$. These two operators mix through a 2×2 matrix

$$\gamma^n = -\frac{g^2}{(4\pi)^2} \begin{pmatrix} a_{ff}^n & a_{fg}^n \\ a_{gf}^n & a_{gg}^n \end{pmatrix}, \quad (18.180)$$

where

$$\begin{aligned} a_{ff}^n &= -\frac{8}{3} \left[1 + 4 \sum_2^n \frac{1}{j} - \frac{2}{n(n+1)} \right], \\ a_{fg}^n &= 4 \frac{n^2 + n + 2}{n(n+1)(n+2)}, \\ a_{gf}^n &= \frac{16}{3} \frac{n^2 + n + 2}{n(n^2 - 1)}, \\ a_{gg}^n &= -6 \left[\frac{1}{3} + \frac{2}{9} n_f + 4 \sum_2^n \frac{1}{j} - \frac{4}{n(n-1)} - \frac{4}{(n+1)(n+2)} \right]. \end{aligned} \quad (18.181)$$

Notice that this matrix is not symmetric. In the last line, n_f is the number of quark flavors, equal to 1 in this case; this term comes from (16.74).

In the realistic case, QCD contains several quark flavors— u , d , s , and also c and b when we work at momenta sufficiently large that we can ignore the masses of these particles. Then the anomalous dimension matrix γ^n has size $(n_f + 1) \times (n_f + 1)$. The submatrix acting on quark operators is diagonal, with all of the diagonal entries being given by a_{ff}^n in (18.181). The quark-gluon and gluon-quark entries are all given by a_{fg}^n and a_{gf}^n , respectively, and are independent of the flavor. The gluon diagonal entry is given by a_{gg}^n in (18.181) with the realistic value of n_f . This means that the gluon operator mixes with only one linear combination of quark operators:

$$\sum_f \mathcal{O}_f^{(n)}; \quad (18.182)$$

the orthogonal linear combinations are simply rescaled, with the exponent given by a_{ff}^n or (18.172).

Let us now apply this analysis of operator mixing to the evaluation of the moment sum rules. For odd n , there is no operator mixing, and so the Q^2 dependence of the right-hand side of (18.155) is correctly given by the simple rescaling (18.160).

For even n , we must take operator mixing into account. The right-hand side of the sum rule (18.154) is the proton matrix element of a twist-2 operator normalized at the scale Q . Let us write an arbitrary linear combination of these operators as

$$c_i^n [\mathcal{O}_i^{(n)}]_Q, \quad (18.183)$$

where the index i runs over g and the various flavors f . To rescale this operator to a fixed reference momentum μ , we rewrite the coefficients in a basis of *left* eigenvectors of γ^n and rescale each eigenvector according to (18.159). In terms of the matrix a_{ij}^n of rescaling coefficients, we can write the rescaling abstractly as

$$c_i^n [\mathcal{O}_i^{(n)}]_Q = c_i^n \left\{ \left(\frac{\log(Q^2/\Lambda^2)}{\log(\mu^2/\Lambda^2)} \right)^{a^n/2b_0} \right\}_{ij} [\mathcal{O}_j^{(n)}]_\mu. \quad (18.184)$$

This rescaling, acting with c_i^n to the left of the matrix (a^n) , is precisely the prescription required by Eq. (18.79).

Let us work this out explicitly for the case $n = 2$. The right-hand side of the moment sum rule (18.154) is given by the matrix element of $\mathcal{O}_f^{(2)}$. We rewrite this as

$$\mathcal{O}_f^{(2)} = (\mathcal{O}_f^{(2)} - \frac{1}{n_f} \sum_{f'} \mathcal{O}_{f'}^{(2)}) + \frac{1}{n_f} \sum_{f'} \mathcal{O}_{f'}^{(2)}. \quad (18.185)$$

The first term is simply rescaled; the second term mixes with the gluon operator $\mathcal{O}_g^{(2)}$. The anomalous dimension matrix acting on $(\sum_f \mathcal{O}_f, \mathcal{O}_g)$ for $n = 2$

has coefficients

$$\begin{pmatrix} a_{ff}^2 & a_{fg}^2 \\ a_{gf}^2 n_f & a_{gg}^2 \end{pmatrix} = \begin{pmatrix} -\frac{64}{9} & \frac{4}{3} n_f \\ \frac{64}{9} & -\frac{4}{3} n_f \end{pmatrix}. \quad (18.186)$$

The left eigenvectors of this matrix, and their corresponding eigenvalues, are

$$\begin{aligned} (1, 1) &\rightarrow a^2 = 0 \\ \left(\frac{16}{3}, -n_f\right) &\rightarrow a^2 = -\frac{4}{3}\left(\frac{16}{3} + n_f\right). \end{aligned} \quad (18.187)$$

Notice that the first eigenvector gives a linear combination of operators $c_i^2 \mathcal{O}_i^{(2)}$ with zero anomalous dimension. This operator is in fact the total energy momentum tensor of QCD,

$$T^{\mu\nu} = \sum_f \mathcal{O}_f^{(2)\mu\nu} + \mathcal{O}_g^{(2)\mu\nu}, \quad (18.188)$$

which must have $\gamma = 0$. If we expand the second term in (18.185) in terms of the components (18.187), we can compute the full form of the operator rescaling. We find

$$\begin{aligned} [\mathcal{O}_f^{(2)}]_Q &= \frac{1}{16/3 + n_f} T \\ &+ \frac{1}{n_f(\frac{16}{3} + n_f)} \left(\frac{\log(Q^2/\Lambda^2)}{\log(\mu^2/\Lambda^2)} \right)^{-(\frac{16}{3} + n_f)/2b_0} \left[\frac{16}{3} \sum_f \mathcal{O}_f^{(2)} - n_f \mathcal{O}_g^{(2)} \right]_\mu \\ &+ \left(\frac{\log(Q^2/\Lambda^2)}{\log(\mu^2/\Lambda^2)} \right)^{-32/3b_0} \left[\mathcal{O}_f^{(2)} - \frac{1}{n_f} \sum_{f'} \mathcal{O}_{f'}^{(2)} \right]_\mu, \end{aligned} \quad (18.189)$$

where T is the energy-momentum tensor (18.188). The right-hand side of the $n = 2$ moment sum rule is given by the coefficient of the proton matrix element of this operator. To evaluate this coefficient, we need to define gluon analogues of the A_f^n , by writing, analogously to (18.134),

$$\langle P | \mathcal{O}_g^{(n)\mu_1 \dots \mu_n} | P \rangle = A_g^n \cdot 2P^{\mu_1} \dots P^{\mu_n} - \text{traces}. \quad (18.190)$$

For the case $n = 2$, we note in particular that

$$\langle P | T^{\mu\nu} | P \rangle = 2P^\mu P^\nu; \quad (18.191)$$

thus, (18.188) implies

$$\sum_f A_f^2 + A_g^2 = 1. \quad (18.192)$$

If we replace each operator in (18.189) by the corresponding coefficient $A_i^2(\mu)$, we will have an expression for the right-hand side of the $n = 2$ moment sum rule which makes its Q^2 dependence explicit.

Although expression (18.189) is rather complicated, it has a simple form in the extreme limit $Q^2 \rightarrow \infty$. At asymptotic Q^2 , the last two terms of (18.189)

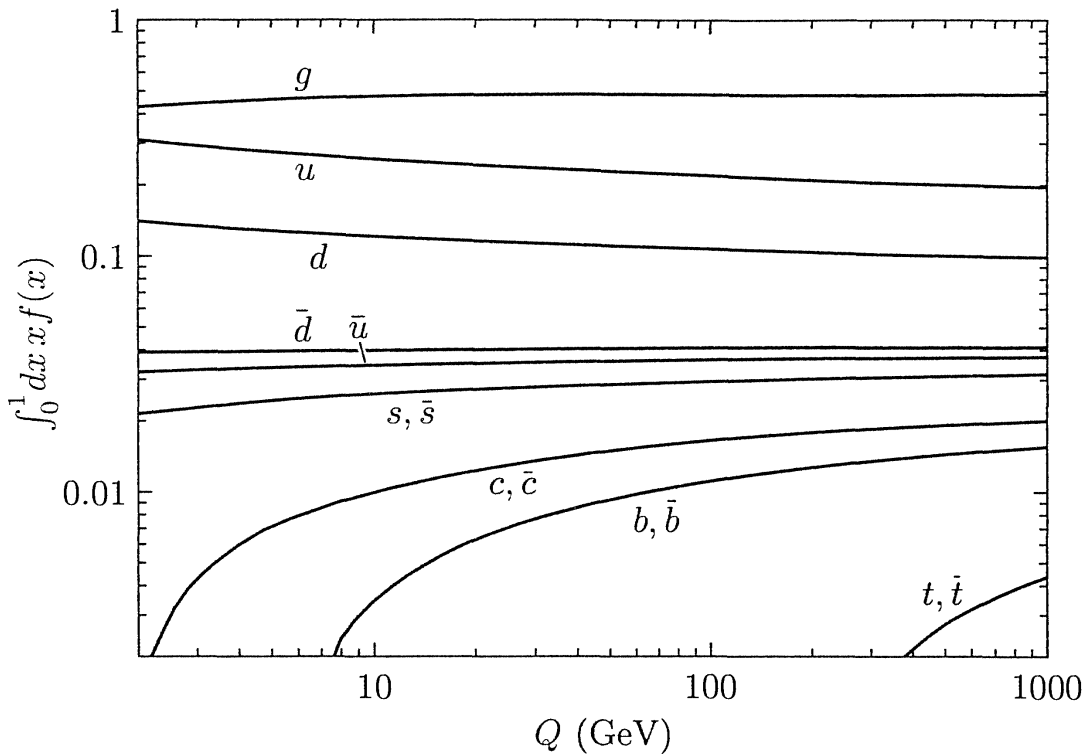


Figure 18.16. Fractions of the total energy-momentum of the proton carried by various parton species, as a function of Q , according to the CTEQ fit to deep inelastic scattering data described in Fig. 17.6. The Q dependence of the curves is calculated from the QCD evolution equations.

tend to zero, and the right-hand side of (18.189) becomes a fixed number times the energy-momentum tensor. Then, using (18.191), we can evaluate the $n = 2$ moment sum rule completely:

$$\int_0^1 dx x f_f^+(x) \rightarrow \frac{1}{16/3 + n_f}. \quad (18.193)$$

In this extreme limit, we find that each quark flavor carries the same fixed fraction of the energy-momentum of the proton. By (18.192), the remainder is carried by the gluons. To illustrate, in a theory with $n_f = 4$, each quark flavor carries $3/28$ of the total momentum of the proton, and the gluons carry the remaining $4/7$. Figure 18.16 shows how slowly these asymptotic results are approached starting from realistic parton distributions.

Relation to the Altarelli-Parisi Equations

The operator mixing analysis just described gives predictions for the moments of parton distributions which imply that these integrals are Q^2 dependent. Of the various moment integrals that do not involve operator mixing, only the $n = 1$ integrals which give the flavor quantum numbers of the proton are constant as a function of Q^2 . The rest decrease as powers of $\log Q^2$. Similarly, one linear combination of the matrix elements of $n = 2$ twist-2 operators

remains constant with Q^2 . This relation is expression by the sum rule (18.192). To write this relation more clearly, let us introduce the parton distribution of gluons as a smooth function satisfying the relations

$$\int_0^1 dx x^{n-1} f_g(x, Q^2) = A_g^{(n)}(Q^2). \quad (18.194)$$

Then (18.192) becomes just the total momentum sum rule for parton distributions (17.39):

$$\int_0^1 dx x \left[\sum_f f_f^+(x) + f_g(x) \right] = 1. \quad (18.195)$$

It is not difficult to verify that, for $n > 2$, all of the eigenvalues of the matrix a_{ij}^n of anomalous dimension coefficients are negative. Thus, all of the higher moment sum rules decrease, subject to the flavor charge and momentum conservation laws. In other words, the operator renormalization analysis predicts that parton distributions shift down to smaller values of x as $\log Q^2$ increases. It is pleasing that this is the same conclusion that we reached in Section 17.5, where we derived the Altarelli-Parisi equations to describe this evolution of the parton distributions.

Given that the operator analysis and the Altarelli-Parisi equations imply the same qualitative behavior for the parton distributions, how do these analyses compare quantitatively? To compare them directly, we should work out what predictions the Altarelli-Parisi equations make for the moments of the parton distribution functions. Let us begin with the simpler case of $f_f^-(x) = f_f(x) - f_{\bar{f}}(x)$.

To find the Altarelli-Parisi equation for this quantity, subtract the last two equations of (17.128). The term involving the gluon distribution cancels, and we find

$$\frac{d}{d \log Q^2} f_f^-(x) = \frac{\alpha_s(Q^2)}{2\pi} \int_x^1 \frac{dz}{z} P_{q \leftarrow q}(z) f_f^-(\frac{x}{z}). \quad (18.196)$$

Now define

$$M_{fn}^- = \int_0^1 dx x^{n-1} f_f^-(x). \quad (18.197)$$

This quantity obeys the differential equation

$$\frac{d}{d \log Q^2} M_{fn}^- = \frac{\alpha_s(Q^2)}{2\pi} \int_0^1 dx x^{n-1} \int_x^1 \frac{dz}{z} P_{q \leftarrow q}(z) f_f^-(\frac{x}{z}). \quad (18.198)$$

Interchange the order of integration on the right-hand side, and change variables to $y = x/z$:

$$\begin{aligned}
 \int_0^1 dx x^{n-1} \int_x^1 \frac{dz}{z} &= \int_0^1 \frac{dz}{z} \int_0^z dx x^{n-1} \\
 &= \int_0^1 \frac{dz}{z} \int_0^1 dy y^{n-1} z^n \\
 &= \int_0^1 dz z^{n-1} \int_0^1 dy y^{n-1}. \tag{18.199}
 \end{aligned}$$

Then the right-hand side of the differential equation neatly factorizes:

$$\frac{d}{d \log Q^2} M_{nf}^- = \frac{\alpha_s(Q^2)}{2\pi} \left[\int_0^1 dz z^{n-1} P_{q \leftarrow q}(z) \right] \cdot \int_0^1 dy y^{n-1} f_f^-(y); \tag{18.200}$$

the last factor is again M_{fn}^- . The coefficient in this relation is the n th moment of the splitting function $P_{q \leftarrow q}(z)$. We can compute this from the explicit form of this function given in (17.129):

$$\int_0^1 dz z^{n-1} P_{q \leftarrow q}(z) = \int_0^1 dz z^{n-1} \frac{4}{3} \left[\frac{1+z^2}{(1-z)_+} + \frac{3}{2} \delta(1-z) \right]. \tag{18.201}$$

The integral over the distribution is done by using the definition (17.105):

$$\begin{aligned}
 \int_0^1 dz z^{n-1} \frac{1}{(1-z)_+} &= \int_0^1 dz \frac{z^{n-1} - 1}{(1-z)} \\
 &= \int_0^1 dz (-1 - z - \dots - z^{n-2}) \\
 &= - \sum_1^{n-1} \frac{1}{j}. \tag{18.202}
 \end{aligned}$$

Then

$$\begin{aligned}
 \int_0^1 dz z^{n-1} P_{q \leftarrow q}(z) &= -\frac{4}{3} \left[\sum_1^{n-1} \frac{1}{j} + \sum_3^{n+1} \frac{1}{j} + \frac{3}{2} \right] \\
 &= -\frac{2}{3} \left[1 + 4 \sum_2^n \frac{1}{j} - \frac{2}{n(n+1)} \right]. \tag{18.203}
 \end{aligned}$$

Remarkably, this is just $a_f^n/4$, as the anomalous dimension coefficient is given in (18.172) or (18.181). Thus, according to the Altarelli-Parisi equations, the n th moment of $f_f^-(x)$ obeys

$$\frac{d}{d \log Q^2} M_{f^n}^- = \frac{\alpha_s(Q^2)}{8\pi} a_f^n \cdot M_{f^n}^-. \quad (18.204)$$

To integrate this equation, we need the explicit form of $\alpha_s(Q^2)$. Inserting expression (17.17), we find

$$\frac{d}{d \log Q^2} M_{f^n}^- = \frac{a_f^n}{2b_0} \frac{1}{\log(Q^2/\Lambda^2)} M_{f^n}^-. \quad (18.205)$$

The solution of this equation, derived from the Altarelli-Parisi equations, is precisely the function (18.160) that we derived from the operator analysis of the moment sum rules for f_f^- .

It is not difficult to check that this conclusion is more general. By taking the n th moment of the full Altarelli-Parisi equations (17.128), we convert these equations to a set of ordinary differential equations for the moments. The linear combination of quark distribution functions

$$\sum_f (f_f(x) + f_{\bar{f}}(x)) \quad (18.206)$$

couples to the gluon distribution and leads to a 2×2 set of equations. All orthogonal linear combinations separate from the gluon distribution and thus have moments that obey equations identical to (18.205). To analyze the coupled equations, define

$$M_n^+ = \int_0^1 dx x^{n-1} \sum_f (f_f(x) + f_{\bar{f}}(x)); \quad M_{gn} = \int_0^1 dx x^{n-1} f_g(x). \quad (18.207)$$

Then one can show, by the manipulations that led to (18.205), that the Altarelli-Parisi equations predict for these moments the set of coupled equations

$$\begin{aligned} \frac{d}{d \log Q^2} M_n^+ &= \frac{1}{2b_0} \frac{1}{\log(Q^2/\Lambda^2)} [a_{ff}^n M_n^+ + a_{fg}^n M_{gn}], \\ \frac{d}{d \log Q^2} M_{gn} &= \frac{1}{2b_0} \frac{1}{\log(Q^2/\Lambda^2)} [n_f a_{gf}^n M_n^+ + a_{gg}^n M_{gn}], \end{aligned} \quad (18.208)$$

where the coefficients a_{ij}^n are proportional to the n th moments of the splitting functions given in (17.129) and (17.130). In all cases, one can see that these coefficients agree precisely with the corresponding coefficients in (18.181). Thus, the solution of these equations gives the same Q^2 dependence for the moments of parton distribution functions that we found from the operator analysis.

Remarkably, the analysis of parton splitting functions given in Chapter 17 and the analysis of operator renormalization factors given above have turned out to be two views of the same basic phenomenon. Both sets of equations

express the manner in which the constituents of hadrons in QCD are resolved, layer by layer, by hard-scattering processes at successively higher values of the momentum transfer. Our understanding that a quark, when studied on a fine scale, is resolved into a set of quarks, antiquarks, and gluons indicates that we have gone far beyond the simple notions of one-particle relativistic mechanics. Our two complementary derivations of this idea reinforce its fundamental character as a prediction of quantum field theory. It is especially pleasing that, as we saw at the end of Section 17.5, Nature apparently accepts this prediction and makes this consequence of quantum field theory an essential part of the structure of hadrons.

Problems

18.1 Matrix element for proton decay. Some advanced theories of particle interactions include heavy particles X whose couplings violate the conservation of baryon number. Integrating out these particles produces an effective interaction that allows the proton to decay to a positron and a photon or a pion. This effective interaction is most easily written using the definite-helicity components of the quark and electron fields: If u_L, d_L, u_R, e_R are two-component spinors, then this effective interaction is

$$\Delta\mathcal{L} = \frac{2}{m_X^2} \epsilon_{abc} \epsilon^{\alpha\beta} \epsilon^{\gamma\delta} e_{R\alpha} u_{Ra\beta} u_{Lb\gamma} d_{Lc\delta}.$$

A typical value for the mass of the X boson is $m_X = 10^{16}$ GeV.

- (a) Estimate, in order of magnitude, the value of the proton lifetime if the proton is allowed to decay through this interaction.
- (b) Show that the three-quark operator in $\Delta\mathcal{L}$ has an anomalous dimension

$$\gamma = -4 \frac{g^2}{(4\pi)^2}.$$

Estimate the enhancement of the proton decay rate due to the leading QCD corrections.

18.2 Parity-violating deep inelastic form factor. In this problem, we first motivate the presence of additional deep inelastic form factors that are proportional to *differences* of quark and antiquark distribution functions. Then we define these functions formally and work out their properties.

- (a) Analyze neutrino-proton scattering following the method used at the beginning of Section 18.5. Define

$$J_+^\mu = \bar{u} \gamma^\mu \left(\frac{1 - \gamma^5}{2} \right) d, \quad J_-^\mu = \bar{d} \gamma^\mu \left(\frac{1 - \gamma^5}{2} \right) u.$$

Let

$$W^{\mu\nu(\nu)} = 2i \int d^4x e^{iq \cdot x} \langle P | T\{ J_-^\mu(x) J_+^\nu(0) \} | P \rangle,$$

averaged over the proton spin. Show that the cross section for deep inelastic neutrino scattering can be computed from $W^{\mu\nu(\nu)}$ according to

$$\frac{d^2\sigma}{dxdy}(\nu p \rightarrow \mu^- X) = \frac{G_F^2 y}{2\pi^2} \cdot (k_\mu k'_\nu + k'_\nu k'_\mu - g_{\mu\nu} k \cdot k' - i\epsilon^{\mu\nu\alpha\beta} k'_\alpha k'_\beta) \text{Im } W^{\mu\nu(\nu)}(P, q).$$

- (b) Show that any term in $\text{Im } W^{\mu\nu(\nu)}$ proportional to q^μ or q^ν gives zero when contracted with the lepton momentum tensor in the formula above. Thus we can expand $W^{\mu\nu(\nu)}$ with three scalar form factors,

$$W^{\mu\nu(\nu)} = -g^{\mu\nu} W_1^{(\nu)} + P^\mu P^\nu W_2^{(\nu)} + i\epsilon^{\mu\nu\lambda\sigma} P_\lambda q_\sigma W_3^{(\nu)} + \dots,$$

where the additional terms do not contribute to the deep inelastic cross section. Find the formula for the deep inelastic cross section in terms of the imaginary parts of $W_1^{(\nu)}$, $W_2^{(\nu)}$, and $W_3^{(\nu)}$.

- (c) Evaluate the form factors $W_i^{(\nu)}$ in the parton model, and show that

$$\begin{aligned} \text{Im } W_1^{(\nu)} &= \pi(f_d(x) + f_{\bar{u}}(x)), \\ \text{Im } W_2^{(\nu)} &= \frac{4\pi}{ys} x(f_d(x) + f_{\bar{u}}(x)), \\ \text{Im } W_3^{(\nu)} &= \frac{2\pi}{ys}(f_d(x) - f_{\bar{u}}(x)). \end{aligned}$$

Insert these expressions into the formula derived in part (b) and show that the result reproduces the first line of Eq. (17.35).

- (d) This analysis motivates the following definition: For a single quark flavor f , let

$$J_{fL}^\mu = \bar{f} \gamma^\mu \left(\frac{1 - \gamma^5}{2} \right) f.$$

Define

$$W_{fL}^{\mu\nu} = 2i \int d^4x e^{iq \cdot x} \langle P | T\{ J_{fL}^\mu(x) J_{fL}^\nu(0) \} | P \rangle.$$

Decompose this tensor according to

$$W_{fL}^{\mu\nu} = -g^{\mu\nu} W_{1fL} + P^\mu P^\nu W_{2fL} + i\epsilon^{\mu\nu\lambda\sigma} P_\lambda q_\sigma W_{3fL} + \dots,$$

where the remaining terms are proportional to q^μ or q^ν . Evaluate the W_{iL} in the parton model. Show that the quantities W_{1fL} and W_{2fL} reproduce the expressions for W_{1f} and W_{2f} given by Eqs. (18.120) and (18.144), and that W_{3fL} is given by

$$\text{Im } W_{3fL} = \frac{2\pi}{ys}(f_f(x) - f_{\bar{f}}(x)).$$

- (e) Compute the operator product of the currents in the expression for $W_{fL}^{\mu\nu}$, and write the terms in this product that involve twist-2 operators. Show that the expressions for W_{1fL} and W_{2fL} that follow from this analysis reproduce the expressions for W_{1f} and W_{2f} given by Eqs. (18.144) and (18.145). Find the corresponding expression for W_{3fL} .

- (f) Define the parton distribution f_f^- by the relation

$$f_f^-(x, Q^2) = \frac{ys}{2\pi} \operatorname{Im} W_{3fL}(x, Q^2).$$

Show that, by virtue of this definition, the distribution function f_f^- satisfies the sum rule (18.155) for odd n .

18.3 Anomalous dimensions of gluon twist-2 operators.

- (a) Compute the divergent parts of the diagrams in Fig. 18.14, and use these to derive the second line of Eq. (18.181). Notice that this result holds only for n even. Show that the two diagrams cancel for n odd.
- (b) Compute the divergent parts of the diagrams in Fig. 18.5, and use these to derive the third and fourth lines of Eq. (18.181).

18.4 Deep inelastic scattering from a photon. Consider the problem of deep-inelastic scattering of an electron from a photon. This process can actually be measured by analyzing the reaction $e^+e^- \rightarrow e^+e^- + X$ in the regime where the positron goes forward, with emission of a collinear photon, which then has a hard reaction with the electron. Let us analyze this process to leading order in QED and to leading-log order in QCD. To predict the photon structure functions, it is reasonable to integrate the renormalization group equations with the initial condition that the parton distribution for photons in the photon is $\delta(x-1)$ at $Q^2 = (\frac{1}{2} \text{ GeV})^2$. Take $\Lambda = 150 \text{ MeV}$. Assume for simplicity that there are four flavors of quarks, u , d , c , and s , with charges $2/3$, $-1/3$, $2/3$, $-1/3$, respectively, and that it is always possible to ignore the masses of these quarks.

- (a) Use the Altarelli-Parisi equations to compute the parton distributions for quarks and antiquarks in the photon, to leading order in QED and to zeroth order in QCD. Compute also the probability that the photon remains a photon as a function of Q^2 .
- (b) Formulate the problem of computing the moments of W_2 for the photon as a problem in operator mixing. Compute the relevant anomalous dimension matrix γ . You should be able to assemble this matrix from familiar ingredients without doing further Feynman diagram computations.
- (c) Compute the $n = 2$ moments of the photon structure functions as a function of Q^2 .
- (d) Describe qualitatively the evolution of the photon structure function as a function of x and Q^2 .

Perturbation Theory Anomalies

In many examples, we have seen that loop corrections can have an important effect on the predictions of quantum field theory. We have studied examples in which the relative importance of operators is shifted by radiative corrections, and in which the form of the interactions they mediate is altered. However, in specific circumstances, radiative corrections can have an even more significant effect: They can destroy symmetries of the classical equations of motion.

The most important effect of this type involves the chiral symmetries of theories with massless fermions. In Section 3.4, we saw that the massless Dirac Lagrangian has an enhanced symmetry associated with the separate number conservation of left- and right-handed fermions. This symmetry is generated by the axial vector current $j^{\mu 5} = \bar{\psi} \gamma^\mu \gamma^5 \psi$. Classically,

$$\partial_\mu j^{\mu 5} = 0 \quad (19.1)$$

for zero-mass fermions. This equation of motion is true not only in free fermion theory but also, as a classical field equation, in massless QED and QCD.

However, in this chapter, we will see that the true picture is not so simple. We will show that, in gauge theories, the conservation of the axial vector current is actually incompatible with gauge invariance, and that radiative corrections in gauge theories supply a nonzero operator that appears on the right-hand side of Eq. (19.1). This new conservation equation for the axial current has a number of remarkable consequences, which we will discuss in Sections 19.3 and 19.4.

19.1 The Axial Current in Two Dimensions

Eventually, we will want to analyze the current conservation equation for the axial current in massless QCD. However, this discussion will involve some technical complication, so we will first study the physics that violates axial current conservation in a context in which the calculations are relatively simple. A particularly simple model problem is that of two-dimensional massless QED.

The Lagrangian of two-dimensional QED is

$$\mathcal{L} = \bar{\psi} (i \not{D}) \psi - \frac{1}{4} (F_{\mu\nu})^2, \quad (19.2)$$

with $\mu, \nu = 0, 1$ and $D_\mu = \partial_\mu + ieA_\mu$. The Dirac matrices must be chosen to satisfy the Dirac algebra

$$\{\gamma^\mu, \gamma^\nu\} = 2g^{\mu\nu}. \quad (19.3)$$

In two dimensions, this set of relations can be represented by 2×2 matrices; we choose

$$\gamma^0 = \begin{pmatrix} 0 & -i \\ i & 0 \end{pmatrix}, \quad \gamma^1 = \begin{pmatrix} 0 & i \\ i & 0 \end{pmatrix}. \quad (19.4)$$

The Dirac spinors will be two-component fields.

The product of the Dirac matrices, which anticommutes with each of the γ^μ , is

$$\gamma^5 = \gamma^0\gamma^1 = \begin{pmatrix} 1 & 0 \\ 0 & -1 \end{pmatrix}. \quad (19.5)$$

Then, just as in four dimensions, there are two possible currents,

$$j^\mu = \bar{\psi}\gamma^\mu\psi, \quad j^{\mu 5} = \bar{\psi}\gamma^\mu\gamma^5\psi, \quad (19.6)$$

and both are conserved if there is no mass term in the Lagrangian.

To make the conservation laws quite explicit, we label the components of the fermion field ψ in this spinor basis as

$$\psi = \begin{pmatrix} \psi_+ \\ \psi_- \end{pmatrix}. \quad (19.7)$$

The subscript indicates the γ^5 eigenvalue. Then, using the explicit representations (19.4) and (19.7), we can rewrite the fermionic part of (19.2) as

$$\mathcal{L} = \psi_+^\dagger i(D_0 + D_1)\psi_+ + \psi_-^\dagger i(D_0 - D_1)\psi_-. \quad (19.8)$$

In the free theory, the field equation of ψ_+ would be

$$i(\partial_0 + \partial_1)\psi_+ = 0; \quad (19.9)$$

the solutions to this equation are waves that move to the right in the one-dimensional space at the speed of light. We will thus refer to the particles associated with ψ_+ as *right-moving* fermions. The quanta associated with ψ_- are, similarly, *left-moving*. This distinction is analogous to the distinction between left- and right-handed particles which gives the physical interpretation of γ^5 in four dimensions. Since the Lagrangian (19.8) contains no terms that mix left- and right-moving fields, it seems obvious that the number currents for these fields are separately conserved. Thus,

$$\partial_\mu \left(\bar{\psi}\gamma^\mu \left(\frac{1-\gamma^5}{2} \right) \psi \right) = 0, \quad \partial_\mu \left(\bar{\psi}\gamma^\mu \left(\frac{1+\gamma^5}{2} \right) \psi \right) = 0. \quad (19.10)$$

It is a curious property of two-dimensional spacetime that the vector and axial vector fermionic currents are not independent of each other. Let $\epsilon^{\mu\nu}$ be

the totally antisymmetric symbol in two dimensions, with $\epsilon^{01} = +1$. Then the two-dimensional Dirac matrices obey the identity

$$\gamma^\mu \gamma^5 = -\epsilon^{\mu\nu} \gamma_\nu. \quad (19.11)$$

The currents $j^{\mu 5}$ and j^μ have the same relation. Thus we can study the properties of the axial vector current by using results that we have already derived for the vector current.

Vacuum Polarization Diagrams

In Section 7.5, we computed the lowest-order vacuum polarization of QED in dimensional regularization. In the limit of zero mass, we found, in Eq. (7.90),

$$i\Pi^{\mu\nu}(q) = -i(q^2 g^{\mu\nu} - q^\mu q^\nu) \frac{2e^2}{(4\pi)^{d/2}} \text{tr}[1] \int_0^1 dx x(1-x) \frac{\Gamma(2-\frac{d}{2})}{(-x(1-x)q^2)^{2-d/2}}, \quad (19.12)$$

where $\text{tr}[1] = 4$ gives the convention for tracing over Dirac matrices given in Eq. (7.88). If we set $\text{tr}[1] = 2$ to be consistent with (19.4) and then set $d = 2$ in (19.12), we find the finite and well-defined result

$$\begin{aligned} i\Pi^{\mu\nu}(q) &= i(q^2 g^{\mu\nu} - q^\mu q^\nu) \frac{2e^2}{4\pi} \cdot 2 \cdot \frac{1}{q^2} \\ &= i\left(g^{\mu\nu} - \frac{q^\mu q^\nu}{q^2}\right) \frac{e^2}{\pi}. \end{aligned} \quad (19.13)$$

Notice that this expression has the structure of a photon mass term; the photon receives the mass

$$m_\gamma^2 = \frac{e^2}{\pi}. \quad (19.14)$$

Schwinger showed that this result is exact, and that the photon of two-dimensional QED is a free massive boson.* In the discussion below Eq. (7.72), we pointed out that it is not possible for a vacuum polarization amplitude consistent with the Ward identity to generate a mass for the photon unless it also contains a pole at $q^2 = 0$. In two dimensions, such a pole can arise from the infrared behavior of the fermion-antifermion intermediate state, and we see this behavior explicitly in (19.13).

Once we have an explicit expression for the vacuum polarization, we can find the expectation value of the current induced by a background electromagnetic field. This quantity is generated by the diagram of Fig. 19.1, which gives

$$\int d^2x e^{iq \cdot x} \langle j^\mu(x) \rangle = (-ie)^{-1} (i\Pi^{\mu\nu}(q)) = -\left(g^{\mu\nu} - \frac{q^\mu q^\nu}{q^2}\right) \cdot \frac{e}{\pi} A_\nu(q), \quad (19.15)$$

*J. Schwinger, *Phys. Rev.* **128**, 2425 (1962).

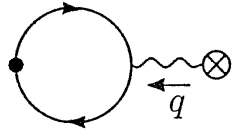


Figure 19.1. Computation of $\langle j^\mu \rangle$ in a background electromagnetic field.

where $A_\nu(q)$ is the Fourier transform of the background field. This quantity manifestly satisfies the current conservation relation $q_\mu \langle j^\mu(q) \rangle = 0$.

The identity (19.11) between the vector and axial vector currents allows us to derive from (19.15) the corresponding expectation value of $j^{\mu 5}$. We find

$$\begin{aligned} \langle j^{\mu 5}(q) \rangle &= -\epsilon^{\mu\nu} \langle j_\nu(q) \rangle \\ &= \epsilon^{\mu\nu} \frac{e}{\pi} \left(A_\nu(q) - \frac{q_\nu q^\lambda}{q^2} A_\lambda(q) \right). \end{aligned} \quad (19.16)$$

If the axial vector current were conserved, this object would satisfy the Ward identity. Instead, we find

$$q_\mu \langle j^{\mu 5}(q) \rangle = \frac{e}{\pi} \epsilon^{\mu\nu} q_\mu A_\nu(q). \quad (19.17)$$

This is the Fourier transform of the field equation

$$\partial_\mu j^{\mu 5} = \frac{e}{2\pi} \epsilon^{\mu\nu} F_{\mu\nu}. \quad (19.18)$$

Apparently, the axial vector current is not conserved in the presence of electromagnetic fields, as the result of an anomalous behavior of its vacuum polarization diagram.

How could this happen? The Feynman diagrams formally satisfy the Ward identity both for the vector and for the axial vector current. The problem must come in the regularization of the vacuum polarization diagram. By dimensional analysis, we know that this diagram has the form

$$\text{Diagram: a wavy line enters a loop from the left, and a wavy line exits the loop to the right.} = ie^2 \left(A g^{\mu\nu} - B \frac{q^\mu q^\nu}{q^2} \right). \quad (19.19)$$

The coefficient B is a finite integral, and is, in any event, unambiguously determined by the low-energy structure of the theory since it is the residue of the pole in q^2 . However, the integral A is logarithmically divergent, so its value depends on the regularization. Dimensional regularization automatically subtracts this integral to set $A = B$; then the vector current Ward identity is satisfied. But then we are led directly to (19.17). We could, alternatively, regularize the integral A so that $A = 0$. Working through the steps of the previous paragraph with this modification, we now find $q_\mu \langle j^{\mu 5}(q) \rangle = 0$, but

$$q_\mu \langle j^\mu(q) \rangle = \frac{e}{\pi} q^\nu A_\nu(q). \quad (19.20)$$

Though the result (19.17) is unpleasant, the result (19.20) would be a complete disaster, since it depends on the unphysical gauge degrees of freedom

of the vector potential. We conclude that it is not possible to regularize two-dimensional QED so that, simultaneously, the theory is gauge invariant and the axial vector current is conserved. The price of requiring gauge invariance is the anomalous nonconservation of the axial current shown in (19.18).

The Axial Vector Current Operator Equation

To understand what happened to the axial current from another viewpoint, we now study the operator equation for the divergence of $j^{\mu 5}$. Varying the Lagrangian (19.2), we find the following equations of motion for the fermion fields:

$$\partial\psi = -ie\mathcal{A}\psi, \quad \partial_\mu \bar{\psi} \gamma^\mu = ie\bar{\psi}\mathcal{A}. \quad (19.21)$$

By using these equations of motion in the most straightforward way, it is easy to conclude that $\partial_\mu j^{\mu 5} = 0$. However, a closer look at these manipulations reveals some subtleties, which alter the final conclusion.

The axial vector current is a composite operator built out of fermion fields. In the previous chapter we saw that products of local operators are often singular, so we will define the current by placing the two fermion fields at distinct points separated by a distance ϵ and then carefully taking the limit as the two fields approach each other. Explicitly, we define

$$j^{\mu 5} = \text{symm lim}_{\epsilon \rightarrow 0} \left\{ \bar{\psi}(x + \frac{\epsilon}{2}) \gamma^\mu \gamma^5 \exp \left[-ie \int_{x - \epsilon/2}^{x + \epsilon/2} dz \cdot A(z) \right] \psi(x - \frac{\epsilon}{2}) \right\}. \quad (19.22)$$

Notice that, because we have placed ψ and $\bar{\psi}$ at different points, we must introduce a Wilson line (15.53) in order that the operator be locally gauge invariant. To give $j^{\mu 5}$ the correct transformation properties under Lorentz transformations, the limit $\epsilon \rightarrow 0$ should be taken symmetrically,

$$\text{symm lim}_{\epsilon \rightarrow 0} \left\{ \frac{\epsilon^\mu}{\epsilon^2} \right\} = 0, \quad \text{symm lim}_{\epsilon \rightarrow 0} \left\{ \frac{\epsilon^\mu \epsilon^\nu}{\epsilon^2} \right\} = \frac{1}{d} g^{\mu\nu}, \quad (19.23)$$

with $d = 2$ in this case.

We now compute the divergence of the axial current defined as in (19.22):

$$\begin{aligned} \partial_\mu j^{\mu 5} = & \text{symm lim}_{\epsilon \rightarrow 0} \left\{ (\partial_\mu \bar{\psi}(x + \frac{\epsilon}{2})) \gamma^\mu \gamma^5 \exp \left[-ie \int_{x - \epsilon/2}^{x + \epsilon/2} dz \cdot A(z) \right] \psi(x - \frac{\epsilon}{2}) \right. \\ & + \bar{\psi}(x + \frac{\epsilon}{2}) \gamma^\mu \gamma^5 \exp \left[-ie \int_{x - \epsilon/2}^{x + \epsilon/2} dz \cdot A(z) \right] (\partial_\mu \psi(x - \frac{\epsilon}{2})) \\ & \left. + \bar{\psi}(x + \frac{\epsilon}{2}) \gamma^\mu \gamma^5 [-ie \epsilon^\nu \partial_\mu A_\nu(x)] \psi(x - \frac{\epsilon}{2}) \right\}. \end{aligned} \quad (19.24)$$

Using the equations of motion (19.21), and keeping terms up to order ϵ , we can reduce this to

$$\begin{aligned}\partial_\mu j^{\mu 5} &= \text{symm} \lim_{\epsilon \rightarrow 0} \left\{ \bar{\psi}(x + \frac{\epsilon}{2}) [ie\mathcal{A}(x + \frac{\epsilon}{2}) - ie\mathcal{A}(x - \frac{\epsilon}{2}) \right. \\ &\quad \left. - ie\epsilon^\nu \gamma^\mu \partial_\mu A_\nu(x)] \gamma^5 \psi(x - \frac{\epsilon}{2}) \right\} \\ &= \text{symm} \lim_{\epsilon \rightarrow 0} \left\{ \bar{\psi}(x + \frac{\epsilon}{2}) [-ie\gamma^\mu \epsilon^\nu (\partial_\mu A_\nu - \partial_\nu A_\mu)] \gamma^5 \psi(x - \frac{\epsilon}{2}) \right\}. \end{aligned} \quad (19.25)$$

Expression (19.25) seems to vanish in the limit $\epsilon \rightarrow 0$. However, we must take account of the fact that the product of the fermion operators is singular. In two dimensions, the contraction of fermion fields is

$$\begin{aligned}\overline{\psi(y)\psi(z)} &= \int \frac{d^2 k}{(2\pi)^2} e^{-ik \cdot (y-z)} \frac{i k}{k^2} \\ &= -\not{\partial} \left(\frac{i}{4\pi} \log(y-z)^2 \right) \\ &= \frac{-i}{2\pi} \frac{\gamma^\alpha (y-z)_\alpha}{(y-z)^2}. \end{aligned} \quad (19.26)$$

Thus,

$$\overline{\bar{\psi}(x + \frac{\epsilon}{2}) \Gamma \psi(x - \frac{\epsilon}{2})} = \frac{-i}{2\pi} \text{tr} \left[\frac{\gamma^\alpha \epsilon_\alpha}{\epsilon^2} \Gamma \right]. \quad (19.27)$$

Notice that the result (19.27) contains an extra minus sign from the interchange of fermion operators.

Because the contraction of fermion fields is singular as $\epsilon \rightarrow 0$, the terms of order ϵ in the last line of (19.25) can give a finite contribution. Taking the contraction according to (19.27), we find

$$\partial_\mu j^{\mu 5} = \text{symm} \lim_{\epsilon \rightarrow 0} \left\{ \frac{-i}{2\pi} \text{tr} \left[\frac{\gamma^\alpha \epsilon_\alpha}{\epsilon^2} \gamma^\mu \gamma^5 \right] \cdot (-ie\epsilon^\nu F_{\mu\nu}) \right\}. \quad (19.28)$$

In two dimensions, $\text{tr}[\gamma^\alpha \gamma^\mu \gamma^5] = 2\epsilon^{\alpha\mu}$. Thus,

$$\partial_\mu j^{\mu 5} = \frac{e}{2\pi} \text{symm} \lim_{\epsilon \rightarrow 0} \left\{ 2 \frac{\epsilon^\mu \epsilon^\nu}{\epsilon^2} \right\} \epsilon^{\mu\alpha} F_{\nu\alpha}. \quad (19.29)$$

Now take the symmetric limit according to the prescription (19.23). We find precisely the anomalous nonconservation equation (19.18). In this derivation, (19.18) appears as an operator relation, rather than in a simple matrix element. Notice that, as in our first derivation of this equation, the assumption of local gauge invariance played a crucial role. If we had defined the axial vector current by reversing the sign of the Wilson line in (19.22), a prescription that would have done violence to local gauge invariance, we would have found the various contributions canceling on the right-hand side of (19.29).

An Example with Fermion Number Nonconservation

To complete our discussion of the two-dimensional axial vector current, we will show that the nonconservation equation (19.18) also has a global aspect. In free fermion theory, the integral of the axial current conservation law gives

$$\int d^2x \partial_\mu j^{\mu 5} = N_R - N_L = 0. \quad (19.30)$$

This relation implies that the difference in the number of right-moving and left-moving fermions cannot be changed in any possible process. Combining this with the conservation law for the vector current, we conclude that the number of each type of fermion is separately conserved. From (19.8), we might conclude that these separate conservation laws hold also in two-dimensional QED. However, we have already found that we must be careful in making statements about the axial current.

In two-dimensional QED, the conservation equation for the axial current is replaced by the anomalous nonconservation equation (19.18). If the right-hand side of this equation were the total derivative of a quantity falling off sufficiently rapidly at infinity, its integral would vanish and we would still retain the global conservation law. In fact, $\epsilon^{\mu\nu} F_{\mu\nu}$ is a total derivative:

$$\epsilon^{\mu\nu} F_{\mu\nu} = 2\partial_\mu (\epsilon^{\mu\nu} A_\nu). \quad (19.31)$$

However, it is easy to imagine examples where the integral of this quantity does not vanish, for example, a world with a constant background electric field. In such a world, the conservation law (19.30) must be violated. But how can this happen?

Let us analyze this problem by thinking about fermions in one space dimension in a background A^1 field that is constant in space and has a very slow time dependence. We will assume that the system has a finite length L , with periodic boundary conditions. Notice that the constant A^1 field cannot be removed by a gauge transformation that satisfies the periodic boundary conditions. One way to see this is to note that the system gives a nonzero value to the Wilson line

$$\exp \left[-ie \int_0^L dx A_1(x) \right], \quad (19.32)$$

which forms a gauge-invariant closed loop due to the periodic boundary conditions.

Following the derivation of the three-dimensional Hamiltonian, Eq. (3.84), we find that the Hamiltonian of this one-dimensional system is

$$H = \int d^2x \psi^\dagger (-i\alpha^1 D_1) \psi, \quad (19.33)$$

where $\alpha = \gamma^0 \gamma^1 = \gamma^5$. In the components (19.7),

$$H = \int d^2x \left\{ -i\psi_+^\dagger (\partial_1 - ieA^1) \psi_+ + i\psi_-^\dagger (\partial_1 - ieA^1) \psi_- \right\}. \quad (19.34)$$

For a constant A^1 field, it is easy to diagonalize this Hamiltonian. The eigenstates of the covariant derivatives are wavefunctions

$$e^{ik_n x}, \quad \text{with} \quad k_n = \frac{2\pi n}{L}, \quad n = -\infty, \dots, \infty, \quad (19.35)$$

to satisfy the periodic boundary conditions. Then the single-particle eigenstates of H have energies

$$\begin{aligned} \psi_+ : \quad E_n &= + (k_n - eA^1), \\ \psi_- : \quad E_n &= - (k_n - eA^1). \end{aligned} \quad (19.36)$$

Each type of fermion has an infinite tower of equally spaced levels. To find the ground state of H , we fill the negative energy levels and interpret holes created among these filled states as antiparticles.

Now adiabatically change the value of A^1 . The fermion energy levels slowly shift in accord with the relations (19.36). If A^1 changes by the finite amount

$$\Delta A^1 = \frac{2\pi}{eL}, \quad (19.37)$$

which brings the Wilson loop (19.32) back to its original value, the spectrum of H returns to its original form. In this process, each level of ψ_+ moves down to the next position, and each level of ψ_- moves up to the next position, as shown in Fig. 19.2. The occupation numbers of levels should be maintained in this adiabatic process. Thus, remarkably, one right-moving fermion disappears from the vacuum and one extra left-moving fermion appears. At the same time,

$$\begin{aligned} \int d^2x \left(\frac{e}{\pi} \epsilon^{\mu\nu} F_{\mu\nu} \right) &= \int dt dx \frac{e}{\pi} \partial_0 A_1 \\ &= \frac{e}{\pi} L (-\Delta A^1) \\ &= -2, \end{aligned} \quad (19.38)$$

where we have inserted (19.37) in the last line. Thus the integrated form of the anomalous nonconservation equation (19.18) is indeed satisfied:

$$N_R - N_L = \int d^2x \left(\frac{e}{2\pi} \epsilon^{\mu\nu} F_{\mu\nu} \right). \quad (19.39)$$

Even in this simple example, we see that it is not possible to escape the question of ultraviolet regularization in analyzing the chiral conservation law. Right-moving fermions are lost and left-moving fermions appear from the depths of the fermionic spectrum, $E \rightarrow -\infty$. In computing the changes in the separate fermion numbers, we have assumed that the vacuum cannot change the charge it contains at large negative energies. This prescription is gauge invariant, but it leads to the nonconservation of the axial vector current.

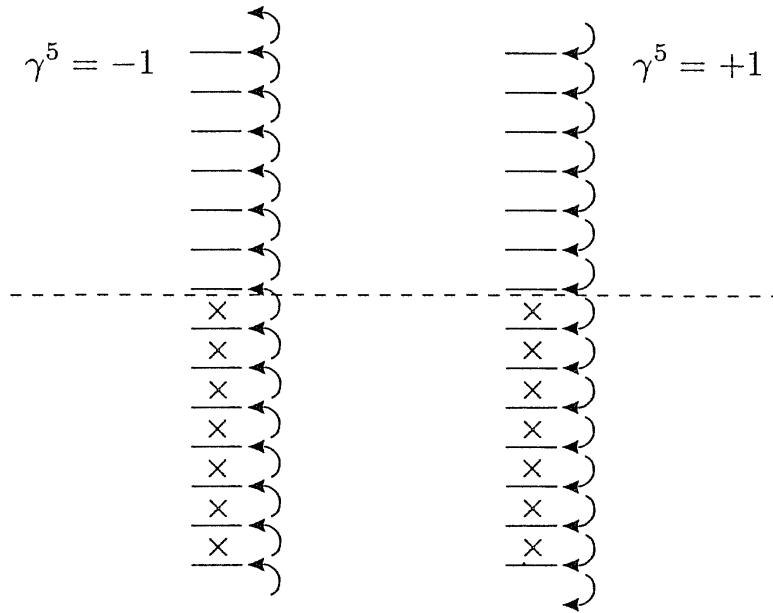


Figure 19.2. Effect on the vacuum state of the Hamiltonian H of one-dimensional QED due to an adiabatic change in the background A^1 field.

19.2 The Axial Current in Four Dimensions

All of the derivations we have just given for the two-dimensional axial current have analogues in four dimensions. In Eq. (3.40), we showed that, in the case of massless fermions, the four-dimensional Dirac equation splits neatly into separate equations for left- and right-handed fermions. If we couple the Dirac equation to a gauge field, we replace derivatives by covariant derivatives. This does not seem to affect the manifest separation between the two helicity components. Thus it seems clear that both the vector and axial vector currents should remain conserved. However, after the analysis we have just completed for the two-dimensional case, we know that we should not take these conservation laws for granted. We will now make a more careful analysis of the axial vector conservation law in four dimensions.

The Axial Vector Current Operator Equation

We begin with the case of massless four-dimensional QED. Of the three arguments that we gave in the previous section for the two-dimensional axial current conservation law, the operator derivation generalizes most easily. The fermion field equations (19.21) are identical in the four-dimensional case. We can again adopt the gauge-invariant definition of the axial vector current (19.22). When we take the divergence of this current, all of the manipulations leading to Eq. (19.25) are still correct.

From this point, we must compute the singular terms in the operator product of the two fermion fields in the limit $\epsilon \rightarrow 0$. As in two dimensions, the leading term is given by contracting the two operators using a free-field

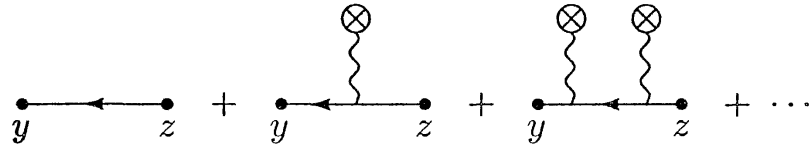


Figure 19.3. Expansion of $\psi(y)\bar{\psi}(z)$ in the presence of a background gauge field.

propagator. This contribution gives

$$\begin{aligned}
 \overline{\psi(y)\bar{\psi}(z)} &= \int \frac{d^4 k}{(2\pi)^4} e^{-ik \cdot (y-z)} \frac{i k}{k^2} \\
 &= -\not{\partial} \left(\frac{i}{2\pi^2} \frac{1}{(y-z)^2} \right) \\
 &= \frac{-i}{\pi^2} \frac{\gamma^\alpha (y-z)_\alpha}{(y-z)^4}.
 \end{aligned} \tag{19.40}$$

This is highly singular as $(y-z) \rightarrow 0$, but it gives zero when traced with $\gamma^\mu \gamma^5$. To find a nonzero result, we must consider terms of higher order in the expansion of the product of operators.

In a nonzero background gauge field, the contraction of fermion fields is given by the series of diagrams shown in Fig. 19.3. We have computed the leading term in this series in (19.40). The higher terms give less singular terms as $(y-z) \rightarrow 0$. The second term in the series is given by

$$\begin{aligned}
 \text{Diagram: } & \text{A fermion line from } y \text{ to } z \text{ with a gauge field loop attached to the } z \text{ end, followed by a circled cross symbol.} \\
 &= \int \frac{d^4 k}{(2\pi)^4} \frac{d^4 p}{(2\pi)^4} e^{-i(k+p) \cdot y} e^{ik \cdot z} \frac{i(k+p)}{(k+p)^2} (-ie\mathcal{A}(p)) \frac{i k}{k^2}.
 \end{aligned} \tag{19.41}$$

This contribution leads to

$$\begin{aligned}
 & \langle \bar{\psi}(x + \frac{\epsilon}{2}) \gamma^\mu \gamma^5 \psi(x - \frac{\epsilon}{2}) \rangle \\
 &= \int \frac{d^4 k}{(2\pi)^4} \frac{d^4 p}{(2\pi)^4} e^{ik \cdot \epsilon} e^{-ip \cdot x} \text{tr} \left[(-\gamma^\mu \gamma^5) \frac{i(k+p)}{(k+p)^2} (-ie\mathcal{A}(p)) \frac{i k}{k^2} \right] \\
 &= \int \frac{d^4 k}{(2\pi)^4} \frac{d^4 p}{(2\pi)^4} e^{ik \cdot \epsilon} e^{-ip \cdot x} \frac{4e\epsilon^{\mu\alpha\beta\gamma} (k+p)_\alpha A_\beta(p) k_\gamma}{k^2 (k+p)^2}.
 \end{aligned} \tag{19.42}$$

To evaluate the limit $\epsilon \rightarrow 0$, we can expand the integrand for large k . Then

$$\begin{aligned}
 \langle \bar{\psi}(x + \frac{\epsilon}{2}) \gamma^\mu \gamma^5 \psi(x - \frac{\epsilon}{2}) \rangle &\sim 4e\epsilon^{\mu\alpha\beta\gamma} \int \frac{d^4 p}{(2\pi)^4} e^{-ip \cdot x} p_\alpha A_\beta(p) \int \frac{d^4 k}{(2\pi)^4} e^{ik \cdot \epsilon} \frac{k_\gamma}{k^4} \\
 &= 4e\epsilon^{\alpha\beta\mu\gamma} (\partial_\alpha A_\beta(x)) \frac{\partial}{\partial \epsilon^\gamma} \left(\frac{i}{16\pi^2} \log \frac{1}{\epsilon^2} \right) \\
 &= 2e\epsilon^{\alpha\beta\mu\gamma} F_{\alpha\beta}(x) \left(\frac{-i}{8\pi^2} \frac{\epsilon_\gamma}{\epsilon^2} \right).
 \end{aligned} \tag{19.43}$$

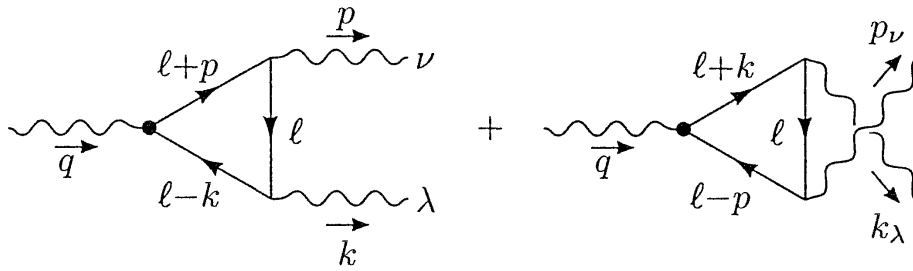


Figure 19.4. Diagrams contributing to the two-photon matrix element of the divergence of the axial vector current.

Substituting this expression into (19.25), we find

$$\partial_\mu j^{\mu 5} = \text{symm lim}_{\epsilon \rightarrow 0} \left\{ \frac{e}{4\pi^2} \epsilon^{\alpha\beta\mu\gamma} F_{\alpha\beta} \left(\frac{-i\epsilon\gamma}{\epsilon^2} \right) (-ie\epsilon^\nu F_{\mu\nu}) \right\}. \quad (19.44)$$

Now take the symmetric limit $\epsilon \rightarrow 0$ in four dimensions. We find

$$\partial_\mu j^{\mu 5} = -\frac{e^2}{16\pi^2} \epsilon^{\alpha\beta\mu\nu} F_{\alpha\beta} F_{\mu\nu}. \quad (19.45)$$

This equation, which expresses the anomalous nonconservation of the four-dimensional axial current, is known as the Adler-Bell-Jackiw anomaly. Adler and Bardeen proved that this operator relation is actually correct to all orders in QED perturbation theory and receives no further radiative corrections.[†]

Triangle Diagrams

We can confirm the Adler-Bell-Jackiw relation by checking, in standard perturbation theory, that the divergence of the axial vector current has a nonzero matrix element to create two photons. To do this, we must analyze the matrix element

$$\int d^4x e^{-iq \cdot x} \langle p, k | j^{\mu 5}(x) | 0 \rangle = (2\pi)^4 \delta^{(4)}(p + k - q) \epsilon_\nu^*(p) \epsilon_\lambda^*(k) \mathcal{M}^{\mu\nu\lambda}(p, k). \quad (19.46)$$

The leading-order diagrams contributing to $\mathcal{M}^{\mu\nu\lambda}$ are shown in Fig. 19.4. The first diagram gives the contribution

$$\text{Diagram} = (-1)(-ie)^2 \int \frac{d^4\ell}{(2\pi)^4} \text{tr} \left[\gamma^\mu \gamma^5 \frac{i(\ell - k)}{(\ell - k)^2} \gamma^\lambda \frac{i\ell}{\ell^2} \gamma^\nu \frac{i(\ell + p)}{(\ell + p)^2} \right], \quad (19.47)$$

and the second diagram gives an identical contribution with (p, ν) and (k, λ) interchanged.

It is easy to give a formal argument that the matrix element of the divergence of the axial current vanishes at this order. Taking the divergence of the axial current in (19.46) is equivalent to dotting this quantity with iq_μ .

[†]S. Adler and W. A. Bardeen, *Phys. Rev.* **182**, 1517 (1969); S. Adler, in Deser, et. al. (1970).

Now we operate on the right-hand side of (19.47) as we do to prove a Ward identity. Replace

$$q_\mu \gamma^\mu \gamma^5 = (\ell + p - \ell + k) \gamma^5 = (\ell + p) \gamma^5 + \gamma^5 (\ell - k). \quad (19.48)$$

Each momentum factor combines with the numerator adjacent to it to cancel the corresponding denominator. This brings (19.47) into the form

$$iq_\mu \cdot \text{Diagram} = e^2 \int \frac{d^4 \ell}{(2\pi)^4} \text{tr} \left[\gamma^5 \frac{(\ell - k)}{(\ell - k)^2} \gamma^\lambda \frac{\ell}{\ell^2} \gamma^\nu + \gamma^5 \gamma^\lambda \frac{\ell}{\ell^2} \gamma^\nu \frac{(\ell + p)}{(\ell + p)^2} \right]. \quad (19.49)$$

Now pass γ^ν through γ^5 in the second term and shift the integral over the first term according to $\ell \rightarrow (\ell + k)$:

$$iq_\mu \cdot \text{Diagram} = e^2 \int \frac{d^4 \ell}{(2\pi)^4} \text{tr} \left[\gamma^5 \frac{\ell}{\ell^2} \gamma^\lambda \frac{(\ell + k)}{(\ell + k)^2} \gamma^\nu - \gamma^5 \frac{\ell}{\ell^2} \gamma^\nu \frac{(\ell + p)}{(\ell + p)^2} \gamma^\lambda \right]. \quad (19.50)$$

This expression is manifestly antisymmetric under the interchange of (p, ν) and (k, λ) , so the contribution of the second diagram in Fig. 19.4 precisely cancels (19.47).

However, because this derivation involves a shift of the integration variable, we should look closely at whether this shift is allowed by the regularization. From (19.47), we see that the integral that must be shifted is divergent. If the diagram is regulated with a simple momentum cutoff, or even with Pauli-Villars regularization, it turns out that the shift leaves over a finite, nonzero term. In Chapter 7, we encountered a similar problem in our discussion of the QED vacuum polarization diagram. We evaded the problem there by using dimensional regularization. Dimensional regularization of the diagrams of Fig. 19.4 will automatically insure the validity of the QED Ward identities for the photon emission vertices,

$$p_\nu \mathcal{M}^{\mu\nu\lambda} = k_\lambda \mathcal{M}^{\mu\nu\lambda} = 0. \quad (19.51)$$

But in the analysis of the axial vector current, even dimensional regularization has an extra subtlety, because γ^5 is an intrinsically four-dimensional object. In their original paper on dimensional regularization,[†] 't Hooft and Veltman suggested using the definition

$$\gamma^5 = i \gamma^0 \gamma^1 \gamma^2 \gamma^3 \quad (19.52)$$

in d dimensions. This definition has the consequence that γ^5 anticommutes with γ^μ for $\mu = 0, 1, 2, 3$ but commutes with γ^μ for other values of μ .

In the evaluation of (19.47), the external indices and the momenta p , k , q all live in the physical four dimensions, but the loop momentum ℓ has components in all dimensions. Write

$$\ell = \ell_{\parallel} + \ell_{\perp}, \quad (19.53)$$

[†]G. 't Hooft and M. J. G. Veltman, *Nucl. Phys.* **B44**, 189 (1972).

where the first term has nonzero components in dimensions 0, 1, 2, 3 and the second term has nonzero components in the other $d-4$ dimensions. Because γ^5 commutes with the γ^μ in these extra dimensions, identity (19.48) is modified to

$$q_\mu \gamma^\mu \gamma^5 = (\not{\ell} + \not{k}) \gamma^5 + \gamma^5 (\not{\ell} - \not{p}) - 2\gamma^5 \not{\ell}_\perp. \quad (19.54)$$

The first two terms cancel according to the argument given above; the shift in (19.50) is justified by the dimensional regularization. However, the third term of (19.54) gives an additional contribution:

$$iq_\mu \cdot \text{Diagram} = e^2 \int \frac{d^4 \ell}{(2\pi)^4} \text{tr} \left[-2\gamma^5 \not{\ell}_\perp \frac{(\not{\ell} - \not{k})}{(\ell - k)^2} \gamma^\lambda \frac{\not{\ell}}{\ell^2} \gamma^\nu \frac{(\not{\ell} + \not{p})}{(\ell + p)^2} \right]. \quad (19.55)$$

To evaluate this contribution, combine denominators in the standard way, and shift the integration variable $\ell \rightarrow \ell + P$, where $P = xk - yp$. In expanding the numerator, we must retain one factor each of γ^ν , γ^λ , \not{p} , and \not{k} to give a nonzero trace with γ^5 . This leaves over one factor of $\not{\ell}_\perp$ and one factor of $\not{\ell}$ which must also be evaluated with components in extra dimensions in order to give a nonzero integral. The factors $\not{\ell}_\perp$ anticommute with the other Dirac matrices in the problem and thus can be moved to adjacent positions. Then we must evaluate the integral

$$\int \frac{d^4 \ell}{(2\pi)^4} \frac{\not{\ell}_\perp \not{\ell}_\perp}{(\ell^2 - \Delta)^3}, \quad (19.56)$$

where Δ is a function of k , p , and the Feynman parameters. Using

$$(\not{\ell}_\perp)^2 = \ell_\perp^2 \rightarrow \frac{(d-4)}{d} \ell^2 \quad (19.57)$$

under the symmetrical integration, we can evaluate (19.56) as

$$\frac{i}{(4\pi)^{d/2}} \frac{(d-4)}{2} \frac{\Gamma(2-\frac{d}{2})}{\Gamma(3)\Delta^{2-d/2}} \xrightarrow{d \rightarrow 4} \frac{-i}{2(4\pi)^2}. \quad (19.58)$$

Notice the behavior in which a logarithmically divergent integral contributes a factor $(d-4)$ in the denominator and allows an anomalous term, formally proportional to $(d-4)$, to give a finite contribution. The remainder of the algebra in the evaluation of (19.55) is straightforward. The terms involving the momentum shift P cancel, and we find

$$\begin{aligned} iq_\mu \cdot \text{Diagram} &= e^2 \left(\frac{-i}{2(4\pi)^2} \right) \text{tr} [2\gamma^5 (-\not{k}) \gamma^\lambda \not{p} \gamma^\nu] \\ &= \frac{e^2}{4\pi^2} \epsilon^{\alpha\lambda\beta\nu} k_\alpha p_\beta. \end{aligned} \quad (19.59)$$

This term is symmetric under the interchange of (p, ν) with (k, λ) , so the second diagram of Fig. 19.4 gives an equal contribution. Thus,

$$\begin{aligned} \langle p, k | \partial_\mu j^{\mu 5}(0) | 0 \rangle &= -\frac{e^2}{2\pi^2} \epsilon^{\alpha\nu\beta\lambda} (-ip_\alpha) \epsilon_\nu^*(p) (-ik_\beta) \epsilon_\lambda^*(k) \\ &= -\frac{e^2}{16\pi^2} \langle p, k | \epsilon^{\alpha\nu\beta\lambda} F_{\alpha\nu} F_{\beta\lambda}(0) | 0 \rangle, \end{aligned} \quad (19.60)$$

as we would expect from the Adler-Bell-Jackiw anomaly equation.

Chiral Transformation of the Functional Integral

A third way of understanding the Adler-Bell-Jackiw anomaly comes from analyzing the conservation law for the axial vector current from the functional integral for the fermion field. In Section 9.6, we used the functional integral to derive the current conservation equations and the Ward identities associated with any symmetry of the Lagrangian. It is instructive to see how this argument breaks down when we apply it to the chiral symmetry of massless fermions.

We first review the standard derivation of the axial vector Ward identities following the method of Section 9.6. Starting from the fermionic functional integral

$$Z = \int \mathcal{D}\psi \mathcal{D}\bar{\psi} \exp \left[i \int d^4x \bar{\psi}(iD)\psi \right], \quad (19.61)$$

make the change of variables

$$\begin{aligned} \psi(x) &\rightarrow \psi'(x) = (1 + i\alpha(x)\gamma^5)\psi(x), \\ \bar{\psi}(x) &\rightarrow \bar{\psi}'(x) = \bar{\psi}(1 + i\alpha(x)\gamma^5). \end{aligned} \quad (19.62)$$

Since the global chiral rotation, with constant α , is a symmetry of the Lagrangian, the only new terms in the Lagrangian that result from (19.62) contain derivatives of α . Thus,

$$\begin{aligned} \int d^4x \bar{\psi}'(iD)\psi' &= \int d^4x [\bar{\psi}(iD)\psi - \partial_\mu \alpha(x) \bar{\psi}\gamma^\mu\gamma^5\psi] \\ &= \int d^4x [\bar{\psi}(iD)\psi + \alpha(x)\partial_\mu(\bar{\psi}\gamma^\mu\gamma^5\psi)]. \end{aligned} \quad (19.63)$$

Then, by varying the Lagrangian with respect to $\alpha(x)$, we derive the classical conservation equation for the axial current. By carrying out a similar manipulation on the functional expression for a correlation function, as in Eq. (9.102), we would derive the associated Ward identities.

In the argument just given, we assumed that the functional measure does not change when we change variables from $\psi'(x)$ to ψ . This seems reasonable, because the relation of ψ' and ψ in (19.62) looks like a unitary transformation. However, we should examine this point more closely.* First, we must carefully

*K. Fujikawa, *Phys. Rev. Lett.* **42**, 1195 (1979); *Phys. Rev. D* **21**, 2848 (1980).

define the functional measure. To do this, expand the fermion field in a basis of eigenstates of \not{D} . Define right and left eigenvectors of \not{D} by

$$(i\not{D})\phi_m = \lambda_m \phi_m, \quad \hat{\phi}_m(i\not{D}) = -iD_\mu \hat{\phi}_m \gamma^\mu = \lambda_m \hat{\phi}_m. \quad (19.64)$$

For zero background A_μ field, these eigenstates are Dirac wavefunctions of definite momentum; the eigenvalues satisfy

$$\lambda_m^2 = k^2 = (k^0)^2 - (\mathbf{k})^2. \quad (19.65)$$

For a fixed A_μ field, this is also the asymptotic form of the eigenvalues for large k . These eigenfunctions give us a basis that we can use to expand ψ and $\bar{\psi}$:

$$\psi(x) = \sum_m a_m \phi_m(x), \quad \bar{\psi}(x) = \sum_m \hat{a}_m \hat{\phi}_m(x), \quad (19.66)$$

where a_m, \hat{a}_m are anticommuting coefficients multiplying the c-number eigenfunctions (19.64). The functional measure over $\psi, \bar{\psi}$ can then be defined as

$$\mathcal{D}\psi \mathcal{D}\bar{\psi} = \prod_m da_m d\hat{a}_m, \quad (19.67)$$

and the functional measure over $\psi', \bar{\psi}'$ can be defined in the same way.

If $\psi'(x) = (1 + i\alpha(x)\gamma^5)\psi(x)$, the expansion coefficients of ψ and ψ' are related by a infinitesimal linear transformation $(1 + C)$, computed as follows:

$$a'_m = \sum_n \int d^4x \phi_m^\dagger(x) (1 + i\alpha(x)\gamma^5) \phi_n(x) a_n = \sum_n (\delta_{mn} + C_{mn}) a_n. \quad (19.68)$$

Then

$$\mathcal{D}\psi' \mathcal{D}\bar{\psi}' = \mathcal{J}^{-2} \cdot \mathcal{D}\psi \mathcal{D}\bar{\psi}, \quad (19.69)$$

where \mathcal{J} is the Jacobian determinant of the transformation $(1 + C)$. The inverse of \mathcal{J} appears in (19.69) as a result of the rule (9.63) or (9.69) for fermionic integration. To evaluate \mathcal{J} , we write

$$\mathcal{J} = \det(1 + C) = \exp[\text{tr} \log(1 + C)] = \exp\left[\sum_n C_{nn} + \dots\right], \quad (19.70)$$

and we can ignore higher order terms in the last line because C is infinitesimal. Thus,

$$\log \mathcal{J} = i \int d^4x \alpha(x) \sum_n \phi_n^\dagger(x) \gamma^5 \phi_n(x). \quad (19.71)$$

The coefficient of $\alpha(x)$ looks like $\text{tr}[\gamma^5] = 0$. However, we must regularize the sum over eigenstates n in a gauge-invariant way. The natural choice is

$$\sum_n \phi_n^\dagger(x) \gamma^5 \phi_n(x) = \lim_{M \rightarrow \infty} \sum_n \phi_n^\dagger(x) \gamma^5 \phi_n(x) e^{\lambda_n^2/M^2}. \quad (19.72)$$

As (19.65) indicates, the sign of λ_n^2 will be negative at large momentum after a Wick rotation; thus, the sign in the exponent of the convergence factor is given correctly. We can write (19.72) in an operator form

$$\begin{aligned} \sum_n \phi_n^\dagger(x) \gamma^5 \phi_n(x) &= \lim_{M \rightarrow \infty} \sum_n \phi_n^\dagger(x) \gamma^5 e^{(iD)^2/M^2} \phi_n(x) \\ &= \lim_{M \rightarrow \infty} \langle x | \text{tr} [\gamma^5 e^{(iD)^2/M^2}] | x \rangle, \end{aligned} \quad (19.73)$$

where, in the second line, we trace over Dirac indices.

To evaluate (19.73), we rewrite $(iD)^2$ according to (16.107). In our present conventions, this equation reads

$$(iD)^2 = -D^2 + \frac{e}{2} \sigma^{\mu\nu} F_{\mu\nu}, \quad (19.74)$$

with $\sigma^{\mu\nu} = \frac{i}{2} [\gamma^\mu, \gamma^\nu]$. Since we are taking the limit $M \rightarrow \infty$, we can concentrate our attention on the asymptotic part of the spectrum, where the momentum k is large and we can expand in powers of the gauge field. To obtain a nonzero trace with γ^5 , we must bring down four Dirac matrices from the exponent. The leading term is given by expanding the exponent to order $(\sigma \cdot F)^2$, and then ignoring the background A_μ field in all other terms. This gives

$$\begin{aligned} &\lim_{M \rightarrow \infty} \langle x | \text{tr} [\gamma^5 e^{(-D^2 + (e/2)\sigma \cdot F)/M^2}] | x \rangle \\ &= \lim_{M \rightarrow \infty} \text{tr} \left[\gamma^5 \frac{1}{2!} \left(\frac{e}{2M^2} \sigma^{\mu\nu} F_{\mu\nu}(x) \right)^2 \right] \langle x | e^{-\partial^2/M^2} | x \rangle. \end{aligned} \quad (19.75)$$

The matrix element in (19.75) can be evaluated by a Wick rotation:

$$\begin{aligned} \langle x | e^{-\partial^2/M^2} | x \rangle &= \lim_{x \rightarrow y} \int \frac{d^4 k}{(2\pi)^4} e^{-ik \cdot (x-y)} e^{k^2/M^2} \\ &= i \int \frac{d^4 k_E}{(2\pi)^4} e^{-k_E^2/M^2} \\ &= i \frac{M^4}{16\pi^2}. \end{aligned} \quad (19.76)$$

Then (19.75) reduces to

$$\begin{aligned} &\lim_{M \rightarrow \infty} \frac{-ie^2}{8 \cdot 16\pi^2} M^4 \text{tr} \left[\gamma^5 \gamma^\mu \gamma^\nu \gamma^\lambda \gamma^\sigma \frac{1}{(M^2)^2} F_{\mu\nu} F_{\lambda\sigma}(x) \right] \\ &= -\frac{e^2}{32\pi^2} \epsilon^{\alpha\beta\mu\nu} F_{\alpha\beta} F_{\mu\nu}(x). \end{aligned} \quad (19.77)$$

Thus,

$$\mathcal{J} = \exp \left[-i \int d^4 x \alpha(x) \left(\frac{e^2}{16\pi^2} \epsilon^{\mu\nu\lambda\sigma} F_{\mu\nu} F_{\lambda\sigma}(x) \right) \right]. \quad (19.78)$$

In all, we find that, after the change of variables (19.62), the functional integral (19.61) takes the form

$$Z = \int \mathcal{D}\psi \mathcal{D}\bar{\psi} \exp \left[i \int d^4x \left(\bar{\psi}(iD)\psi + \alpha(x) \left\{ \partial_\mu j^{\mu 5} + \frac{e^2}{16\pi^2} \epsilon^{\mu\nu\lambda\sigma} F_{\mu\nu} F_{\lambda\sigma} \right\} \right) \right]. \quad (19.79)$$

Varying the exponent with respect to $\alpha(x)$, we find precisely the Adler-Bell-Jackiw anomaly equation.

This derivation of the axial vector anomaly is especially interesting because it generalizes readily to any even dimensionality. The functional derivation always picks out for the right-hand side of the anomaly equation the pseudoscalar operator built from gauge fields that has the same dimension, d , as the divergence of the current. In two dimensions, this derivation leads immediately to (19.18). As long as d is even, we can always construct a matrix γ^5 that anticommutes with all of the Dirac matrices by taking their product. Then, the functional derivation leads straightforwardly to the result

$$\partial_\mu j^{\mu 5} = (-1)^{n+1} \frac{2e^n}{n!(4\pi)^n} \epsilon^{\mu_1\mu_2\cdots\mu_{2n}} F_{\mu_1\mu_2} \cdots F_{\mu_{2n-1}\mu_{2n}}, \quad (19.80)$$

where $n = d/2$.

At the end of the previous section, we argued that the axial vector anomaly leads to global nonconservation of fermionic charges in a two-dimensional system with a macroscopic electric field. In the same way, the four-dimensional anomaly equation leads to global nonconservation of the number of left- and right-handed fermions in background fields in which the right-hand side of (19.45) is nonzero. These are field configurations with parallel electric and magnetic fields. In Problem 19.1, we work out an example of four-dimensional massless fermions in a simple situation of this type and show that the fermion numbers are indeed violated, in a manner similar to what we saw at the end of Section 19.1, in accord with the Adler-Bell-Jackiw anomaly.

19.3 Goldstone Bosons and Chiral Symmetries in QCD

The Adler-Bell-Jackiw anomaly has a number of important implications for QCD. To describe these, we must first discuss the chiral symmetries of QCD systematically. In this discussion, we will ignore all but the lightest quarks u and d . In many analyses of the low-energy structure of the strong interactions, one also treats the s quark as light; this gives results that naturally generalize the ones we will find below.

The fermionic part of the QCD Lagrangian is

$$\mathcal{L} = \bar{u}iD\bar{u} + \bar{d}iD\bar{d} - m_u \bar{u}u - m_d \bar{d}d. \quad (19.81)$$

If the u and d quarks are very light, the last two terms are small and can be neglected. Let us study the implications of making this approximation. If

we ignore the u and d masses, the Lagrangian (19.81) of course has isospin symmetry, the symmetry of an $SU(2)$ unitary transformation mixing the u and d fields. However, because the classical Lagrangian for massless fermions contains no coupling between left- and right-handed quarks, this Lagrangian actually is symmetric under the separate unitary transformations

$$\begin{pmatrix} u \\ d \end{pmatrix}_L \rightarrow U_L \begin{pmatrix} u \\ d \end{pmatrix}_L, \quad \begin{pmatrix} u \\ d \end{pmatrix}_R \rightarrow U_R \begin{pmatrix} u \\ d \end{pmatrix}_R. \quad (19.82)$$

It is useful to separate the $U(1)$ and $SU(2)$ parts of these transformations; then the symmetry group of the classical, massless QCD Lagrangian is $SU(2) \times SU(2) \times U(1) \times U(1)$. Let Q denote the quark doublet, with chiral components

$$Q_L = \left(\frac{1-\gamma^5}{2} \right) \begin{pmatrix} u \\ d \end{pmatrix}, \quad Q_R = \left(\frac{1+\gamma^5}{2} \right) \begin{pmatrix} u \\ d \end{pmatrix}. \quad (19.83)$$

Then we can write the currents associated with these symmetries as

$$\begin{aligned} j_L^\mu &= \bar{Q}_L \gamma^\mu Q_L, & j_R^\mu &= \bar{Q}_R \gamma^\mu Q_R, \\ j_L^{\mu a} &= \bar{Q}_L \gamma^\mu Q_L \tau^a, & j_R^{\mu a} &= \bar{Q}_R \gamma^\mu \tau^a Q_R, \end{aligned} \quad (19.84)$$

where $\tau^a = \sigma^a/2$ represent the generators of $SU(2)$. The sums of left- and right-handed currents give the baryon number and isospin currents

$$j^\mu = \bar{Q} \gamma^\mu Q, \quad j^{\mu a} = \bar{Q} \gamma^\mu \tau^a Q. \quad (19.85)$$

The corresponding symmetries are the transformations (19.82) with $U_L = U_R$. The differences of the currents (19.84) give the corresponding axial vector currents $j^{\mu 5}$, $j^{\mu 5a}$:

$$j^{\mu 5} = \bar{Q} \gamma^\mu \gamma^5 Q, \quad j^{\mu 5a} = \bar{Q} \gamma^\mu \gamma^5 \tau^a Q. \quad (19.86)$$

In the discussion to follow, we will derive conclusions about the strong interactions by assuming that the classical conservation laws for these currents are not spoiled by anomalies. We will show below that this assumption is correct for the isotriplet currents $j^{\mu 5a}$ but not for $j^{\mu 5}$.

The vector $SU(2) \times U(1)$ transformations are manifest symmetries of the strong interactions, and the associated currents lead to familiar conservation laws. What about the orthogonal, axial vector, transformations? These do not correspond to any obvious symmetry of the strong interactions. In 1960, Nambu and Jona-Lasinio hypothesized that these are accurate symmetries of the strong interactions that are spontaneously broken.[†] This idea has led to a correct and surprisingly detailed description of the properties of the strong interactions at low energy.

[†]Y. Nambu and G. Jona-Lasinio, *Phys. Rev.* **122**, 345 (1961).

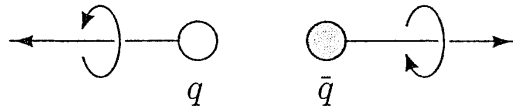


Figure 19.5. A quark-antiquark pair with zero total momentum and angular momentum.

Spontaneous Breaking of Chiral Symmetry

Before we describe the consequences of spontaneously broken chiral symmetry, let us ask why we might expect the chiral symmetries to be spontaneously broken in the first place. In the theory of superconductivity, a small electron-electron attraction leads to the appearance of a condensate of electron pairs in the ground state of a metal. In QCD, quarks and antiquarks have strong attractive interactions, and, if these quarks are massless, the energy cost of creating an extra quark-antiquark pair is small. Thus we expect that the vacuum of QCD will contain a condensate of quark-antiquark pairs. These fermion pairs must have zero total momentum and angular momentum. Thus, as Fig. 19.5 shows, they must contain net chiral charge, pairing left-handed quarks with the antiparticles of right-handed quarks. The vacuum state with a quark pair condensate is characterized by a nonzero vacuum expectation value for the scalar operator

$$\langle 0 | \bar{Q} Q | 0 \rangle = \langle 0 | \bar{Q}_L Q_R + \bar{Q}_R Q_L | 0 \rangle \neq 0, \quad (19.87)$$

which transforms under (19.82) with $U_L \neq U_R$. The expectation value signals that the vacuum mixes the two quark helicities. This allows the u and d quarks to acquire effective masses as they move through the vacuum. Inside quark-antiquark bound states, the u and d quarks would appear to move as if they had a sizable effective mass, even if they had zero mass in the original QCD Lagrangian.

The vacuum expectation value (19.87) signals the spontaneous breaking of the full symmetry group (19.82) down to the subgroup of vector symmetries with $U_L = U_R$. Thus there are four spontaneously broken continuous symmetries, associated with the four axial vector currents. At the end of Section 11.1, we proved Goldstone's theorem, which states that every spontaneously broken continuous symmetry of a quantum field theory leads to a massless particle with the quantum numbers of a local symmetry rotation. This means that, in QCD with massless u and d quarks, we should find four spin-zero particles with the correct quantum numbers to be created by the four axial vector currents.

The real strong interactions do not contain any massless particles, but they do contain an isospin triplet of relatively light mesons, the pions. These particles are known to have odd parity (as we expect if they are quark-antiquark bound states). Thus, they can be created by the axial isospin currents. We can parametrize the matrix element of $j^{\mu 5a}$ between the vacuum

and an on-shell pion by writing

$$\langle 0 | j^{\mu 5a}(x) | \pi^b(p) \rangle = -ip^\mu f_\pi \delta^{ab} e^{-ip \cdot x}, \quad (19.88)$$

where a, b are isospin indices and f_π is a constant with the dimensions of (mass)¹. We show in Problem 19.2 that the value of f_π can be determined from the rate of π^+ decay through the weak interaction; one finds $f_\pi = 93$ MeV. For this reason, f_π is often called the *pion decay constant*. If we contract (19.88) with p_μ and use the conservation of the axial currents, we find that an on-shell pion must satisfy $p^2 = 0$, that is, it must be massless, as required by Goldstone's theorem.

If we now restore the quark mass terms in (19.81), the axial currents are no longer exactly conserved. The equation of motion of the quark field is now

$$iD^\mu Q = \mathbf{m}Q, \quad -iD_\mu \bar{Q}\gamma^\mu = \bar{Q}\mathbf{m}, \quad (19.89)$$

where

$$\mathbf{m} = \begin{pmatrix} m_u & 0 \\ 0 & m_d \end{pmatrix} \quad (19.90)$$

is the quark mass matrix. Then one can readily compute

$$\partial_\mu j^{\mu 5a} = i\bar{Q}\{\mathbf{m}, \tau^b\}Q. \quad (19.91)$$

Using this equation together with (19.88), we find

$$\langle 0 | \partial_\mu j^{\mu 5a}(0) | \pi^b(p) \rangle = -p^2 f_\pi \delta^{ab} = \langle 0 | i\bar{Q}\{\mathbf{m}, \tau^a\} | \pi^b(p) \rangle. \quad (19.92)$$

The last expression is an invariant quantity times

$$\text{tr}[\{\mathbf{m}, \tau^a\}\tau^b] = \frac{1}{2}\delta^{ab}(m_u + m_d). \quad (19.93)$$

Thus, the quark mass terms give the pions masses of the form

$$m_\pi^2 = (m_u + m_d) \frac{M^2}{f_\pi}. \quad (19.94)$$

The mass parameter M has been estimated to be of order 400 MeV. Thus, to give the observed pion mass of 140 MeV, one needs only $(m_u + m_d) \sim 10$ MeV. This is a small perturbation on the strong interactions.

This argument has an interesting implication for the nature of the isospin symmetry of the strong interactions. In the limit in which the u and d quarks have zero mass in the Lagrangian, these quarks acquire large, equal effective masses from the vacuum with spontaneously broken chiral symmetry. As long as the masses m_u and m_d in the Lagrangian are small compared to the effective mass, the u and d quarks will behave inside hadrons as though they are approximately degenerate. Thus the isospin symmetry of the strong interactions need have nothing to do with a fundamental symmetry linking u and d ; it follows for any arbitrary relation between m_u and m_d , provided that both of these parameters are much less than 300 MeV. Similarly, the approximate $SU(3)$ symmetry of the strong interactions follows if the fundamental mass of the s quark is also small compared to the strong interaction scale. The best

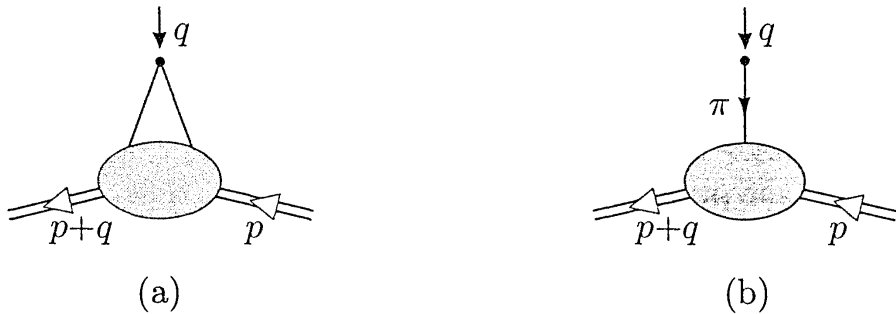


Figure 19.6. Matrix element of the axial isospin current in the nucleon: (a) kinematics of the amplitude; (b) contribution that leads to a pole in q^2 .

current estimates of the mass ratios $m_u : m_d : m_s$ are in fact $1 : 2 : 40$, so that the fundamental Lagrangian of the strong interactions shows no sign of flavor symmetry among the quark masses.[‡]

The identification of the pions as Goldstone bosons of broken chiral symmetry has a number of implications for hadronic matrix elements. Here we will give only one example. In the following argument, we will work in the limit of exact chiral symmetry, ignoring the small corrections from the u and d masses.

The matrix element of the axial isospin current in the nucleon, a quantity that enters the theory of neutron and nuclear β decay, can be written in terms of form factors as follows:

$$\langle N | j^{\mu 5a}(q) | N \rangle = \bar{u} \left[\gamma^\mu \gamma^5 F_1^5(q^2) + \frac{i \sigma^{\mu\nu} q_\nu}{2m} F_2^5(q^2) + q^\mu \gamma^5 F_3^5(q^2) \right] u. \quad (19.95)$$

The kinematics of the vertex is shown in Fig. 19.6. Notice that there is one more possible form factor than in the vector case, Eq. (6.33). The value of F_1^5 at $q^2 = 0$ is not restricted by the value of any manifestly conserved charge. Conventionally, one writes simply

$$F_1^5(0) = g_A. \quad (19.96)$$

However, we will now show that the value of this quantity can be computed.

If we ignore quark masses, the axial vector current in (19.95) is conserved, so the form factors satisfy

$$\begin{aligned} 0 &= \bar{u}(p') \left[q^\mu \gamma^5 F_1^5(q^2) + q^2 \gamma^5 F_3^5(q^2) \right] u(p) \\ &= \bar{u}(p') \left[(p' - p)^\mu \gamma^5 F_1^5(q^2) + q^2 \gamma^5 F_3^5(q^2) \right] u(p) \\ &= \bar{u}(p') \left[2m_N \gamma^5 F_1^5(q^2) + q^2 \gamma^5 F_3^5(q^2) \right] u(p). \end{aligned} \quad (19.97)$$

[‡]The determination of the fundamental quark masses is reviewed by J. Gasser and H. Leutwyler, *Phys. Repts.* **8**, 77 (1982).

Thus, we find

$$g_A = \lim_{q^2 \rightarrow 0} \frac{q^2}{2m_N} F_3^5(q^2). \quad (19.98)$$

This equation implies that $g_A = 0$ unless F_3^5 contains a pole in q^2 . Such a pole would imply the presence of a physical massless particle, but fortunately, there is one available—the massless pion. The process in which the current creates a pion that is then absorbed by the nucleon indeed leads to a pole in $F_3^5(q^2)$, as shown in Fig. 19.6(b).

Let us now compute this pole term and use it to determine g_A . The low-energy pion-nucleon interaction is conventionally parametrized by the Lagrangian

$$\Delta\mathcal{L} = ig_{\pi NN}\pi^a \bar{N} \gamma^5 \sigma^a N. \quad (19.99)$$

The amplitude for the current $j^{\mu 5a}$ to create the pion is given by (19.88). Then the contribution of Fig. 19.6(b) to the current vertex is

$$-g_{\pi NN}\bar{u}(2\tau^a\gamma^5)u \cdot \frac{i}{q^2} \cdot (iq^\mu f_\pi). \quad (19.100)$$

Thus,

$$F_3^5(q^2) = \frac{1}{q^2} \cdot 2f_\pi g_{\pi NN}. \quad (19.101)$$

We find that g_A is given by a combination of f_π , the nucleon mass, and the pion-nucleon coupling constant:

$$g_A = \frac{m_N}{f_\pi} g_{\pi NN}. \quad (19.102)$$

This strange identity, called the *Goldberger-Trieman relation*, is satisfied experimentally to 5% accuracy.

The identification of the pion as the Goldstone boson of spontaneously broken chiral symmetry leads to numerous other predictions for current matrix elements and pion scattering amplitudes. In particular, the leading terms of the pion-pion and pion-nucleon scattering amplitudes at low energy can be computed directly in terms of f_π by arguments similar to one just given.*

Anomalies of Chiral Currents

Up to this point, we have discussed the chiral symmetries of QCD according to the classical current conservation equations. We must now ask whether these equations are affected by the Adler-Bell-Jackiw anomaly, and what the consequences of that modification are.

To begin, we study the modification of the chiral conservation laws due to the coupling of the quark currents to the gluon fields of QCD. The arguments given in the previous section go through equally well in the case of

*The detailed consequences of spontaneously broken chiral symmetry are worked out in a very clear manner in Georgi (1984).

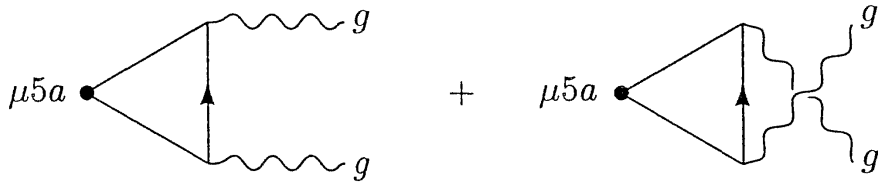


Figure 19.7. Diagrams that lead to an axial vector anomaly for a chiral current in QCD.

massless fermions coupling to a non-Abelian gauge field, so we expect that an axial vector current will receive an anomalous contribution from the diagrams shown in Fig. 19.7. The anomaly equation should be the Abelian result, supplemented by an appropriate group theory factor. In addition, since the axial current is gauge invariant, the anomaly must also be gauge invariant. That is, it must contain the full non-Abelian field strength, including its nonlinear terms. These terms are actually included in the functional derivation of the anomaly given at the end of Section 19.2.

For the axial currents of QCD, written in (19.86), we can read the group theory factors for the Adler-Bell-Jackiw anomaly from the diagrams of Fig. 19.7. For the axial isospin currents,

$$\partial_\mu j^{\mu 5a} = -\frac{g^2}{16\pi^2} \epsilon^{\alpha\beta\mu\nu} F_{\alpha\beta}^c F_{\mu\nu}^d \cdot \text{tr}[\tau^a t^c t^d], \quad (19.103)$$

where $F_{\mu\nu}^c$ is a gluon field strength, τ^a is an isospin matrix, t^c is a color matrix, and the trace is taken over colors and flavors. In this case, we find

$$\text{tr}[\tau^a t^c t^d] = \text{tr}[\tau^a] \text{tr}[t^c t^d] = 0, \quad (19.104)$$

since the trace of a single τ^a vanishes. Thus the conservation of the axial isospin currents is unaffected by the Adler-Bell-Jackiw anomaly of QCD. However, in the case of the isospin singlet axial current, the matrix τ^a is replaced by the matrix 1 on flavors, and we find

$$\partial_\mu j^{\mu 5} = -\frac{g^2 n_f}{32\pi^2} \epsilon^{\alpha\beta\mu\nu} F_{\alpha\beta}^c F_{\mu\nu}^c, \quad (19.105)$$

where n_f is the number of flavors; $n_f = 2$ in our current model.

Thus, the isospin singlet axial current is not in fact conserved in QCD. The divergence of this current is equal to a gluon operator with nontrivial matrix elements between hadron states. Some subtle questions remain concerning the effects of this operator. In particular, it can be shown, as we saw for the two-dimensional axial anomaly in Eq. (19.31), that the right-hand side of (19.105) is a total divergence. Nevertheless, again in accord with our experience in two dimensions, there are physically reasonable field configurations in which the four-dimensional integral of this term takes a nonzero value. This topic is discussed further at the end of Section 22.3. In any event, Eq. (19.105) indeed implies that QCD has no isosinglet axial symmetry and no associated Goldstone boson. This equation explains why the strong interactions contain

no light isosinglet pseudoscalar meson with mass comparable to that of the pions.

Though the axial isospin currents have no axial anomaly from QCD interactions, they do have an anomaly associated with the coupling of quarks to electromagnetism. Again referring to the diagrams of Fig. 19.7, we see that the electromagnetic anomaly of the axial isospin currents is given by

$$\partial_\mu j^{\mu 5a} = -\frac{e^2}{16\pi^2} \epsilon^{\alpha\beta\mu\nu} F_{\alpha\beta} F_{\mu\nu} \cdot \text{tr}[\tau^a Q^2], \quad (19.106)$$

where $F_{\mu\nu}$ is the electromagnetic field strength, Q is the matrix of quark electric charges,

$$Q = \begin{pmatrix} \frac{2}{3} & 0 \\ 0 & -\frac{1}{3} \end{pmatrix}, \quad (19.107)$$

and the trace again runs over flavors and colors. Since the matrices in the trace do not depend on color, the color sum simply gives a factor of 3. The flavor trace is nonzero only for $a = 3$; in that case, the electromagnetic anomaly is

$$\partial_\mu j^{\mu 53} = -\frac{e^2}{32\pi^2} \epsilon^{\alpha\beta\mu\nu} F_{\alpha\beta} F_{\mu\nu}. \quad (19.108)$$

Because the current $j^{\mu 53}$ annihilates a π^0 meson, Eq. (19.108) indicates that the axial vector anomaly contributes to the matrix element for the decay $\pi^0 \rightarrow 2\gamma$. We will now show that, in fact, it gives the leading contribution to this amplitude. Again, we work in the limit of massless u and d quarks, so that the chiral symmetries are exact up to the effects of the anomaly.

Consider the matrix element of the axial current between the vacuum and a two-photon state:

$$\langle p, k | j^{\mu 53}(q) | 0 \rangle = \epsilon_\nu^* \epsilon_\lambda^* \mathcal{M}^{\mu\nu\lambda}(p, k). \quad (19.109)$$

This is the same matrix element (19.46) that we studied in QED perturbation theory in Section 19.2. Now, however, we will study the general properties of this matrix element by expanding it in form factors. In general, the amplitude can be decomposed by writing all possible tensor structures and applying the restrictions that follow from symmetry under the interchange of (p, ν) and (k, λ) and the QED Ward identities (19.51). This leaves three possible structures:

$$\begin{aligned} \mathcal{M}^{\mu\nu\lambda} = & q^\mu \epsilon^{\nu\lambda\alpha\beta} p_\alpha k_\beta \mathcal{M}_1 + (\epsilon^{\mu\nu\alpha\beta} k^\lambda - \epsilon^{\mu\lambda\alpha\beta} p^\nu) k_\alpha p_\beta \mathcal{M}_2 \\ & + [(\epsilon^{\mu\nu\alpha\beta} p^\lambda - \epsilon^{\mu\lambda\alpha\beta} k^\nu) k_\alpha p_\beta - \epsilon^{\mu\nu\lambda\sigma} (p - k)_\sigma p \cdot k] \mathcal{M}_3. \end{aligned} \quad (19.110)$$

The second term satisfies (19.51) by virtue of the on-shell conditions $p^2 = k^2 = 0$.

Now contract (19.110) with (iq_μ) to take the divergence of the axial vector current. We find

$$iq_\mu \mathcal{M}^{\mu\nu\lambda} = iq^2 \epsilon^{\nu\lambda\alpha\beta} p_\alpha k_\beta \mathcal{M}_1 - i\epsilon^{\mu\nu\lambda\sigma} q_\mu (p - k)_\sigma p \cdot k \mathcal{M}_3; \quad (19.111)$$

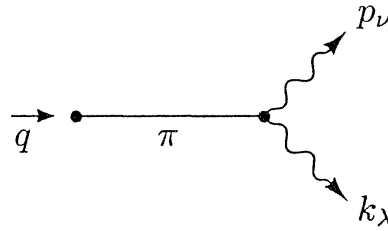


Figure 19.8. Contribution that leads to a pole in the axial vector current form factor \mathcal{M}_1 .

the other terms automatically give zero. Using $q = p + k$, $q^2 = 2p \cdot k$, we can simplify this to

$$iq_\mu \mathcal{M}^{\mu\nu\lambda} = iq^2 \epsilon^{\nu\lambda\alpha\beta} p_\alpha k_\beta (\mathcal{M}_1 + \mathcal{M}_3). \quad (19.112)$$

The whole quantity is proportional to q^2 and apparently vanishes in the limit $q^2 \rightarrow 0$. This contrasts with the prediction of the axial vector anomaly. Taking the matrix element of the right-hand side of (19.108), we find

$$iq_\mu \mathcal{M}^{\mu\nu\lambda} = -\frac{e^2}{4\pi^2} \epsilon^{\nu\lambda\alpha\beta} p_\alpha k_\beta. \quad (19.113)$$

The conflict can be resolved if one of the form factors appearing in (19.112) contains a pole in q^2 . Such a pole can arise through the process shown in Fig. 19.8, in which the current creates a π^0 meson which subsequently decays to two photons. The amplitude for the current to create the meson is given by (19.88). Let us parametrize the pion decay amplitude as

$$i\mathcal{M}(\pi^0 \rightarrow 2\gamma) = iA \epsilon_\nu^* \epsilon_\lambda^* \epsilon^{\nu\lambda\alpha\beta} p_\alpha k_\beta, \quad (19.114)$$

where A is a constant to be determined. Then the contribution of the process of Fig. 19.8 to the amplitude $\mathcal{M}^{\mu\nu\lambda}$ defined in (19.109) is

$$(iq^\mu f_\pi) \frac{i}{q^2} (iA \epsilon^{\nu\lambda\alpha\beta} p_\alpha k_\beta). \quad (19.115)$$

This is a contribution to the form factor \mathcal{M}_1 ,

$$\mathcal{M}_1 = \frac{-i}{q^2} f_\pi \cdot A, \quad (19.116)$$

plus terms regular at $q^2 = 0$. Now, by equating (19.112) to (19.113), we determine A in terms of the coefficient of the anomaly:

$$A = \frac{e^2}{4\pi^2} \frac{1}{f_\pi}. \quad (19.117)$$

From the decay matrix element (19.114), it is straightforward to work out the decay rate of the π^0 . Note that, though we have worked out the decay matrix element in the limit of a massless π^0 , we must supply the physically

correct kinematics which depends on the π^0 mass. Including a factor $1/2$ for the phase space of identical particles, we find

$$\begin{aligned}\Gamma(\pi^0 \rightarrow 2\gamma) &= \frac{1}{2m_\pi} \frac{1}{8\pi} \frac{1}{2} \sum_{\text{pol.}} |\mathcal{M}(\pi^0 \rightarrow 2\gamma)|^2 \\ &= \frac{1}{32\pi m_\pi} \cdot A^2 \cdot 2(p \cdot k)^2 \\ &= A^2 \cdot \frac{m_\pi^3}{64\pi}.\end{aligned}\quad (19.118)$$

Thus, finally,

$$\Gamma(\pi^0 \rightarrow 2\gamma) = \frac{\alpha^2}{64\pi^3} \frac{m_\pi^3}{f_\pi^2}. \quad (19.119)$$

This relation, which provides a direct measure of the coefficient of the Adler-Bell-Jackiw anomaly, is satisfied experimentally to an accuracy of a few percent.

19.4 Chiral Anomalies and Chiral Gauge Theories

Up to this point, we have coupled gauge fields to fermions in a parity-symmetric manner, replacing the derivative in the Dirac equation by a covariant derivative. This procedure couples the gauge field to the vector current of fermions. However, this procedure gives only a subset of the possible couplings of fermions to gauge bosons. In this section we will construct more general, parity-asymmetric, couplings and discuss their interplay with the axial vector anomaly.

We will focus primarily on theories of massless fermions. If the Lagrangian contains no fermion mass terms, it has no terms that mix the two helicity states of a Dirac fermion. Thus, in a theory that contains massless Dirac fermions ψ_i , we can write the kinetic energy term in the helicity basis (3.36) as

$$\mathcal{L} = \psi_{Li}^\dagger i\bar{\sigma} \cdot \partial \psi_{Li} + \psi_{Ri}^\dagger i\sigma \cdot \partial \psi_{Ri}. \quad (19.120)$$

There is no difficulty in coupling this system to a gauge field by assigning the left-handed fields ψ_{Li} to one representation of the gauge group G and assigning the right-handed fields to a different representation. For example, we might assign the left-handed fields to a representation r of G and take the right-handed fields to be invariant under G . This gives

$$\mathcal{L} = \psi_{Li}^\dagger i\bar{\sigma} \cdot D \psi_{Li} + \psi_{Ri}^\dagger i\sigma \cdot \partial \psi_{Ri}, \quad (19.121)$$

with $D_\mu = \partial_\mu - igA_\mu^a t_r^a$. In more conventional notation, (19.121) becomes

$$\mathcal{L} = \bar{\psi} i \left(\partial_\mu - igA_\mu^a t_r^a \left(\frac{1-\gamma^5}{2} \right) \right) \psi. \quad (19.122)$$

It is straightforward to verify that the classical Lagrangian (19.122) is invariant to the local gauge transformation

$$\begin{aligned}\psi &\rightarrow \left(1 + i\alpha^a t^a \left(\frac{1-\gamma^5}{2}\right)\right) \psi, \\ A_\mu^a &\rightarrow A_\mu^a + \frac{1}{g} \partial_\mu \alpha^a + f^{abc} A_\mu^b \alpha^c,\end{aligned}\tag{19.123}$$

which generalizes (15.46). Since the right-handed fields are free fields, we can even eliminate these fields and write a gauge-invariant Lagrangian for purely left-handed fermions.

The idea of gauge fields that couple only to left-handed fermions plays a central role in the construction of a theory of weak interactions. The coupling of the W boson to quarks and leptons described in (17.31) can be derived by assigning the left-handed components of quarks and leptons to doublets of an $SU(2)$ gauge symmetry

$$Q_L = \begin{pmatrix} u \\ d \end{pmatrix}_L, \quad L_L = \begin{pmatrix} \nu \\ \ell \end{pmatrix}_L, \tag{19.124}$$

and then identifying the W bosons as gauge fields that couple to this $SU(2)$ group. In this picture, it is the restriction of the symmetry to left-handed fields that leads to the helicity structure of the weak interaction effective Lagrangian. We will discuss a complete, explicit model of weak interactions, incorporating this idea, in the next chapter.

To work out the general properties of chirally coupled fermions, it is useful to rewrite their Lagrangian with one further transformation. Below Eq. (3.38), we noted that the quantity $\sigma^2 \psi_R^*$ transforms under Lorentz transformations as a left-handed field. Thus it is useful to rewrite the right-handed components in (19.120) as new left-handed fermions, by defining

$$\psi'_{Li} = \sigma^2 \psi_{Ri}^*, \quad \psi'^\dagger_{Li} = \psi_{Ri}^T \sigma^2. \tag{19.125}$$

This transformation relabels the right-handed fermions as antifermions and calls their left-handed antiparticles a new species of left-handed fermions. By using (3.38), we can rewrite the Lagrangian for the right-handed fermions as

$$\int d^4x \psi_{Ri}^\dagger i\sigma \cdot \partial \psi_{Ri} = \int d^4x \psi'^\dagger_{Li} i\bar{\sigma} \cdot \partial \psi'_{Li}. \tag{19.126}$$

The minus sign from fermion interchange cancels the minus sign from integration by parts. Notice that, if the fermions are coupled to gauge fields in the representation r , this manipulation changes the covariant derivative as follows:

$$\begin{aligned}\psi_R^\dagger i\sigma \cdot (\partial - ig A^a t_r^a) \psi_R &= \psi'^\dagger_{Li} i\bar{\sigma} \cdot (\partial + ig A^a (t_r^a)^T) \psi'_{Li} \\ &= \psi'^\dagger_{Li} i\bar{\sigma} \cdot (\partial - ig A^a t_{\bar{r}}^a) \psi'_{Li}.\end{aligned}\tag{19.127}$$

Thus the new fields ψ'_L belong to the conjugate representation to r , for which the representation matrices are given by (15.82). In this notation, QCD with

n_f flavors of massless fermions is rewritten as an $SU(3)$ gauge theory coupled to n_f massless fermions in the 3 and n_f massless fermions in the $\bar{3}$ representation of $SU(3)$. The most general gauge theory of massless fermions would simply assign left-handed fermions to an arbitrary, reducible representation R of the gauge group G . We have just seen that rewriting a system of Dirac fermions leads to $R = r \oplus \bar{r}$, a *real* representation in the sense described below (15.82). Conversely, if R is not a real representation, then the theory cannot be rewritten in terms of Dirac fermions and is intrinsically chiral.

The rewriting (19.125) transforms the mass term of the QCD Lagrangian as follows:

$$m\bar{\psi}_i\psi_i = m(\psi_R^\dagger\psi_L + \text{h.c.}) = -m(\psi_{Li}^T\sigma^2\psi_{Li} + \text{h.c.}). \quad (19.128)$$

This has the form of the *Majorana* mass term that we encountered in Problem 3.4. The most general mass term that can be built purely from left-handed fermion fields is

$$\Delta\mathcal{L}_M = M_{ij}\psi_{Li}^T\sigma^2\psi_{Lj} + \text{h.c.} \quad (19.129)$$

The matrix M_{ij} is symmetric under $i \leftrightarrow j$, since the minus sign from the antisymmetry of σ^2 is compensated by a minus sign from fermion interchange. This mass term is gauge invariant if M_{ij} is invariant under G . For example, the mass term in (19.128) couples 3 and $\bar{3}$ indices together in an $SU(3)$ singlet combination. In general, a gauge-invariant mass term exists if the representation containing the fermions is *strictly real*, in the sense described below (15.82). In an intrinsically chiral theory, there is no possible gauge-invariant mass term. We will see in the next chapter that, in the gauge theory of the weak interactions, mass terms for the quarks and leptons are forbidden by gauge invariance. We will present a solution to this problem in Section 20.2.

At the classical level, there is no restriction on the representation R of the left-handed fermions. However, at the level of one-loop corrections, many possible choices become inconsistent due to the axial vector anomaly. In a gauge theory of left-handed massless fermions, consider computing the diagrams of Fig. 19.9, in which the external fields are non-Abelian gauge bosons and the marked vertex represents the gauge symmetry current

$$j^{\mu a} = \bar{\psi}\gamma^\mu\left(\frac{1-\gamma^5}{2}\right)t^a\psi. \quad (19.130)$$

The gauge boson vertices also contain factors of $(1 - \gamma^5)/2$. The three projectors can be moved together into a single factor. Then, if we regularize this diagram as in Section 19.2, the term containing a γ^5 has an axial vector anomaly that leads to the relation

$$\langle p, \nu, b; k, \lambda, c | \partial_\mu j^{\mu a} | 0 \rangle = \frac{g^2}{8\pi^2} \epsilon^{\alpha\nu\beta\lambda} p_\alpha k_\beta \cdot \mathcal{A}^{abc}, \quad (19.131)$$

where \mathcal{A}^{abc} is a trace over group matrices in the representation R :

$$\mathcal{A}^{abc} = \text{tr}[t^a \{t^b, t^c\}]. \quad (19.132)$$

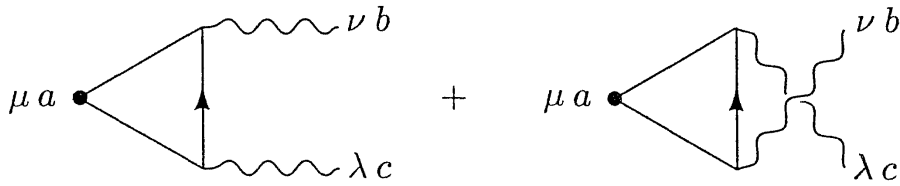


Figure 19.9. Diagrams contributing to the anomaly of a gauge symmetry current in a chiral gauge theory.

This equation implies that, unless \mathcal{A}^{abc} vanishes, the current $j^{\mu a}$ is not conserved. The factor (19.132) is totally symmetric in (a, b, c) , so this condition is independent of which current is treated as an external operator. As we described in Sections 19.1 and 19.2, we can change the regularization of the diagram so that the external current is conserved, but only at the price of violating the conservation of one of the other two currents in the diagram.

Since the whole construction of a theory with local gauge invariance is based on the existence of an exact global symmetry, the violation of the conservation of $j^{\mu a}$ does violence to the structure of the theory. For example, triangle diagrams of the form of Fig. 19.9 will now generate divergent gauge boson mass terms and will upset the delicate relations between three- and four-point vertices discussed in Chapter 16. These relations, following from the Ward identity, were necessary to insure the cancellation of unphysical states and the unitarity of the S -matrix. The only way to avoid this problem is to insist that $\mathcal{A}^{abc} = 0$ as a fundamental consistency condition for chiral gauge theories.[†] Gauge theories satisfying this condition are said to be *anomaly free*.

As an example of the application of this condition, consider the prototype weak interaction gauge theory that we presented in (19.124). If the two gauge bosons in Fig. 19.8 are $SU(2)$ gauge bosons and the current $j^{\mu a}$ is an $SU(2)$ gauge current, we would evaluate (19.132) by substituting $t^a = \tau^a = \sigma^a/2$ and using the relation $\{\sigma^b, \sigma^c\} = 2\delta^{bc}$. This gives

$$\mathcal{A}^{abc} = \frac{1}{8} \text{tr}[\sigma^a \cdot 2\delta^{bc}] = 0, \quad (19.133)$$

so the consistency condition is satisfied. If the fermions in (19.124) also couple to electromagnetism, there is an additional consistency condition that we would find by taking the current in Fig. 19.8 to be the electromagnetic current. The factor \mathcal{A}^{abc} for this case is

$$\text{tr}[Q\{\tau^b, \tau^c\}], \quad (19.134)$$

where Q is the matrix of electric charges. If we simplify as in (19.133), the trace (19.134) becomes

$$\frac{1}{2} \text{tr}[Q] \delta^{bc}. \quad (19.135)$$

[†]D. J. Gross and R. Jackiw, *Phys. Rev. D* **6**, 477 (1972).

This factor is proportional to the sum of the fermion electric charges, which does not vanish either for quarks or for leptons. However, if we sum over one quark doublet and one lepton doublet, with a factor 3 for colors, we find

$$\text{tr}[Q] = 3 \cdot \left(\frac{2}{3} - \frac{1}{3}\right) + (0 - 1) = 0. \quad (19.136)$$

Remarkably, the weak interaction gauge theory described by (19.124) can be consistently combined with QED only if the theory contains equal numbers of quark and lepton doublets.

We complete this section by working out more generally the condition that a chiral gauge theory be anomaly free. We will first derive some basic properties of the anomaly factor \mathcal{A}^{abc} and then apply these to chiral gauge theories with simple gauge groups.

If the fermion representation R is real, R is equivalent to its conjugate representation \bar{R} . Thus, as we described below (15.82), t_R^a is related by a unitary transformation to $t_{\bar{R}}^a = -(t_R^a)^T$. Since (19.132) is invariant to unitary transformations of the t^a , we can replace t_R^a by $t_{\bar{R}}^a$. Then

$$\begin{aligned} \mathcal{A}^{abc} &= \text{tr}[(-t^a)^T \{(-t^b)^T, (-t^c)^T\}] \\ &= -\text{tr}[\{t^c, t^b\} t^a] \\ &= -\mathcal{A}^{abc}. \end{aligned} \quad (19.137)$$

Thus, if R is real, the gauge theory is automatically anomaly free. As a special case, any gauge theory of Dirac fermions is anomaly free.

In more general circumstances, we can simplify the calculation of \mathcal{A}^{abc} by noting that it is an invariant of the gauge group G that is totally symmetric with three indices in the adjoint representation. For some possible groups, a suitable invariant may not exist, and in those cases \mathcal{A}^{abc} must vanish. For example, in $SU(2)$ the adjoint representation has spin 1. The symmetric product of two spin-1 multiplets gives spin 0 plus spin 2, with no spin-1 component. Thus, there is no symmetric tensor coupling two spin-1 indices to give a spin 1. The factor (19.132) must then vanish in any $SU(2)$ gauge theory. We saw this happen in an explicit example in Eq. (19.133).

In $SU(n)$ groups, $n \geq 3$, there is a unique symmetric invariant d^{abc} of the required type. It appears in the anticommutator of representation matrices of the fundamental representation:

$$\{t_n^a, t_n^b\} = \delta^{ab} + d^{abc} t_n^c. \quad (19.138)$$

The uniqueness of this invariant implies that, in an $SU(n)$ gauge theory, any trace of the form of (19.132) is proportional to d^{abc} . For each representation r , we can define an *anomaly coefficient* $A(r)$ by

$$\text{tr}[t_r^a \{t_r^b, t_r^c\}] = \frac{1}{2} A(r) d^{abc}. \quad (19.139)$$

For the fundamental representation, we can see from (19.138) that $A(n) = 1$. It follows from the argument of (19.137) that

$$A(\bar{r}) = -A(r). \quad (19.140)$$

For higher representations, the anomaly coefficients can be worked out using methods similar to those we used in Section 15.3 to compute $C_2(r)$. For example, we show in Problem 19.3 that, if a and s are the $SU(n)$ representations corresponding to antisymmetric and symmetric two-index tensors, then

$$A(a) = n - 4, \quad A(s) = n + 4. \quad (19.141)$$

An $SU(n)$ gauge theory is anomaly free if the anomaly coefficients of the various irreducible components of the fermion multiplet R sum to zero. For example, the $SU(n)$ gauge theory of left-handed fermions with representation content

$$R = a + (n - 4)\bar{n} \quad (19.142)$$

is anomaly free.

Of the various simple Lie groups listed below (15.72), only $SU(n)$, $SO(4n + 2)$, and E_6 have complex representations. Of these, only $SU(n)$ and $SO(6)$, which has the same Lie algebra as $SU(4)$, have a symmetric invariant of the type required to build the anomaly. Gauge theories based on $SO(4n+2)$, $n \geq 2$, and on E_6 are automatically anomaly free. The groups $SO(10)$ and E_6 have been suggested as candidates for the *grand unified* gauge symmetry of particle physics, which we will discuss in Section 22.2.

There is one further constraint on the representation content of a chiral gauge theory, which comes from considering its coupling to gravity. It is possible to show that the diagrams of Fig. 19.9 give an anomaly contribution when computed with a gauge current $j^{\mu a}$ and external gravitational fields. The group-theory factor that multiplies this diagram is

$$\text{tr}[t_R^a]. \quad (19.143)$$

This factor automatically vanishes if the gauge group is non-Abelian. However, if the gauge group of the theory contains $U(1)$ factors, the theory cannot be consistently coupled to gravity unless each of the $U(1)$ generators is traceless.[‡]

Once we have constructed a consistent chiral gauge theory, we have an additional problem of finding a prescription for calculating in this theory consistently. In a vector-like gauge theory, we can define ultraviolet-divergent diagrams with dimensional regularization. This guarantees that the divergent diagrams will be regulated in a way that respects the Ward identities of local gauge invariance. To generalize dimensional regularization to chiral gauge theories, we need to introduce a dimensional continuation of γ^5 . The 't Hooft-Veltman definition used to define the chiral current in Section 19.2 is not satisfactory, because this definition does not manifestly respect the conservation of the gauge currents. A useful alternative procedure is to define γ^5 formally as an object that anticommutes with all of the γ^μ . This prescription gives unambiguous, gauge-invariant results for amplitudes that are not proportional to $\epsilon^{\mu\nu\lambda\sigma}$, at least through two-loop order. In Section 21.3, we will

[‡]L. Alvarez-Gaumé and E. Witten, *Nucl. Phys.* **B234**, 269 (1984).

use this prescription to compute loop diagrams in weak interaction theory. As a last resort, one can always compute with a non-gauge-invariant regulator and add non-gauge-invariant counterterms to the theory so that the gauge theory Ward identities remain valid.

19.5 Anomalous Breaking of Scale Invariance

There is one more important example of a symmetry that is an invariance at the classical level and is broken by quantum corrections. This is the classical scale invariance of a massless field theory with a dimensionless coupling constant. In Chapter 12, we saw that a quantum field theory with no classical dimensionful parameters still depends on a mass scale through the regularization of ultraviolet divergences, or, equivalently, through the running of coupling constants. We have already seen how to analyze this induced dependence on the renormalization scale using the Callan-Symanzik equation. In this section, we will show how the violation of classical scale invariance by quantum corrections can be described as a current conservation anomaly.

In this book we have avoided giving a careful treatment of the energy-momentum tensor of a quantum field theory. In Section 2.2, we used Noether's theorem to demonstrate that the invariance of a quantum field theory under spacetime translations implies the presence of a conserved tensor $T^{\mu\nu}$. In Section 9.6, we gave an alternative derivation of this result using the functional integral formalism. However, to discuss the theory of scale invariance, we will need some more detailed properties of the energy-momentum tensor. We will now simply state these properties and refer elsewhere for their derivations.*

The tensor $T^{\mu\nu}$ defined by expressions (2.17) and (9.99) is called the *canonical energy-momentum tensor*. The expressions that defined this tensor do not imply that $T^{\mu\nu}$ is symmetric. In fact, this tensor need not be symmetric, and, in a gauge theory, it need not be gauge-invariant. However, it is always possible to convert $T^{\mu\nu}$ into a symmetric and gauge-invariant tensor $\Theta^{\mu\nu}$ by the addition

$$\Theta^{\mu\nu} = T^{\mu\nu} + \partial_\lambda \Sigma^{\mu\nu\lambda}, \quad (19.144)$$

where $\Sigma^{\mu\nu\lambda}$ is antisymmetric under interchange of μ and λ . The form of the added term implies that $\Theta^{\mu\nu}$ is conserved if $T^{\mu\nu}$ is, and that the global energy-momentum four-vector is unchanged,

$$P^\nu = \int d^3x T^{0\nu} = \int d^3x \Theta^{0\nu}. \quad (19.145)$$

A scale transformation of a scalar field theory can be defined as a transformation of variables

$$\phi(x) \rightarrow e^{-D\sigma} \phi(xe^{-\sigma}), \quad (19.146)$$

*The conclusions presented in the next three paragraphs are derived with care in C. G. Callan, S. Coleman, and R. Jackiw, *Ann. Phys.* **59**, 42 (1970).

with $D = 1$, the canonical mass dimension of the field. The scale transformation is defined similarly in theories of fermion and gauge fields. If this transformation is an invariance of the classical Lagrangian, as it will be if there are no dimensionful couplings, this theory will possess a conserved current D^μ , called the *dilatation current*. The dilatation current has a simple relation to the symmetric energy-momentum tensor $\Theta^{\mu\nu}$: $D^\mu = \Theta^{\mu\nu}x_\nu$, so that

$$\partial_\mu D^\mu = \Theta^{\mu\mu}. \quad (19.147)$$

The derivation of these results from Noether's theorem is not straightforward. There is a simpler derivation, which, however, uses formalism beyond the scope of this book. If the quantum field theory under consideration is coupled to gravity, then the energy-momentum tensor can be identified as the source of the gravitational field. This energy-momentum tensor can be found by varying the Lagrangian \mathcal{L}_m of matter fields with respect to the spacetime metric $g_{\mu\nu}(x)$. This construction gives a manifestly symmetric and gauge-invariant tensor, which turns out to be $\Theta^{\mu\nu}$:

$$\Theta^{\mu\nu} = 2 \frac{\delta}{\delta g_{\mu\nu}(x)} \int d^4x \mathcal{L}_m. \quad (19.148)$$

A scale transformation can be represented as a change in the spacetime metric

$$g_{\mu\nu}(x) \rightarrow e^{2\sigma} g_{\mu\nu}(x). \quad (19.149)$$

Combining (19.148) and (19.149), we see that the change in the Lagrangian induced by this transformation is just the trace of $\Theta^{\mu\nu}$. This will be equal by Noether's theorem to the divergence of the corresponding current, giving us back Eq. (19.147).

In QED, it is not hard to guess the form of the symmetric energy-momentum tensor:

$$\Theta^{\mu\nu} = -F^{\mu\lambda}F^\nu_\lambda + \frac{1}{4}g^{\mu\nu}(F_{\lambda\sigma})^2 + \frac{1}{2}\bar{\psi}i(\gamma^\mu D^\nu + \gamma^\nu D^\mu)\psi - g^{\mu\nu}\bar{\psi}(iD - m)\psi. \quad (19.150)$$

This is a gauge-invariant symmetric tensor that leads to the familiar expression for the total energy,

$$H = \int d^3x \left\{ \frac{1}{2}(E^2 + B^2) + \psi^\dagger(-i\gamma^0\gamma \cdot \nabla + m)\psi \right\}. \quad (19.151)$$

For future reference, we note that these results are true at the classical level in any spacetime dimension d . In four dimensions, the trace of the gauge field terms cancels automatically. After using the Dirac equation, which is valid as an operator equation of motion, we find that the trace of $\Theta^{\mu\nu}$ is given by

$$\Theta^\mu_\mu = m\bar{\psi}\psi \quad (19.152)$$

and indeed vanishes, classically, if $m = 0$.

When quantum corrections are included, we know that a scale transformation is not a symmetry of the theory, since the same theory referred to a

larger scale contains a different value of the renormalized coupling constant. The shift of the renormalized coupling is

$$g \rightarrow g + \sigma\beta(g), \quad (19.153)$$

and the corresponding change in the Lagrangian is

$$\sigma\beta(g) \frac{\partial}{\partial g} \mathcal{L}. \quad (19.154)$$

Thus, when quantum corrections are included, the equation for the dilatation current in a classically scale-invariant theory should read

$$\partial_\mu D^\mu = \Theta^\mu_\mu = \beta(g) \frac{\partial}{\partial g} \mathcal{L}. \quad (19.155)$$

In massless QED, we can write this formula most usefully by rescaling the gauge fields so that the coupling constant e is removed from the covariant derivative: $eA^\mu \rightarrow A^\mu$. Then e appears only in the term

$$\mathcal{L} = -\frac{1}{4e^2} (F_{\lambda\sigma})^2 + \dots, \quad (19.156)$$

and Eq. (19.155) reads

$$\Theta^\mu_\mu = \frac{\beta(e)}{2e^3} (F_{\lambda\sigma})^2. \quad (19.157)$$

This relation, which says that the trace of the symmetric energy-momentum tensor takes a nonzero value as a result of quantum corrections, is known as the *trace anomaly*.

We should be able to check the trace anomaly equation (19.157) directly in perturbation theory. We now evaluate the trace of $\Theta^{\mu\nu}$ explicitly to one-loop order. The formalism we have set up is very similar to that of the background field calculation of the β function done in Section 16.6. As in that section, we will integrate over the fluctuating parts of quantum fields in the presence of a background field with a nonzero $F_{\mu\nu}$. Equation (19.157) predicts that this integration will lead to the expression

$$\langle \Theta^\mu_\mu \rangle = C \int \frac{d^4 k}{(2\pi)^4} A_\mu(-k) (k^2 g^{\mu\nu} - k^\mu k^\nu) A_\nu(k), \quad (19.158)$$

where A_μ is the background field and the constant C is equal to $\beta(e)/e^3$.

Since we will be using dimensional regularization, we should begin by writing the trace of $\Theta^{\mu\nu}$ in d dimensions:

$$\Theta^\mu_\mu = -\frac{4-d}{4} (F_{\lambda\sigma})^2 + (1-d) \bar{\psi} i \not{D} \psi. \quad (19.159)$$

The one-loop matrix element of this quantity proportional to two powers of the background field arises from the three diagrams shown in Fig. 19.10. Since the second term on the right-hand side of (19.159) vanishes by the equation of motion of $\psi(x)$, one might expect that this term gives zero contribution to the trace. Indeed, it is easy to check that the first two diagrams in Fig.

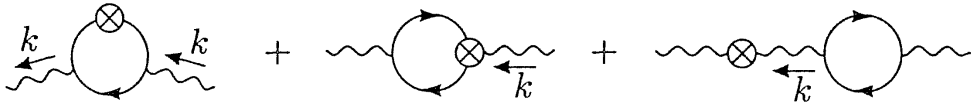


Figure 19.10. One-loop diagrams contributing to the anomalous trace of $\Theta^{\mu\nu}$.

19.10 cancel: These diagrams have the same structure, since the first has an extra propagator and an extra factor \not{p} from the operator matrix element, and opposite overall signs.

The first term on the left-hand side of (19.159) is unexpected, since it apparently vanishes in four dimensions. However, the fermion loop diagram is divergent, and in dimensional regularization, this introduces a factor $1/(2 - d/2)$. As a result, this diagram gives a nonzero contribution to the operator matrix element. In massless QED, the fermion loop diagram has the value

$$\text{Diagram} = -i(k^2 g^{\mu\nu} - k^\mu k^\nu) \frac{4}{3(4\pi)^2} (\Gamma(2 - \frac{d}{2}) + (\text{finite})). \quad (19.160)$$

Then the complete expression for the third diagram in Fig. 19.10 is

$$\int \frac{d^4 k}{(2\pi)^4} A_\mu(-k) \left(-2 \frac{4-d}{4} \right) (k^2 g^{\mu\nu} - k^\mu k^\nu) \frac{-i}{k^2} \left(-ik^2 \frac{4}{3(4\pi)^2} \frac{1}{2-d/2} \right). \quad (19.161)$$

This is of the form of (19.158), with

$$C = \frac{1}{12\pi^2}, \quad (19.162)$$

which is indeed the first β function coefficient in massless QED.

This discussion generalizes to QCD and other gauge theories. In a non-Abelian gauge theory, $\Theta^{\mu\nu}$ is given by the obvious generalization of (19.150) with the Abelian field-strength tensor $F_{\mu\nu}$ replaced by the non-Abelian expression $F_{\mu\nu}^a$. The trace of $\Theta^{\mu\nu}$ is again given by

$$\Theta^\mu_\mu = -\frac{4-d}{4} (F_{\lambda\sigma}^a)^2, \quad (19.163)$$

plus terms that vanish by the equations of motion. In the background field gauge, the one-loop diagrams with the operator Θ^μ_μ inserted into the loop cancel as above. We saw in Section 16.6 that the two-point functions in this gauge sum to

$$\text{Diagram} = -i(k^2 g^{\mu\nu} - k^\mu k^\nu) \left[\frac{-b_0}{(4\pi)^2} \right] (\Gamma(2 - \frac{d}{2}) + (\text{finite})), \quad (19.164)$$

where $\beta(g) = -b_0 g^3 / (4\pi)^2$. Following through the logic of the previous paragraph, we again find the result (19.158) with the identification of C as the first β function coefficient.

As with the axial vector anomaly, the trace anomaly can be found in many different ways. For each possible method of regulating a quantum field theory, there is a derivation of the trace anomaly that exploits the possible pathology of that particular regulator. For example, if one uses a Pauli-Villars regulator with heavy fermions to cancel the divergence of the QED fermion loop diagram, the heavy fermions Ψ contribute a term $M\bar{\Psi}\Psi$ to the trace of $\Theta^{\mu\nu}$. The loop diagram with this term inserted turns out to have a finite limit as $M \rightarrow \infty$, which precisely reproduces the trace anomaly. This computation is worked out in Problem 19.4.

As with the axial vector anomaly, each derivation of the anomaly with a different regulator, taken individually, seems artificial, as if there were a problem with the field theory that we are not quite clever enough to fix. Eventually, though, we are forced to conclude that the quantum field theory is trying to tell us something. The anomalous symmetries of the classical theory cannot be promoted to symmetries of the quantum theory. Instead, the anomalous conservation laws require profound and qualitative changes in the theory from the classical to the quantum level.

Problems

19.1 Fermion number nonconservation in parallel E and B fields.

- (a) Show that the Adler-Bell-Jackiw anomaly equation leads to the following law for global fermion number conservation: If N_R and N_L are, respectively, the numbers of right- and left-handed massless fermions, then

$$\Delta N_R - \Delta N_L = -\frac{e^2}{2\pi^2} \int d^4x \mathbf{E} \cdot \mathbf{B}.$$

To set up a solvable problem, take the background field to be $A^\mu = (0, 0, Bx^1, A)$, with B constant and A constant in space and varying only adiabatically in time.

- (b) Show that the Hamiltonian for massless fermions represented in the components (3.36) is

$$H = \int d^3x \left[\psi_R^\dagger (-i\sigma \cdot \mathbf{D}) \psi_R - \psi_L^\dagger (-i\sigma \cdot \mathbf{D}) \psi_L \right],$$

with $D^i = \nabla^i - ieA^i$. Concentrate on the term in the Hamiltonian that involves right-handed fermions. To diagonalize this term, one must solve the eigenvalue equation $-i\sigma \cdot \mathbf{D} \psi_R = E\psi_R$.

- (c) The ψ_R eigenvectors can be written in the form

$$\psi_R = \begin{pmatrix} \phi_1(x^1) \\ \phi_2(x^1) \end{pmatrix} e^{i(k_2 x^2 + k_3 x^3)}.$$

The functions ϕ_1 and ϕ_2 , which depend only on x^1 , obey coupled first-order differential equations. Show that, when one of these functions is eliminated, the other obeys the equation of a simple harmonic oscillator. Use this observation to find the single-particle spectrum of the Hamiltonian. Notice that the eigenvalues do not depend on k_2 .

- (d) If the system of fermions is set up in a box with sides of length L and periodic boundary conditions, the momenta k_2 and k_3 will be quantized:

$$k_i = \frac{2\pi n_i}{L}.$$

By looking back to the harmonic oscillator equation in part (c), show that the condition that the center of the oscillation is inside the box leads to the condition

$$k_2 < eBL.$$

Combining these two conditions, we see that each level found in part (c) has a degeneracy of

$$\frac{eL^2 B}{2\pi}.$$

- (e) Now consider the effect of changing the background A adiabatically by an amount (19.37). Show that the vacuum loses right-handed fermions. Repeating this analysis for the left-handed spectrum, one sees that the vacuum gains the same number of left-handed fermions. Show that these numbers are in accord with the global nonconservation law given in part (a).

19.2 Weak decay of the pion.

- (a) In the effective Lagrangian for semileptonic weak interactions (18.28), the hadronic part of the operator is a left-handed current involving the u and d quarks. Show that this current is related to the quark currents of Section 19.3 as follows:

$$\bar{u}_L \gamma^\mu d_L = \frac{1}{4} (j^{\mu 1} + ij^{\mu 2} - j^{\mu 51} - ij^{\mu 52}),$$

where 1, 2 are isospin indices. Using this identification and (19.88), show that the amplitude for the decay $\pi^+ \rightarrow \ell^+ \nu$ is given by

$$i\mathcal{M} = G_F f_\pi \bar{u}(q) \not{p} (1 - \gamma^5) v(k),$$

where p, k, q are the momenta of the π^+ , ℓ^+ , ν .

- (b) Compute the decay rate of the pion. Show that this rate vanishes in the limit of zero lepton mass, and that the relative rate of pion decay to muons and electrons is given by

$$\frac{\Gamma(\pi^+ \rightarrow e^+ \nu)}{\Gamma(\pi^+ \rightarrow \mu^+ \nu)} = \left(\frac{m_e}{m_\mu}\right)^2 \frac{(1 - m_e^2/m_\pi^2)}{(1 - m_\mu^2/m_\pi^2)} = 10^{-4}.$$

From the measured pion lifetime, $\tau_\pi = 2.6 \times 10^{-8}$ sec, and the pion and muon masses, $m_\pi = 140$ MeV, $m_\mu = 106$ MeV, determine the value of f_π .

19.3 Computation of anomaly coefficients.

- (a) Consider a product $r_1 \times r_2$ of $SU(n)$ representations, which is decomposed into irreducible representations as in (15.98). Using the explicit form of the generators given in (15.99), show that the anomaly coefficients satisfy

$$d_1 A(r_2) + d_2 A(r_1) = \sum_i A(r_i).$$

- (b) As we saw in Problem 15.5, the two-index symmetric and anitsymmetric tensors form irreducible representations of $SU(n)$, which we will call s and a , respectively. In $SU(3)$, the representation a is three-dimensional. Show that it is equivalent to the $\bar{3}$. Compute the anomaly coefficients for a and s , making use of the identity in part (a).
- (c) Since $SU(n)$ has a unique three-index symmetric tensor d^{abc} which is already nonvanishing in an $SU(3)$ subgroup, we can compute the anomaly coefficient in $SU(n)$ by restricting our attention to three generators in this subgroup. By decomposing $SU(n)$ representations into $SU(3)$ representations, compute the anomaly coefficients for a and s in $SU(n)$ and derive Eq. (19.141). Find the anomaly coefficient of the j -index totally antisymmetric tensor representation of $SU(n)$. Why does the result always vanish when $2j = n$?

19.4 Large fermion mass limits. In the text, we derived the Adler-Bell-Jackiw and trace anomalies by the use of dimensional regularization. As an alternative, one could imagine deriving these results using Pauli-Villars regularization. In that technique, one regularizes the value of a fermion loop integral by subtracting the value of the same loop diagram computed with fermions Ψ of large mass M . The parameter M plays the role of the cutoff and should be taken to infinity at the end of the calculation. The anomalies arise because some pieces of the diagrams computed for very heavy fermions do not disappear in the limit $M \rightarrow \infty$. These nontrivial $M \rightarrow \infty$ limits are interesting in their own right and can have physical applications (for example, in part (c) of the Final Project for Part III).

- (a) Show that the Adler-Bell-Jackiw anomaly equation is equivalent to the following large-mass limit of a fermion matrix element between the vacuum and a two-photon state:

$$\lim_{M \rightarrow \infty} \left\{ \langle p, k | 2iM \bar{\Psi} \gamma^5 \Psi | 0 \rangle \right\} = -\frac{e^2}{2\pi^2} \epsilon^{\alpha\nu\beta\lambda} p_\alpha \epsilon_\nu^*(p) k_\beta \epsilon_\lambda^*(k).$$

- (b) Show that the trace anomaly, at one-loop order, is equivalent to the following large-mass limit:

$$\lim_{M \rightarrow \infty} \left\{ \langle p, k | M \bar{\Psi} \Psi | 0 \rangle \right\} = +\frac{e^2}{6\pi^2} [p \cdot k \epsilon^*(p) \cdot \epsilon^*(k) - p \cdot \epsilon^*(k) k \cdot \epsilon^*(p)].$$

- (c) Show that the matrix element in part (a) is ultraviolet-finite before the $M \rightarrow \infty$ limit is taken. Evaluate the matrix element explicitly at one-loop order and verify the limit claimed in part (a).
- (d) The matrix element in part (b) has a potential ultraviolet divergence. However, show that the coefficient of $(p \cdot \epsilon^*(k) k \cdot \epsilon^*(p))$ is ultraviolet-finite, and that the rest of the expression is determined by gauge invariance. Compute the full matrix element using dimensional regularization as a gauge-invariant regulator and verify the result claimed in part (b).

Gauge Theories with Spontaneous Symmetry Breaking

In the course of this book, we have discussed three distinct fashions in which symmetries can be realized in a quantum field theory. The simplest case is a global symmetry that is manifest, leading to particle multiplets with restricted interactions. A second possibility is a global symmetry that is spontaneously broken. Then, as discussed in Chapter 11,* the symmetry currents are still conserved and interactions are similarly restricted, but the vacuum state does not respect the symmetry and the particles do not form obvious symmetry multiplets. Instead, such a theory contains massless particles, Goldstone bosons, one for each generator of the spontaneously broken symmetry. The third case is that of a local, or gauge, symmetry. As we saw in Chapter 15, such a symmetry requires the existence of a massless vector field for each symmetry generator, and the interactions among these fields are highly restricted.

It is now only natural to consider a fourth possibility: What happens if we include both local gauge invariance and spontaneous symmetry breaking in the same theory? In this chapter and the next, we will find that this combination of ingredients leads to new possibilities for the construction of quantum field theory models. We will see that spontaneous symmetry breaking requires gauge vector bosons to acquire mass. However, the interactions of these massive bosons are still constrained by the underlying gauge symmetry, and these constraints can have observable consequences.

In elementary particle physics, the principal application of spontaneously broken local symmetry is in the currently accepted model of weak interactions. This model, due to Glashow, Weinberg, and Salam, is introduced in Section 20.2. There we will see that it makes a number of precise and successful predictions for weak interaction phenomena. Remarkably, this model also unifies the weak interactions with electromagnetism in a single larger gauge theory.

*Section 11.1 is necessary background for the present chapter, but the rest of Chapter 11 is not.

20.1 The Higgs Mechanism

In this section we analyze some simple examples of gauge theories with spontaneous symmetry breaking. We begin with an Abelian gauge theory, and then study several examples of non-Abelian models.

An Abelian Example

As our first example, consider a complex scalar field coupled both to itself and to an electromagnetic field:

$$\mathcal{L} = -\frac{1}{4}(F_{\mu\nu})^2 + |D_\mu\phi|^2 - V(\phi), \quad (20.1)$$

with $D_\mu = \partial_\mu + ieA_\mu$. This Lagrangian is invariant under the local $U(1)$ transformation

$$\phi(x) \rightarrow e^{i\alpha(x)}\phi(x), \quad A_\mu(x) \rightarrow A_\mu(x) - \frac{1}{e}\partial_\mu\alpha(x). \quad (20.2)$$

If we choose the potential in \mathcal{L} to be of the form

$$V(\phi) = -\mu^2\phi^*\phi + \frac{\lambda}{2}(\phi^*\phi)^2, \quad (20.3)$$

with $\mu^2 > 0$, the field ϕ will acquire a vacuum expectation value and the $U(1)$ global symmetry will be spontaneously broken. The minimum of this potential occurs at

$$\langle\phi\rangle = \phi_0 = \left(\frac{\mu^2}{\lambda}\right)^{1/2}, \quad (20.4)$$

or at any other value related by the $U(1)$ symmetry (20.2).

Let us expand the Lagrangian (20.1) about the vacuum state (20.4). Decompose the complex field $\phi(x)$ as

$$\phi(x) = \phi_0 + \frac{1}{\sqrt{2}}(\phi_1(x) + i\phi_2(x)). \quad (20.5)$$

The potential (20.3) is rewritten

$$V(\phi) = -\frac{1}{2\lambda}\mu^4 + \frac{1}{2} \cdot 2\mu^2\phi_1^2 + \mathcal{O}(\phi_i^3), \quad (20.6)$$

so that the field ϕ_1 acquires the mass $m = \sqrt{2}\mu$ and ϕ_2 is the massless Goldstone boson. So far, this whole analysis follows that in Section 11.1.

But now consider how the kinetic energy term of ϕ is transformed. Inserting the expansion (20.5), we rewrite

$$|D_\mu\phi|^2 = \frac{1}{2}(\partial_\mu\phi_1)^2 + \frac{1}{2}(\partial_\mu\phi_2)^2 + \sqrt{2}e\phi_0 \cdot A_\mu\partial^\mu\phi_2 + e^2\phi_0^2A_\mu A^\mu + \dots, \quad (20.7)$$

where we have omitted terms cubic and quartic in the fields A_μ , ϕ_1 , and ϕ_2 . The last term written explicitly in (20.7) is a photon mass term

$$\Delta\mathcal{L} = \frac{1}{2}m_A^2A_\mu A^\mu, \quad (20.8)$$

where the mass

$$m_A^2 = 2e^2 \phi_0^2 \quad (20.9)$$

arises from the nonvanishing vacuum expectation value of ϕ . Notice that the sign of this mass term is correct; the physical spacelike components of A^μ appear in (20.8) as

$$\Delta\mathcal{L} = -\frac{1}{2}m_A^2(A^i)^2,$$

with the correct sign for a potential energy term.

In Chapter 7, and again in Chapter 16 for the non-Abelian case, we argued that a gauge boson cannot obtain a mass, unless this mass term is associated with a pole in the vacuum polarization amplitude. There is a counterexample to this result in two-dimensional spacetime; there, as we saw in Section 19.1, a pole of the required form can arise from the infrared singularity generated by a massless fermion pair. However, in four dimensions, a pole in the vacuum polarization amplitude can be created only by a massless scalar particle. Typically, in situations with unbroken symmetry, no such particle is available.

However, a model with a spontaneously broken continuous symmetry must have massless Goldstone bosons. These scalar particles have the quantum numbers of the symmetry currents, and therefore have just the right quantum numbers to appear as intermediate states in the vacuum polarization. In the model we are now discussing, we can see this pole arise explicitly in the following way: The third term in Eq. (20.7) couples the gauge boson directly to the Goldstone boson ϕ_2 ; this gives a vertex of the form

$$\mu \sim \sim \sim \bullet \quad \begin{matrix} \leftarrow \\ k \end{matrix} = i\sqrt{2}e\phi_0(-ik^\mu) = m_A k^\mu. \quad (20.10)$$

If we also treat the mass term (20.8) as a vertex in perturbation theory, then the leading-order contributions to the vacuum polarization amplitude give the expression

$$\begin{aligned} \text{---} \bullet \sim \sim \sim &= \sim \sim \bullet \sim \sim \sim + \sim \sim \bullet \sim \sim \sim \\ &= im_A^2 g^{\mu\nu} + (m_A k^\mu) \frac{i}{k^2} (-m_A k^\nu) \\ &= im_A^2 \left(g^{\mu\nu} - \frac{k^\mu k^\nu}{k^2} \right). \end{aligned} \quad (20.11)$$

The Goldstone boson supplies exactly the right pole to make the vacuum polarization amplitude properly transverse.

Although the Goldstone boson plays an important formal role in this theory, it does not appear as an independent physical particle. The easiest way to see this is to make a particular choice of gauge, called the *unitarity gauge*. Using the local $U(1)$ gauge symmetry (20.2), we can choose $\alpha(x)$ in such a way that $\phi(x)$ becomes real-valued at every point x . With this choice, the field ϕ_2 is removed from the theory. The Lagrangian (20.1) becomes

$$\mathcal{L} = -\frac{1}{4}(F_{\mu\nu})^2 + (\partial_\mu \phi)^2 + e^2 \phi^2 A_\mu A^\mu - V(\phi). \quad (20.12)$$

If the potential $V(\phi)$ favors a nonzero vacuum expectation value of ϕ , the gauge field acquires a mass; it also retains a coupling to the remaining, physical field ϕ_1 .

This mechanism, by which spontaneous symmetry breaking generates a mass for a gauge boson, was explored and generalized to the non-Abelian case by Higgs, Kibble, Guralnik, Hagen, Brout, and Englert, and is now known as the *Higgs mechanism*. However, this mechanism had an earlier application to the theory of superconductivity. In Chapter 8, we constructed the Landau description of a second-order phase transition. To describe a superconductor, Landau and Ginzburg coupled this theory to an external electromagnetic field; they obtained precisely the Lagrangian (20.1). Since the gauge field acquires a nonzero mass, external electromagnetic fields penetrate a superconductor only to the depth m_A^{-1} . This explains the *Meissner effect*, the observed exclusion of macroscopic magnetic fields from a superconductor.

The role of the Goldstone boson in the Higgs mechanism is intricate, and seems mysterious at this level of the discussion. We first saw that the involvement of the Goldstone boson is necessary, as a matter of principle, in order for the gauge boson to acquire a mass. We then saw that the Goldstone boson can be formally eliminated from the theory. However, we might argue that the Goldstone boson has not completely disappeared. A massless vector boson has only two physical polarization states; we saw in Chapter 16 that the longitudinal polarization state cannot be produced, and appears in the formalism only to cancel other unphysical contributions. However, a massive vector boson must have three physical polarization states: In its rest frame, it is a spin-1 object, which can make no distinction between transverse and longitudinal polarizations. It is tempting to say that the gauge boson acquired its extra degree of freedom by *eating* the Goldstone boson. In Sections 21.1 and 21.2 we will clarify this picture, by studying the quantization and gauge-fixing of spontaneously broken gauge theories.

Systematics of the Higgs Mechanism

The Higgs mechanism extends straightforwardly to systems with non-Abelian gauge symmetry. It is not difficult to derive the general relation by which a set of scalar field vacuum expectation values leads to the appearance of gauge boson masses. Let us work out this relation and then apply it in a number of examples.

Consider a system of scalar fields ϕ_i that appear in a Lagrangian invariant under a symmetry group G , represented by the transformation

$$\phi_i \rightarrow (1 + i\alpha^a t^a)_{ij} \phi_j. \quad (20.13)$$

It is convenient to write the ϕ_i as real-valued fields, for example, writing n complex fields as $2n$ real fields. Then the group representation matrices t^a must be pure imaginary and, since they are Hermitian, antisymmetric. Let us

write

$$t_{ij}^a = iT_{ij}^a, \quad (20.14)$$

so that the T^a are real and antisymmetric.

If we promote the symmetry group G to a local gauge symmetry, the covariant derivative on the ϕ_i is

$$D_\mu \phi = (\partial_\mu - ig A_\mu^a t^a) \phi = (\partial_\mu + g A_\mu^a T^a) \phi.$$

Then the kinetic energy term for the ϕ_i is

$$\frac{1}{2} (D_\mu \phi_i)^2 = \frac{1}{2} (\partial_\mu \phi_i)^2 + g A_\mu^a (\partial_\mu \phi_i T_{ij}^a \phi_j) + \frac{1}{2} g^2 A_\mu^a A^{b\mu} (T^a \phi)_i (T^b \phi)_i. \quad (20.15)$$

Now let the ϕ_i acquire vacuum expectation values

$$\langle \phi_i \rangle = (\phi_0)_i, \quad (20.16)$$

and expand the ϕ_i about these values. The last term in Eq. (20.15) contains a term with the structure of a gauge boson mass,

$$\Delta \mathcal{L} = \frac{1}{2} m_{ab}^2 A_\mu^a A^{b\mu}, \quad (20.17)$$

with the mass matrix

$$m_{ab}^2 = g^2 (T^a \phi_0)_i (T^b \phi_0)_i. \quad (20.18)$$

This matrix is positive semidefinite, since its diagonal elements are

$$m_{aa}^2 = g^2 (T^a \phi_0)^2 \geq 0 \quad (\text{no sum}).$$

Thus, generically, all of the gauge bosons will receive positive masses. However, it may be that some particular generator T^a of G leaves the vacuum invariant:

$$T^a \phi_0 = 0.$$

In that case, the generator T^a will give no contribution to (20.18), and the corresponding gauge boson will remain massless.

As in the Abelian case, the gauge boson propagator receives a contribution from the Goldstone bosons, which is necessary to make the vacuum polarization amplitude transverse. To compute this contribution, we need the vertex that mixes gauge bosons and Goldstone bosons. This comes from the second term of the Lagrangian (20.15). When we insert the vacuum expectation value of the scalar field (20.16), this term becomes

$$\Delta \mathcal{L} = g A_\mu^a \partial_\mu \phi_i (T^a \phi_0)_i. \quad (20.19)$$

This interaction term does not involve all of the components of ϕ —only those that are parallel to a vector $T^a \phi_0$ for some choice of T^a . These vectors represent the infinitesimal rotations of the vacuum; thus the components ϕ_i that appear in (20.19) are precisely the Goldstone bosons. Using the fact that these

bosons are massless, we can compute the counterpart, for the non-Abelian case, of the Goldstone boson diagram in Eq. (20.11):

$$a^\mu \text{---} \bullet \text{---} b^\nu = \sum_j (gk^\mu(T^a\phi_0)_j) \frac{i}{k^2} (-gk^\nu(T^b\phi_0)_j). \quad (20.20)$$

The sum runs over those components j with a nonzero projection onto the space spanned by the $T^a\phi_0$, or equally well, over all j . This diagram is therefore proportional to the mass matrix (20.18). Combining this expression with the contribution to the vacuum polarization from (20.17), we find a properly transverse result,

$$\text{---} \bullet \text{---} = im_{ab}^2 \left(g^{\mu\nu} - \frac{k^\mu k^\nu}{k^2} \right), \quad (20.21)$$

where m_{ab}^2 is given by Eq. (20.18).

Non-Abelian Examples

Let us now apply this general formalism to some specific examples of non-Abelian gauge theories. Consider first a model with an $SU(2)$ gauge field coupled to a scalar field ϕ that transforms as a spinor of $SU(2)$. The covariant derivative acting on ϕ is

$$D_\mu \phi = (\partial_\mu - igA_\mu^a \tau^a) \phi, \quad (20.22)$$

where $\tau^a = \sigma^a/2$. The square of this expression is the scalar field kinetic energy term.

If ϕ acquires a vacuum expectation value, we can use the freedom of $SU(2)$ rotations to write this expectation value in the form

$$\langle \phi \rangle = \frac{1}{\sqrt{2}} \begin{pmatrix} 0 \\ v \end{pmatrix}. \quad (20.23)$$

Then the gauge boson masses arise from

$$|D_\mu \phi|^2 = \frac{1}{2} g^2 \begin{pmatrix} 0 & v \end{pmatrix} \tau^a \tau^b \begin{pmatrix} 0 \\ v \end{pmatrix} A_\mu^a A^{b\mu} + \dots \quad (20.24)$$

We can symmetrize the matrix product under the interchange of a and b ; using $\{\tau^a, \tau^b\} = \frac{1}{2}\delta^{ab}$, we find the mass term

$$\Delta \mathcal{L} = \frac{g^2 v^2}{8} A_\mu^a A^{a\mu}. \quad (20.25)$$

All three gauge bosons receive the mass

$$m_A = \frac{gv}{2}, \quad (20.26)$$

signaling that all three generators of $SU(2)$ are broken equally well by (20.23).

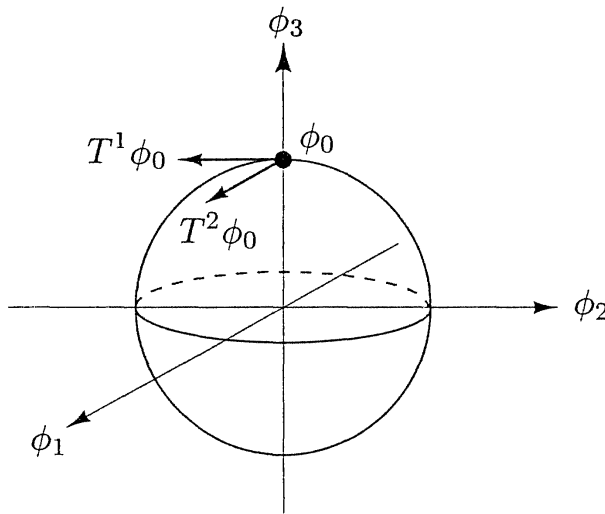


Figure 20.1. The space of configurations for a scalar field in the vector representation of $SU(2)$. When the $SU(2)$ symmetry is spontaneously broken, the allowed vacuum states lie on a spherical surface. If the vacuum expectation value ϕ_0 lies in the 3 direction, then the generator T^3 leaves ϕ_0 unchanged, while T^1 and T^2 rotate ϕ_0 in the directions shown.

What if we had taken ϕ to transform according to the vector representation of $SU(2)$? If we take ϕ to be a real-valued vector under $SU(2)$, we must assign it the covariant derivative

$$(D_\mu \phi)_a = \partial_\mu \phi_a + g \epsilon_{abc} A_\mu^b \phi_c. \quad (20.27)$$

Again, the ϕ kinetic energy term is the square of this object, and so, if ϕ acquires a vacuum expectation value, we find the gauge boson mass term

$$\Delta \mathcal{L} = \frac{1}{2} (D_\mu \phi)^2 = \frac{g^2}{2} (\epsilon_{abc} A_\mu^b (\phi_0)_c)^2 + \dots \quad (20.28)$$

If a vector of $SU(2)$ acquires an expectation value ϕ_0 , we can choose our coordinates so that this vector points in any particular direction in the internal space. We will choose it to point in the 3 direction, as indicated in Fig. 20.1:

$$\langle \phi_c \rangle = (\phi_0)_c = V \delta_{c3}. \quad (20.29)$$

Inserting (20.29) into (20.28), we find

$$\Delta \mathcal{L} = \frac{g^2}{2} V^2 (\epsilon_{ab3} A_\mu^b)^2 = \frac{g^2}{2} V^2 ((A_\mu^1)^2 + (A_\mu^2)^2). \quad (20.30)$$

The gauge bosons corresponding to the generators 1 and 2 acquire masses

$$m_1 = m_2 = gV, \quad (20.31)$$

while the boson corresponding to the generator 3 remains massless. It is easy to see the reason for this distinction by glancing at Fig. 20.1. The vacuum expectation value of ϕ_c destroys the symmetry of rotation about the axes 1 and 2, but it preserves the symmetry of rotation about the 3 axis. As we saw

in our general analysis, gauge bosons corresponding to unbroken symmetry generators remain massless.

It is interesting that this model contains both massive and massless gauge bosons, with the distinction between these bosons created by spontaneous symmetry breaking. If we interpret the massive bosons as W bosons and the massless gauge boson as the photon, it is tempting to interpret this theory as a unified model of weak and electromagnetic interactions. Georgi and Glashow proposed this model as a serious candidate for the theory of weak interactions.[†] However, Nature chooses a different model, which we will discuss in the next section.

We turn next to a more complicated example. Consider an $SU(3)$ gauge theory with a scalar field in the adjoint representation. The covariant derivative of ϕ takes the form

$$D_\mu \phi_a = \partial_\mu \phi_a + g f_{abc} A_\mu^b \phi_c, \quad (20.32)$$

and so the gauge field masses arise from the term

$$\Delta \mathcal{L} = \frac{g^2}{2} (f_{abc} A_\mu^b \phi_c)^2. \quad (20.33)$$

We can write this more clearly by defining the quantity

$$\Phi = \phi_c t^c, \quad (20.34)$$

where t^c are the 3×3 traceless Hermitian matrices that represent the generators of $SU(3)$. Using this notation and the definition (15.68) of the structure constants, we can rewrite the mass term (20.33) as

$$\Delta \mathcal{L} = -g^2 \text{tr}[[t^a, \Phi][t^b, \Phi]] A_\mu^a A^{b\mu}. \quad (20.35)$$

Now let Φ acquire a vacuum expectation value

$$\langle \Phi \rangle = \Phi_0. \quad (20.36)$$

Since Φ_0 is a traceless Hermitian matrix, we should analyze its effects by diagonalizing it. In principle, Φ_0 could have three arbitrary eigenvalues that sum to zero. However, when one minimizes explicit potential energy functions, one often finds expectation values that preserve some of the original symmetry. We will consider two examples.

First, Φ_0 might have the orientation

$$\Phi_0 = |\phi| \cdot \begin{pmatrix} 1 & & \\ & 1 & \\ & & -2 \end{pmatrix}. \quad (20.37)$$

[†]H. Georgi and S. L. Glashow, *Phys. Rev. Lett.* **28**, 1494 (1972).

This matrix commutes with the four $SU(3)$ generators

$$t^a = \begin{pmatrix} \tau^a & 0 \\ 0 & 0 \end{pmatrix}, \quad t^8 = \frac{1}{\sqrt{6}} \begin{pmatrix} 1 & & \\ & 1 & \\ & & -2 \end{pmatrix}. \quad (20.38)$$

Thus, the expectation value (20.37) breaks $SU(3)$ spontaneously to $SU(2) \times U(1)$ and leaves the gauge bosons corresponding to these four generators massless. The remaining four generators of $SU(3)$,

$$\begin{aligned} t^4 &= \frac{1}{2} \begin{pmatrix} & 1 \\ & 0 \\ 1 & 0 & 0 \end{pmatrix}, & t^5 &= \frac{1}{2} \begin{pmatrix} & i \\ & 0 \\ -i & 0 & 0 \end{pmatrix}, \\ t^6 &= \frac{1}{2} \begin{pmatrix} & 0 \\ & 1 \\ 0 & 1 & 0 \end{pmatrix}, & t^7 &= \frac{1}{2} \begin{pmatrix} & 0 \\ & -i \\ 0 & i & 0 \end{pmatrix}, \end{aligned} \quad (20.39)$$

acquire the masses

$$m^2 = (3g|\phi|)^2, \quad (20.40)$$

as one can check by substituting these matrices into Eq. (20.35).

Another possible orientation for Φ_0 is

$$\Phi_0 = |\phi| \cdot \begin{pmatrix} 1 & & \\ & -1 & \\ & & 0 \end{pmatrix}. \quad (20.41)$$

In this case, only t^3 and t^8 commute with Φ_0 , so the original $SU(3)$ symmetry is broken down to $U(1) \times U(1)$. By substituting into (20.35), one can determine that the gauge bosons corresponding to the remaining generators of $SU(3)$ acquire the masses

$$t^1, t^2 : \quad m^2 = (2g|\phi|)^2, \quad t^4, t^5, t^6, t^7 : \quad m^2 = (g|\phi|)^2. \quad (20.42)$$

Still larger symmetry groups offer a wider variety of symmetry-breaking patterns, and more complex mass matrices. We consider one further example in Problem 20.1.

Formal Description of the Higgs Mechanism

Up to this point, our study of the Higgs mechanism has been based on the explicit analysis of scalar field Lagrangians coupled to gauge fields. Scalar field theories provide the simplest examples of systems with spontaneous symmetry breaking, and the explicit calculations they allow are useful for visualization. But symmetries can be broken in other ways. In the theory of superconductivity, for example, the Abelian gauge invariance of electromagnetism is broken by pairs of electrons that condense in the ground state of a metal. In Section 19.3, we argued that, in the approximation that quark masses are very small, QCD possesses global symmetries that are spontaneously broken by a

condensation of quark-antiquark pairs. In these examples, spontaneous symmetry breaking is the result of strong interactions beyond perturbation theory. We would like to understand whether these more general mechanisms of spontaneous symmetry breaking can also give mass to vector bosons, and, if so, how the masses can be calculated.

To carry out this analysis, we will need to abstract several ideas from the preceding discussion. First, we will discuss in general terms the relations between gauge bosons, Goldstone bosons, and global symmetry currents. Then we will use this information to construct the gauge boson mass matrix without making direct use of the Lagrangian.

Consider, first, an arbitrary quantum field theory \mathcal{L}_0 with a global symmetry G . In Section 9.6, we derived the Noether current corresponding to the G symmetry by varying the Lagrangian by a local gauge transformation with infinitesimal parameter $\alpha^a(x)$. Transforming with a constant α^a should leave \mathcal{L}_0 unchanged. Then the more general variation of \mathcal{L}_0 must take the form

$$\delta\mathcal{L}_0 = -(\partial_\mu\alpha^a)J^{\mu a}, \quad (20.43)$$

for some set of vector operators $J^{\mu a}$ built from the fields of \mathcal{L}_0 . The variational principle then tells us that

$$\partial_\mu J^{\mu a} = 0. \quad (20.44)$$

We can identify the $J^{\mu a}$ as the Noether currents of the global gauge symmetry.

We can now couple this globally symmetric theory to non-Abelian gauge fields, promoting the global symmetry to a local symmetry. To first order in g , the new Lagrangian should take the form

$$\mathcal{L} = \mathcal{L}_0 + gA_\mu^a J^{\mu a} + \mathcal{O}(A^2). \quad (20.45)$$

To check this, note that the transformation (20.43) compensates the variation due to a gauge transformation of A_μ^a , Eq. (15.46), to leading order in g . The terms of order A^2 and higher can in general be arranged to compensate the higher-order terms in the gauge transformation. Thus, matrix elements involving only one insertion of the gauge field can be evaluated using properties of the Noether currents of the original globally symmetric theory. Note in particular that the conservation law for these currents, Eq. (20.44), guarantees that the Ward identities for these matrix elements are satisfied.

If the global symmetry of the theory \mathcal{L}_0 is spontaneously broken, this theory will contain Goldstone bosons, which will stand in a special relation to the Noether currents. At long wavelength, the Goldstone bosons become infinitesimal symmetry rotations of the vacuum, $Q^a |0\rangle$, where Q^a is the global charge associated with $J^{\mu a}$. Thus, the operators $J^{\mu a}$ have the correct quantum numbers to create Goldstone bosons from the vacuum. Let $|\pi_k\rangle$ denote a Goldstone boson state. In general, there will be a current $J^{\mu a}$ that can create or destroy this boson; we can parametrize the corresponding matrix element as

$$\langle 0 | J^{\mu a}(x) | \pi_k(p) \rangle = -ip^\mu F^a_k e^{-ip \cdot x}, \quad (20.46)$$

where p^μ is the on-shell momentum of the boson and F^a_k is a matrix of constants. The elements F^a_k vanish when a denotes a generator of an unbroken symmetry. Then the nonvanishing matrix elements of F^a_k connect the currents of the spontaneously broken symmetries to their corresponding Goldstone bosons. Since the currents $J^{\mu a}$ are conserved, we find

$$0 = \partial_\mu \langle 0 | J^{\mu a}(x) | \pi_k(p) \rangle = -p^2 F^a_k e^{-ip \cdot x}, \quad (20.47)$$

which implies that the bosons with nonzero matrix elements (20.46) satisfy $p^2 = 0$ on shell and so are massless. This is another proof of Goldstone's theorem.[†]

Since the scalar field theory that we examined earlier in this section should be a special case of this analysis, we should find there an example of the relation given in Eq. (20.46). Comparing Eqs. (20.15) and (20.45), we see that, for the scalar field theory,

$$J^{\mu a} = \partial_\mu \phi_i T_{ij}^a \phi_j, \quad (20.48)$$

which is indeed the Noether current corresponding to the global gauge symmetry. Inserting the vacuum expectation value (20.16), we find

$$J^{\mu a} = \partial_\mu \phi_i (T^a \phi_0)_i, \quad (20.49)$$

which leads to the set of matrix elements

$$\langle 0 | J^{\mu a}(x) | \phi_i(p) \rangle = -ip^\mu (T^a \phi_0)_i e^{-ip \cdot x}. \quad (20.50)$$

Using this relation, we can identify

$$F^a_i = T_{ij}^a \phi_{0j} \quad (20.51)$$

for the Higgs mechanism in a weakly coupled scalar field theory. To be more precise, the index i runs over all components of the scalar field ϕ . However, we saw in the discussion below Eq. (20.19) that (20.51) is nonzero only for components ϕ_i that are Goldstone bosons, and only for symmetry generators a that are spontaneously broken. Thus the nonzero components of (20.51) form precisely the structure (20.46).

As a concrete illustration of the way that the objects $T^a \phi_0$ link spontaneously broken generators and Goldstone bosons, consider the situation of $SU(2)$ symmetry broken by a scalar field in the vector representation, as in Eq. (20.29) and Fig. 20.1. According to the figure, rotations about the 1 axis tip the vacuum expectation value of ϕ into the 2 direction, rotations about the 2 axis tip this expectation value into the 1 direction, and rotations about 3 leave $\langle \phi \rangle$ invariant. Thus the gauge generators T^1 and T^2 are spontaneously broken, and the scalar field components ϕ^2 and ϕ^1 are the corresponding Goldstone bosons. This accords with the result of computing the elements of $(T^a \phi_0)_i$ explicitly: Using $(T^a)_{bc} = \epsilon^{bac}$, we find

$$(T^a \phi_0)_b = \epsilon_{bac} \langle \phi^c \rangle = V \epsilon^{ba3}. \quad (20.52)$$

[†]A special case of this argument appeared in the discussion of Eq. (19.88).

Inserting this result into formula (20.50), we see that the current of each spontaneously broken symmetry creates and destroys its own Goldstone boson.

Now we can use this formalism to study the working of the Higgs mechanism in this general context. Consider the original theory \mathcal{L}_0 coupled to gauge bosons of G . To see how the Higgs mechanism operates, we must compute the vacuum polarization amplitude. This amplitude is required by the Ward identity to be transverse, so it is necessarily of the form

$$a \sim \text{---} \text{---} b = i \left(g^{\mu\nu} - \frac{k^\mu k^\nu}{k^2} \right) \cdot (m_{ab}^2 + \mathcal{O}(k^2)). \quad (20.53)$$

It is not easy to compute the nonsingular terms in (20.53) in this general situation, but it is straightforward to compute the singular term, which comes from contributions with an intermediate Goldstone boson. Combining Eqs. (20.45) and (20.46), we see that the amplitude for a gauge boson to convert to a Goldstone boson is

$$\text{---} \leftarrow \bullet \text{---} \sim \sim \sim \mu = -g k^\mu F^a{}_j. \quad (20.54)$$

Then the pole contribution to the vacuum polarization is

$$\text{Diagram: Two wavy lines with a dot between them.} = (gk^\mu F^a_j) \frac{i}{k^2} (-gk^\nu F^b_j). \quad (20.55)$$

Comparing (20.55) with (20.21), we identify

$$m_{ab}^2 = g^2 F^a_j F^b_j. \quad (20.56)$$

Notice that, in the case in which the symmetry is broken by a scalar field, this result reverts to (20.18). However, Eq. (20.56) applies to any theory of spontaneously broken symmetry, whether the symmetry breaking is apparent from the Lagrangian or whether it requires strong interactions or other non-perturbative effects. It is a general result, then, that any gauge boson coupled to the current of a spontaneously broken symmetry acquires a mass.

20.2 The Glashow-Weinberg-Salam Theory of Weak Interactions

We are now ready to write down the spontaneously broken gauge theory that gives the experimentally correct description of the weak interactions, a model introduced by Glashow, Weinberg, and Salam (GWS). Like the second $SU(2)$ model considered in the previous section, this model gives a unified description of weak and electromagnetic interactions, in which the massless photon corresponds to a particular combination of symmetry generators that remains unbroken.

Again we begin with a theory with $SU(2)$ gauge symmetry. To break the symmetry spontaneously, we introduce a scalar field in the spinor representation of $SU(2)$, as in Eq. (20.22). However, we know that this theory leads

to a system with no massless gauge bosons. We therefore introduce an additional $U(1)$ gauge symmetry. We assign the scalar field a charge $+1/2$ under this $U(1)$ symmetry, so that its complete gauge transformation is

$$\phi \rightarrow e^{i\alpha^a \tau^a} e^{i\beta/2} \phi. \quad (20.57)$$

(Here $\tau^a = \sigma^a/2$.) If the field ϕ acquires a vacuum expectation value of the form

$$\langle \phi \rangle = \frac{1}{\sqrt{2}} \begin{pmatrix} 0 \\ v \end{pmatrix}, \quad (20.58)$$

then a gauge transformation with

$$\alpha^1 = \alpha^2 = 0, \quad \alpha^3 = \beta \quad (20.59)$$

leaves $\langle \phi \rangle$ invariant. Thus, the theory will contain one massless gauge boson, corresponding to this particular combination of generators. The remaining three gauge bosons will acquire masses from the Higgs mechanism.

Gauge Boson Masses

It is straightforward to work out the details of the mass spectrum by using the methods of the previous section. The covariant derivative of ϕ is

$$D_\mu \phi = (\partial_\mu - ig A_\mu^a \tau^a - i\frac{1}{2}g' B_\mu) \phi, \quad (20.60)$$

where A_μ^a and B_μ are, respectively, the $SU(2)$ and $U(1)$ gauge bosons. Since the $SU(2)$ and $U(1)$ factors of the gauge group commute with one another, they can have different coupling constants, which we have called g and g' .

The gauge boson mass terms come from the square of Eq. (20.60), evaluated at the scalar field vacuum expectation value (20.58). The relevant terms are

$$\Delta \mathcal{L} = \frac{1}{2} (0 \quad v) \left(g A_\mu^a \tau^a + \frac{1}{2} g' B_\mu \right) \left(g A_\mu^b \tau^b + \frac{1}{2} g' B_\mu \right) \begin{pmatrix} 0 \\ v \end{pmatrix}. \quad (20.61)$$

If we evaluate the matrix product explicitly, using $\tau^a = \sigma^a/2$, we find

$$\Delta \mathcal{L} = \frac{1}{2} \frac{v^2}{4} [g^2 (A_\mu^1)^2 + g^2 (A_\mu^2)^2 + (-g A_\mu^3 + g' B_\mu)^2]. \quad (20.62)$$

There are three massive vector bosons, which we will notate as follows:

$$\begin{aligned} W_\mu^\pm &= \frac{1}{\sqrt{2}} (A_\mu^1 \mp i A_\mu^2) & \text{with mass} \quad m_W &= g \frac{v}{2}; \\ Z_\mu^0 &= \frac{1}{\sqrt{g^2 + g'^2}} (g A_\mu^3 - g' B_\mu) & \text{with mass} \quad m_Z &= \sqrt{g^2 + g'^2} \frac{v}{2}. \end{aligned} \quad (20.63)$$

The fourth vector field, orthogonal to Z_μ^0 , remains massless:

$$A_\mu = \frac{1}{\sqrt{g^2 + g'^2}} (g' A_\mu^3 + g B_\mu) \quad \text{with mass} \quad m_A = 0. \quad (20.64)$$

We will identify this field with the electromagnetic vector potential.

From now on it will be more convenient to write all expressions in terms of these mass eigenstate fields. Consider, for instance, the coupling of the vector fields to fermions. For a fermion field belonging to a general $SU(2)$ representation, with $U(1)$ charge Y , the covariant derivative takes the form

$$D_\mu = \partial_\mu - ig A_\mu^a T^a - ig' Y B_\mu. \quad (20.65)$$

In terms of the mass eigenstate fields, this becomes

$$\begin{aligned} D_\mu = \partial_\mu - i \frac{g}{\sqrt{2}} (W_\mu^+ T^+ + W_\mu^- T^-) - i \frac{1}{\sqrt{g^2 + g'^2}} Z_\mu (g^2 T^3 - g'^2 Y) \\ - i \frac{gg'}{\sqrt{g^2 + g'^2}} A_\mu (T^3 + Y), \end{aligned} \quad (20.66)$$

where $T^\pm = (T^1 \pm iT^2)$. The normalization is chosen so that, in the spinor representation of $SU(2)$,

$$T^\pm = \frac{1}{2} (\sigma^1 \pm i\sigma^2) = \sigma^\pm. \quad (20.67)$$

The last term of Eq. (20.66) makes explicit the fact that the massless gauge boson A_μ couples to the gauge generator $(T^3 + Y)$, which generates precisely the symmetry operation (20.59).

To put expression (20.66) into a more useful form, we should identify the coefficient of the electromagnetic interaction as the electron charge e ,

$$e = \frac{gg'}{\sqrt{g^2 + g'^2}}, \quad (20.68)$$

and identify the electric charge quantum number as

$$Q = T^3 + Y. \quad (20.69)$$

These substitutions, with $Q = -1$ for the electron, give the conventional form of the coupling of the electromagnetic field.

To simplify expression (20.66) further, we define the *weak mixing angle*, θ_w , to be the angle that appears in the change of basis from (A^3, B) to (Z^0, A) :

$$\begin{pmatrix} Z^0 \\ A \end{pmatrix} = \begin{pmatrix} \cos \theta_w & -\sin \theta_w \\ \sin \theta_w & \cos \theta_w \end{pmatrix} \begin{pmatrix} A^3 \\ B \end{pmatrix},$$

that is,

$$\cos \theta_w = \frac{g}{\sqrt{g^2 + g'^2}}, \quad \sin \theta_w = \frac{g'}{\sqrt{g^2 + g'^2}}. \quad (20.70)$$

Then, with the manipulation in the Z^0 coupling

$$g^2 T^3 - g'^2 Y = (g^2 + g'^2) T^3 - g'^2 Q,$$

we can rewrite the covariant derivative (20.66) in the form

$$D_\mu = \partial_\mu - i \frac{g}{\sqrt{2}} (W_\mu^+ T^+ + W_\mu^- T^-) - i \frac{g}{\cos \theta_w} Z_\mu (T^3 - \sin^2 \theta_w Q) - ie A_\mu Q, \quad (20.71)$$

where

$$g = \frac{e}{\sin \theta_w}. \quad (20.72)$$

We see here that the couplings of all of the weak bosons are described by two parameters: the well-measured electron charge e , and a new parameter θ_w . The couplings induced by W and Z exchange will also involve the masses of these particles. However, these masses are not independent, since it follows from Eqs. (20.63) that

$$m_W = m_Z \cos \theta_w. \quad (20.73)$$

All effects of W and Z exchange processes, at least at tree level, can be written in terms of the three basic parameters e , θ_w , and m_W .

Coupling to Fermions

The covariant derivative (20.71) uniquely determines the coupling of the W and Z^0 fields to fermions, once the quantum numbers of the fermion fields are specified. To determine these quantum numbers, we must take account of the fact, mentioned in Section 17.3, that the W boson couples only to left-handed helicity states of quarks and leptons.

At the level of the classical Lagrangian, there is no difficulty in constructing theories in which the left- and right-handed components of a fermion field couple differently to gauge bosons.* Already in Section 3.2 we saw that the kinetic energy term for Dirac fermions splits into separate pieces for the left- and right-handed fields:

$$\bar{\psi} i \not{\partial} \psi = \bar{\psi}_L i \not{\partial} \psi_L + \bar{\psi}_R i \not{\partial} \psi_R. \quad (20.74)$$

When we couple ψ to a gauge field, we can assign ψ_L and ψ_R to different representations of the gauge group. Then the two terms on the right-hand side of (20.74) will contain two different covariant derivatives, and these will imply two different sets of couplings.

In the GWS model, we can use this technique to insure that only the left-handed components of the quark and lepton fields couple to the W bosons. We assign the left-handed fermion fields to doublets of $SU(2)$, while making the right-handed fermion fields singlets under this group. Once we have specified the T^3 value for each fermion field, the value of Y that we must assign follows from Eq. (20.69). This means that the Y assignments will also be different for

*In Section 19.4, we argued that there is a possible problem with this strategy at the level of quantum corrections. We will check below whether the specific model we construct avoids this problem.

the left- and right-handed components of quarks and leptons. For the right-handed fields, $T^3 = 0$, and so we reproduce the standard electric charges by assigning Y to equal the electric charge. For example, for the right-handed u quark field, $Y = +2/3$; for e_R^- , $Y = -1$. For the left-handed fields,

$$E_L = \begin{pmatrix} \nu_e \\ e^- \end{pmatrix}_L, \quad Q_L = \begin{pmatrix} u \\ d \end{pmatrix}_L, \quad (20.75)$$

the assignments $Y = -1/2$ and $Y = +1/6$, respectively, combine with $T^3 = \pm 1/2$ to give the correct electric charge assignments. Since the left- and right-handed fermions live in different representations of the fundamental gauge group, it is often useful to think of these components as distinct particles, which are mixed by the fermion mass terms.

In fact, the construction of fermion mass terms is a serious problem, because all possible such terms are forbidden by global gauge invariances. For example, we cannot write an electron mass term

$$\Delta \mathcal{L} = -m_e (\bar{e}_L e_R + \bar{e}_R e_L), \quad (20.76)$$

because the fields e_L and e_R belong to different $SU(2)$ representations and have different $U(1)$ charges. For the next few pages, we will ignore this problem by treating all fermion fields as massless. This description will suffice to analyze the structure of the weak interactions at high energies, where the quark and lepton masses can be ignored. At the end of this section we will return to the problem of writing quark and lepton mass terms in the GWS theory. The solution to this problem will reinforce the idea that the left- and right-handed fermion fields are fundamentally independent entities, mixed to form massive fermions by some subsidiary process.

If we ignore fermion masses, the Lagrangian for the weak interactions of quarks and leptons follows directly from the charge assignments given above. The fermion kinetic energy terms for e , ν , u , and d are

$$\mathcal{L} = \bar{E}_L(i\cancel{D})E_L + \bar{e}_R(i\cancel{D})e_R + \bar{Q}_L(i\cancel{D})Q_L + \bar{u}_R(i\cancel{D})u_R + \bar{d}_R(i\cancel{D})d_R. \quad (20.77)$$

In each term, the covariant derivative is given by Eq. (20.65), with T^a and Y evaluated in the particular representation to which that fermion field belongs. For example,

$$\bar{Q}_L(i\cancel{D})Q_L = \bar{Q}_L i\gamma^\mu (\partial_\mu - igA_\mu^a \tau^a - i\frac{1}{6}g' B_\mu) Q_L. \quad (20.78)$$

A right-handed neutrino would have zero coupling both to $SU(2)$ and to $U(1)$, so we have simply omitted this field from Eq. (20.77).

To work out the physical consequences of the fermion-vector boson couplings, we should write Eq. (20.77) in terms of the vector boson mass eigenstates, using the form of the covariant derivative given in Eq. (20.71). Equation (20.77) then takes the form

$$\begin{aligned} \mathcal{L} = & \bar{E}_L(i\cancel{D})E_L + \bar{e}_R(i\cancel{D})e_R + \bar{Q}_L(i\cancel{D})Q_L + \bar{u}_R(i\cancel{D})u_R + \bar{d}_R(i\cancel{D})d_R \\ & + g(W_\mu^+ J_W^{\mu+} + W_\mu^- J_W^{\mu-} + Z_\mu^0 J_Z^\mu) + e A_\mu J_{EM}^\mu, \end{aligned} \quad (20.79)$$

where

$$\begin{aligned}
 J_W^{\mu+} &= \frac{1}{\sqrt{2}} (\bar{\nu}_L \gamma^\mu e_L + \bar{u}_L \gamma^\mu d_L); \\
 J_W^{\mu-} &= \frac{1}{\sqrt{2}} (\bar{e}_L \gamma^\mu \nu_L + \bar{d}_L \gamma^\mu u_L); \\
 J_Z^\mu &= \frac{1}{\cos \theta_w} \left[\bar{\nu}_L \gamma^\mu \left(\frac{1}{2}\right) \nu_L + \bar{e}_L \gamma^\mu \left(-\frac{1}{2} + \sin^2 \theta_w\right) e_L + \bar{e}_R \gamma^\mu (\sin^2 \theta_w) e_R \right. \\
 &\quad + \bar{u}_L \gamma^\mu \left(\frac{1}{2} - \frac{2}{3} \sin^2 \theta_w\right) u_L + \bar{u}_R \gamma^\mu \left(-\frac{2}{3} \sin^2 \theta_w\right) u_R \\
 &\quad \left. + \bar{d}_L \gamma^\mu \left(-\frac{1}{2} + \frac{1}{3} \sin^2 \theta_w\right) d_L + \bar{d}_R \gamma^\mu \left(\frac{1}{3} \sin^2 \theta_w\right) d_R \right]; \\
 J_{EM}^\mu &= \bar{e} \gamma^\mu (-1) e + \bar{u} \gamma^\mu (+\frac{2}{3}) u + \bar{d} \gamma^\mu (-\frac{1}{3}) d. \tag{20.80}
 \end{aligned}$$

Here we have used Eq. (20.67) to simplify the W boson currents. Notice that the current J_{EM}^μ associated with the photon field is indeed the standard electromagnetic current.

Anomaly Cancellation

As we have just seen, there is no difficulty in writing a Lagrangian that couples the GWS gauge bosons to fermions in a chiral fashion. However, these chiral couplings do present a potential problem that appears at the level of one-loop corrections. In Section 19.2, we saw that an axial current that is conserved at the level of the classical equations of motion can acquire a nonzero divergence through one-loop diagrams that couple this current to a pair of gauge bosons. The Feynman diagram that contains this anomalous contribution is a triangle diagram with the axial current and the two gauge currents at its vertices. In a gauge theory in which gauge bosons couple to a chiral current, the dangerous triangle diagrams appear in the one-loop corrections to the three-gauge-boson vertex function. The anomalous terms violate the Ward identity for this amplitude. Thus, as we argued in Section 19.4, theories in which gauge bosons couple to chiral currents can be gauge invariant only if the anomalous contribution somehow disappears. Fortunately, as we saw there, the anomalous terms can be arranged to cancel when one sums over all possible fermion species that can circulate in these diagrams.[†]

Within the GWS theory, the requirement from experiment that the weak interaction currents are left-handed forced us to choose a chiral gauge coupling. Now we must check that the anomalous terms from the triangle diagrams cancel as required. We will find that they do, but only through a subtle and rather magical interplay of the quantum numbers of quarks and leptons.

The anomalous term of a triangle diagram of three gauge bosons A_μ^a , A_ν^b ,

[†]If you have not read Chapter 19, but you are willing to assume that the fermion triangle diagram contains a contribution that violates gauge invariance, you should still be able to follow the argument that follows.

and A_λ^c is proportional to the group theoretic invariant

$$\text{tr}[\gamma^5 t^a \{t^b, t^c\}], \quad (20.81)$$

where the trace is taken over all fermion species. The anticommutator comes from taking the sum of two triangle diagrams in which the fermions circle in opposite directions. The factor γ^5 registers the fact that the anomaly is associated with chiral currents; this factor equals -1 for left-handed fermions and $+1$ for right-handed fermions. In theories such as QED or QCD in which the gauge bosons couple equally to right- and left-handed species, the anomalies automatically cancel. This bookkeeping method is a special case of the more general method presented in Section 19.4.

To evaluate the anomalies of the GWS theory, it is easiest to work in the basis of $SU(2) \times U(1)$ gauge bosons, before the mixing to the photon and Z^0 mass eigenstates. It suffices to evaluate the triangle diagrams for massless fermions, so that right- and left-handed fermions have distinct quantum numbers. However, we must consider not only the anomalies of diagrams with three $SU(2) \times U(1)$ gauge bosons, but also diagrams with both weak-interaction gauge bosons and color $SU(3)$ gauge bosons of QCD. If we consider effects of gravity on the weak-interaction gauge theory, there is also a possibly anomalous diagram with one weak-interaction gauge boson and two gravitons. We can omit diagrams, such as the anomaly of three $SU(3)$ bosons or of one $SU(3)$ boson and two gravitons, in which all of the couplings are left-right symmetric. Then the full set of diagrams with possible anomalous terms is shown in Fig. 20.2. All of the possible anomalies must cancel if the Ward identities of the $SU(2) \times U(1)$ gauge theory are to be satisfied.

It is a special property of $SU(2)$ gauge theory that the anomaly of three $SU(2)$ gauge bosons always vanishes; this result follows from the property of Pauli sigma matrices $\{\sigma^a, \sigma^b\} = 2\delta^{ab}$, which implies that the trace (20.81) vanishes. The anomalies containing one $SU(3)$ boson or one $SU(2)$ boson are proportional to

$$\text{tr}[t^a] = 0 \quad \text{or} \quad \text{tr}[\tau^a] = 0. \quad (20.82)$$

The remaining nontrivial anomalies are those of one $U(1)$ boson with two $SU(2)$ bosons or two $SU(3)$ bosons, the anomaly of three $U(1)$ bosons, and the gravitational anomaly with one $U(1)$ gauge boson.

The anomaly of one $U(1)$ boson with two $SU(3)$ bosons is proportional to the group theory factor

$$\text{tr}[t^a t^b Y] = \frac{1}{2} \delta^{ab} \cdot \sum_q Y_q, \quad (20.83)$$

where the sum runs over left-handed quarks and right-handed quarks, with an extra (-1) for the left-handed contributions. Inserting the charge assignments given above for u_L , d_L , u_R , and d_R , we find

$$\sum_q Y_q = -2 \cdot \frac{1}{6} + \left(\frac{2}{3}\right) + \left(-\frac{1}{3}\right) = 0. \quad (20.84)$$

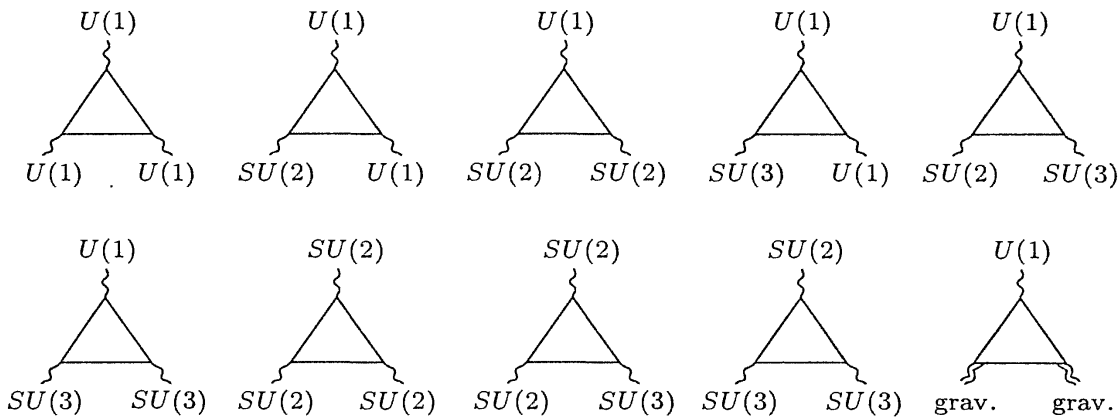


Figure 20.2. Possible gauge anomalies of weak interaction theory. All of these anomalies must vanish for the Glashow-Weinberg-Salam theory to be consistent.

Similarly, the anomaly of a $U(1)$ boson with two $SU(2)$ bosons is proportional to

$$\text{tr}[\tau^a \tau^b Y] = \frac{1}{2} \delta^{ab} \sum_{fL} Y_{fL}, \quad (20.85)$$

where the sum runs over the left-handed fermions E_L and Q_L . Thus,

$$\sum_{fL} Y_{fL} = -(-\frac{1}{2}) - 3 \cdot \frac{1}{6} = 0; \quad (20.86)$$

the factor 3 counts the color states of the quarks. The anomaly of three $U(1)$ gauge bosons is proportional to a sum involving left- and right-handed leptons and quarks:

$$\text{tr}[Y^3] = -2(-\frac{1}{2})^3 + (-1)^3 - 3[2(\frac{1}{6})^3 - (\frac{2}{3})^3 - (-\frac{1}{3})^3] = 0. \quad (20.87)$$

Finally, the gravitational anomaly with one $U(1)$ gauge boson is proportional to

$$\text{tr}[Y] = -2(-\frac{1}{2}) + (-1) - 3[2(\frac{1}{6}) - (\frac{2}{3}) - (-\frac{1}{3})] = 0. \quad (20.88)$$

The Glashow-Weinberg-Salam theory is thus a chiral gauge theory that is completely free of axial vector anomalies among the gauge currents. However, the cancellation of anomalies requires that leptons and quarks appear in complete multiplets with the structure of $(E_L, e_R, Q_L, u_R, d_R)$. This set of fields is often called a *generation* of quarks and leptons. The consistency of the theory requires that quarks and leptons appear in Nature in equal numbers, organizing themselves into successive generations in this way.

Experimental Consequences of the GWS Theory

Now that we have a fundamental theory for the coupling of W and Z bosons to fermions, we can work out the consequences of this theory for observable processes mediated by weak bosons. This analysis should reproduce the effective Lagrangian description of the weak interactions used in Chapters 17

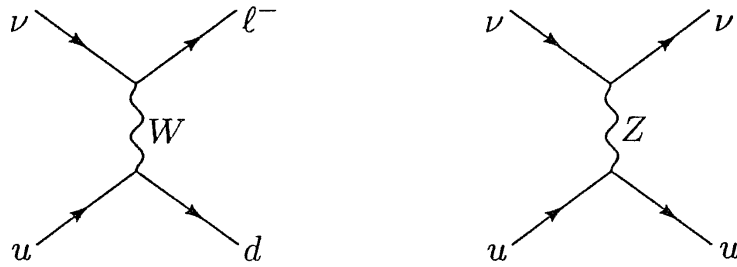


Figure 20.3. Some processes with virtual W and Z boson exchange.

and 18, and also predict additional observable effects of weak boson exchange. In our discussion here, we will derive only the most basic relations in this subject; we do not have space for a systematic survey of the phenomenology of weak interactions. However, we encourage the reader to study the experimental foundations of the weak interactions, which contain many beautiful illustrations of the principles of quantum field theory.[‡]

At energies low compared to the vector boson masses, the couplings of the weak bosons have their major effects through processes that involve virtual weak boson exchange. These processes are shown in Fig. 20.3. We will derive the Feynman rules for massive gauge bosons in Chapter 21. Meanwhile, it is reasonable to guess that the W and Z boson propagators are given by

$$\langle W^{\mu+}(p)W^{\nu-}(-p) \rangle = \frac{-ig^{\mu\nu}}{p^2 - m_W^2}, \quad \langle Z^{\mu}(p)Z^{\nu}(-p) \rangle = \frac{-ig^{\mu\nu}}{p^2 - m_Z^2}. \quad (20.89)$$

We will see in Section 21.1 that these propagators give correct expressions for diagrams with W and Z exchange up to terms of order (m_f/m_W) , where m_f is a fermion mass.

First consider the W exchange diagram in Fig. 20.3, in the limit of energies low compared to the W mass. We can then neglect the p^2 term in the denominator of the W propagator (20.89). Taking the W coupling from Eq. (20.79), we find that the diagram can be described by the effective Lagrangian

$$\begin{aligned} \Delta\mathcal{L}_W &= \frac{g^2}{m_W^2} J_W^{\mu-} J_{\mu W}^+ \\ &= \frac{g^2}{2m_W^2} (\bar{e}_L \gamma^\mu \nu_L + \bar{d}_L \gamma^\mu u_L) (\bar{\nu}_L \gamma_\mu e_L + \bar{u}_L \gamma_\mu d_L). \end{aligned} \quad (20.90)$$

The coefficient is often written in terms of the *Fermi constant*,

$$\frac{G_F}{\sqrt{2}} = \frac{g^2}{8m_W^2}. \quad (20.91)$$

The various terms in this effective Lagrangian reproduce the expressions we have already written in Eqs. (17.31), (18.28), and (18.29). Since these interactions among leptons and quarks are mediated by the exchange of an

[‡]The experimental successes of the theory of weak interactions are reviewed in the book of Commins and Bucksbaum (1983).

electrically charged vector boson, they are called collectively *charged-current* interactions. The effective Lagrangian (20.90) turns out to provide an impressively successful description of the phenomenology of charged-current weak interactions. We have described its use in high-energy neutrino scattering, but it has comparable successes in nuclear β -decay, muon decay, and a variety of other processes.

In a similar way, we can work out the effective Lagrangian resulting from virtual Z^0 exchange. We find

$$\begin{aligned}\Delta\mathcal{L}_Z &= \frac{g^2}{m_Z^2} J_Z^\mu J_{\mu Z} \\ &= \frac{8G_F}{\sqrt{2}} \left(\sum_f \bar{f} \gamma^\mu (T^3 - \sin^2 \theta_w Q) f \right)^2,\end{aligned}\quad (20.92)$$

where the sum in the second line runs over all left-handed and right-handed flavors, and we have used relation (20.73) to simplify the prefactor. We say that the effective Lagrangian (20.92) mediates *neutral current* weak interaction processes. Notice that, if we define $SU(2)$ gauge currents as

$$J^{\mu a} = \sum_f \bar{f} \gamma^\mu T^a f, \quad (20.93)$$

then the effective Lagrangians of W and Z exchange can be written together in the simple form

$$\Delta\mathcal{L}_W + \Delta\mathcal{L}_Z = \frac{8G_F}{\sqrt{2}} \left[(J^{\mu 1})^2 + (J^{\mu 2})^2 + (J^{\mu 3} - \sin^2 \theta_w J_{EM}^\mu)^2 \right]. \quad (20.94)$$

This expression becomes manifestly invariant under an unbroken global $SU(2)$ symmetry in the limit $g' \rightarrow 0$ or $\sin^2 \theta_w \rightarrow 0$. We will discuss this observation further at the end of this section.

The neutral current effective Lagrangian (20.92) contains terms that couple together all of the various species of quarks and leptons. These terms violate parity, and so distinguish themselves from the effects of strong and electromagnetic interactions. For example, Eq. (20.92) predicts the existence of neutral current deep inelastic neutrino scattering events, in which a high-energy neutrino shatters a nucleon but does not convert to a final-state muon or electron. This process is analyzed in Problem 20.4. Similarly, the neutral-current interaction predicts the presence of parity-violating effects in electron deep inelastic scattering. It also predicts a parity-violating electron-nucleon interaction that should mix atomic energy levels, and a similar parity-violating nucleon-nucleon interaction. Within the GWS theory, the strengths of all of these various effects are predicted in terms of the Fermi constant and one additional parameter, the value of $\sin^2 \theta_w$. Thus, the GWS theory can be tested by observing each of these effects and asking whether a single value of this parameter can account for the strengths of all of these disparate processes.

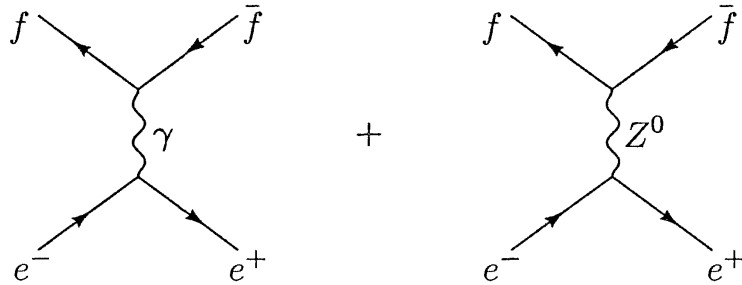


Figure 20.4. Diagrams contributing to the process $e^+e^- \rightarrow f\bar{f}$ in the Glashow-Weinberg-Salam theory.

Further tests of the GWS theory are available at higher energies. The process $e^+e^- \rightarrow f\bar{f}$ is affected in an essential way, since the theory contains a new diagram with s -channel Z^0 exchange, which interferes with the standard photon exchange diagram, as shown in Fig. 20.4. It is straightforward to work out the effects of this interference using the methods of Section 5.2, so we have left this analysis as Problem 20.3.

As the center-of-mass energy approaches m_Z , the Z^0 appears directly as a resonance in the e^+e^- annihilation cross section. Similarly, both the W and the Z can be observed as resonances in quark-antiquark annihilation, viewed as a parton subprocess in proton-antiproton scattering. The positions of these resonances are predicted from G_F , $\sin^2 \theta_w$, and the value of e or α , according to Eqs. (20.72) and (20.91). Using these relations, we find

$$m_W^2 = \frac{\pi\alpha}{\sqrt{2}G_F \sin^2 \theta_w}, \quad m_Z^2 = \frac{\pi\alpha}{\sqrt{2}G_F \sin^2 \theta_w \cos^2 \theta_w}. \quad (20.95)$$

The detailed shape of the Z^0 resonance is shown in Fig. 20.5. The experimental measurements shown are compared to a theoretical curve with the resonance position adjusted for the best fit. The height and width of the resonance are then predicted by the GWS theory. The resonance is broadened to higher energies by processes in which the electron and positron radiate collinear photons before annihilation; this correction was discussed in Problem 5.5.

Because the Lagrangian of the GWS theory treats left- and right-handed fermions as distinct species with completely different quantum numbers, the couplings of the Z^0 to left- and right-handed fermions differ significantly. One manifestation of this is the presence of a *polarization asymmetry*, a net polarization of fermions produced in the decay $Z^0 \rightarrow f\bar{f}$, or an asymmetry in the inverse process of Z^0 production. This asymmetry can be read directly from the form of the Z^0 current given in (20.80):

$$\begin{aligned} A_{LR}^f &= \frac{\Gamma(Z^0 \rightarrow f_L \bar{f}_R) - \Gamma(Z^0 \rightarrow f_R \bar{f}_L)}{\Gamma(Z^0 \rightarrow f_L \bar{f}_R) + \Gamma(Z^0 \rightarrow f_R \bar{f}_L)} \\ &= \frac{(\frac{1}{2} - |Q_f| \sin^2 \theta_w)^2 - (Q_f \sin^2 \theta_w)^2}{(\frac{1}{2} - |Q_f| \sin^2 \theta_w)^2 + (Q_f \sin^2 \theta_w)^2}. \end{aligned} \quad (20.96)$$

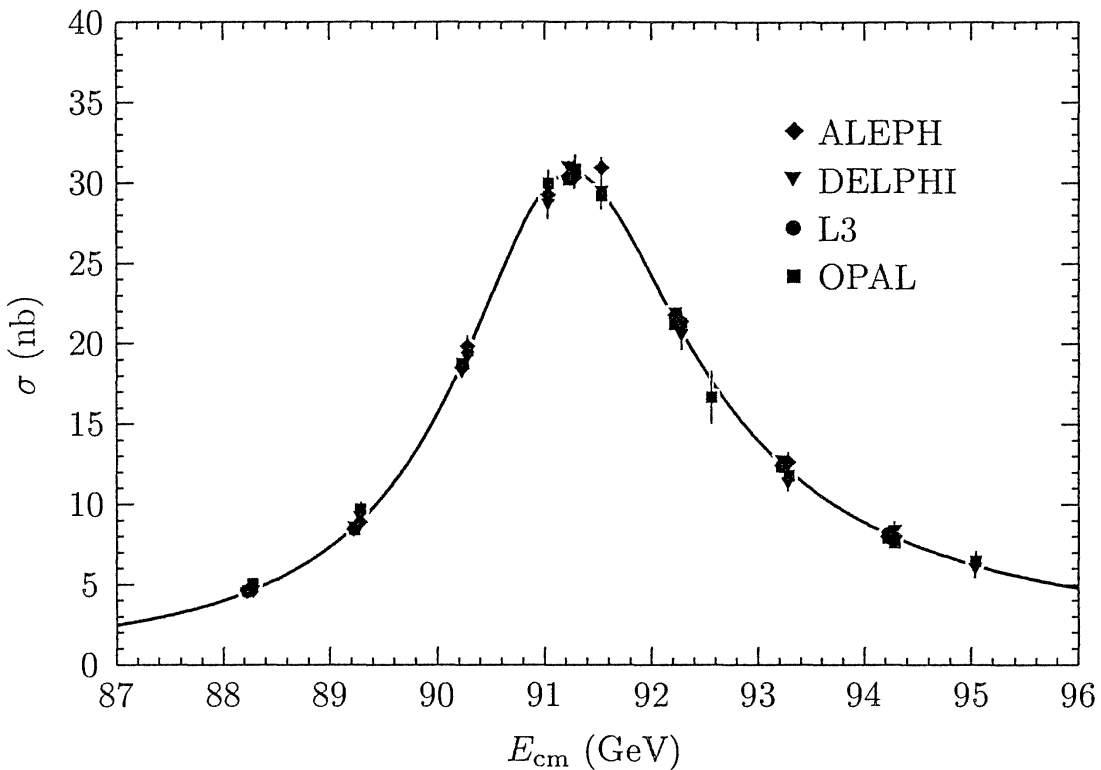


Figure 20.5. The total cross section for e^+e^- annihilation to hadrons for E_{cm} close to the Z^0 boson mass, as measured by the ALEPH, DELPHI, L3, and OPAL experiments and compiled by the Particle Data Group. *Phys. Rev. D50*, (1994), Fig. 32.14. References to the original articles are given there. The solid curve is the prediction of the GWS theory.

For a realistic value $\sin^2 \theta_w = 0.23$, this expression gives a 15% asymmetry for charged leptons and a 95% asymmetry for d , s , and b quarks. The asymmetry can be checked experimentally for leptons by measuring the polarization of τ leptons at the Z^0 resonance, or by measuring the relative cross sections for producing the resonance using left- versus right-handed electrons. For quarks, the asymmetry can be determined indirectly from the forward-backward production asymmetry on the resonance, as explained in Problem 20.3.

Because the weak neutral current has so many different manifestations, the GWS theory of weak interactions can be subjected to a stringent test by comparing the values of the parameter $\sin^2 \theta_w$ needed to account for each of its predicted effects. Table 20.1 presents the values of $\sin^2 \theta_w$ extracted from a wide variety of weak interaction neutral current effects and asymmetries. In all cases, one-loop radiative corrections must be included to analyze the experiment at the required level of accuracy. These radiative corrections involve some subtlety. First, one must adopt a specific renormalization convention that defines $\sin^2 \theta_w$ and use it consistently in all calculations. The table shows results for two different choices of this convention. In both conventions, the values of weak-interaction observables are taken to be functions of α , G_F , and a third independent parameter. In the first column this parameter is the mass ratio m_W/m_Z , and, following the tree-level expression (20.73), we consider

Table 20.1. Values of $\sin^2 \theta_w$ from Weak Interaction Experiments

Observed Quantity or Process	s_W^2	$\sin^2 \theta_{w \overline{MS}}$
m_Z	0.2247 (21)	0.2320 (6)
m_W	0.2264 (25)	0.2338 (22)
Γ_Z	0.2250(18)	0.2322 (6)
Lepton f-b asymmetries at the Z^0	0.2243 (17)	0.2315 (11)
All pair-production asymmetries at the Z^0	0.2245 (17)	0.2317 (8)
A_{LR}^e at the Z^0	0.2221 (17)	0.2292 (10)
Deep inelastic neutrino scattering	0.2260 (48)	0.233 (5)
Neutrino-proton elastic scattering	0.205 (31)	0.212 (32)
Neutrino-electron elastic scattering	0.224 (9)	0.231 (9)
Atomic parity violation	0.216 (8)	0.223 (8)
Parity violation in inelastic e^- scattering	0.216 (17)	0.223 (18)

The values listed here are obtained by fitting experimental observations by adjusting the value of s_W^2 or $\sin^2 \theta_{w \overline{MS}}$, taking α and G_F as accurately known parameters. The numbers in parentheses are the standard errors in the last displayed digits. The conversion from the experimentally measured quantities to s_W^2 or $\sin^2 \theta_{w \overline{MS}}$ depends on the value of the top quark mass and the mass of the Higgs boson. These values assume a top quark mass of 169 GeV and a Higgs mass of 300 GeV; the quoted errors include an uncertainty of 17 GeV in the top quark mass and a range from 60 GeV to 1000 GeV for the Higgs mass. The differences in the relative errors between the two columns reflect the importance of this theoretical uncertainty. Some observables depend weakly on α_s ; these values assume $\alpha_s(m_Z) = 0.120 \pm .007$. This table is taken from the article of P. Langacker and J. Erler for the Particle Data Group, *Phys. Rev. D* **50**, 1304 (1994). That article contains a full set of references and a discussion of the sources of uncertainty in these determinations.

this ratio to define a renormalized value of $\sin^2 \theta_w$:

$$s_W^2 \equiv 1 - \frac{m_W^2}{m_Z^2}. \quad (20.97)$$

In the second column, the third parameter is $\sin^2 \theta_w$ computed from the weak interaction coupling constants defined by minimal subtraction (Eq. (11.77)). The differences between different definitions of $\sin^2 \theta_w$ appear at the level of one-loop computations and can reveal interesting physics; this subject is discussed in Section 21.3.

A second subtlety is that the one-loop corrections to weak neutral current processes depend on the value of the t quark mass, which has only recently been determined and is still somewhat poorly known. The dependence on the t quark mass is relatively strong, for interesting reasons that we will discuss in Section 21.3. The one-loop corrections also depend weakly on properties of the particles responsible for the spontaneous symmetry breaking.

We can see from Table 20.1 that a wide variety of effects due to the weak neutral current have been observed, with magnitudes accounted for by a single, consistent value of $\sin^2 \theta_w$. This remarkable concordance of theory and experiment gives us confidence that the Glashow-Weinberg-Salam theory is indeed the correct description of weak and electromagnetic interactions.

Fermion Mass Terms

We now return to the problem of writing mass terms for the quarks and leptons. Recall that one cannot put ordinary mass terms into the Lagrangian, because the left- and right-handed components of the various fermion fields have different gauge quantum numbers and so simple mass terms violate gauge invariance. To give masses to the quarks and leptons, we must again invoke the mechanism of spontaneous symmetry breaking.

We began this section by assuming that a scalar field ϕ acquires a vacuum expectation value (20.58), in order to give mass to the W and Z bosons. This scalar field needed to be a spinor under $SU(2)$ and to have $Y = 1/2$ in order to produce the correct pattern of gauge boson masses. With these quantum numbers, we can also write a gauge-invariant coupling linking e_L , e_R , and ϕ , as follows:

$$\Delta\mathcal{L}_e = -\lambda_e \bar{E}_L \cdot \phi e_R + \text{h.c.} \quad (20.98)$$

Here the $SU(2)$ indices of the doublets E_L and ϕ are contracted; notice also that the charges Y of the various fields sum to zero. The parameter λ_e is a new dimensionless coupling constant. If we replace ϕ in this expression by its vacuum expectation value (20.58), we obtain

$$\Delta\mathcal{L}_e = -\frac{1}{\sqrt{2}}\lambda_e v \bar{e}_L e_R + \text{h.c.} + \dots \quad (20.99)$$

This is a mass term for the electron. The size of the mass is set by the vacuum expectation value of ϕ , rescaled by the new dimensionless coupling:

$$m_e = \frac{1}{\sqrt{2}}\lambda_e v. \quad (20.100)$$

Since the electron mass is proportional to v , one might expect that the masses of the electron and the W boson should be of the same order. In fact, taking the observed values, $m_e/m_W \sim 6 \times 10^{-6}$. Since λ_e is a renormalizable coupling, it must be treated as an input to the theory. Thus the GWS theory allows the electron to be very light, but it cannot explain why the electron is so light compared to the W boson.

We can write mass terms for the quark fields in the same way. Notice that, in the following expression, both terms are invariant under $SU(2)$ and have zero net Y :

$$\Delta\mathcal{L}_q = -\lambda_d \bar{Q}_L \cdot \phi d_R - \lambda_u \epsilon^{ab} \bar{Q}_{La} \phi_b^\dagger u_R + \text{h.c.} \quad (20.101)$$

Substituting the vacuum expectation value of ϕ from Eq. (20.58), these terms become

$$\Delta\mathcal{L}_q = -\frac{1}{\sqrt{2}}\lambda_d v \bar{d}_L d_R - \frac{1}{\sqrt{2}}\lambda_u v \bar{u}_L u_R + \text{h.c.} + \dots, \quad (20.102)$$

standard mass terms for the d and u quarks. The GWS theory thus gives the relations

$$m_d = \frac{1}{\sqrt{2}}\lambda_d v, \quad m_u = \frac{1}{\sqrt{2}}\lambda_u v. \quad (20.103)$$

As with the electron, the theory parametrizes but does not explain the small values of the d and u quark masses observed experimentally.

When additional generations of quarks are introduced into the theory, there can be additional coupling terms that mix generations. Alternatively, we can diagonalize the Higgs couplings by choosing a new basis for the quark fields. We will show that this is always possible in Section 20.3. However, this simplification of the Higgs couplings causes a complication in the gauge couplings. Let

$$u_L^i = (u_L, c_L, t_L), \quad d_L^i = (d_L, s_L, b_L) \quad (20.104)$$

denote the up- and down-type quarks in their original basis, and let $u_L'^i$ and $d_L'^i$ denote the quarks in the basis that diagonalizes their Higgs couplings. This latter basis is the physical one, since it is the basis that diagonalizes the mass matrix. The two bases are related by unitary transformations:

$$u_L'^i = U_u^{ij} u_L^j, \quad d_L'^i = U_d^{ij} d_L^j. \quad (20.105)$$

In this new basis, the W boson current takes the form

$$J_W^{\mu+} = \frac{1}{\sqrt{2}}\bar{u}_L^i \gamma^\mu d_L^i = \frac{1}{\sqrt{2}}\bar{u}_L'^i \gamma^\mu (U_u^\dagger U_d)_{ij} d_L'^j. \quad (20.106)$$

This expression is conventionally written

$$J_W^{\mu+} = \frac{1}{\sqrt{2}}\bar{u}_L'^i \gamma^\mu V_{ij} d_L'^j, \quad (20.107)$$

where V_{ij} is a unitary matrix called the Cabibbo-Kobayashi-Maskawa (CKM) matrix. The off-diagonal terms in V_{ij} allow weak-interaction transitions between quark generations. For example, restricting to two generations for simplicity and writing

$$V_{1j} d_L'^j = \cos \theta_c d_L' + \sin \theta_c s_L', \quad (20.108)$$

the term proportional to $\sin \theta_c$ allows an s quark to decay weakly to a u quark. We have made use of this structure in our discussion of the effective Lagrangian for K meson decays in Section 18.2. We will discuss CKM flavor mixing and its symmetry properties in more detail in Section 20.3.

It is interesting to note that there is no term within the structure we have described that gives a mass to the neutrino. If we wanted to generalize Eq. (20.98) to allow a neutrino mass term, we would have to introduce a new

fermion field ν_R that is completely neutral under $SU(2) \times U(1)$. Then we could write the Higgs coupling

$$\Delta\mathcal{L}_\nu = -\lambda_\nu \epsilon^{ab} \bar{E}_{La} \phi_b^\dagger \nu_R + \text{h.c.}, \quad (20.109)$$

which would give the ν_e a mass, presumably comparable to that of the electron. But we know from experiment that neutrino masses are extremely small; the mass of the ν_e is known to be less than 10 eV. This extreme suppression of the neutrino masses would be naturally explained if the states ν_R do not exist. We will show in Section 20.3 that this assumption also implies that there are no transitions between leptons of different generations; this result is also in accord with very strong experimental bounds.

The Higgs Boson

This discussion of fermion mass generation emphasizes that the scalar field that causes spontaneous breaking of the gauge symmetry is an important ingredient in the structure of the Glashow-Weinberg-Salam theory. We should therefore ask whether it has any more direct manifestations.

To investigate this question, we will work in the *unitarity gauge*, analogous to that used for the Abelian model in Eq. (20.12). Let us parametrize the scalar field ϕ by writing

$$\phi(x) = U(x) \frac{1}{\sqrt{2}} \begin{pmatrix} 0 \\ v + h(x) \end{pmatrix}. \quad (20.110)$$

The two-component spinor on the right has an arbitrary real-valued lower component, given by the vacuum expectation value of ϕ plus a fluctuating real-valued field $h(x)$ with $\langle h(x) \rangle = 0$. This spinor is acted on by a general $SU(2)$ gauge transformation $U(x)$ to produce the most general complex-valued two-component spinor. We can now make a gauge transformation to eliminate $U(x)$ from the Lagrangian. This reduces ϕ to a field with one physical degree of freedom.

An explicit renormalizable Lagrangian that leads to a vacuum expectation value for ϕ is

$$\mathcal{L} = |D_\mu \phi|^2 + \mu^2 \phi^\dagger \phi - \lambda (\phi^\dagger \phi)^2. \quad (20.111)$$

The minimum of the potential energy occurs at

$$v = \left(\frac{\mu^2}{\lambda} \right)^{1/2}. \quad (20.112)$$

In the unitarity gauge, the potential energy terms in (20.111) take the form

$$\begin{aligned} \mathcal{L}_V &= -\mu^2 h^2 - \lambda v h^3 - \frac{1}{4} \lambda h^4 \\ &= -\frac{1}{2} m_h^2 h^2 - \sqrt{\frac{\lambda}{2}} m_h h^3 - \frac{1}{4} \lambda h^4. \end{aligned} \quad (20.113)$$

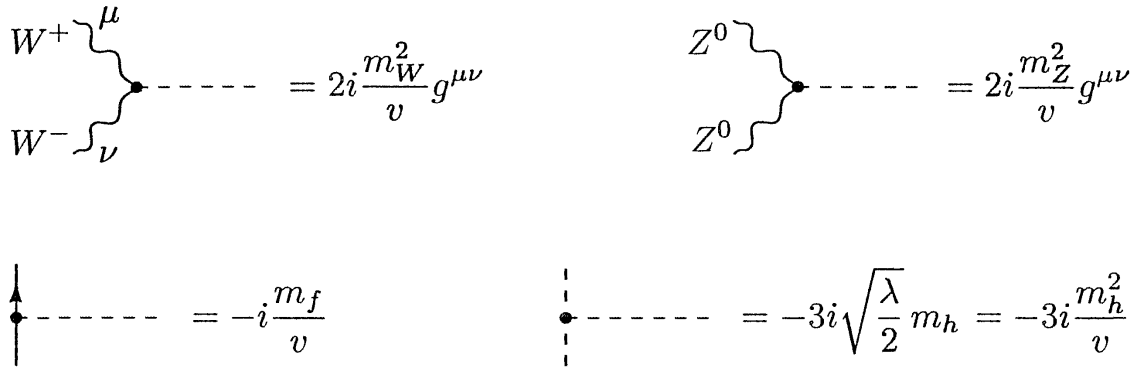


Figure 20.6. Feynman rules for the couplings of the Higgs boson to vector bosons, to fermions, and to itself.

The quantum of the field $h(x)$ is a scalar particle with mass

$$m_h = \sqrt{2}\mu^2 = \sqrt{\frac{\lambda}{2}}v. \quad (20.114)$$

This particle is known as the *Higgs boson*. As for the fermions in the GWS theory, the Higgs boson has a mass whose general magnitude is controlled by the vacuum expectation value v , but whose precise value is determined by a new, unspecified, renormalizable coupling constant.

The expansion of the kinetic energy term of (20.111) in unitarity gauge yields the gauge boson mass term (20.62), plus additional terms involving the Higgs boson field. Explicitly,

$$\mathcal{L}_K = \frac{1}{2}(\partial_\mu h)^2 + \left[m_W^2 W^{\mu+} W_\mu^- + \frac{1}{2} m_Z^2 Z^\mu Z_\mu \right] \cdot \left(1 + \frac{h}{v} \right)^2, \quad (20.115)$$

where m_W and m_Z are given by Eqs. (20.63).

Finally, the fermion mass terms in Eqs. (20.98) and (20.101) lead to direct couplings of the Higgs boson to fermions. Evaluating these terms in unitarity gauge, we find that, for any quark or lepton flavor, the Higgs boson couples according to

$$\mathcal{L}_f = -m_f \bar{f} f \left(1 + \frac{h}{v} \right). \quad (20.116)$$

The Higgs boson couplings in Eqs. (20.113), (20.115), and (20.116) lead to the Feynman rules shown in Fig. 20.6.

In general, the couplings of the Higgs boson to other particles of the weak interaction theory are proportional to the masses of those particles. Thus, the particles that are most easily made in the laboratory have very weak couplings to the Higgs boson, which makes it difficult to observe this particle. In any event, the Higgs boson has not yet been found. As of this writing, the Higgs boson that we have just described has been searched for and excluded for values of m_h below 60 GeV. If the self-coupling λ is large, however, the Higgs boson could have a mass as large as 1000 GeV; thus, a large dynamic range remains unexplored.

The phenomenological properties of the Higgs boson are worked out in more detail in the Final Project of Part III.

A Higgs Sector?

Since there is no experimental evidence for the existence of the simple Higgs boson contained in the GWS model, it is worth asking whether the W and Z bosons might acquire mass by a more complicated mechanism. There are two aspects to this question.

First, Is it certain that the W and Z bosons are gauge bosons of a spontaneously broken $SU(2) \times U(1)$ symmetry? The evidence for this idea comes from the universality of the couplings of the various quarks and leptons to the weak interactions. This universality is tested in the fact that the same value of the Fermi constant describes all charged-current weak-interaction processes, and that this same strength of coupling combined with a single value of $\sin^2 \theta_w$ describes the whole range of weak neutral current phenomena. We have seen, especially in the discussion of Chapter 16, that the principle of local gauge invariance leads naturally to the prediction of universal, flavor-independent, coupling constants. No other principle is known that would explain this striking regularity. Thus there is compelling evidence that the underlying theory of the weak interactions is a spontaneously broken gauge theory.

However, it is quite possible that the mechanism of the spontaneous breaking of $SU(2) \times U(1)$ is more complicated than the simple model of a single scalar field that we have written in Eq. (20.111). In principle, the breaking of $SU(2) \times U(1)$ might be the result of the dynamics of a complicated new set of particles and interactions, which we will refer to as the *Higgs sector*. Experiment gives us only three properties of this new sector: First, it must generate the masses of the quarks and leptons. Second, it must generate the masses of the W and Z bosons. The third piece of information, which is the only non-trivial one, comes from the relation (20.73) between weak boson masses in the GWS theory,

$$m_W = m_Z \cos \theta_w. \quad (20.117)$$

This relation is satisfied experimentally to better than 1% accuracy, that is, to the level of one-loop radiative corrections. Whatever complicated mechanism we invoke to generate the spontaneous breaking of $SU(2) \times U(1)$, it should reproduce this relation in a natural way.

To understand the implications of relation (20.117), we must analyze the gauge boson mass matrix without assuming that $SU(2) \times U(1)$ is broken by the expectation value of a scalar field. Actually, it is possible to compute the gauge boson mass matrix under much less restrictive assumptions, using the argument given at the very end of Section 20.1. There we constructed the gauge boson mass matrix from the matrix elements for gauge currents to create or destroy Goldstone bosons. We will now show that relation (20.117) follows for a large class of models of $SU(2) \times U(1)$ breaking for which these matrix elements satisfy certain simple properties.

Any model of weak-interaction symmetry breaking must contain some set of fields that is responsible for the spontaneous breaking of $SU(2) \times U(1)$. Think of this sector of the theory as a field theory with a global $SU(2) \times U(1)$ symmetry, which is promoted to a local symmetry through its coupling to gauge bosons. In the theory with global symmetry, this symmetry is spontaneously broken to $U(1)$. Since three continuous symmetries are spontaneously broken, this sector must supply three Goldstone bosons, which will eventually be eaten by W^+ , W^- , and Z^0 . Call these three bosons π_a , where $a = 1, 2, 3$. Let $J^{\mu a}$ be the $SU(2)$ symmetry currents of the new sector, and let $J^{\mu Y}$ be the $U(1)$ current. The gauge boson mass matrix will then be constructed from the matrix elements (20.46), which here take the form

$$\langle 0 | J^{\mu A} | \pi_b(p) \rangle = -ip^\mu F^A_b, \quad (20.118)$$

with $A = 1, 2, 3, Y$ and $b = 1, 2, 3$. Using the method of Eq. (20.55), we find that the gauge boson vacuum polarization contains the pole term

$$-\frac{i}{k^2} (g_A F^A_c) (g_B F^B_c), \quad (20.119)$$

summed over c , where $g_A = g$ for $A = 1, 2, 3$ and $g_A = g'$ for $A = Y$. Then we can identify the gauge boson mass matrix as

$$m_{AB}^2 = g_A g_B F^A_c F^B_c. \quad (20.120)$$

To reproduce the known form of the weak gauge boson mass matrix, we must now place constraints on the F^A_b . First we must insure that the photon remains massless. This follows if the linear combination of charges (20.69) annihilates the vacuum. In the language of Eq. (20.118), we must insist that the corresponding linear combination of currents cannot excite a Goldstone boson:

$$\langle 0 | (J^{\mu 3} + J^{\mu Y}) | \pi^a(p) \rangle = 0. \quad (20.121)$$

We can also achieve relation (20.117), using the following additional assumption: The symmetry-breaking sector has an $SU(2)$ global symmetry, under which the three Goldstone bosons and the three $SU(2)$ gauge currents transform as triplets, which remains exact when the $SU(2)$ gauge symmetry is spontaneously broken. This global $SU(2)$ symmetry implies that, if $A = a = 1, 2, 3$ in Eq. (20.118),

$$\langle 0 | J^{\mu a} | \pi^b(p) \rangle = -iF p^\mu \delta^{ab}, \quad (20.122)$$

where F is a parameter with the dimensions of mass. Combining (20.122) and (20.121), we have

$$\langle 0 | J^{\mu Y} | \pi^3(p) \rangle = +iF p^\mu. \quad (20.123)$$

Inserting this form for F^A_b into (20.120), we find the gauge boson mass matrix

$$m^2 = F^2 \begin{pmatrix} g^2 & & & \\ & g^2 & & \\ & & g^2 & -gg' \\ & & -gg' & g'^2 \end{pmatrix}, \quad (20.124)$$

where the matrix acts on the gauge boson $(A_\mu^1, A_\mu^2, A_\mu^3, B_\mu)$. The eigenvectors of this matrix are precisely (20.63) and (20.64). To reproduce the eigenvalues, we need only define

$$v = 2F. \quad (20.125)$$

We have now shown that the GWS relation between the W and Z boson masses is not special to the situation in which the gauge symmetry is broken by a single scalar field. This relation follows from the much more general assumption of an unbroken global $SU(2)$ symmetry of the Higgs sector. This symmetry is often called *custodial $SU(2)$ symmetry*.* We have seen this symmetry already as the global $SU(2)$ symmetry of the weak-interaction effective Lagrangian (20.94).

For the case of a single scalar field, the custodial symmetry arises in the following way: If we write the field ϕ in terms of its four real components, the Lagrangian (20.111) (ignoring the gauge couplings) has $O(4)$ global symmetry. The vacuum expectation value of ϕ breaks this symmetry down to $O(3)$, that is, $SU(2)$.

However, there are many other quantum field theories that break $SU(2)$ spontaneously while leaving another global $SU(2)$ symmetry unbroken. One rather complex example is given by QCD with two massless flavors, if we identify the gauged $SU(2)$ with the symmetry generated by U_L in (19.82) and identify the custodial $SU(2)$ with vectorial isospin symmetry. A copy of the familiar strong interactions with a mass scale large enough to give $F = 125$ GeV would be a perfectly acceptable model for the Higgs sector. (Unfortunately, it is not easy in this model to generate masses for the quarks and leptons.)

The question of the nature of the Higgs sector and the explicit mechanism of $SU(2) \times U(1)$ breaking is probably the most pressing open problem in the theory of elementary particles. We will discuss this question further in the Epilogue.

20.3 Symmetries of the Theory of Quarks and Leptons

Putting together the theory of strong interactions described in Chapter 17 and the theory of weak and electromagnetic interactions described in the previous section, we have now constructed a complete description of elementary particle interactions. It is interesting to investigate the symmetries of this theory, to ask what might be the fundamental symmetries of the underlying description of Nature.

We have already seen, in the arguments leading up to Eq. (15.17), that the Lagrangian of a gauge theory is highly restricted by the conditions of renormalizability and gauge invariance. In this section, we will construct the

*P. Sikivie, L. Susskind, M. Voloshin, and V. Zakharov, *Nucl. Phys.* **B173**, 189 (1980).

most general renormalizable Lagrangian consistent with the $SU(3) \times SU(2) \times U(1)$ gauge symmetries of the strong, weak and electromagnetic interactions. We can then ask what further global symmetries we must impose on this theory in order to give it the global symmetries that we see in Nature.

As a first step, we will ignore the Higgs scalar field and the mass terms of quarks, leptons, and gauge bosons. Then the Lagrangian of the theory of quarks and leptons is entirely specified by gauge invariance and renormalizability. We have

$$\mathcal{L}_K = -\frac{1}{4} \sum_i (F_{i\mu\nu}^a)^2 + \sum_J \bar{\psi}_J (iD) \psi_J, \quad (20.126)$$

where the index i runs over the three factors of the gauge group and the index J runs over the various multiplets of chiral fermions.

In principle, we could add to (20.126) the following pseudoscalar pure gauge operators:

$$\Delta \mathcal{L}_\theta = \sum_i \frac{\theta_i g_i^2}{64\pi^2} \epsilon^{\mu\nu\lambda\sigma} F_{i\mu\nu}^a F_{i\lambda\sigma}^a. \quad (20.127)$$

These terms are apparently odd under both P and T . However, we saw at the end of Section 19.2 that terms of this form can be generated or canceled by making a change of variables in the effective action. For example, the change of variables on the right-handed electron field

$$e_R \rightarrow e^{i\alpha} e_R \quad (20.128)$$

produces, according to (19.78) or (19.79), a correction to the Lagrangian involving the P - and T -odd combination of field strengths for the $U(1)$ gauge field

$$\Delta \mathcal{L} = \alpha \cdot \frac{g'^2}{32\pi^2} \epsilon^{\mu\nu\lambda\sigma} F_{\mu\nu} F_{\lambda\sigma}. \quad (20.129)$$

The coefficient of (20.129) differs from the corresponding coefficient in (19.79) because we transform only the right-handed chiral component of the electron field. If we were to transform another fermion field, of hypercharge Y , we would find a similar shift, with the coefficient proportional to Y^2 . If this new field coupled to the $SU(2)$ or $SU(3)$ gauge fields, we would also find terms proportional to those field strengths. Thus, we can eliminate the term in (20.127) involving the $U(1)$ field strengths by making the change of variables (20.128) with $\alpha = -\frac{1}{2}\theta_1$. We can eliminate all three terms in (20.127) by making appropriate chiral rotations on three fermion multiplets, say, e_R , E_L , and Q_L . The change of variables (20.128), which rotates the right-handed electron field, is not symmetric under parity and, in fact, changes the definition of the parity operation. By making this change of variables, we are choosing new coordinates in which the P and T transformation properties of the whole theory are as simple as possible.

Let us now investigate the properties of the Lagrangian (20.126) under P , C , and T . The couplings of the QCD gauge bosons are invariant to each

of these symmetries separately. However, the couplings of the $SU(2)$ gauge bosons violate P and C as much as possible. Recall from Section 3.6 that P converts a left-handed electron to a right-handed electron, and that C converts a left-handed electron to a left-handed positron. Each of these operations converts a particle that couples to $SU(2)$ gauge bosons to one that does not. However, the combination of these two operations interchanges left-handed particles with right-handed antiparticles. Thus the combined operation CP is a symmetry of (20.126). This Lagrangian is also invariant under time reversal.

Thus, we see that the discrete symmetries of C and P , on the one hand, and CP and T , on the other, stand on a very different footing in gauge field theories. Any chiral gauge theory will naturally violate C and P . At this level in our analysis, it is a mystery why C and P should be observed to be approximate symmetries of Nature. On the other hand, every theory of gauge bosons and massless fermions respects CP and T . It is known experimentally that Nature contains some interaction that violates CP , since the CP selection rules are weakly violated in the decays of the K^0 meson. But to find a source for this violation, we must add terms to our basic gauge theory (20.126).

We must, first of all, add dynamics to (20.126) that will cause the spontaneous breaking of $SU(2) \times U(1)$. We will begin by working with the simplest model with one Higgs scalar field ϕ . The most general renormalizable Lagrangian for ϕ is

$$\mathcal{L}_\phi = |D_\mu \phi|^2 + \mu^2 \phi^\dagger \phi - \lambda(\phi^\dagger \phi)^2. \quad (20.130)$$

The Hermiticity of \mathcal{L}_ϕ implies that the parameters μ^2 and λ are real. Thus this Lagrangian respects P , C , and T . As discussed at the end of the previous section, this Lagrangian also automatically has the custodial $SU(2)$ symmetry required to produce the mass relation (20.117).

Finally, we must add the terms that couple the Higgs field to the quarks and leptons. Here, renormalizability and gauge invariance provide the weakest constraints, and there are many allowed interactions. We will first analyze the coupling of ϕ to the quark fields, and then generalize this discussion to the leptons.

In writing the Higgs field couplings to the quarks, we should recall that there are known to be three generations of quarks and leptons. Thus there are three doublets of left-handed quarks:

$$Q_L^i = \begin{pmatrix} u^i \\ d^i \end{pmatrix}_L = \left(\begin{pmatrix} u \\ d \end{pmatrix}_L, \begin{pmatrix} c \\ s \end{pmatrix}_L, \begin{pmatrix} t \\ b \end{pmatrix}_L \right). \quad (20.131)$$

There are six right-handed quarks, three with $Y = \frac{2}{3}$ and three with $Y = -\frac{1}{3}$:

$$u_R^i = (u_R, c_R, t_R), \quad d_R^i = (d_R, s_R, b_R). \quad (20.132)$$

When we couple gauge fields to these quarks, we replace the ordinary derivatives with covariant derivatives. This automatically gives all of the quarks the same coupling to QCD and all quarks of the same type the same coupling to

the weak interactions. It does not allow mixing between the various quark flavors. However, the coupling of the Higgs field to the quarks does not follow from a gauge principle and so need not have any of these restrictions. Unless we require quark flavor conservation by postulating a new discrete symmetry of the theory, the Higgs couplings will, in general, mix the various flavors.

If we do not impose any additional symmetries on the theory, we must write the most general renormalizable gauge-invariant coupling with the structure of Eq. (20.101):

$$\mathcal{L}_m = -\lambda_d^{ij} \bar{Q}_L^i \cdot \phi d_R^j - \lambda_u^{ij} \bar{Q}_{La}^i \phi_b^\dagger u_R^j + \text{h.c.}, \quad (20.133)$$

where λ_d^{ij} and λ_u^{ij} are general, not necessarily symmetric or Hermitian, complex-valued matrices. The operation of CP interchanges the operators written in (20.133) with their Hermitian conjugates without changing the coefficients; thus, CP is equivalent to the substitutions

$$\lambda_d^{ij} \rightarrow (\lambda_d^{ij})^*, \quad \lambda_u^{ij} \rightarrow (\lambda_u^{ij})^*. \quad (20.134)$$

CP would be a symmetry of (20.133) if the matrices λ^{ij} were real-valued; however, there is no principle that requires this. Without the imposition of further symmetry requirements, it seems that (20.133) does maximum violence to all discrete and flavor conservation symmetries.

However, just as we were able to eliminate the T -violating terms (20.127) by making a chiral rotation, we can simplify the form of (20.133) by appropriate chiral transformations. To find the required transformations, diagonalize the Hermitian matrices obtained by squaring λ_d and λ_u . Define unitary matrices U_u and W_u by

$$\lambda_u \lambda_u^\dagger = U_u D_u^2 U_u^\dagger, \quad \lambda_u^\dagger \lambda_u = W_u D_u^2 W_u^\dagger, \quad (20.135)$$

where D_u^2 is a diagonal matrix with positive eigenvalues. Then

$$\lambda_u = U_u D_u W_u^\dagger, \quad (20.136)$$

where D_u is the diagonal matrix whose diagonal elements are the positive square roots of the eigenvalues of (20.135). We can define unitary matrices U_d and W_d in a similar way and decompose λ_d as

$$\lambda_d = U_d D_d W_d^\dagger. \quad (20.137)$$

Now make the change of variables

$$u_R^i \rightarrow W_u^{ij} u_R^j, \quad d_R^i \rightarrow W_d^{ij} d_R^j. \quad (20.138)$$

This eliminates the unitary matrices W_u and W_d from the Higgs coupling (20.133). Since each of the three u_R^i and each of the three d_R^i have the same coupling to the gauge fields, W_u and W_d commute with the corresponding covariant derivatives. Thus, under (20.138),

$$\sum_i (\bar{u}_R^i (iD) u_R^i + \bar{d}_R^i (iD) d_R^i) \rightarrow \sum_i (\bar{u}_R^i (iD) u_R^i + \bar{d}_R^i (iD) d_R^i), \quad (20.139)$$

and so W_u and W_d disappear from the theory.

The analogous transformation on the left-handed fields also makes a dramatic simplification. Make the change of variables

$$u_L^i \rightarrow U_u^{ij} u_L^j, \quad d_L^i \rightarrow U_d^{ij} d_L^j. \quad (20.140)$$

This transformation eliminates U_u , U_d from the terms in (20.133) that involve the lower component of the Higgs field. In unitarity gauge, only these terms survive. By combining the diagonal elements of D_u and D_d with the vacuum expectation value of the Higgs field, we can relate these elements to quark masses:

$$m_u^i = \frac{1}{\sqrt{2}} D_u^{ii} v, \quad m_d^i = \frac{1}{\sqrt{2}} D_d^{ii} v. \quad (20.141)$$

With this replacement, (20.133) takes the form

$$\mathcal{L}_m = -m_d^i \bar{d}_L^i d_R^j \left(1 + \frac{h}{v}\right) - m_u^i \bar{u}_L^i u_R^j \left(1 + \frac{h}{v}\right) + \text{h.c.} \quad (20.142)$$

This has the standard form of quark mass terms and Higgs boson couplings. The transformations (20.138) and (20.140) thus convert the quark fields to the basis of mass eigenstates. In this basis, the mass terms and Higgs couplings are diagonal in flavor and conserve P , C , and T .

Since left-handed u and d quarks have identical couplings to QCD, the matrices U_u and U_d commute with the QCD couplings in the covariant derivative. However, u_L and d_L are mixed by the weak interactions, and so we must investigate the effect of (20.140) on the $SU(2) \times U(1)$ couplings more carefully. This is most easily done by referring to the Lagrangian (20.79). The matrices U_u and U_d cancel out of the pure kinetic terms in the first line of (20.79). They also cancel out of the electromagnetic current J_{EM}^μ ; for example,

$$\bar{u}_L^i \gamma^\mu u_L^i \rightarrow \bar{u}_L^i U_u^{\dagger ij} \gamma^\mu U_u^{jk} u_L^k = \bar{u}_L^i \gamma^\mu u_L^i. \quad (20.143)$$

By the same logic, U_u and U_d cancel out of the Z^0 boson current.

However, in the current that couples to the W boson field, we find

$$J^{\mu+} = \frac{1}{\sqrt{2}} \bar{u}_L^i \gamma^\mu d_L^i \rightarrow \frac{1}{\sqrt{2}} \bar{u}_L^i \gamma^\mu (U_u^\dagger U_d)^{ij} d_L^j. \quad (20.144)$$

That is, the charge-changing weak interactions link the three u_L^i quarks with a unitary rotation of the triplet of d_L^i quarks, with this rotation given by the unitary matrix

$$V = U_u^\dagger U_d. \quad (20.145)$$

The matrix V is known as the *Cabibbo-Kobayashi-Maskawa* (CKM) mixing matrix.

The matrix V can have complex elements, but we can remove phases from V by performing phase rotations of the various quark fields. Before analyzing the case of three generations, it is useful to consider the case of two

generations— u , d , c , and s . In this case, V is a 2×2 unitary matrix. Such a matrix has 4 parameters; we can write its most general form as

$$V = \begin{pmatrix} \cos \theta_c e^{i\alpha} & \sin \theta_c e^{i\beta} \\ -\sin \theta_c e^{i(\alpha+\gamma)} & \cos \theta_c e^{i(\beta+\gamma)} \end{pmatrix}. \quad (20.146)$$

One parameter of V is a rotation angle, and the other three are phases. We can remove these phases by performing the change of variables on the quark fields

$$q_L^i \rightarrow \exp[i\alpha^i] q_L^i. \quad (20.147)$$

This global phase rotation has no effect on any term of the Lagrangian except for the weak charged current (20.144). A phase rotation that is equal for all four quark flavors cancels out of (20.144). However, the other three possible phase transformations are just what we need to eliminate α , β , and γ .

When we have chosen the phases of the quark fields in this way, V takes the form

$$V = \begin{pmatrix} \cos \theta_c & \sin \theta_c \\ -\sin \theta_c & \cos \theta_c \end{pmatrix}. \quad (20.148)$$

Then the quark terms in the weak charged current can be written

$$J^{\mu+} = \frac{1}{\sqrt{2}} (\cos \theta_c \bar{u}_L \gamma^\mu d_L + \sin \theta_c \bar{u}_L \gamma^\mu s_L - \sin \theta_c \bar{c}_L \gamma^\mu d_L + \cos \theta_c \bar{c}_L \gamma^\mu s_L). \quad (20.149)$$

We have already seen, in Eqs. (18.31) and (18.32), that this is the way the s quark enters the weak interactions. The angle θ_c is the Cabibbo angle, as defined in Eq. (18.30).

The same set of arguments can be made for the theory with three generations. Here V is a general unitary 3×3 matrix. Such a matrix has 9 parameters. Of these, 3 are rotation angles; this is the number of parameters of an $O(3)$ rotation. The remaining 6 parameters are phases. We can remove these phases by making phase rotations of quark fields as in (20.147), but the overall phase is redundant, so we can remove only 5 of these phases. The final form of V contains 3 angles, of which one is the Cabibbo angle, and one phase. After all the transformations we have made, this one phase that makes some couplings of the W^+ to quarks complex is the only remaining parameter that violates CP .

We began this argument from a Lagrangian for the quark-Higgs boson coupling that seemed to violate all possible flavor symmetries and all discrete spacetime symmetries. However, by making changes of variables on the fermion fields, we have been able to dramatically simplify the form of the Lagrangian. If we keep only those terms involving the massless gauge bosons, the photon and the gluons, plus the mass terms and interactions written in (20.142), we see that this set of terms conserves P , C , T , and all flavor symmetries. This dramatic simplification occurs because the unbroken gauge symmetry of Nature, the gauge symmetry of QCD and QED, is nonchiral and can be written as acting on Dirac fermions. Since we have omitted only the

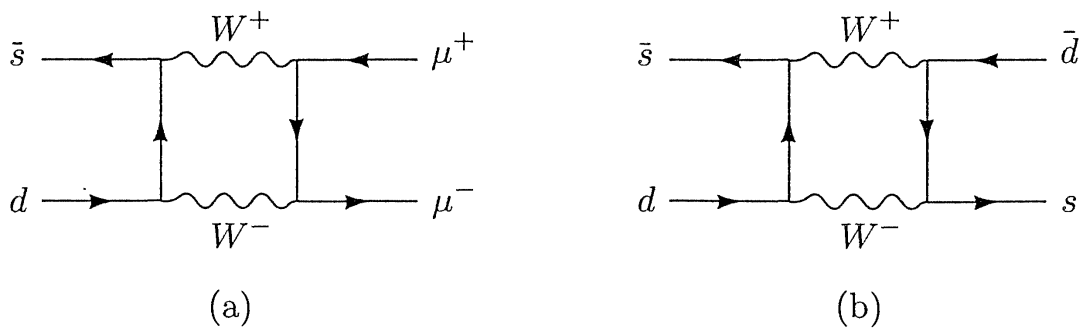


Figure 20.7. Higher-order diagrams that seem to give the leading contributions to flavor-changing weak neutral current processes: (a) $K^0 \rightarrow \mu^+ \mu^-$; (b) $K^0 \leftrightarrow \bar{K}^0$.

effects mediated by the massive W and Z bosons, this much of the analysis already guarantees that Nature will appear, to a high degree of approximation, to respect the three separate discrete symmetries and all quark flavor conservation laws. Notice that we did not assume any fundamental global symmetries, but depended only on the assignment of gauge quantum numbers in the $SU(3) \times SU(2) \times U(1)$ gauge theory.

If we include the Z boson and the weak neutral current, we have a theory that violates P and C through Z exchange but that respects CP . In addition, this theory respects all flavor conservation laws. We describe this situation by saying that there is no flavor-changing weak neutral current. The experimental evidence for this statement is quite impressive. The best tests come from the study of the neutral K^0 meson, which is an $s\bar{d}$ bound state and so could decay by Z^0 exchange if this boson coupled to a flavor-changing current. In fact, the decay $K^0 \rightarrow \mu^+ \mu^-$ is highly suppressed, to the level of the one-loop weak interaction correction shown in Fig. 20.7(a). Similarly, the interconversion of K^0 and \bar{K}^0 , which could proceed directly if the Z^0 could change flavor, is suppressed to the level of the contribution shown in Fig. 20.7(b).

On the other hand, W bosons couple to currents that can change quark flavor, in a pattern parametrized by the Cabibbo angle and the other angles in the CKM matrix. Thus, heavy quark flavors decay by W boson exchange processes. Since the W couples to a current that contains only left-handed quarks, it mediates an interaction that violates P and C maximally. This violation of discrete symmetries is concealed from our ordinary experience because the amplitude for W exchange is small. However, this P and C violation is a dramatic qualitative feature of weak decays.

Since the coupling of the W to quarks contains an irreducible phase, these couplings in principle can violate CP . However, we have seen that this phase can be removed in a theory with only two generations. This means that the phase of the CKM matrix can have physical consequences only in a process that involves all three generations. Typically, this means that the CKM phase can contribute only to weak interaction loop corrections or to complicated exclusive decay processes. Thus the $SU(3) \times SU(2) \times U(1)$ theory can account

for CP violation, and also explains why this effect is much weaker even than the weak interactions. It is interesting to note that Kobayashi and Maskawa originally proposed the existence of the third generation in order to provide a mechanism for CP violation.[†]

On the other hand, at this moment there is no conclusive evidence that the origin of CP violation is indeed the phase of the CKM matrix. All of the arguments we have given in this section have used the simplest model of the Higgs sector, in which this sector consists of a single scalar field. More general models of the Higgs sector may leave behind a more complicated set of quark-Higgs couplings than appear in (20.142), and some of these may violate CP . In addition, there may be terms in the Higgs sector itself that lead to CP violation. The origin of the observed CP violation is still an open problem that needs both theoretical and experimental exploration.

Before leaving this subject, we must discuss one more aspect of this argument that is still mysterious. To simplify the Lagrangian of the gauge theory of quarks to its final form, we needed to make chiral changes of variables in the functional integral. We saw in Section 19.2, and we reviewed at the beginning of this section, that such changes of variables produce the new P - and T -violating terms written in Eq. (20.127). It can be shown, using the fact that these terms are total derivatives, that the terms involving $SU(2)$ and $U(1)$ field strengths have no observable effects. However, the term involving QCD field strengths can induce an electric dipole moment for the neutron, a T -violating effect that has been searched for and excluded at an impressive level of accuracy. Thus the P - and T -violating combination of QCD field strengths cannot be allowed to appear in the Lagrangian. On the other hand, if the original up and down quark Higgs coupling matrices were of the most general possible form, it seems that this cannot be avoided. This problem is known as the *strong CP problem*. To solve this problem, one must either constrain the Higgs coupling matrices, violating the spirit of the argument we have just concluded, or one must add additional structure to the Higgs sector.[‡]

Finally, let us discuss the general form and simplification of the Higgs boson couplings to leptons. When we wrote the Glashow-Weinberg-Salam Lagrangian in the previous section, we noted that no gauge field coupled to the right-handed neutrino. Thus, we chose to eliminate this particle from the theory. We might need right-handed components of the neutrinos to construct neutrino mass terms, but at the moment there is no evidence for nonzero neutrino masses. Thus, in the remainder of this section, we will assume that there are no right-handed neutrinos and work out the consequences of this assumption.*

[†]M. Kobayashi and T. Maskawa, *Prog. Theor. Phys.* **49**, 652 (1973).

[‡]The strong CP problem, its proposed solutions, and their unexpected implications are reviewed by R. D. Peccei in *CP Violation*, C. Jarlskog, ed. (World Scientific, 1989).

*In generalizations of the $SU(2) \times U(1)$ model, neutrinos can acquire Majorana

Generalizing Eq. (20.133), we can write the most general coupling of a Higgs boson to three generations of leptons. Since there are no right-handed neutrinos, the only possible coupling is

$$\mathcal{L}_m = -\lambda_\ell^{ij} \bar{E}_L^i \cdot \phi e_R^j + \text{h.c.} \quad (20.150)$$

To diagonalize this coupling, represent λ_ℓ in the form

$$\lambda_\ell = U_\ell D_\ell W_\ell^\dagger, \quad (20.151)$$

and eliminate the matrices U_ℓ and W_ℓ by the changes of variables

$$e_L^i \rightarrow U_\ell^{ij} e_L^j, \quad \nu_L^i \rightarrow U_\ell^{ij} \nu_L^j, \quad e_R^i \rightarrow W_\ell^{ij} e_R^j. \quad (20.152)$$

Since we are now making the same change of variables on the two components of the weak doublet E_L^i , this change of variables commutes with the $SU(2)$ interactions in the covariant derivative. Thus the unitary matrices U_ℓ and W_ℓ completely disappear from the theory. The result is a theory of leptons that conserves CP exactly and also conserves the lepton number of each generation. This last result is very accurately tested experimentally. For example, there is no evidence for the generation-changing muon decay processes $\mu^- \rightarrow e^- \gamma$ or $\mu^- \rightarrow e^- e^- e^+$; the branching ratios for these processes are known to be below 10^{-10} .

We have seen, then, that the $SU(3) \times SU(2) \times U(1)$ gauge theory of quarks and leptons does an excellent job of accounting for the symmetries and conservation laws that are observed in elementary particle phenomena. It predicts which symmetries should be exact in Nature and which should be approximate. For approximate symmetries, it gives an accurate estimate of the level of symmetry violation. Most remarkably (except for the one issue of the strong CP problem), none of these predictions depend on any underlying global discrete or flavor symmetries in the fundamental equations. The global symmetries that we observe in Nature follow only from gauge invariance and the specific representation assignments that we made in constructing our gauge theory description.

mass terms that are naturally very small. These models also respect the constraints on lepton flavor mixing described in the next paragraph. For an introduction to these ideas on neutrino mass, see P. Ramond, in *Perspectives in the Standard Model*, R. K. Ellis, C. T. Hill, and J. D. Lykken, eds. (World Scientific, 1992).

Problems

20.1 Spontaneous breaking of $SU(5)$. Consider a gauge theory with the gauge group $SU(5)$, coupled to a scalar field Φ in the adjoint representation. Assume that the potential for this scalar field forces it to acquire a nonzero vacuum expectation value. Two possible choices for this expectation value are

$$\langle \Phi \rangle = A \begin{pmatrix} 1 & & & & \\ & 1 & & & \\ & & 1 & & \\ & & & 1 & \\ & & & & -4 \end{pmatrix} \quad \text{and} \quad \langle \Phi \rangle = B \begin{pmatrix} 2 & & & & \\ & 2 & & & \\ & & 2 & & \\ & & & -3 & \\ & & & & -3 \end{pmatrix}.$$

For each case, work out the spectrum of gauge bosons and the unbroken symmetry group.

20.2 Decay modes of the W and Z bosons.

- (a) Compute the partial decay widths of the W boson into pairs of quarks and leptons. Assume that the top quark mass m_t is larger than m_W , and ignore the other quark masses. The decay widths to quarks are enhanced by QCD corrections. Show that the correction is given, to order α_s , by Eq. (17.9). Using $\sin^2 \theta_w = 0.23$, find a numerical value for the total width of the W^+ .
- (b) Compute the partial decay widths of the Z boson into pairs of quarks and leptons, treating the quarks in the same way as in part (a). Determine the total width of the Z boson and the fractions of the decays that give hadrons, charged leptons, and invisible modes $\nu\bar{\nu}$.

20.3 $e^+e^- \rightarrow$ hadrons with photon- Z^0 interference

- (a) Consider a fermion species f with electric charge Q_f and weak isospin I_L^3 for its left-handed component. Ignore the mass of the f . Compute the differential cross section for the process $e^+e^- \rightarrow f\bar{f}$ in the standard electroweak model. Include the effect of the Z^0 width using the Breit-Wigner formula, Eq. (7.60). Plot the behavior of the total cross section as a function of CM energy through the Z^0 resonance, for u , d , and μ .
- (b) Compute the forward-backward asymmetry for $e^+e^- \rightarrow f\bar{f}$, defined as

$$A_{FB}^f = \frac{\left(\int_0^1 - \int_{-1}^0 \right) d \cos \theta (d\sigma / d \cos \theta)}{\left(\int_0^1 + \int_{-1}^0 \right) d \cos \theta (d\sigma / d \cos \theta)},$$

as a function of center of mass energy.

- (c) Show that, just on the Z^0 resonance, the forward-backward asymmetry is given by

$$A_{FB}^f = \frac{3}{4} A_{LR}^e A_{LR}^f.$$

- (d) Show that the cross section at the peak of the Z^0 resonance is given by

$$\sigma_{\text{peak}} = \frac{12\pi}{m_Z^2} \frac{\Gamma(Z^0 \rightarrow e^+e^-) \Gamma(Z^0 \rightarrow f\bar{f})}{\Gamma_Z^2},$$

where Γ_Z is the total width of the Z^0 . Notice that both the total width of the Z^0 and the peak height are affected by the presence of extra invisible decay modes. Compute the shifts in Γ_Z and σ_{peak} that would be produced by a hypothetical fourth neutrino species, and compare these shifts to the cross section measurements shown in Fig. 20.5.

20.4 Neutral-current deep inelastic scattering.

- (a) In Eq. (17.35), we wrote formulae for neutrino and antineutrino deep inelastic scattering with W^\pm exchange. Neutrinos and antineutrinos can also scatter by exchanging a Z^0 . This process, which leads to a hadronic jet but no observable outgoing lepton, is called the *neutral current* reaction. Compute $d\sigma/dxdy$ for neutral current deep inelastic scattering of neutrinos and antineutrinos from protons, accounting for scattering from u and d quarks and antiquarks.
- (b) Next, consider deep inelastic scattering from a nucleus A with equal numbers of protons and neutrons. For such a target, $f_u(x) = f_d(x)$, and similarly for antiquarks. Show that the formulae in part (a) simplify in such a situation. In particular, let R^ν , $R^{\bar{\nu}}$ be defined as

$$R^\nu = \frac{d\sigma/dxdy(\nu A \rightarrow \nu X)}{d\sigma/dxdy(\nu A \rightarrow \mu^- X)}, \quad R^{\bar{\nu}} = \frac{d\sigma/dxdy(\bar{\nu} A \rightarrow \bar{\nu} X)}{d\sigma/dxdy(\bar{\nu} A \rightarrow \mu^+ X)}.$$

Show that R^ν and $R^{\bar{\nu}}$ are given by the following simple formulae:

$$R^\nu = \frac{1}{2} - \sin^2 \theta_w + \frac{5}{9} \sin^4 \theta_w (1 + r),$$

$$R^{\bar{\nu}} = \frac{1}{2} - \sin^2 \theta_w + \frac{5}{9} \sin^4 \theta_w (1 + \frac{1}{r}),$$

where

$$r = \frac{d\sigma/dxdy(\bar{\nu} A \rightarrow \mu^+ X)}{d\sigma/dxdy(\nu A \rightarrow \mu^- X)}.$$

These formulae remain true when R^ν and $R^{\bar{\nu}}$ are redefined to be the ratios of neutral- to charged-current cross sections integrated over the region of x and y that is observed in a given experiment.

- (c) By setting r equal to the observed value—say, $r = 0.4$ —and varying $\sin^2 \theta_w$, the relations of part (b) generate a curve in the plane of R^ν versus $R^{\bar{\nu}}$ that is known as *Weinberg's nose*. Sketch this curve. The observed values of R^ν , $R^{\bar{\nu}}$ lie close to this curve, near the point corresponding to $\sin^2 \theta_w = 0.23$.

20.5 A model with two Higgs fields.

- (a) Consider a model with two scalar fields ϕ_1 and ϕ_2 , which transform as $SU(2)$ doublets with $Y = 1/2$. Assume that the two fields acquire parallel vacuum expectation values of the form (20.23) with vacuum expectation values v_1 , v_2 . Show that these vacuum expectation values produce the same gauge boson mass matrix that we found in Section 20.2, with the replacement

$$v^2 \rightarrow (v_1^2 + v_2^2).$$

- (b) The most general potential function for a model with two Higgs doublets is quite complex. However, if we impose the discrete symmetry $\phi_1 \rightarrow -\phi_1$, $\phi_2 \rightarrow \phi_2$,

the most general potential is

$$V(\phi_1, \phi_2) = -\mu_1^2 \phi_1^\dagger \phi_1 - \mu_2^2 \phi_2^\dagger \phi_2 + \lambda_1 (\phi_1^\dagger \phi_1)^2 + \lambda_2 (\phi_2^\dagger \phi_2)^2 + \lambda_3 (\phi_1^\dagger \phi_1)(\phi_2^\dagger \phi_2) + \lambda_4 (\phi_1^\dagger \phi_2)(\phi_2^\dagger \phi_1) + \lambda_5 ((\phi_1^\dagger \phi_2)^2 + \text{h.c.})$$

Find conditions on the parameters μ_i and λ_i so that the configuration of vacuum expectation values required in part (a) is a locally stable minimum of this potential.

- (c) In the unitarity gauge, one linear combination of the upper components of ϕ_1 and ϕ_2 is eliminated, while the other remains as a physical field. Show that the physical charged Higgs field has the form

$$\phi^+ = \sin \beta \phi_1^+ - \cos \beta \phi_2^+,$$

where β is defined by the relation

$$\tan \beta = \frac{v_2}{v_1}.$$

- (d) Assume that the two Higgs fields couple to quarks by the set of fundamental couplings

$$\mathcal{L}_m = -\lambda_d^{ij} \bar{Q}_L^i \cdot \phi_1 d_R^j - \lambda_u^{ij} \bar{Q}_{La}^i \phi_{2b}^\dagger u_R^j + \text{h.c.}$$

Find the couplings of the physical charged Higgs boson of part (c) to the mass eigenstates of quarks. These couplings depend only on the values of the quark masses and $\tan \beta$ and on the elements of the CKM matrix.

Quantization of Spontaneously Broken Gauge Theories

In Chapter 20 we saw that when a gauge symmetry is spontaneously broken, the gauge bosons acquire mass. This phenomenon allowed us to construct a realistic theory of the weak interactions. Up to this point, however, we have discussed spontaneously broken gauge theories only in a simplistic way. To isolate the physical degrees of freedom, we have used the device of going to the unitarity gauge. However, it is not at all clear what the rules of perturbation theory are in this gauge, or how the unitarity gauge constraint is maintained when we compute Feynman diagrams. We have also seen that the Goldstone bosons that are absorbed into the massive gauge bosons play an important role in formal arguments about these theories, so we would like to quantize these theories in a gauge that does not eliminate these particles from the beginning.

In this chapter we will address these problems, by carrying out the formal gauge-fixing of theories with spontaneously broken gauge symmetry using the Faddeev-Popov method. We will define a class of gauges, called the R_ξ gauges, almost all of which contain the Goldstone bosons of the original spontaneous symmetry breaking. These particles cancel the effects of other unphysical particles in the formalism to maintain the unitarity of the theory. These cancellations are a more intricate version of the cancellations between gauge and ghost degrees of freedom that we saw in Chapter 16. However, we will see in Section 21.2 that a theory does not forget that it contains Goldstone bosons and that, under some circumstances, the properties of the Goldstone bosons in the theory without gauge couplings can carry over to the theory with massive gauge bosons.

Finally, having defined the perturbation theory and clarified the role of the Goldstone bosons in spontaneously broken gauge theories, we will carry out some explicit loop calculations of interest in the theory of weak interactions. Here we will see applications of the ideas of Chapter 11, that a theory with spontaneously broken symmetry can be renormalized with the counterterms of the symmetric Lagrangian. In Section 21.3 we will show through some examples that this result applies with equal force to gauge theories, and that it endows the weak-interaction gauge theory with substantial predictive power.

21.1 The R_ξ Gauges

In our discussion of the low-energy effective Lagrangian for weak interactions, we proposed in Eq. (20.89) the following expression for the propagator of a massive gauge boson:

$$\langle A^\mu(p)A^\nu(-p) \rangle \stackrel{?}{=} \frac{-ig^{\mu\nu}}{p^2 - m^2}. \quad (21.1)$$

This expression is a natural first guess, generalizing the Feynman-'t Hooft gauge. However, it is unsatisfactory in a number of ways.

The most important of these defects concerns the treatment of gauge boson polarization states. The propagator (21.1) contains four components, corresponding to the transverse, longitudinal, and timelike polarizations. We saw in Chapters 5 and 16 that, for massless gauge bosons, the unphysical longitudinal and timelike components cancel in computations. For a massive gauge boson, however, the longitudinal polarization state corresponds to a real physical particle; we do not want it to cancel. Expression (21.1) does not take this change into account.

An Abelian Example

To understand this and other formal problems that arise for gauge theories with spontaneously broken symmetry, we need to carefully redo the Faddeev-Popov quantization of these theories. To begin, we will quantize the spontaneously broken Abelian gauge theory introduced in Eq. (20.1):

$$\mathcal{L} = -\frac{1}{4}(F_{\mu\nu})^2 + |D_\mu\phi|^2 - V(\phi), \quad (21.2)$$

with $D_\mu = \partial_\mu + ieA_\mu$. Here $\phi(x)$ is a complex scalar field. However, it will be most convenient to analyze the model by writing ϕ in terms of its real components,

$$\phi = \frac{1}{\sqrt{2}}(\phi^1 + i\phi^2). \quad (21.3)$$

Then the infinitesimal local symmetry transformation is

$$\delta\phi^1 = -\alpha(x)\phi^2, \quad \delta\phi^2 = \alpha(x)\phi^1, \quad \delta A_\mu = -\frac{1}{e}\partial_\mu\alpha. \quad (21.4)$$

Let us assume that $V(\phi)$ forces the scalar field to acquire a vacuum expectation value: $\langle\phi^1\rangle = v$. Then we should change variables by a shift:

$$\phi^1(x) = v + h(x); \quad \phi^2 = \varphi. \quad (21.5)$$

The field ϕ^2 or φ is the Goldstone boson. The Lagrangian (21.2) now takes the form

$$\mathcal{L} = -\frac{1}{4}(F_{\mu\nu})^2 + \frac{1}{2}(\partial_\mu h - eA_\mu\varphi)^2 + \frac{1}{2}(\partial_\mu\varphi + eA_\mu(v + h))^2 - V(\phi). \quad (21.6)$$

This Lagrangian is still invariant under an exact local symmetry,

$$\delta h = -\alpha(x)\varphi, \quad \delta\varphi = \alpha(x)(v + h), \quad \delta A_\mu = -\frac{1}{e}\partial_\mu\alpha. \quad (21.7)$$

Thus, in order to define the functional integral over the variables (h, φ, A_μ) , we must introduce Faddeev-Popov gauge fixing.

Starting from the functional integral

$$Z = \int \mathcal{D}A \mathcal{D}h \mathcal{D}\varphi e^{i\int \mathcal{L}[A, h, \varphi]}, \quad (21.8)$$

we can introduce a gauge-fixing constraint as we did in Section 9.4. Following the steps leading from Eq. (9.50) to Eq. (9.54), we find

$$Z = C \cdot \int \mathcal{D}A \mathcal{D}h \mathcal{D}\varphi e^{i\int \mathcal{L}[A, h, \varphi]} \delta(G(A, h, \varphi)) \det\left(\frac{\delta G}{\delta \alpha}\right), \quad (21.9)$$

where C is a constant proportional to the volume of the gauge group and $G(A, h, \varphi)$ is a gauge-fixing condition. Alternatively, we can introduce the gauge-fixing constraint as $\delta(G(x) - \omega(x))$ and integrate over $\omega(x)$ with a Gaussian weight, as in the derivation of Eq. (9.56). This gives

$$Z = C' \cdot \int \mathcal{D}A \mathcal{D}h \mathcal{D}\varphi \exp\left[i\int d^4x (\mathcal{L}[A, h, \varphi] - \frac{1}{2}(G)^2)\right] \det\left(\frac{\delta G}{\delta \alpha}\right). \quad (21.10)$$

The gauge-fixing function G is arbitrary, but we can simplify our formalism by choosing it appropriately.

An especially convenient choice of the gauge-fixing function is

$$G = \frac{1}{\sqrt{\xi}}(\partial_\mu A^\mu - \xi ev\varphi). \quad (21.11)$$

When we form G^2 , the term quadratic in A_μ will provide the same gauge-dependent addition to the gauge field action that we saw in the derivation of Eqs. (9.58) and (16.29). In addition, the cross term between A_μ and φ is engineered to cancel the quadratic term of the form $\partial_\mu\varphi A^\mu$ coming from the third term of (21.6). With this choice, the quadratic terms of the gauge-fixed Lagrangian ($\mathcal{L} - \frac{1}{2}G^2$) are

$$\begin{aligned} \mathcal{L}_2 = & -\frac{1}{2}A_\mu\left(-g^{\mu\nu}\partial^2 + \left(1 - \frac{1}{\xi}\right)\partial^\mu\partial^\nu - (ev)^2g^{\mu\nu}\right)A_\nu \\ & + \frac{1}{2}(\partial_\mu h)^2 - \frac{1}{2}m_h^2h^2 + \frac{1}{2}(\partial_\mu\varphi)^2 - \frac{\xi}{2}(ev)^2\varphi^2. \end{aligned} \quad (21.12)$$

The mass term for the h field comes from the expansion of $V(\phi)$, as in (20.6). The mass term for the gauge field comes from the Higgs mechanism, that is, from the third term of (21.6). Notice that the formalism also produces a mass for the Goldstone boson φ :

$$m_\varphi^2 = \xi(ev)^2 = \xi m_A^2. \quad (21.13)$$

The fact that this mass is gauge-dependent is a signal that the Goldstone boson is a fictitious field, which will not be produced in physical processes.

To complete the Faddeev-Popov quantization procedure, we must derive the Lagrangian of the ghosts. This Lagrangian depends on the gauge variation of G , which can be computed by inserting (21.7) into (21.11). We find

$$\frac{\delta G}{\delta \alpha} = \frac{1}{\sqrt{\xi}} \left(-\frac{1}{e} \partial^2 - \xi ev(v + h) \right). \quad (21.14)$$

The determinant of this operator can be accounted for by including a set of Faddeev-Popov ghosts with the Lagrangian,

$$\mathcal{L}_{\text{ghost}} = \bar{c} \left[-\partial^2 - \xi m_A^2 \left(1 + \frac{h}{v} \right) \right] c, \quad (21.15)$$

where $m_A = ev$ as in Eq. (21.13). Since this is an Abelian gauge theory, the ghost field does not couple directly to the gauge field. It does, however, couple to the physical Higgs field, so it cannot be completely ignored as in QED.

From the quadratic terms in the Lagrangians for A_μ , h , φ , and the ghosts, we can readily find the propagators for these fields. All four propagators are shown in Fig. 21.1. The only complicated case is that of the gauge field. The term in (21.12) involving A_μ involves an operator whose Fourier transform is

$$\begin{aligned} g^{\mu\nu} k^2 - \left(1 - \frac{1}{\xi} \right) k^\mu k^\nu - m_A^2 g^{\mu\nu} \\ = \left(g^{\mu\nu} - \frac{k^\mu k^\nu}{k^2} \right) (k^2 - m_A^2) + \left(\frac{k^\mu k^\nu}{k^2} \right) \frac{1}{\xi} (k^2 - \xi m_A^2). \end{aligned} \quad (21.16)$$

The inverse of this matrix gives the A_μ field propagator:

$$\begin{aligned} \langle A_\mu(k) A_\nu(-k) \rangle &= \frac{-i}{k^2 - m_A^2} \left(g^{\mu\nu} - \frac{k^\mu k^\nu}{k^2} \right) + \frac{-i\xi}{k^2 - \xi m_A^2} \left(\frac{k^\mu k^\nu}{k^2} \right) \\ &= \frac{-i}{k^2 - m_A^2} \left(g^{\mu\nu} - \frac{k^\mu k^\nu}{k^2 - \xi m_A^2} (1 - \xi) \right). \end{aligned} \quad (21.17)$$

Notice that the transverse components of the A field and the component h of the Higgs field acquire the masses m_A , m_h that we found in Section 20.1. The unphysical components of A , the Goldstone bosons, and the ghosts all acquire the same gauge-dependent mass $\sqrt{\xi} m_A$.

ξ Dependence in Perturbation Theory

Because the parameter ξ was introduced only in the gauge fixing, we expect it to cancel out of all computations of expectation values of gauge-invariant operators and of S -matrix elements. This cancellation can be proved to all orders in perturbation theory by using the BRST symmetry of the gauge-fixed Lagrangian.* Here, however, we will simply illustrate the cancellation of ξ in a simple example.

*See, for example, Taylor (1976).

$$\begin{aligned}
 A_\mu: \quad \mu \sim \sim \sim \sim \nu &= \frac{-i}{k^2 - m_A^2} \left(g^{\mu\nu} - \frac{k^\mu k^\nu}{k^2 - \xi m_A^2} (1 - \xi) \right) \\
 h: \quad \text{---} \xleftarrow{k} \text{---} &= \frac{i}{k^2 - m_h^2} \\
 \varphi: \quad \text{---} \xleftarrow{k} \text{---} &= \frac{i}{k^2 - \xi m_A^2} \\
 c: \quad \text{.....} \xleftarrow{k} \text{.....} &= \frac{i}{k^2 - \xi m_A^2}
 \end{aligned}$$

Figure 21.1. Propagators of the gauge field, Higgs fields, and ghosts in the Abelian model with spontaneously broken symmetry.

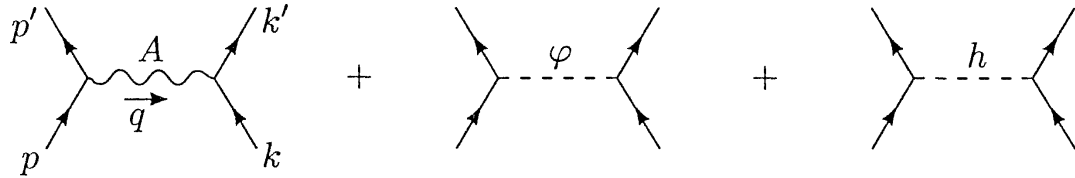


Figure 21.2. Diagrams contributing to fermion-fermion scattering at leading order in the Abelian model with spontaneous symmetry breaking.

Consider coupling a fermion to the spontaneously broken gauge theory through a chiral interaction:

$$\mathcal{L}_f = \bar{\psi}_L (iD) \psi_L + \bar{\psi}_R (i\partial) \psi_R - \lambda_f (\bar{\psi}_L \phi \psi_R + \bar{\psi}_R \phi^* \psi_L), \quad (21.18)$$

with $D_\mu = \partial_\mu + ieA_\mu$ as before. This is a stripped-down, Abelian version of the coupling of fermions to the weak interaction gauge theory. The fermion ψ receives a mass

$$m_f = \lambda_f \frac{v}{\sqrt{2}} \quad (21.19)$$

from the spontaneous symmetry breaking. (This theory has an axial vector anomaly that would render loop calculations inconsistent, but we will analyze it only at the level of tree diagrams.)

In this theory, the leading-order diagrams contributing to fermion-fermion scattering are those shown in Fig. 21.2. Notice that the contribution from the exchange of the unphysical particle φ must be included, since this particle appears in the Feynman rules. The ghosts do not appear in this process until the one-loop level. Since the propagator of the physical Higgs particle h is independent of ξ , the cancellation of the ξ dependence must take place between the transverse and longitudinal components of A_μ and the Goldstone boson φ .

The graph with exchange of the Goldstone boson has the value

$$i\mathcal{M}_\varphi = \left(\frac{\lambda_f}{\sqrt{2}}\right)^2 \bar{u}(p')\gamma^5 u(p) \frac{i}{q^2 - \xi m_A^2} \bar{u}(k')\gamma^5 u(k). \quad (21.20)$$

The ξ dependence of this expression must be canceled by that of the gauge boson exchange diagram,

$$\begin{aligned} i\mathcal{M}_A &= (-ie)^2 \bar{u}(p')\gamma_\mu \left(\frac{1-\gamma^5}{2}\right) u(p) \\ &\quad \times \frac{i}{q^2 - m_A^2} \left(g^{\mu\nu} - \frac{q^\mu q^\nu}{q^2 - \xi m_A^2} (1-\xi)\right) \bar{u}(k')\gamma_\nu \left(\frac{1-\gamma^5}{2}\right) u(k). \end{aligned} \quad (21.21)$$

The ξ dependence of this term looks quite intricate. However, we can make some simplifications by rewriting the gauge boson propagator as

$$\begin{aligned} &\frac{-i}{q^2 - m_A^2} \left(g^{\mu\nu} - \frac{q^\mu q^\nu}{m_A^2} + q^\mu q^\nu \left[\frac{1}{m_A^2} - \frac{1}{q^2 - \xi m_A^2} (1-\xi)\right]\right) \\ &= \frac{-i}{q^2 - m_A^2} \left(g^{\mu\nu} - \frac{q^\mu q^\nu}{m_A^2}\right) + \frac{-i}{q^2 - \xi m_A^2} \left(\frac{q^\mu q^\nu}{m_A^2}\right). \end{aligned} \quad (21.22)$$

The first term of (21.22) is ξ -independent. The second term can be simplified in (21.21) by using the identity

$$\begin{aligned} q^\mu \bar{u}(p')\gamma_\mu \left(\frac{1-\gamma^5}{2}\right) u(p) &= \frac{1}{2} \bar{u}(p') [(\not{p} - \not{p}') - (\not{p} - \not{p}')\gamma^5] u(p) \\ &= \frac{1}{2} \bar{u}(p') [\not{p}'\gamma^5 + \gamma^5 \not{p}] u(p) \\ &= m_f \bar{u}(p')\gamma^5 u(p), \end{aligned} \quad (21.23)$$

and the analogous identity on the other fermion line. After making these rearrangements and inserting the explicit values $m_f = \lambda_f v / \sqrt{2}$ and $m_A = ev$, the gauge boson exchange amplitude (21.21) takes the form

$$\begin{aligned} i\mathcal{M}_A &= (-ie)^2 \bar{u}(p')\gamma_\mu \left(\frac{1-\gamma^5}{2}\right) u(p) \frac{i}{q^2 - m_A^2} \left(g^{\mu\nu} - \frac{q^\mu q^\nu}{m_A^2}\right) \bar{u}(k')\gamma_\nu \left(\frac{1-\gamma^5}{2}\right) u(k) \\ &\quad + \left(\frac{\lambda_f}{\sqrt{2}}\right)^2 \bar{u}(p')\gamma^5 u(p) \frac{-i}{q^2 - \xi m_A^2} \bar{u}(k')\gamma^5 u(k). \end{aligned} \quad (21.24)$$

The second term of (21.24) precisely cancels the Goldstone boson exchange diagram (21.20). The terms that remain in the fermion-fermion scattering amplitude are independent of ξ .

This demonstration merits two additional comments. First, throughout this book, we have become accustomed to dotting the gauge boson momentum into a gauge boson vertex and finding zero or contact terms. However, in spontaneously broken gauge theories, we typically find a different result. The fermionic current $\bar{\psi}\gamma^\mu(1-\gamma^5)\psi$ is not conserved, with the nonconservation being proportional to the fermion mass. This allows the manipulation (21.23) to contribute terms proportional to the Higgs boson vacuum expectation value,

which interplay with the Goldstone boson contributions. We will discuss this point further, and find a physical application of it, in Section 21.2.

The second point concerns the final form of the gauge-invariant sum of the gauge boson and Goldstone boson exchange diagrams. These give just the result we would have found by neglecting the Goldstone boson and computing the gauge boson exchange using the first term of (21.22) as the propagator:

$$\langle A_\mu(q) A_\nu(-q) \rangle = \frac{-i}{q^2 - m_A^2} \left(g^{\mu\nu} - \frac{q^\mu q^\nu}{m_A^2} \right). \quad (21.25)$$

The tensor structure represents a gauge boson polarization sum. To identify what vectors are summed over, notice that, if the vector boson is on-shell, and if we boost to its rest frame, this structure becomes precisely the projection onto the three purely spatial directions. These are the three polarization states of an on-shell massive vector particle. In a general frame, still for q^μ on-shell, the tensor in (21.25) remains the projection onto physical polarization states:

$$\sum_{\epsilon^\mu q_\mu = 0} \epsilon^\mu \epsilon^{\nu*} = - \left(g^{\mu\nu} - \frac{q^\mu q^\nu}{m_A^2} \right). \quad (21.26)$$

Thus, in the cancellation of the ξ -dependent parts of the gauge boson propagator, we also find that the Goldstone boson diagram cancels the contribution of the unphysical timelike polarization state of the gauge boson, leaving over the required three physical polarizations.

The perturbation theory rules that we have developed have a very different character for different values of ξ . Thus, it is even more true in the case of spontaneously broken symmetry that we can find different special simplifications by choosing different values of this gauge parameter. For $\xi = 0$, Lorentz gauge, the Goldstone boson is massless and has exactly the couplings it has in the ungauged model of symmetry breaking, while the gauge boson propagator is purely transverse:

$$\overbrace{\mu \leftarrow \nu}^k = \frac{-i}{k^2 - m_A^2} \left(g^{\mu\nu} - \frac{k^\mu k^\nu}{k^2} \right); \quad \overbrace{\quad \quad \quad \quad \quad}^k = \frac{-i}{k^2}. \quad (21.27)$$

This gauge is especially useful for analyzing models of symmetry breaking. Both propagators have poles at $k^2 = 0$. However, we know that there are no corresponding physical particles, because these poles move away from $k^2 = 0$ as we change ξ , while the S -matrix must be ξ -independent.

For $\xi = 1$, we recover the simple form of the gauge boson propagator given in (21.1). This choice of the gauge boson propagator is not consistent, however, unless we also include Goldstone boson exchanges in which the Goldstone boson is also assigned the mass m_A :

$$\overbrace{\mu \leftarrow \nu}^k = \frac{-ig^{\mu\nu}}{k^2 - m_A^2}; \quad \overbrace{\quad \quad \quad \quad \quad}^k = \frac{-i}{k^2 - m_A^2}. \quad (21.28)$$

This gauge, still called the Feynman-'t Hooft gauge, is the most convenient one for general higher-order computations.

For any finite value of ξ , the gauge boson and Goldstone boson propagators fall off as $1/k^2$ and thus obey the general power-counting analysis of Section 10.1. It follows that, in any one of these gauges, the perturbation theory will be renormalizable, in the sense that the divergences are removed by a finite set of counterterms. Furthermore, the analysis of Section 11.6 tells us that the only counterterms required are those that are symmetric under the original global symmetry of the theory. However, we should require one further condition of our renormalization procedure: We should insist that the counterterms preserve local gauge invariance, and, in particular, preserve the property that S -matrix elements and the matrix elements of gauge-invariant operators are independent of ξ . This result was proved to all orders in perturbation theory by 't Hooft and Veltman and by Lee and Zinn-Justin.[†] Thus, in the gauge defined by any finite value of ξ , we can, in principle, straightforwardly compute a physical quantity to any order. The gauges defined by the possible values of ξ are known as the *renormalizability*, or R_ξ , gauges.

By taking the limit $\xi \rightarrow \infty$ of the R_ξ gauges, we find a gauge with very different simplifying features. In this limit, the unphysical degrees of freedom, which have masses proportional to $\sqrt{\xi}$, disappear from the theory. The gauge boson and Goldstone boson propagators become:

$$\overbrace{\mu}^{\text{wavy line}} \overbrace{\nu}^{\text{wavy line}} = \frac{-i}{k^2 - m_A^2} \left(g^{\mu\nu} - \frac{k^\mu k^\nu}{m_A^2} \right); \quad \overbrace{k}^{\text{dashed line}} = 0. \quad (21.29)$$

The gauge boson propagator contains exactly the three spacelike polarization states. In this gauge, the only singularities of Feynman diagrams correspond to the propagation of physical intermediate states. Thus, the unitarity of the S -matrix follows from the Cutkosky rules, as in the globally symmetric theories considered in Section 7.3, without the need to worry about the cancellation of unphysical states.[‡] The $\xi \rightarrow \infty$ limit of the R_ξ gauges thus gives the quantum-mechanical realization of the *unitarity* (or U) gauge, introduced in Eq. (20.12).

It is not straightforward to prove renormalizability directly in the U gauge. In this gauge, the gauge boson propagator falls off more slowly than $1/k^2$ at large k . This signals trouble for the evaluation of loop diagrams. Typically, in fact, individual loop diagrams will diverge as $\log \xi$ or worse as $\xi \rightarrow \infty$. Still, the gauge invariance of the S -matrix implies that these divergences must cancel in the sum of all diagrams contributing to a given process, so that this sum has a smooth limit as $\xi \rightarrow \infty$. There is no difficulty of principle with the fact that we use one gauge to prove the renormalizability of spontaneously

[†]G. 't Hooft and M. J. G. Veltman, *Nucl. Phys.* **B50**, 318 (1972), B. W. Lee and J. Zinn-Justin, *Phys. Rev. D5*, 3121, 3137, 3155 (1972), **D7**, 1049 (1973).

[‡]In the more sophisticated language of Section 16.4, the crucial identity (16.54), which is required for the unitarity of the S -matrix, is true manifestly.

broken gauge theories and another gauge to prove their unitarity. In fact, this method of argumentation makes natural use of the underlying symmetries of the theory.

Non-Abelian Analysis

Now that we have thoroughly examined the R_ξ gauges for an Abelian gauge theory, we are ready to generalize to the non-Abelian case. There is no difficulty in being completely general, so let us consider a Yang-Mills gauge theory with gauge group G , spontaneously broken by the vacuum expectation value of a scalar field.

We will build on our classical analysis of this system following Eq. (20.13). As in that analysis, it will be most convenient to write the scalars as a multiplet ϕ_i of real-valued fields. Then the gauge transformation of the ϕ_i takes the form

$$\delta\phi_i = -\alpha^a(x)T_{ij}^a\phi_j, \quad (21.30)$$

where the T_{ij}^a are real, antisymmetric representation matrices of G . Similarly, the transformation of the gauge fields is

$$\delta A_\mu^a = \frac{1}{g}\partial_\mu\alpha^a - f^{abc}\alpha^b A_\mu^c = \frac{1}{g}(D_\mu\alpha)^a. \quad (21.31)$$

(If the gauge group is not simple, the coupling g need not be the same for every a .) The Lagrangian invariant under these gauge transformations is

$$\mathcal{L} = -\frac{1}{4}(F_{\mu\nu}^a)^2 + \frac{1}{2}(D_\mu\phi)^2 - V(\phi), \quad (21.32)$$

with

$$D_\mu\phi_i = \partial_\mu\phi_i + gA_\mu^a T_{ij}^a\phi_j. \quad (21.33)$$

Assume that the potential $V(\phi)$ is minimized at a point where some of the components of ϕ acquire vacuum expectation values. As in (20.16), define

$$\langle\phi_i\rangle = (\phi_0)_i. \quad (21.34)$$

We will expand ϕ_i about this value:

$$\phi_i(x) = \phi_{0i} + \chi_i(x). \quad (21.35)$$

It will be convenient to divide the space of values χ_i into two subspaces. The vectors $T^a\phi_0$ correspond to symmetry transformations of the vacuum expectation value of ϕ . The field fluctuations along these directions are the Goldstone bosons. Let $\{n_i\}$ be an orthonormal basis for this subspace; then the unit vectors n_i are in 1-to-1 correspondence with the Goldstone bosons. The field fluctuations orthogonal to all of the vectors $T^a\phi_0$ correspond to the (massive) physical scalar fields of the spontaneously broken gauge theory.

In the discussion to follow, the vectors $T^a\phi_0$ will play an important role. We should then recall the notation for these vectors that we introduced in Eq. (20.51):

$$F_i^a = T_{ij}^a\phi_{0j}. \quad (21.36)$$

The matrix F^a_i is not generally square; it has one row for each gauge generator, and one column for each component of ϕ . However, many of its elements are zero. Its nonzero elements connect the spontaneously broken gauge generators and the Goldstone bosons. In Eq. (20.56), we showed that the gauge boson masses generated through the Higgs mechanism can be written

$$m_{ab}^2 = g^2 F^a_j F^b_j. \quad (21.37)$$

To give a concrete example of a matrix F^a_j , let us compute it in the GWS electroweak theory. Following the conventions introduced in Eq. (20.14), we should rewrite the Higgs field of the GWS model in terms of four real scalar fields. A convenient parametrization is

$$\phi = \frac{1}{\sqrt{2}} \begin{pmatrix} -i(\phi^1 - i\phi^2) \\ v + (h + i\phi^3) \end{pmatrix}. \quad (21.38)$$

The fields ϕ^i are the Goldstone bosons, and h is the massive Higgs boson. The vacuum state is simply

$$\phi_0 = \frac{1}{\sqrt{2}} \begin{pmatrix} 0 \\ v \end{pmatrix}.$$

The real representation matrices are

$$T^a = -i\tau^a = -i\frac{\sigma^a}{2}, \quad T^Y = -iY = -i\frac{1}{2}.$$

A simple computation then shows, for instance, that $T^1\phi_0$ equals $v/2$ times a unit vector in the ϕ^1 direction. Filling in the remaining components of F^a_i , with $a = 1, 2, 3, Y$ and $i = 1, 2, 3$, we find

$$gF^a_i = \frac{v}{2} \begin{pmatrix} g & 0 & 0 \\ 0 & g & 0 \\ 0 & 0 & g \\ 0 & 0 & -g' \end{pmatrix}. \quad (21.39)$$

We do not need to include the components of F^a_i along the direction of the physical Higgs field h ; the vectors $T^a\phi_0$ are all orthogonal to this direction.

If we insert (21.35) into (21.32) as a change of variables, we find, for the quadratic terms in the Lagrangian,

$$\begin{aligned} \mathcal{L}_2 = & -\frac{1}{2} A_\mu^a (-g^{\mu\nu} \partial^2 + \partial^\mu \partial^\nu) A_\nu^a + \frac{1}{2} (\partial_\mu \chi)^2 \\ & + g \partial^\mu \chi_i A_\mu^a F^a_i + \frac{1}{2} (m_A^2)^{ab} A_\mu^a A^{\mu b} - \frac{1}{2} M_{ij} \chi_i \chi_j, \end{aligned} \quad (21.40)$$

where $(m_A^2)^{ab}$ is the gauge boson mass matrix (21.37) and

$$M_{ij} = \left. \frac{\partial^2}{\partial \phi_i \partial \phi_j} V(\phi) \right|_{\phi_0}. \quad (21.41)$$

We proved in Eq. (11.13) that

$$n_i M_{ij} = 0 \quad (21.42)$$

for all possible directions n_i in the subspace spanned by the $T^a\phi_0$, so the Goldstone bosons are massless.

To study the quantum theory of this system we start with the functional integral

$$Z = \int \mathcal{D}A \mathcal{D}\chi e^{i \int \mathcal{L}[A, \chi]}. \quad (21.43)$$

Using the Faddeev-Popov gauge-fixing procedure, we define this integral, analogously to (21.10), as

$$Z = C' \cdot \int \mathcal{D}A \mathcal{D}\chi \exp \left[i \int d^4x (\mathcal{L}[A, \chi] - \frac{1}{2}(G)^2) \right] \det \left(\frac{\delta G}{\delta \alpha} \right), \quad (21.44)$$

for an arbitrary gauge-fixing function $G(A, \chi)$. The R_ξ gauges are defined by the choice

$$G^a = \frac{1}{\sqrt{\xi}} (\partial_\mu A^{a\mu} - \xi g F^a_i \chi_i). \quad (21.45)$$

Note that G involves only the components of χ that lie in the subspace of the Goldstone bosons.

The gauge-fixing term adds to the Lagrangian the following set of quadratic terms:

$$(-\frac{1}{2}G^2)_2 = \frac{1}{2} A_\mu^a \left(\frac{1}{\xi} \partial^\mu \partial^\nu \right) A_\nu^a + g \partial_\mu A^{a\mu} F^a_i \chi_i - \frac{1}{2} \xi g^2 [F^a_i \chi_i]^2. \quad (21.46)$$

The term that mixes A_μ^a and χ_i is arranged to cancel between (21.40) and (21.46). The final quadratic Lagrangian for the gauge and Goldstone boson fields is

$$\begin{aligned} \mathcal{L}_2 = & -\frac{1}{2} A_\mu^a \left(\left[-g^{\mu\nu} \partial^2 + \left(1 - \frac{1}{\xi} \right) \partial^\mu \partial^\nu \right] \delta^{ab} - g^2 F^a_i F^b_i \right) A_\nu^b \\ & + \frac{1}{2} (\partial_\mu \chi)^2 - \frac{1}{2} \xi g^2 F^a_i F^a_j \chi_i \chi_j. \end{aligned} \quad (21.47)$$

The mass matrices of gauge bosons and Goldstone bosons in this Lagrangian are closely related to one another. The gauge boson mass matrix is

$$(m_A^2)^{ab} = g^2 F^a_i F^b_i = g^2 (FF^T)^{ab}. \quad (21.48)$$

In an R_ξ gauge, the timelike components of the gauge bosons acquire the mass matrix

$$\xi m_A^2 = \xi g^2 (FF^T)^{ab}. \quad (21.49)$$

At the same time, the Goldstone bosons acquire the mass matrix

$$(m_G^2)_{ij} = \xi g^2 F^a_i F^a_j = \xi g^2 (F^T F)_{ij}. \quad (21.50)$$

The two matrices (21.49) and (21.50) have different numbers of zero eigenvalues, but their nonzero eigenvalues are in 1-to-1 correspondence. This is precisely the correspondence induced by the Higgs mechanism between the massive gauge bosons and the Goldstone bosons that they absorbed to gain mass.

Finally, we must construct the ghost Lagrangian. This is found from the gauge variation of the gauge-fixing term G^a . Inserting (21.30) and (21.31) into (21.45), we find

$$\frac{\delta G^a}{\delta \alpha^b} = \frac{1}{\sqrt{\xi}} \left(\frac{1}{g} (\partial_\mu D^\mu)^{ab} + \xi g (T^a \phi_0) \cdot T^b (\phi_0 + \chi) \right). \quad (21.51)$$

Thus, the ghost Lagrangian is

$$\mathcal{L}_{\text{ghost}} = \bar{c}^a [-(\partial_\mu D^\mu)^{ab} - \xi g^2 (T^a \phi_0) \cdot T^b (\phi_0 + \chi)] c^b. \quad (21.52)$$

Notice that the ghosts have exactly the same mass matrix (21.49) as the unphysical components of the gauge bosons. This Lagrangian also contains both the familiar coupling of the ghosts to the gauge fields and the coupling to the physical Higgs fields that we found in the Abelian case (21.15).

We have now computed the kinetic energy terms for gauge fields, scalar fields, and ghosts in an R_ξ gauge. It is straightforward to convert these results to the calculation of propagators for these fields; the computations are exactly the same as in the Abelian case. We find for the three propagators

$$\begin{aligned} \text{a} \begin{array}{c} \text{---} \\ \text{---} \\ \text{---} \end{array} \text{b} &= \left(\frac{-i}{k^2 - g^2 F F^T} \left[g^{\mu\nu} - \frac{k^\mu k^\nu}{k^2 - \xi g^2 F F^T} (1 - \xi) \right] \right)^{ab}, \\ \text{i} \begin{array}{c} \text{---} \\ \text{---} \\ \text{---} \end{array} \text{j} &= \left(\frac{-i}{k^2 - \xi g^2 F^T F - M^2} \right)_{ij}, \\ \text{a} \begin{array}{c} \text{---} \\ \text{---} \\ \text{---} \end{array} \text{b} &= \left(\frac{-i}{k^2 - \xi g^2 F F^T} \right)^{ab}. \end{aligned} \quad (21.53)$$

All of these equations involve the matrix F defined in Eq. (21.36); the appearance of a matrix in the denominator should be interpreted as a matrix inverse. The scalar field propagator also includes the mass matrix (21.41) of the physical Higgs bosons. There is no conflict between this matrix and the mass matrix of the Goldstone bosons, since they project onto orthogonal subspaces.

Although the preceding discussion has been extremely abstract, it is not hard to specialize to a particular example. So consider, once again, the GWS electroweak theory, for which the matrix F^a_i is given by Eq. (21.39).

The gauge boson mass matrix in the GWS theory is

$$g^2 F F^T = \frac{v^2}{4} \begin{pmatrix} g^2 & 0 & 0 & 0 \\ 0 & g^2 & 0 & 0 \\ 0 & 0 & g^2 & -gg' \\ 0 & 0 & -gg' & g'^2 \end{pmatrix},$$

in agreement with Eq. (20.124). (The g on the left-hand side should be interpreted as g' for the fourth component of F .) Diagonalizing this matrix gives the familiar relations (20.62). Thus, in the basis of mass eigenstates, the four

gauge-boson propagators decouple to give simply

$$\mu \overbrace{\sim \sim \sim}^k \nu = \frac{-i}{k^2 - m^2} \left[g^{\mu\nu} - \frac{k^\mu k^\nu}{k^2 - \xi m^2} (1 - \xi) \right], \quad (21.54)$$

where m^2 is m_W^2 , m_Z^2 , or, for the photon, zero. Notice that, for the photon, this expression precisely reproduces Eq. (9.58).

The mass matrix of the Goldstone bosons in the GWS theory is

$$g^2 F^T F = \frac{v^2}{4} \begin{pmatrix} g^2 & 0 & 0 \\ 0 & g^2 & 0 \\ 0 & 0 & g^2 + g'^2 \end{pmatrix}.$$

These fields therefore have the propagator

$$\overbrace{\cdots \cdots}^k = \frac{i}{k^2 - \xi m^2}, \quad (21.55)$$

with $m^2 = m_W^2$ for ϕ^1 and ϕ^2 (the bosons eaten by the W^\pm) and $m^2 = m_Z^2$ for ϕ^3 (the boson eaten by the Z). The field $h(x)$, which is the physical Higgs field, propagates independently with a mass determined by the Higgs potential (and no factor of ξ in the propagator).

Finally, there are four ghost fields. According to Eq. (21.53), these have the propagator

$$\overbrace{\cdots \cdots}^k = \frac{i}{k^2 - \xi m^2}, \quad (21.56)$$

with the same values of m^2 as the four gauge bosons.

The Feynman rules for the interaction vertices of these particles are complicated to write out, due to the large number of possible combinations. However, it is quite straightforward to generate these rules by expanding the weak interaction Lagrangian and reading off the vertices term by term. We will work out a few examples in the following section.*

21.2 The Goldstone Boson Equivalence Theorem

From the results of the previous section, we see that perturbative calculations in the R_ξ gauges involve intricate cancellations among unphysical particles. Sometimes, however, these unphysical particles can still leave their footprints in physical observables. In this section we will see that, in the high-energy limit, the unphysical Goldstone boson that is eaten by a massive gauge boson still controls the amplitude for emission or absorption of the gauge boson in its longitudinal polarization state.

*The complete Feynman rules for the weak-interaction gauge theory are given in Appendix B of Cheng and Li (1984).

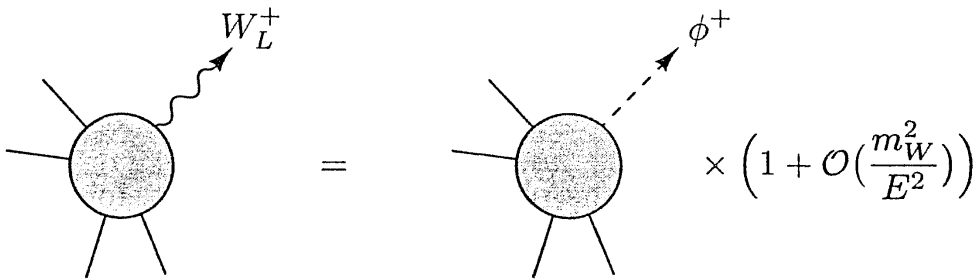


Figure 21.3. The Goldstone boson equivalence theorem. At high energy, the amplitude for emission or absorption of a longitudinally polarized massive gauge boson becomes equal to the amplitude for emission or absorption of the Goldstone boson that was eaten by the gauge boson.

When we introduced the Higgs mechanism for vector boson mass generation, we pointed out that it involves a certain conservation of degrees of freedom. A massless gauge boson, which has two transverse polarization states, combines with a scalar Goldstone boson to produce a massive vector particle, which has three polarization states. When the massive vector particle is at rest, its three polarization states are completely equivalent, but when it is moving relativistically, there is a clear distinction between the transverse and longitudinal polarization directions. This suggests that a rapidly moving, longitudinally polarized massive gauge boson might betray its origin as a Goldstone boson. The strongest version of this idea is expressed in Fig. 12.3: The amplitude for emission or absorption of a longitudinally polarized gauge boson becomes equal, at high energy, to the amplitude for emission or absorption of the Goldstone boson that was eaten. Remarkably, this statement is precisely correct, as a consequence of the underlying local gauge invariance. This *Goldstone boson equivalence theorem* was first proved by Cornwall, Levin, Tiktopoulos, and Vayonakis.[†]

Formal Aspects of Goldstone Boson Equivalence

The proof of the Goldstone boson equivalence theorem is based on the Ward identities of the spontaneously broken gauge theory. To give a complete proof of the theorem, we would have to construct and analyze these Ward identities in some detail. However, it is possible to understand the idea of the proof by examining the special case of the theorem in which a single massive vector boson is emitted or absorbed in a scattering process. The analysis of this special case requires only the relatively simple Ward identity satisfied by a current between on-shell states.[‡]

[†]J. M. Cornwall, D. N. Levin, and G. Tiktopoulos, *Phys. Rev. D* **10**, 1145 (1974); C. E. Vayonakis, *Lett. Nuov. Cim.* **17**, 383 (1976). For an illuminating discussion of the equivalence theorem, see B. W. Lee, C. Quigg, and H. Thacker, *Phys. Rev. D* **16**, 1519 (1977).

[‡]For a careful derivation of the equivalence theorem, including processes involving

To prepare for a discussion of longitudinal vector bosons, we need some simple kinematics. A vector boson at rest has momentum $k^\mu = (m, 0, 0, 0)$ and a polarization vector that is a linear combination of the three orthogonal unit vectors

$$(0, 1, 0, 0), \quad (0, 0, 1, 0), \quad (0, 0, 0, 1). \quad (21.57)$$

If we boost this particle along the \hat{z} axis, its momentum boosts to $k^\mu = (E_k, 0, 0, k)$. The three possible polarization vectors are now the three unit vectors satisfying

$$\epsilon^\mu k_\mu = 0, \quad \epsilon^2 = -1. \quad (21.58)$$

Two of these are the first two vectors in (21.57); these give the transverse polarizations. The third vector satisfying (21.58) is the longitudinal polarization vector

$$\epsilon_L^\mu(k) = \left(\frac{k}{m}, 0, 0, \frac{E_k}{m} \right), \quad (21.59)$$

which is the boost of the third vector in (21.57). An important and somewhat counterintuitive feature of (21.59) is that it becomes increasingly parallel to k^μ as k becomes large. In fact, component by component,

$$\epsilon_L^\mu(k) = \frac{k^\mu}{m} + \mathcal{O}(m/E_k) \quad (21.60)$$

as $k \rightarrow \infty$. Since the components of k^μ are growing as k , this statement is consistent with the requirement that $\epsilon_L \cdot k = 0$ while $k \cdot k = m^2$.

With this kinematic situation in mind, let us analyze the Ward identity satisfied by a gauge current matrix element between on-shell states. It is simplest to work in Lorentz gauge ($\xi = 0$), where the gauge-fixing term (21.45) does not involve the Goldstone boson fields. The Ward identity can then be written as follows:

$$0 = k^\mu \left(\text{shaded circle} \right) = k^\mu \left(\text{1PI} + \text{Goldstone loop} \right). \quad (21.61)$$

In the last expression we have written the matrix element as the sum of two pieces. First, the current can couple directly into a one-particle-irreducible vertex function $\Gamma^\mu(k)$. This gives the class of diagrams that contribute to the scattering of a gauge boson from the external states. However, for a spontaneously broken gauge theory, there is an additional term, which is not one-particle-irreducible, in which the current creates a Goldstone boson and it is this particle that couples to the external states through a 1PI vertex $\Gamma(k)$.

Let us write the relation linking the gauge current and the Goldstone boson state as

$$\langle 0 | J^\mu | \pi(k) \rangle = -iF k^\mu, \quad (21.62)$$

multiple absorptions and emissions of massive vector bosons, see M. S. Chanowitz and M. K. Gaillard, *Nucl. Phys.* **B261**, 379 (1985).

as in Eq. (20.46). Then the argument leading to Eq. (20.56) tells us that the gauge boson mass is given by

$$m = gF, \quad (21.63)$$

where g is the gauge boson coupling constant.

With these identifications, we can write the Ward identity that follows from the conservation of the gauge current:

$$k_\mu \langle J^\mu \rangle = 0, \quad (21.64)$$

between on-shell states. Writing each term shown in (21.61) in terms of the appropriate one-particle-irreducible vertex function, we find

$$k_\mu \Gamma^\mu(k) + k_\mu (igFk^\mu) \frac{i}{k^2} \Gamma(k) = 0. \quad (21.65)$$

Thus,

$$k_\mu \Gamma^\mu(k) = m\Gamma(k). \quad (21.66)$$

Now use this equation in the limit of large gauge boson momentum. Since the gauge boson vertex is one-particle-irreducible, the momenta of propagators inside the vertex are not, in general, collinear with k^μ . Then, according to (21.60), we may replace k^μ/m by the longitudinal polarization vector. Notice that this would not be permissible (but, also, is not necessary) in the second term of (21.65). Our final result is

$$\epsilon_{L\mu}(k)\Gamma^\mu(k) = \Gamma(k), \quad (21.67)$$

as $k \rightarrow \infty$, with an error of order m^2/k^2 . That is, in the high-energy limit, the couplings of longitudinal gauge bosons become precisely those of their associated Goldstone bosons.

The equivalence theorem can be derived in another way, using the counting of physical states in spontaneously broken gauge theories, which we discussed below Eq. (21.26). In the previous section, we saw that, at least at the tree level, unitarity is maintained in spontaneously broken gauge theories by the cancellation of diagrams that produce timelike-polarized gauge bosons against diagrams that produce Goldstone bosons.

The situation is most clear in Feynman-'t Hooft gauge. There, the numerator of the gauge boson propagator is $-g^{\mu\nu}$. We can write this in terms of polarization vectors as

$$-g^{\mu\nu} = \sum_{i=1,2,3} \epsilon_i^\mu(k) \epsilon_i^{\nu*}(k) - \frac{k^\mu k^\nu}{m^2}. \quad (21.68)$$

The last term is the contribution from unphysical timelike polarization states. The unitarity of the S -matrix requires that, when a Cutkosky cut through a diagram puts a gauge boson propagator on-shell, the contribution of this piece

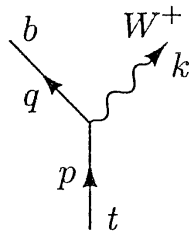
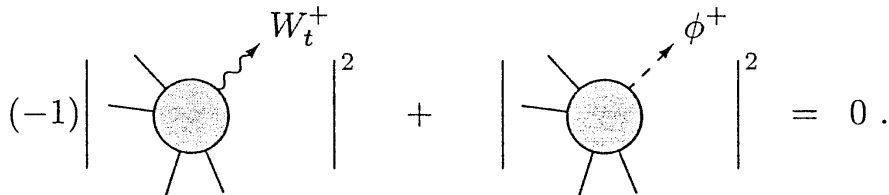


Figure 21.4. Decay of a t quark into $W^+ + b$.

must be canceled by a Cutkosky cut that runs through a Goldstone boson line. The required cancellation is

$$-\left| \frac{k_\mu}{m} \Gamma^\mu(k) \right|^2 + |\Gamma(k)|^2 = 0, \quad (21.69)$$

or, diagrammatically,



Once again, since $\Gamma^\mu(k)$ is a one-particle-irreducible vertex, we can use (21.60) to replace (k^μ/m) by the longitudinal polarization vector $\epsilon_L^\mu(k)$ for a high-energy gauge boson. Then (21.69) becomes just the square of (21.67).

Through these formal arguments, we can see, at least to the tree level in processes with single gauge boson emission, that the equivalence theorem must be valid. However, it is much more illuminating to see the equivalence theorem at work in explicit calculations for interesting physical processes. We will now illustrate its influence in two examples.

Top Quark Decay

The first example is the weak decay of the top quark. This charge $+2/3$ quark is sufficiently heavy that it can decay to a real W^+ through $t \rightarrow W^+ + b$. The diagram for this decay is given by the simple gauge vertex shown in Fig. 21.4.

Let us first try to guess the magnitude of the top quark width. The squared matrix element will contain a factor of g^2 , times some expression with dimensions of mass. Since the width should be large if the top quark mass is heavy, a first guess might be

$$\Gamma \sim \frac{g^2}{4\pi} m_t. \quad (21.70)$$

The correct expression, however, turns out to be enhanced by a factor of $(m_t/m_W)^2$.

The amplitude for this decay can be read from Eq. (20.80):

$$i\mathcal{M} = \frac{ig}{\sqrt{2}} \bar{u}(q) \gamma^\mu \left(\frac{1-\gamma^5}{2} \right) u(p) \epsilon_\mu^*(k). \quad (21.71)$$

(We set the relevant CKM factor equal to 1.) We will now turn this amplitude into an expression for the decay rate of the top quark. For simplicity, we will ignore the mass of the b quark in this computation.

Squaring the amplitude in (21.71) according to our standard methods, and then summing over initial and averaging over final spins, we find

$$\frac{1}{2} \sum_{\text{spins}} |\mathcal{M}|^2 = \frac{g^2}{2} [q^\mu p^\nu + q^\nu p^\mu - g^{\mu\nu} q \cdot p] \sum_{\text{polarizations}} \epsilon_\mu^*(k) \epsilon_\nu(k). \quad (21.72)$$

We can sum explicitly over physical gauge boson polarizations by inserting the expression (21.26) for the polarization sum. This gives

$$\begin{aligned} \frac{1}{2} \sum_{\text{spins}} |\mathcal{M}|^2 &= \frac{g^2}{2} [q^\mu p^\nu + q^\nu p^\mu - g^{\mu\nu} q \cdot p] \left[-g_{\mu\nu} + \frac{k_\mu k_\nu}{m_W^2} \right] \\ &= \frac{g^2}{2} \left[q \cdot p + 2 \frac{(k \cdot q)(k \cdot p)}{m_W^2} \right]. \end{aligned} \quad (21.73)$$

For $m_b = 0$,

$$2q \cdot p = 2q \cdot k = m_t^2 - m_W^2, \quad 2k \cdot p = m_t^2 + m_W^2. \quad (21.74)$$

Then

$$\frac{1}{2} \sum_{\text{spins}} |\mathcal{M}|^2 = \frac{g^2}{4} \frac{m_t^4}{m_W^2} \left(1 - \frac{m_W^2}{m_t^2} \right) \left(1 + 2 \frac{m_W^2}{m_t^2} \right). \quad (21.75)$$

After multiplying by phase space, we find

$$\Gamma = \frac{g^2}{64\pi} \frac{m_t^3}{m_W^2} \left(1 - \frac{m_W^2}{m_t^2} \right)^2 \left(1 + 2 \frac{m_W^2}{m_t^2} \right). \quad (21.76)$$

This is larger than our initial estimate (21.70) by a factor $(m_t/m_W)^2$.

It is not difficult to find the origin of this enhancement, by using the Goldstone boson equivalence theorem. In the gauge theory of weak interactions, the top quark obtains its mass from its coupling to the Higgs sector. The relation between the top-Higgs coupling λ_t and the top quark mass is written in Eq. (20.103). The top quark can be heavy only if λ_t is large. But then the amplitude for the top quark to decay to a Goldstone boson will be enhanced above (21.70) by the factor

$$\frac{\lambda_t^2}{g^2} = \frac{m_t^2}{2m_W^2}, \quad (21.77)$$

which is in fact the enhancement we found in (21.76).

To make the comparison more precise, we will now compute the prediction of the equivalence theorem for the top quark decay rate into a longitudinally polarized W^+ boson. Recall from (20.101) that the term in the weak interaction Lagrangian that couples t and b to the Higgs field is

$$\Delta\mathcal{L} = -\lambda_t \epsilon^{ab} \bar{Q}_{La} \phi_b^\dagger t_R + \text{h.c.} \quad (21.78)$$

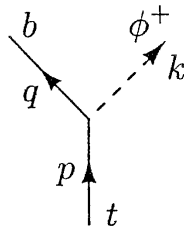


Figure 21.5. Decay of a t quark into a Goldstone boson and a b quark.

Decompose the Higgs field as in (21.38), and write

$$\phi^\pm = \frac{1}{\sqrt{2}}(\phi^1 \pm i\phi^2). \quad (21.79)$$

These are the fields of the charged Goldstone bosons that are eaten by the W^\pm . Including the Goldstone boson in the theory adds a process $t \rightarrow \phi^+ + b$, shown in Fig. 21.5. This process is mediated by the Lagrangian term

$$\Delta\mathcal{L} = \lambda_t \bar{b}_L \phi^+ t_R, \quad (21.80)$$

which leads to the decay amplitude

$$i\mathcal{M} = i\lambda_t \bar{u}(q) \left(\frac{1+\gamma^5}{2} \right) u(p). \quad (21.81)$$

From this expression, we easily find

$$\frac{1}{2} \sum_{\text{spins}} |\mathcal{M}|^2 = \lambda_t^2 q \cdot p. \quad (21.82)$$

If we now ignore the mass of the Goldstone boson, or, equivalently, consider the limit $m_t \gg m_W$, we find for the top quark decay rate

$$\Gamma = \frac{\lambda_t^2}{32\pi} m_t = \frac{g^2}{64\pi} \frac{m_t^3}{m_W^2}, \quad (21.83)$$

in agreement with the leading term of (21.76) in this limit. Our results imply that only the production of the longitudinal polarization state of the W^+ is enhanced; this is easily checked directly by substituting explicit polarization vectors into (21.72).

In our derivation of (21.76), we summed over the physical polarization states of the emitted W^+ ; one might say that we used the prescription of the U gauge to sum over polarizations. We could equally well have used the prescription of Feynman-'t Hooft gauge, replacing

$$\sum_i \epsilon_\mu^*(k) \epsilon_\nu(k) \rightarrow -g_{\mu\nu}, \quad (21.84)$$

and also adding the contribution of the Goldstone boson emission diagram, treating the Goldstone boson as a massive particle with mass m_W . With these

prescriptions, the gauge boson matrix element gives

$$\frac{1}{2} \sum_{\text{spins}} |\mathcal{M}|^2 = \frac{g^2}{2} (2q \cdot p) = \frac{g^2}{2} (m_t^2 - m_W^2). \quad (21.85)$$

The Goldstone boson emission diagram gives

$$\frac{1}{2} \sum_{\text{spins}} |\mathcal{M}|^2 = \lambda_t^2 q \cdot p = \frac{g^2}{4} \frac{m_t^2}{m_W^2} (m_t^2 - m_W^2). \quad (21.86)$$

The sum of these contributions indeed reproduces (21.75) and thus gives the same result (21.76) for the total decay rate. In Feynman-'t Hooft gauge, the enhancement due to the large coupling of the top quark to the Higgs sector shows up explicitly in the Goldstone boson emission contributions to the total rate of W^+ production.

$$e^+ e^- \rightarrow W^+ W^-$$

Our second example is more complicated, but also contains more interesting physics. This is the reaction $e^+ e^- \rightarrow W^+ W^-$. In this reaction, the equivalence theorem does not lead to an enhancement of the cross section, but, rather, directs a cancellation between Feynman diagrams. As we will see, this cancellation is essential for the internal consistency of the theory.

In Problem 9.1, we computed the cross section for $e^+ e^-$ annihilation into a pair of charged scalar particles, as in Fig. 21.6(a), and found the result

$$\frac{d\sigma}{d\cos\theta}(e^+ e^- \rightarrow \phi^+ \phi^-) = \frac{\pi\alpha^2}{4s} \quad (21.87)$$

at energies much larger than the scalar mass. Just as for $e^+ e^-$ annihilation to fermion pairs, this cross section falls as $1/s$ at high energy. It can be shown that this behavior is required by unitarity: Since the electron and positron annihilate through a pointlike vertex, the annihilation takes place in only one partial wave. Unitarity puts a limit on the amplitude in this partial wave, requiring that \mathcal{M} be bounded by a constant, and thus that σ be bounded by $1/s$ at high energy.*

The same unitarity argument applies to $e^+ e^-$ annihilation to vector bosons. Here, however, it is much less obvious that Feynman diagrams actually produce a cross section consistent with unitarity. Consider the contribution of Fig. 21.6(b). We would expect that the square of this diagram should contain a contribution to the cross section of the form of the scalar contribution (21.87) multiplied by the dot product of polarization vectors:

$$\frac{d\sigma}{d\cos\theta}(e^+ e^- \rightarrow W^+ W^-) \sim \frac{\pi\alpha^2}{4s} \cdot |\epsilon(k_+) \cdot \epsilon(k_-)|^2, \quad (21.88)$$

*Partial-wave analysis for relativistic collisions is discussed in Perkins (1987), Chapter 4.

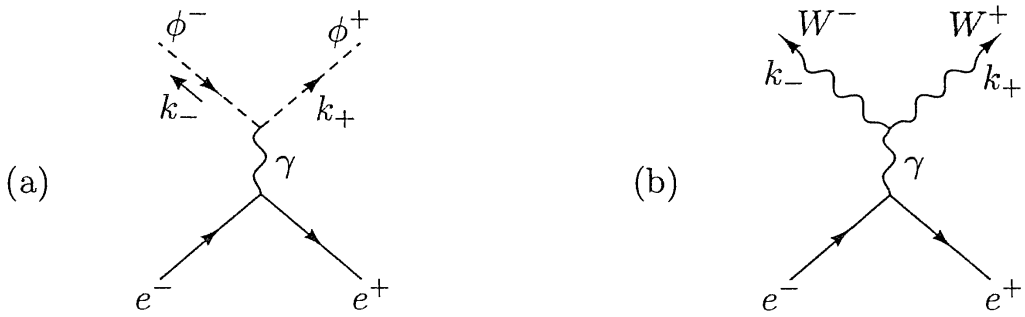


Figure 21.6. Electron-positron annihilation through a virtual photon (a) to charged scalar bosons, (b) to W bosons.

where k_+ and k_- are the momenta of the outgoing W bosons. For transversely polarized W bosons, this term is well behaved, but for longitudinally polarized W 's it leads to problems. Using the approximation (21.60) for the longitudinal polarization vectors, we find

$$\epsilon(k_+) \cdot \epsilon(k_-) \rightarrow \frac{k_+ \cdot k_-}{m_W^2} \rightarrow \frac{s}{4m_W^2} \quad (21.89)$$

for $s \gg m_W^2$. This leads to a cross section that grows much faster than is allowed by unitarity. In principle, the cross section could be brought back down to a proper behavior by the addition of contributions from higher orders in perturbation theory, but this would be a most unpleasant resolution. It would imply that the theory of W bosons becomes strongly coupled at energies such that

$$\frac{s}{4m_W^2} \sim \left(\frac{g^2}{4\pi}\right)^{-1}, \quad (21.90)$$

corresponding to center-of-mass energies of order 1000 GeV. But if the theory of W bosons is strongly coupled at short distances, it is hard to understand why, at large distances, it should become the simple, weak-coupling theory that we observe.

Fortunately, there is another possible resolution of this problem. In the weak interaction gauge theory, there are three Feynman diagrams that contribute to the amplitude for $e^+e^- \rightarrow W^+W^-$ at the tree level; these are shown in Fig. 21.7. Each diagram separately produces a cross section that grows in the same manner as (21.88). However, it is possible that the badly behaved terms might cancel among the three diagrams, leaving a more proper high-energy behavior. If this miraculous cancellation were to occur, it would allow the theory of W bosons to be consistently weakly coupled up to very high energies.

Although such a cancellation seems unlikely at first sight, it is actually required by the Goldstone boson equivalence theorem. The theorem states that, at high energy, the cross section for producing longitudinal W bosons should be equal to the cross section for producing the corresponding scalar Goldstone bosons. But we know that scalar cross sections behave as $1/s$, as

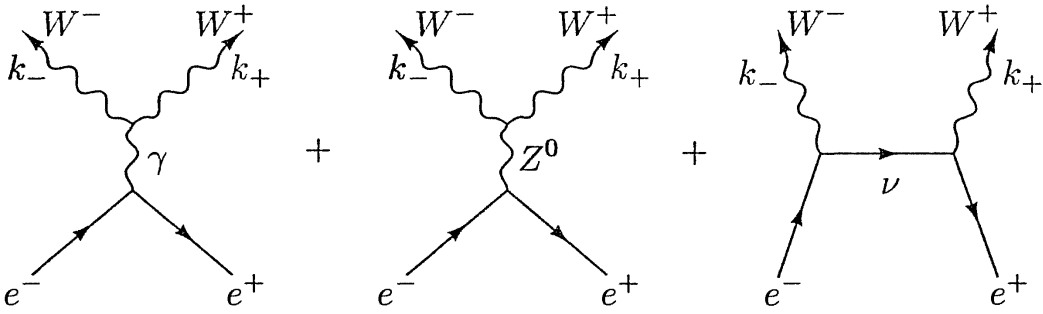


Figure 21.7. Diagrams contributing to $e^+e^- \rightarrow W^+W^-$ in the weak interaction gauge theory.

indicated in (21.87). Thus, somehow, the gauge boson cross section must also conspire to produce this result. We will now show this explicitly. We will see that the required cancellations are directed by the Ward identities of the gauge theory.

To prepare for this calculation, we need the Feynman rules for the vertices shown in Fig. 21.8. The Feynman rules for the couplings of the electron to W , Z , and γ can be read directly from (20.80). The relative strengths of these couplings are determined by the $SU(2) \times U(1)$ quantum numbers of the left- and right-handed components of the electron. It is equally straightforward to construct the couplings of the Goldstone bosons to Z and γ . Since the boson ϕ^+ has electric charge 1, the photon coupling is just that found in Problem 9.1. The Z coupling is determined with the additional information that the ϕ^+ has $I^3 = +1/2$. All of these expressions are shown in Fig. 21.8.

The three-gauge-boson vertices that appear in Fig. 21.7 arise from the cubic terms in the gauge field action. Since the $U(1)$ field strength is linear in gauge fields, these come only from the kinetic term of the $SU(2)$ gauge field. To identify the specific pieces we need, we must rewrite this cubic term in the basis of mass eigenstates given by (20.63) and (20.64). This can be done as follows:

$$\begin{aligned}
 -\frac{1}{4}(F_{\mu\nu}^a)^2 &\rightarrow -\frac{1}{2}(\partial_\mu A_\nu^a - \partial_\nu A_\mu^a)g\epsilon^{abc}A^{\mu b}A^{\nu c} \\
 &= -g(\partial_\mu A_\nu^1 - \partial_\nu A_\mu^1)A^{\mu 2}A^{\nu 3} + g(\partial_\mu A_\nu^2 - \partial_\nu A_\mu^2)A^{\mu 1}A^{\nu 3} \\
 &\quad - g(\partial_\mu A_\nu^3 - \partial_\nu A_\mu^3)A^{\mu 1}A^{\nu 2} \\
 &= ig[(\partial_\mu W_\nu^+ - \partial_\nu W_\mu^+)W^{\mu-}A^{\nu 3} - (\partial_\mu W_\nu^- - \partial_\nu W_\mu^-)W^{\mu+}A^{\nu 3} \\
 &\quad + \frac{1}{2}(\partial_\mu A_\nu^3 - \partial_\nu A_\mu^3)(W^{\mu+}W^{\nu-} - W^{\mu-}W^{\nu+})]. \quad (21.91)
 \end{aligned}$$

Finally, inserting $A_\mu^3 = \cos\theta_w Z_\mu + \sin\theta_w A_\mu$ and $g = e/\sin\theta_w$, we find the Feynman rules shown in Fig. 21.9.

Before examining the amplitude for e^+e^- annihilation to vector boson

Figure 21.8 consists of four Feynman diagrams. The first two diagrams show electron-positron annihilation. The left diagram shows an electron e_L^- and a positron e_R^+ annihilating into a virtual photon γ , which then couples to a virtual photon γ . The right diagram shows an electron e_L^- and a positron e_R^+ annihilating into a virtual photon γ , which then couples to a Z^0 boson. The third diagram shows an electron e_L^- and a positron e_R^+ annihilating into a virtual photon γ , which then couples to a Z^0 boson. The fourth diagram shows an electron e_L^- and a positron e_R^+ annihilating into a virtual photon γ , which then couples to a Z^0 boson.

Figure 21.8. Feynman rules of the weak-interaction gauge theory for electrons and scalars coupling to photons and Z bosons.

Figure 21.9 shows four Feynman diagrams for the WW and WWZ vertices. The top row shows the $WW\gamma$ vertex. The left diagram shows a virtual photon γ with momentum q and helicity λ interacting with a virtual photon γ with momentum k_+ and helicity μ , which then couples to a virtual photon γ with momentum k_- and helicity ν , which finally couples to a WW vertex. The right diagram shows a virtual photon γ with momentum q and helicity λ interacting with a virtual photon γ with momentum k_+ and helicity μ , which then couples to a virtual photon γ with momentum k_- and helicity ν , which finally couples to a WW vertex. The bottom row shows the WWZ vertex. The left diagram shows a virtual photon γ with momentum q and helicity λ interacting with a virtual photon γ with momentum k_+ and helicity μ , which then couples to a virtual photon γ with momentum k_- and helicity ν , which finally couples to a WW vertex. The right diagram shows a virtual photon γ with momentum q and helicity λ interacting with a virtual photon γ with momentum k_+ and helicity μ , which then couples to a virtual photon γ with momentum k_- and helicity ν , which finally couples to a WWZ vertex.

Figure 21.9. Feynman rules of the weak-interaction gauge theory for $WW\gamma$ and WWZ vertices.

pairs, we will first work out the amplitude for production of a pair of charged scalars. The equivalence theorem predicts that the amplitude for production of two longitudinal W bosons should become equal to this amplitude at high energy. Assembling vertices from Fig. 21.8, we find that, for an electron of either helicity, the amplitude to annihilate to scalars through a virtual photon is

$$i\mathcal{M}(ee \rightarrow \gamma^* \rightarrow \phi^+ \phi^-) = ie^2 \bar{v} \gamma_\mu u \frac{1}{q^2} (k_+ - k_-)^\mu, \quad (21.92)$$

where k_+ , k_- are the momenta of the scalars and $q = k_+ + k_-$. The corresponding amplitude for annihilation through a virtual Z^0 depends on the e^+e^- helicities. Adding these contributions to the preceding expression, we

find

$$\begin{aligned} i\mathcal{M}(e_L^- e_R^+ \rightarrow \phi^+ \phi^-) &= ie^2 \bar{v}_L \gamma_\mu u_L \left[\frac{1}{q^2} + \frac{(\frac{1}{2} - \sin^2 \theta_w)^2}{\sin^2 \theta_w \cos^2 \theta_w} \frac{1}{q^2 - m_Z^2} \right] (k_+ - k_-)^\mu, \\ i\mathcal{M}(e_R^- e_L^+ \rightarrow \phi^+ \phi^-) &= ie^2 \bar{v}_R \gamma_\mu u_R \left[\frac{1}{q^2} - \frac{(\frac{1}{2} - \sin^2 \theta_w)}{\cos^2 \theta_w} \frac{1}{q^2 - m_Z^2} \right] (k_+ - k_-)^\mu. \end{aligned} \quad (21.93)$$

Notice that, in the high-energy limit, the amplitude for the annihilation of right-handed electrons cancels down to

$$i\mathcal{M}(e_R^- e_L^+ \rightarrow \phi^+ \phi^-) \rightarrow i \frac{e^2}{2 \cos^2 \theta_w} \bar{v}_R \gamma_\mu u_R \frac{1}{q^2} (k_+ - k_-)^\mu, \quad (21.94)$$

which is just the amplitude for an e_R^- , with $Y = -1$, to couple to a ϕ^+ , with $Y = 1/2$, through the $U(1)$ gauge boson B_μ with coupling constant $g' = e/\cos \theta_w$. This expression reflects the fact that the e_R^- has no direct coupling to the $SU(2)$ gauge bosons. Similarly, the amplitude for left-handed electrons tends to

$$i\mathcal{M}(e_L^- e_R^+ \rightarrow \phi^+ \phi^-) \rightarrow ie^2 \left[\frac{1}{4 \cos^2 \theta_w} + \frac{1}{4 \sin^2 \theta_w} \right] \bar{v}_L \gamma_\mu u_L \frac{1}{q^2} (k_+ - k_-)^\mu \quad (21.95)$$

in the high-energy limit. This has the structure of a coherent sum of amplitudes with B_μ and A_μ^3 exchange. In just the way that we saw in Chapter 11, the symmetry structure of a gauge theory with spontaneously broken symmetry is recovered in the high-energy limit.

Now let us compare these results to a direct calculation of the $W^+ W^-$ production amplitude in the weak interaction gauge theory. Begin with the case of an initial e_R^- . Since the coupling of the electron to the W^- is purely left-handed, the third diagram of Fig. 21.7 vanishes in this case, so the computation is a bit easier. The first two diagrams of Fig. 21.7 have exactly the same structure and sum to

$$\begin{aligned} i\mathcal{M}(e_R^- e_L^+ \rightarrow W^+ W^-) &= \bar{v}_R \gamma_\lambda u_R \left[(-ie) \frac{-i}{q^2} (ie) + \frac{ie \sin \theta_w}{\cos \theta_w} \frac{-i}{q^2 - m_Z^2} \frac{ie \cos \theta_w}{\sin \theta_w} \right] \\ &\cdot [g^{\mu\nu} (k_- - k_+)^{\lambda} + g^{\lambda\nu} (-q - k_-)^\mu + g^{\lambda\mu} (k_+ + q)^\nu] \epsilon_\mu^*(k_+) \epsilon_\nu^*(k_-). \end{aligned} \quad (21.96)$$

This equation is valid in any of the R_ξ gauges, since, if we ignore the electron mass,

$$q^\lambda \bar{v}_R \gamma_\lambda u_R = 0. \quad (21.97)$$

The second line of Eq. (21.96) contains the enhancement for longitudinal W bosons mentioned above. If we approximate the longitudinal polarization vectors by (21.60) and drop terms that do not grow as $s \rightarrow \infty$, this line becomes

$$[g^{\mu\nu} (k_- - k_+)^{\lambda} + g^{\lambda\nu} (-q - k_-)^\mu + g^{\lambda\mu} (k_+ + q)^\nu] \frac{k_{+\mu}}{m_W} \frac{k_{-\nu}}{m_W}$$

$$\begin{aligned}
&= \frac{1}{m_W^2} [k_+ \cdot k_- (k_- - k_+)^{\lambda} - 2k_- \cdot k_+ k_-^{\lambda} + 2k_+ \cdot k_- k_+^{\lambda}] + \mathcal{O}(1) \cdot (k_- - k_+)^{\lambda} \\
&= \frac{s}{2m_W^2} (k_+ - k_-)^{\lambda} + \dots
\end{aligned} \tag{21.98}$$

On the other hand, the expression in brackets in the first line of (21.96) cancels almost completely, to

$$-ie^2 \left(\frac{1}{q^2} - \frac{1}{q^2 - m_Z^2} \right) = +ie^2 \frac{m_Z^2}{q^2(q^2 - m_Z^2)}.$$

Using both of these simplifications, we find

$$i\mathcal{M}(e_R^- e_L^+ \rightarrow W_L^+ W_L^-) = \bar{v}_R \gamma_{\lambda} u_R \left[(ie^2) \frac{m_Z^2}{s^2} \right] \frac{s}{2m_W^2} (k_+ - k_-)^{\lambda}. \tag{21.99}$$

By inserting the relation $m_W = m_Z \cos \theta_w$, we see that this amplitude is identical to (21.94), as required by the equivalence theorem.

For the amplitude with an initial e_L^- , the computation is somewhat more involved. Now all three diagrams of Fig. 21.7 contribute, and since the last diagram has a different kinematic structure, it will be less clear how the diagrams combine together. In what follows, we will demonstrate the cancellation of the unitarity-violating enhanced terms, and we will indicate how the terms one order smaller in m_W^2/s assemble into the correct structure. However, we will not account rigorously for all of these smaller terms. It is actually straightforward, but lengthy, to show that the terms we will omit do not contribute to the high-energy limit of the cross section. This demonstration is included in Problem 21.2.

For the case of an initial e_L^- , the first two diagrams of Fig. 21.7 sum to the expression

$$\begin{aligned}
&\text{Diagram: } W^- \text{ (wavy line)} \rightarrow \gamma, Z \text{ (crossed lines)} \rightarrow W^+ \text{ (wavy line)} \\
&= \bar{v}_L \gamma_{\lambda} u_L \left[(-ie) \frac{-i}{q^2} (ie) + \frac{ie(-\frac{1}{2} + \sin^2 \theta_w)}{\sin \theta_w \cos \theta_w} \frac{-i}{q^2 - m_Z^2} \frac{ie \cos \theta_w}{\sin \theta_w} \right] \\
&\quad \cdot [g^{\mu\nu} (k_- - k_+)^{\lambda} + g^{\lambda\nu} (-q - k_-)^{\mu} + g^{\lambda\mu} (k_+ + q)^{\nu}] \epsilon_{\mu}^*(k_+) \epsilon_{\nu}^*(k_-),
\end{aligned} \tag{21.100}$$

which differs from (21.96) only in the coupling of the electron to the virtual Z^0 . For longitudinal W bosons, we can simplify this expression as we did (21.96), obtaining

$$\begin{aligned}
&\text{Diagram: } W_L^- \text{ (wavy line)} \rightarrow \gamma, Z \text{ (crossed lines)} \rightarrow W_L^+ \text{ (wavy line)} \\
&= \bar{v}_L \gamma_{\lambda} u_L (ie^2) \left[\frac{m_Z^2}{s(s - m_Z^2)} - \frac{1}{2 \sin^2 \theta_w} \frac{1}{s - m_Z^2} \right] \frac{s}{2m_W^2} (k_+ - k_-)^{\lambda}.
\end{aligned} \tag{21.101}$$

The second term in brackets is a potentially dangerous contribution, which must be canceled by the diagram with t -channel neutrino exchange. This

diagram has the value

$$\text{Diagram: } W_L^- \xrightarrow{\nu} W_L^+ = \left(\frac{ig}{\sqrt{2}} \right)^2 \bar{v}_L \gamma^\mu \frac{i(\not{\ell} - \not{k}_-)}{(\ell - k_-)^2} \gamma^\nu u_L(\ell) \epsilon_\mu^*(k_+) \epsilon_\nu^*(k_-), \quad (21.102)$$

where ℓ is the initial electron momentum. Approximating the longitudinal polarization vectors as before, we have

$$\text{Diagram: } W_L^- \xrightarrow{\nu} W_L^+ = -i \frac{g^2}{2} \bar{v}_L \frac{\not{k}_+}{m_W} \frac{(\not{\ell} - \not{k}_-)}{(\ell - k_-)^2} \frac{\not{k}_-}{m_W} u_L(\ell) \epsilon_\mu^*(k_+) \epsilon_\nu^*(k_-). \quad (21.103)$$

Now we manipulate this expression as if we were proving a Ward identity. Using the fact that $u_L(\ell)$ satisfies the Dirac equation,

$$(\not{\ell} - \not{k}_-) \not{k}_- u_L(\ell) = -(\not{\ell} - \not{k}_-)^2 u_L(\ell) = -(\ell - k_-)^2 u_L(\ell), \quad (21.104)$$

expression (21.103) reduces to

$$\text{Diagram: } W_L^- \xrightarrow{\nu} W_L^+ = i \frac{g^2}{2} \bar{v}_L \frac{\not{k}_+}{m_W^2} u_L(\ell). \quad (21.105)$$

Finally, using Eq. (21.97), we can rewrite this expression as

$$\text{Diagram: } W_L^- \xrightarrow{\nu} W_L^+ = ie^2 \frac{1}{2 \sin^2 \theta_w} \frac{1}{2m_W^2} \bar{v}_L \gamma_\lambda u_L(\ell) (k_+ - k_-)^\lambda. \quad (21.106)$$

This term cancels the dangerous high-energy behavior of (21.101). Adding these two amplitudes, we find in the high-energy limit

$$i\mathcal{M}(e_L^- e_R^+ \rightarrow W_L^+ W_L^-) = ie^2 \bar{v}_L \gamma_\lambda u_L(k_+ - k_-)^\lambda \frac{1}{s} \cdot \left[\frac{1}{2 \cos^2 \theta_w} + \frac{1}{4 \cos^2 \theta_w \sin^2 \theta_w} \right]. \quad (21.107)$$

The quantity in brackets can be rewritten as

$$\left[\frac{1}{4 \cos^2 \theta_w} + \frac{1}{4 \sin^2 \theta_w} \right].$$

With this rearrangement, (21.107) agrees precisely with (21.95). In the derivation of (21.107), however, we have dropped higher-order contributions from the polarization vectors (21.60) that are of the same order as the terms we kept; one must show carefully that these terms do not give additional contributions in the high-energy limit.

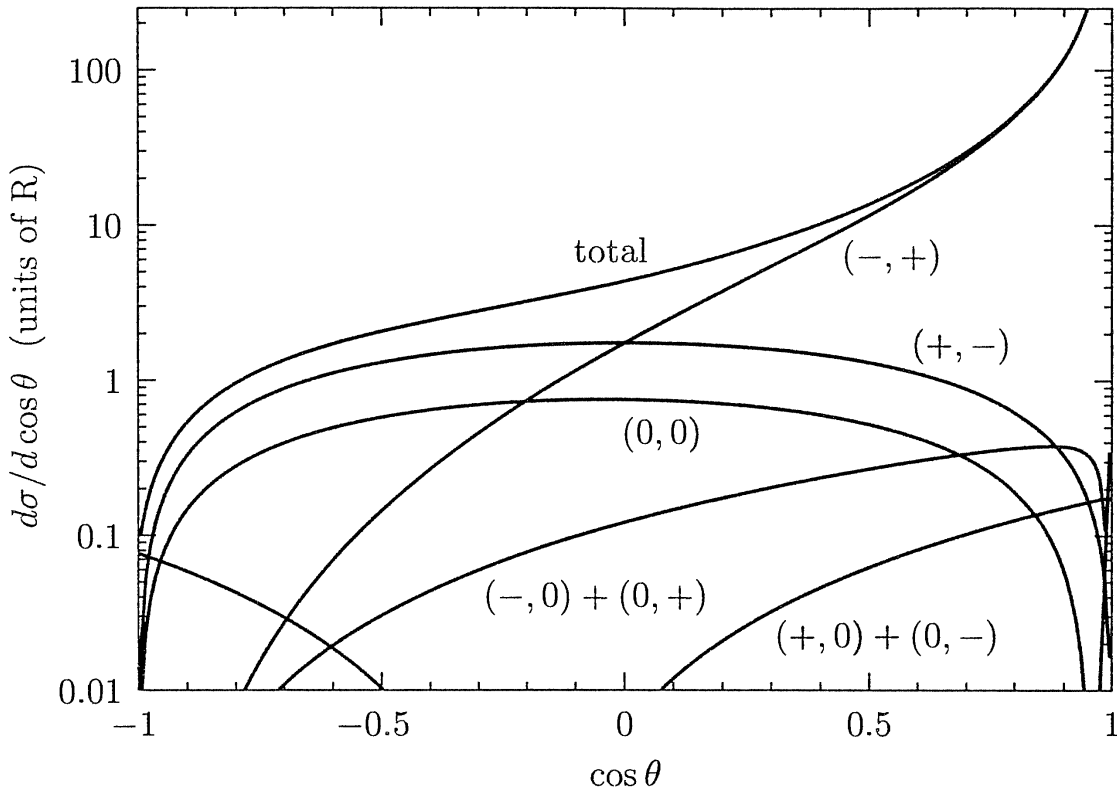


Figure 21.10. The differential cross section for $e_L^- e_R^+ \rightarrow W^+ W^-$, in units of R (Eq. (5.15)), at $E_{\text{cm}} = 1000$ GeV. The various curves show the contributions to the total from individual helicity states of W^- and W^+ ; these are denoted (h_-, h_+) , where each helicity takes the values $(+, -, 0)$. The contributions from the $(+, +)$ and $(-, -)$ states are too small to be visible. Notice that both the $W_L^- W_L^+$ cross section, denoted $(0, 0)$, and the $(+, -)$ cross section become proportional to $\sin^2 \theta$ at very high energy.

The calculation of Problem 21.2 gives for the complete annihilation amplitude

$$\begin{aligned}
 i\mathcal{M}(e_L^- e_R^+ \rightarrow W_L^+ W_L^-) = & ie^2 \bar{v}_L \gamma_\lambda u_L (k_+ - k_-)^\lambda \frac{1}{s} \\
 & \cdot \left[\frac{1}{2 \sin^2 \theta_w} \left\{ -\frac{s}{s - m_Z^2} \left(\frac{m_Z^2}{2m_W^2} + 1 \right) + \frac{2}{\beta^2} \right. \right. \\
 & \left. \left. - \frac{8m_W^2}{s\beta^2(1+\beta^2-2\beta \cos \theta)} \right\} + \frac{m_Z^2}{m_W^2} \left(\frac{\frac{1}{2}s + m_W^2}{s - m_Z^2} \right) \right], \quad (21.108)
 \end{aligned}$$

where $\beta = (1 - 4m_W^2/s)^{1/2}$ is the W boson velocity. The high-energy limit of this expression indeed reproduces (21.101). The contributions to the differential cross section for $e_L^- e_R^+ \rightarrow W^+ W^-$ from this and the other possible helicity states are plotted in Fig. 21.10.

These cancellations among the diagrams of Fig. 21.7 occur by virtue of the Ward identities of the gauge theory. That is, they occur only because the theory has an underlying local gauge invariance. At the beginning of our discussion, we argued that these cancellations are necessary to insure that the theory remains, in a consistent way, weakly coupled up to arbitrarily

high energy. In Section 20.1, we showed that one can generate masses for vector bosons by spontaneously breaking local gauge invariance. We have now argued the converse of that result: that the only theories of massive vector bosons that do not have violent high-energy behavior are those that result from spontaneously broken gauge theories.[†]

21.3 One-Loop Corrections to the Weak-Interaction Gauge Theory

The final topic in our study of spontaneously broken gauge theories is the computation of one-loop corrections in the weak-interaction gauge theory. As we discussed in Section 20.2, tree-level diagrams produce a number of intricate predictions for the couplings of the Z^0 and the cross sections for neutral current reactions. In general, these predictions are modified by the effects of one-loop diagrams. In this section we will study some examples of these one-loop corrections.

As in any renormalizable field theory, the one-loop diagrams of the electroweak gauge theory are typically ultraviolet divergent. These divergences can be absorbed by adjusting the underlying parameters of the theory. These adjustments define a set of counterterms which, by renormalizability, render the full set of one-loop diagrams of the theory finite. Those amplitudes that are not adjusted by hand then become predictions of the theory.

In Chapter 11, we saw that this general procedure, which applies to any renormalizable field theory, gives especially rich information when applied to a theory with spontaneous symmetry breaking. In a theory with spontaneously broken symmetry, the amplitudes of the theory vary markedly for different particles in the same multiplet of the original symmetry. However, the counterterms of the theory respect the symmetry relations. Thus, the adjustment of an amplitude for one particle leads to definite predictions for other particles that are not related by any manifest symmetry.

Theoretical Orientation, and a Specific Problem

At the end of Section 11.6, we presented a useful framework for organizing calculations of the predictions of renormalizable theories with spontaneous symmetry breaking. We defined a *zeroth-order natural relation* to be a relation among observable quantities in the theory that is true for any values of the parameters in the Lagrangian. Since the counterterms of the theory shift the values of the underlying parameters without adding new terms, a zeroth-order natural relation will not be corrected by these counterterms. Thus, if the theory is renormalizable, the one-loop corrections to a zeroth-order natural

[†]This statement is proved systematically in the paper of Cornwall, Levin, and Tiktopoulos cited at the beginning of this section.

relation will be finite, and will in fact be definite predictions from the quantum structure of the field theory. Though we discussed this idea originally in theories with spontaneously broken global symmetry, it applies equally well to theories with spontaneously broken gauge symmetry. In this section, we will apply this idea to derive finite one-loop corrections to relations in the weak-interaction gauge theory.

It is easy to find zeroth-order natural relations in the electroweak theory. The leading-order predictions given in Section 20.2 involve a relatively small number of free parameters. Many of these predictions are made for energies at which the quark and lepton masses can be ignored; then they depend only on the coupling constants g and g' and the vacuum expectation value v , which sets the scale of spontaneous symmetry breaking. The remaining ingredients of the weak-interaction theory are given in terms of these parameters; for example,

$$\begin{aligned} m_W &= g \frac{v}{2}, & m_Z &= \sqrt{g^2 + g'^2} \frac{v}{2}, \\ e &= \frac{gg'}{\sqrt{g^2 + g'^2}}, & \frac{G_F}{\sqrt{2}} &= \frac{g^2}{8m_W^2} = \frac{1}{2v^2}. \end{aligned} \quad (21.109)$$

Even in this set of quantities, we have four relations that depend on three underlying parameters, so there is one relation of observable quantities that is independent of the parameters of the Lagrangian.

Since many of the predictions of the weak interaction gauge theory are determined by the parameter $\sin^2 \theta_w$, it is useful to define $\sin^2 \theta_w$ in terms of observables and then use this definition as a basis for constructing natural relations. In our discussion of the precision tests of electroweak theory in Section 20.2, we used the definition

$$s_W^2 \equiv 1 - \frac{m_W^2}{m_Z^2} \quad (21.110)$$

as a standard for comparison of different experiments. But since the three most accurately known weak-interaction observables are α , G_F , and m_Z , it is useful to construct another physical definition of $\sin^2 \theta_w$ based on these three quantities. Define θ_0 such that

$$\sin 2\theta_0 \equiv \left(\frac{4\pi\alpha_*}{\sqrt{2}G_F m_Z^2} \right)^{1/2}, \quad (21.111)$$

where α_* is the running coupling constant of QED evaluated at the scale $Q^2 = m_Z^2$. The renormalization group insists that it is the value of the electric charge at the weak-interaction scale that enters precision electroweak predictions, and this observation is confirmed by summing radiative correction diagrams involving light quarks and leptons. The current best values of the quantities in Eq. (21.111) give

$$s_0^2 \equiv \sin^2 \theta_0 = 0.2307 \pm 0.0005. \quad (21.112)$$

Thus, this quantity provides a very accurate standard of reference.

Once Eq. (21.111) is taken to define a reference value of $\sin^2 \theta_w$, the equations of Section 20.2 that connect $\sin^2 \theta_w$ to other observables become zeroth-order natural relations. For example, the tree-level equations

$$\frac{m_W^2}{m_Z^2} = \cos^2 \theta_w, \quad A_{LR}^e = \frac{(\frac{1}{2} - \sin^2 \theta_w)^2 - (\sin^2 \theta_w)^2}{(\frac{1}{2} - \sin^2 \theta_w)^2 + (\sin^2 \theta_w)^2} \quad (21.113)$$

are natural relations linking four observables of the weak interactions. The corrections to these relations will be well-defined predictions of the theory.

In principle, we could now compute all of the one-loop diagrams that correct the parameters m_W , m_Z , G_F , α , and A_{LR}^e . However, this is a very complicated exercise, requiring an extensive technical apparatus.[†] In this section we will focus on radiative corrections from one simple source that can be considered independently. Aside from the question of anomalies, the electroweak theory does not restrict the number of quark or lepton generations. Thus, it is sensible, and gauge invariant, to compute the one-loop corrections due to one quark or lepton doublet. For definiteness, we consider the effects of the (t, b) quark doublet.

By focusing on the radiative corrections due to heavy quarks, we dramatically simplify the calculational task before us. The various observables of the weak-interaction gauge theory are extracted from the measurement of scattering amplitudes with light fermions, leptons or quarks, in the initial and final states. For example, G_F is measured from the strength of a low-energy weak-interaction process, usually chosen to be the rate of muon decay: $\mu \rightarrow \nu_\mu e^- \bar{\nu}_e$. For any such process, there are one-loop corrections of many kinds, as shown in Fig. 21.11. In addition to corrections to the vector boson propagator, there are vertex corrections, box diagrams, and diagrams with real photon emission. In general, the contributions of the various classes of diagrams are not gauge invariant; rather, gauge invariance results from cancellations between the classes of diagrams in Fig. 21.11(b), (c), and (d). However, since heavy quarks do not couple directly to the light leptons, the (t, b) doublet contributes only the single diagram shown in Fig. 21.11(f), which must be gauge invariant by itself. This same conclusion applies to the (t, b) correction to other leptonic weak interaction processes. If we ignore the CKM angles that mix the t and b with other species, the conclusion extends also to weak-interaction processes involving light quarks.

A similar situation occurs with other species of particles, such as those of the Higgs sector. The coupling of Higgs sector particles to a light quark or lepton is proportional to the fermion's mass, which we can often ignore. Thus the most important contributions from Higgs-sector particles are propagator corrections. The case in which the spontaneous symmetry breaking is produced by a single scalar field ϕ is particularly straightforward to analyze;

[†]A detailed theoretical discussion of one-loop corrections to the electroweak theory can be found in W. Hollik, *Fortschr. d. Physik* **38**, 165 (1990).

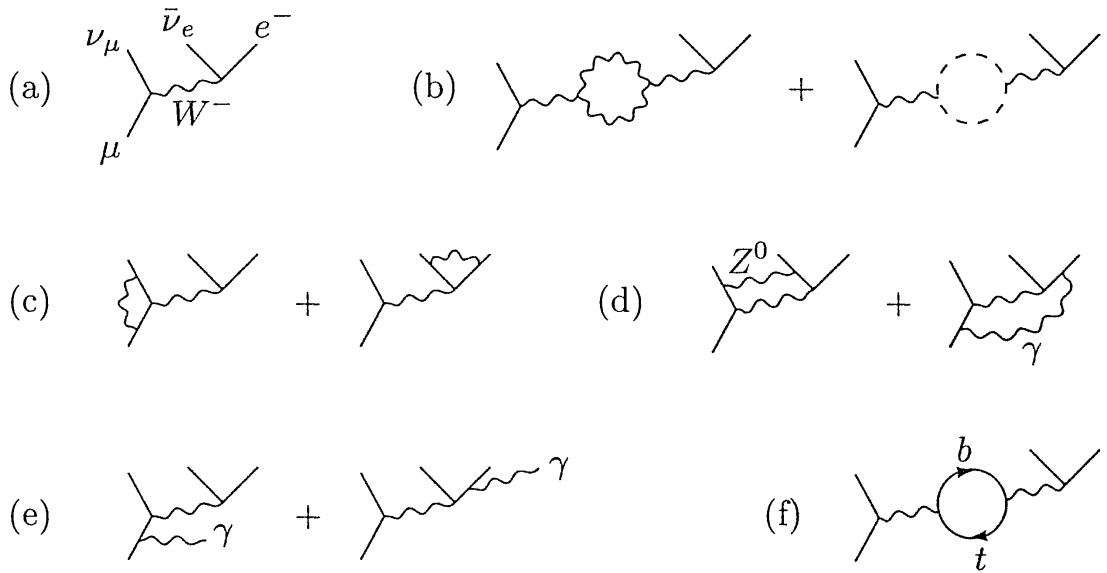


Figure 21.11. Examples of radiative corrections to μ decay in the weak interaction gauge theory: (a) lowest-order diagram; (b) propagator corrections; (c) vertex diagrams; (d) box diagrams; (e) real photon corrections; (f) the contribution of the (t, b) doublet.

this is done in Problem 21.4. Loop corrections from particles that do not couple directly to the external fermions are often termed *oblique*, since they enter the low-energy weak interactions only indirectly.

Influence of Heavy Quark Corrections

Our task, then, is to compute the corrections to relations (21.113) due to the (t, b) doublet. These two relations depend on five observable quantities— m_Z , m_W , A_{LR}^e , α , and G_F —with the last two parameters entering through θ_w and Eq. (21.111). We will express these five quantities as functions of the bare parameters g , g' , and v , with corrections proportional to combinations of t and b vacuum polarization diagrams. The zeroth-order terms will naturally cancel out when we compute the corrections to the relations (21.113).

The loop amplitudes that we require are shown in Fig. 21.12. To deal with these contributions most straightforwardly, we introduce a uniform notation for vacuum polarization amplitudes. Denote the vacuum polarization amplitude involving the gauge bosons I and J as

$$\mu \text{---} \text{---} \text{---} \text{---} \nu = i\Pi_{IJ}^{\mu\nu}(q), \quad (21.114)$$

where I and J may be γ , W , or Z . When the gauge bosons are massive, the vacuum polarization amplitudes need not be transverse by themselves, so $\Pi_{IJ}^{\mu\nu}(q)$ need not vanish at $q^2 = 0$. Thus, we will change our notation from the case of QED and write the decomposition of $\Pi_{IJ}^{\mu\nu}(q)$ into tensor structures as

$$\Pi_{IJ}^{\mu\nu}(q) = \Pi_{IJ}(q^2)g^{\mu\nu} - \Delta(q^2)q^\mu q^\nu. \quad (21.115)$$

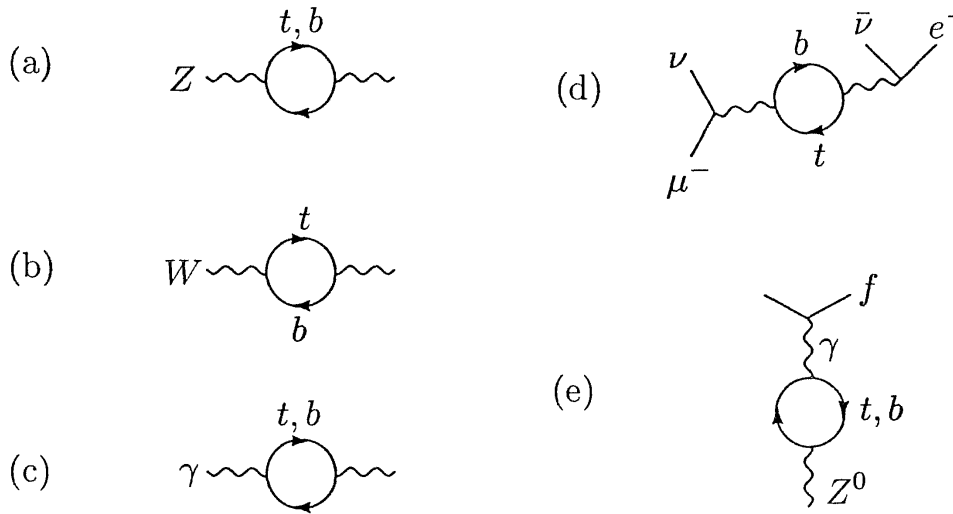


Figure 21.12. One-loop corrections from t and b to weak-interaction observables: (a) m_Z ; (b) m_W ; (c) α ; (d) G_F ; (e) A_{LR}^e .

In all of the examples to follow, the factors q^μ will dot into currents of light leptons, to give zero as in Eq. (21.97). Thus the form factor $\Delta(q^2)$ will drop out of our calculations. Our previous result that $\Pi^{\mu\nu}(q)$ vanishes in QED at $q^2 = 0$ appears in this formalism as the set of constraints

$$\Pi_{\gamma\gamma}(0) = \Pi_{\gamma Z}(0) = 0. \quad (21.116)$$

For the other amplitudes, our sign conventions are chosen so that a positive value of $\Pi_{IJ}(m^2)$ gives a positive mass shift to the gauge boson. Let us also define

$$\Pi'_{\gamma\gamma}(0) = \left. \frac{d\Pi_{\gamma\gamma}}{dq^2} \right|_{q^2=0}; \quad (21.117)$$

this is the quantity we called $\Pi(0)$ in Eq. (7.73).

Now we use this notation to write the loop corrections to each of the five observables. The first two diagrams in Fig. 21.12 are simply mass corrections, and so, straightforwardly,

$$\begin{aligned} m_Z^2 &= (g^2 + g'^2) \frac{v^2}{4} + \Pi_{ZZ}(m_Z^2), \\ m_W^2 &= g^2 \frac{v^2}{4} + \Pi_{WW}(m_W^2). \end{aligned} \quad (21.118)$$

Note that both vacuum polarization amplitudes are evaluated at the poles in the respective propagators. To evaluate the shift of α by one-loop corrections, we consider the effect of Fig. 21.12(c) on the low-energy Coulomb potential. The values of the leading-order propagator and the one-loop correction combine to give the factors

$$\frac{-ie^2}{q^2} \left(1 + i\Pi_{\gamma\gamma}(q^2) \cdot \frac{-i}{q^2} \right), \quad (21.119)$$

where, in this equation, e^2 is given in terms of bare variables as in (21.109). Thus, the observed value of α , in the limit $q^2 \rightarrow 0$, is modified according to the relation

$$4\pi\alpha = \frac{g^2 g'^2}{g^2 + g'^2} (1 + \Pi'_{\gamma\gamma}(0)). \quad (21.120)$$

In a similar way, the diagrams of Fig. 21.12(d) give a modified strength of the 4-fermion weak interaction process that leads to μ decay. The leading and one-loop diagrams sum to

$$\frac{g^2}{q^2 - m_W^2} \left(1 + i\Pi_{WW}(q^2) \frac{-i}{q^2 - m_W^2} \right). \quad (21.121)$$

Then the effective strength of the weak interaction vertex at $q^2 = 0$ is shifted as follows:

$$\frac{G_F}{\sqrt{2}} = \frac{1}{2v^2} \left(1 - \frac{\Pi_{WW}(0)}{m_W^2} \right). \quad (21.122)$$

Notice that, in the approximation of keeping only oblique corrections, the strength of every low-energy weak interaction amplitude is corrected by this same factor.

Finally, the polarization asymmetry A_{LR}^e is corrected by a (t, b) loop diagram according to Fig. 21.12(e). The analogous diagram with an intermediate Z^0 is summed into the Z^0 propagator and does not affect the form of the vertex. At zeroth order, the coupling of the Z^0 to any left- or right-handed light fermion is given, according to Eq. (20.71), by

$$\sqrt{g^2 + g'^2} \left(T^3 - \frac{g'^2}{g^2 + g'^2} Q \right). \quad (21.123)$$

The coefficient of Q is the bare value of $\sin^2 \theta_w$. The loop diagram in Fig. 21.12(e) adds to this a contribution

$$i\Pi_{Z\gamma}(q^2) \frac{-i}{q^2} \cdot (ieQ). \quad (21.124)$$

To discuss asymmetries at the Z^0 resonance, we set $q^2 = m_Z^2$. The term (21.124) adds to the piece of (21.123) proportional to Q ; thus it shifts the bare value of $\sin^2 \theta_w$. When we include this correction, the Z^0 coupling takes the form

$$\sqrt{g^2 + g'^2} \left(T^3 - s_*^2 Q \right), \quad (21.125)$$

where

$$s_*^2 = \frac{g'^2}{g^2 + g'^2} - \frac{e}{\sqrt{g^2 + g'^2}} \frac{\Pi_{\gamma Z}(m_Z^2)}{m_Z^2}. \quad (21.126)$$

The asymmetries at the Z^0 resonance discussed in Section 20.2 are computed as ratios of these couplings. Thus, to include the oblique radiative correction to A_{LR}^f , for any light fermion species f , we reevaluate formula (20.96), using s_*^2 in place of the zeroth-order $\sin^2 \theta_w$.

We might, in fact, say that s_*^2 gives an additional way to define $\sin^2 \theta_w$ from observable quantities, to be compared to the definitions s_W^2 given in (21.110) and s_0^2 given in (21.111). Speaking strictly, the value of $\sin^2 \theta_w$ determined by the asymmetries at the Z^0 depends on the quark or lepton quantum numbers through vertex corrections that are not included in the analysis above. However, these species-dependent corrections are small and can be systematically subtracted to define a universal s_*^2 that determines the weak interaction asymmetries of all fermion species.*

The three definitions of $\sin^2 \theta_w$ all agree at zeroth order but receive different radiative corrections. If we include only the oblique corrections, it is easy to produce compact formulae for the three quantities. From (21.126), we have

$$s_*^2 = \frac{g'^2}{g^2 + g'^2} - \sin \theta_w \cos \theta_w \frac{\Pi_{\gamma Z}}{m_Z^2}. \quad (21.127)$$

In the prefactor of the one-loop correction, we can ignore the distinction between the bare and renormalized values of $\sin^2 \theta_w$. We can obtain a similar expression for s_W^2 by taking the ratio of the two formulae in (21.118):

$$s_W^2 = \frac{g'^2}{g^2 + g'^2} - \frac{1}{m_Z^2} \left(\Pi_{WW}(m_W^2) - \frac{m_W^2}{m_Z^2} \Pi_{ZZ}(m_Z^2) \right). \quad (21.128)$$

Finally, we can evaluate the oblique corrections to $\sin^2 \theta_0$ defined by (21.111). This is most readily done by writing $\delta\theta_0$ for the difference between the true and the bare value of θ_0 , and then expanding (21.111) as follows:

$$2 \cos 2\theta_0 \delta\theta_0 = \frac{1}{2} \sin 2\theta_0 \left[\frac{\delta\alpha}{\alpha} - \frac{\delta G_F}{G_F} - \frac{\delta m_Z^2}{m_Z^2} \right]. \quad (21.129)$$

The shifts of α , G_F , and m_Z^2 can be read from (21.120), (21.122), and (21.118). Then we can reconstruct

$$\sin^2 \theta_0 = \frac{g'^2}{g^2 + g'^2} + 2 \sin \theta_0 \cos \theta_0 \delta \theta_0. \quad (21.130)$$

Assembling the pieces and evaluating the coefficients of the vacuum polarization diagrams to zeroth order, we obtain

$$\begin{aligned} \sin^2 \theta_0 = & \frac{g'^2}{g^2 + g'^2} \\ & + \frac{\sin^2 \theta_w \cos^2 \theta_w}{\cos^2 \theta_w - \sin^2 \theta_w} \left[\Pi'_{\gamma\gamma}(0) + \frac{1}{m_W^2} \Pi_{WW}(0) - \frac{1}{m_Z^2} \Pi_{ZZ}(m_Z^2) \right]. \end{aligned} \quad (21.131)$$

It is not difficult to discover that each of the equations (21.127), (21.128), and (21.131) contains ultraviolet divergences. However, if the weak interaction gauge theory is renormalizable, these divergences should cancel when we

*This is explained clearly in D. Kennedy and B. W. Lynn, *Nucl. Phys.* **B322**, 1 (1989).

compute the corrections to any zeroth-order natural relation. In the situation that we consider, renormalizability implies that the various definitions of $\sin^2 \theta_w$ should differ only by expressions that are ultraviolet-finite.

We are now almost prepared to check this prediction explicitly. We can clarify the structure of the ultraviolet divergences in our relations for the various quantities $\sin^2 \theta_w$ by recasting the vacuum polarization amplitudes to make more explicit the quantum numbers to which the gauge bosons couple. Recall from Eq. (20.71) that the Z boson couples to the combination of $SU(2)$ and electromagnetic quantum numbers ($T^3 - \sin^2 \theta_w Q$). Similarly, the W bosons couple to T^\pm , or, equivalently, to T^1, T^2 . It is useful to break up the vacuum polarization amplitudes into terms that depend on these specific quantum numbers. We will also extract the coupling constants indicated in (20.71). Thus we replace

$$\begin{aligned}\Pi_{\gamma\gamma} &= e^2 \Pi_{QQ}, \\ \Pi_{\gamma Z} &= \left(\frac{e^2}{\sin \theta_w \cos \theta_w} \right) [\Pi_{3Q} - \sin^2 \theta_w \Pi_{QQ}], \\ \Pi_{ZZ} &= \left(\frac{e}{\sin \theta_w \cos \theta_w} \right)^2 [\Pi_{33} - 2 \sin^2 \theta_w \Pi_{3Q} + \sin^4 \theta_w \Pi_{QQ}], \\ \Pi_{WW} &= \left(\frac{e}{\sin \theta_w} \right)^2 \Pi_{11},\end{aligned}\tag{21.132}$$

where Q denotes the electric charge and $1, 2, 3$ denote the components of weak-interaction $SU(2)$.

A vacuum polarization amplitude can always be viewed as an expectation value of a pair of currents. From this viewpoint, the quantities on the right-hand side of (21.132) are expectation values of currents with definite quantum numbers. For example, Π_{33} is an expectation value of a pair of $SU(2)$ currents J^μ . Acting on the standard fermions, J_a^μ is a left-handed current and J_Q^μ is a vector current.

The ultraviolet divergences in the expectation values of currents in (21.132) have the form

$$\begin{aligned}\Pi_{33} &\sim (A + Bq^2) \log \Lambda^2, \\ \Pi_{11} &\sim (A + Bq^2) \log \Lambda^2, \\ \Pi_{3Q} &\sim (Bq^2) \log \Lambda^2, \\ \Pi_{QQ} &\sim (Cq^2) \log \Lambda^2.\end{aligned}\tag{21.133}$$

We will demonstrate this explicitly later in this section. However, we can understand this structure from the following rough argument: Since the symmetry of the theory should be recovered at large momentum, the amplitudes Π_{33} and Π_{11} , which differ only by their orientation in the symmetry space, should have the same ultraviolet divergences. The divergence in the slope of Π_{3Q} should be related to that in the slope of Π_{33} because $Q = T^3 + Y$ and Π_{3Y} is unimportant asymptotically since $\text{tr}[T^3 Y] = 0$. We pointed out

in Eq. (21.116) that Π_{3Q} and Π_{QQ} vanish at $q^2 = 0$; thus they have no q^2 -independent divergences.

Now we will rewrite the two zeroth-order natural relations in (21.113) in such a way that we can apply (21.133). To do this, we take the differences of Eqs. (21.127), (21.128), and (21.131) to obtain

$$\begin{aligned} s_*^2 - \sin^2 \theta_0 &= \frac{\sin^2 \theta_w \cos^2 \theta_w}{\cos^2 \theta_w - \sin^2 \theta_w} \left\{ \frac{\Pi_{ZZ}(m_Z^2)}{m_Z^2} - \frac{\Pi_{WW}(0)}{m_W^2} - \Pi'_{\gamma\gamma}(0) \right. \\ &\quad \left. - \frac{\cos^2 \theta_w - \sin^2 \theta_w}{\sin \theta_w \cos \theta_w} \frac{\Pi_{\gamma Z}(m_Z^2)}{m_Z^2} \right\}, \\ s_W^2 - s_*^2 &= -\frac{\Pi_{WW}(m_W^2)}{m_Z^2} + \frac{m_W^2}{m_Z^2} \frac{\Pi_{ZZ}(m_Z^2)}{m_Z^2} + \sin \theta_w \cos \theta_w \frac{\Pi_{\gamma Z}(m_Z^2)}{m_Z^2}. \end{aligned} \quad (21.134)$$

Inserting (21.132), and also using the relation $m_W = m_Z \cos \theta_w$ in the coefficients of terms already of one-loop order, we find after some algebra

$$\begin{aligned} s_*^2 - \sin^2 \theta_0 &= \frac{e^2}{(\cos^2 \theta_w - \sin^2 \theta_w)m_Z^2} \left\{ [\Pi_{33}(m_Z^2) - \Pi_{11}(0) - \Pi_{3Q}(m_Z^2)] \right. \\ &\quad \left. + \sin^2 \theta_w \cos^2 \theta_w [\Pi_{QQ}(m_Z^2) - m_Z^2 \Pi'_{QQ}(0)] \right\}, \\ s_W^2 - s_*^2 &= \frac{e^2}{\sin^2 \theta_w m_Z^2} [\Pi_{33}(m_Z^2) - \Pi_{11}(m_W^2) - \sin^2 \theta_w \Pi_{3Q}(m_Z^2)]. \end{aligned} \quad (21.135)$$

If indeed the ultraviolet divergences of the vacuum polarization integrals have the structure of (21.133), then the divergent part of each expression in brackets in (21.135) vanishes, and the weak interaction gives definite, finite predictions for the differences of s_*^2 , s_W^2 , and $\sin^2 \theta_0$.

Computation of Vacuum Polarization Amplitudes

We can verify the divergence structure (21.133) by computing the vacuum polarization diagrams for t and b quarks explicitly. Rather than computing these one by one, it is easiest to compute, once and for all, the most general fermionic vacuum polarization amplitudes, and then to recover the amplitudes required in the previous paragraph as special cases of these.

Consider, then, the two vacuum polarization amplitudes shown in Fig. 12.13. The diagrams are built from two fermion propagators with different masses m_1 and m_2 , linked by left- or right-handed currents. We call the vacuum polarization amplitude with two left-handed currents $\Pi_{LL}^{\mu\nu}(q)$, and that with one left and one right-handed current $\Pi_{LR}^{\mu\nu}(q)$. Since the vacuum polarizations depend on only one momentum and two vector indices, there is no way that they can contain an invariant involving $\epsilon^{\mu\nu\rho\sigma}$. Thus, the amplitudes with other combinations of currents are related to these by

$$\Pi_{RR}^{\mu\nu}(q) = \Pi_{LL}^{\mu\nu}(q), \quad \Pi_{RL}^{\mu\nu}(q) = \Pi_{LR}^{\mu\nu}(q). \quad (21.136)$$

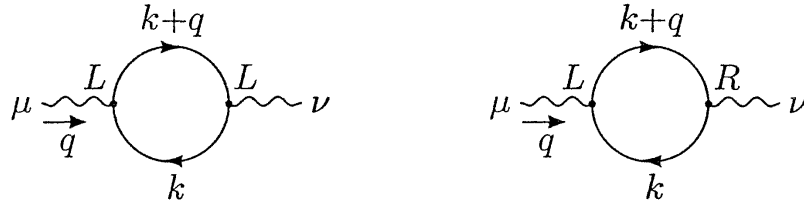


Figure 21.13. Elementary vacuum polarization amplitudes of fermionic currents.

In addition, there is no difficulty in regularizing these diagrams using dimensional regularization with an anticommuting γ^5 , the regularization prescription we endorsed at the end of Section 19.4. The vacuum polarization of a vector current is reconstructed as

$$\Pi_{VL}^{\mu\nu}(q) = \Pi_{LL}^{\mu\nu}(q) + \Pi_{RL}^{\mu\nu}(q). \quad (21.137)$$

The vacuum polarization of purely left-handed currents is given by

$$\begin{aligned} \text{---} \text{---} \text{---} \text{---} \text{---} &= (-1) \int \frac{d^4 k}{(2\pi)^4} \text{tr} \left[(i\gamma^\mu) \left(\frac{1-\gamma^5}{2} \right) \frac{i(k+m_1)}{k^2 - m_1^2} \right. \\ &\quad \left. \cdot (i\gamma^\nu) \left(\frac{1-\gamma^5}{2} \right) \frac{i(k+q+m_2)}{(k+q)^2 - m_2^2} \right] \\ &= - \int \frac{d^4 k}{(2\pi)^4} \text{tr} \left[\gamma^\mu k \gamma^\nu (k+q) \left(\frac{1+\gamma^5}{2} \right) \right] \cdot \frac{1}{(k^2 - m_1^2)((k+q)^2 - m_2^2)}. \end{aligned} \quad (21.138)$$

The prefactor (-1) comes from the fermion loop. There is no possible tensor structure antisymmetric in μ and ν , so we can now drop the γ^5 term. From here, the calculation proceeds as in Section 7.5. We combine denominators using

$$\frac{1}{(k^2 - m_1^2)((k+q)^2 - m_2^2)} = \int_0^1 dx \frac{1}{(\ell^2 - \Delta)^2}, \quad (21.139)$$

where

$$\ell = k + xq, \quad \Delta = xm_2^2 + (1-x)m_1^2 - x(1-x)q^2. \quad (21.140)$$

Then, integrating with dimensional regularization and following the steps leading to Eq. (7.90), we find

$$\begin{aligned} \text{---} \text{---} \text{---} \text{---} \text{---} &= - \frac{4i}{(4\pi)^{d/2}} \int_0^1 dx \frac{\Gamma(2-\frac{d}{2})}{\Delta^{2-d/2}} \left[g^{\mu\nu} (x(1-x)q^2 \right. \\ &\quad \left. - \frac{1}{2}(xm_2^2 + (1-x)m_1^2)) - x(1-x)q^\mu q^\nu \right]. \end{aligned} \quad (21.141)$$

Notice that both $\Pi_{LL}^{\mu\nu}$ and its first derivative with respect to q^2 are logarithmically divergent.

The vacuum polarization amplitude $\Pi_{LR}^{\mu\nu}$ can be obtained in a very similar fashion. From the Feynman rules,

$$\begin{aligned}
 \text{Diagram: } & \text{A loop diagram with two external lines labeled } L \text{ and } R. \text{ The loop is oriented clockwise.} \\
 & = (-1) \int \frac{d^4 k}{(2\pi)^4} \text{tr} \left[(i\gamma^\mu) \left(\frac{1-\gamma^5}{2} \right) \frac{i(k+m_1)}{k^2 - m_1^2} \right. \\
 & \quad \left. \cdot (i\gamma^\nu) \left(\frac{1+\gamma^5}{2} \right) \frac{i(k+q+m_2)}{(k+q)^2 - m_2^2} \right] \\
 & = - \int \frac{d^4 k}{(2\pi)^4} \text{tr} \left[\gamma^\mu m_1 \gamma^\nu m_2 \left(\frac{1+\gamma^5}{2} \right) \right] \frac{1}{(k^2 - m_1^2)((k+q)^2 - m_2^2)}. \tag{21.142}
 \end{aligned}$$

From here, the same manipulations as in the previous paragraph lead to

$$\text{Diagram: } = -\frac{2i}{(4\pi)^{d/2}} \int_0^1 dx \frac{\Gamma(2-\frac{d}{2})}{\Delta^{2-d/2}} [g^{\mu\nu} m_1 m_2]. \tag{21.143}$$

As a check, we can use (21.141), (21.143), and (21.136), setting $m_1 = m_2 = m$, to assemble the QED vacuum polarization of vector currents. We find

$$\begin{aligned}
 \Pi_{VV}^{\mu\nu}(q) &= e^2 [\Pi_{LL}^{\mu\nu} + \Pi_{LR}^{\mu\nu} + \Pi_{RL}^{\mu\nu} + \Pi_{RR}^{\mu\nu}] \\
 &= \frac{-8ie^2}{(4\pi)^{d/2}} \int_0^1 dx \frac{\Gamma(2-\frac{d}{2})}{\Delta^{2-d/2}} [x(1-x)q^2 g^{\mu\nu} - x(1-x)q^\mu q^\nu], \tag{21.144}
 \end{aligned}$$

where now $\Delta = m^2 - x(1-x)q^2$. This coincides precisely with our result from Section 7.5.

As we argued below (21.115), only the terms in the vacuum polarization amplitudes proportional to $g^{\mu\nu}$ will enter our expressions for weak-interaction radiative corrections. Thus, we can summarize the calculation of the basic vacuum polarization amplitudes by quoting the results for this leading form factor:

$$\begin{aligned}
 \Pi_{LL}(q^2) &= \Pi_{RR}(q^2) = -\frac{4}{(4\pi)^{d/2}} \int_0^1 dx \frac{\Gamma(2-\frac{d}{2})}{\Delta^{2-d/2}} [x(1-x)q^2 \\
 & \quad - \frac{1}{2}(xm_2^2 + (1-x)m_1^2)]; \\
 \Pi_{LR}(q^2) &= \Pi_{RL}(q^2) = -\frac{2}{(4\pi)^{d/2}} \int_0^1 dx \frac{\Gamma(2-\frac{d}{2})}{\Delta^{2-d/2}} [m_1 m_2]. \tag{21.145}
 \end{aligned}$$

From these terms, we can assemble any desired vacuum polarization of t and b quarks in the weak-interaction gauge theory. To make use of these expressions more easily, we will expand the quantities (21.145) in the limit $d \rightarrow 4$. If we set $\epsilon = 4 - d$, the integrands of the expressions above simplify according to

$$\frac{1}{(4\pi)^{d/2}} \frac{\Gamma(2-\frac{d}{2})}{\Delta^{2-d/2}} \rightarrow \frac{1}{(4\pi)^2} \left[\frac{2}{\epsilon} - \gamma + \log(4\pi) - \log \Delta \right]. \quad (21.146)$$

Let

$$E = \frac{2}{\epsilon} - \gamma + \log(4\pi) - \log(M^2), \quad (21.147)$$

where M is an arbitrary subtraction scale. It is useful to define

$$\begin{aligned} b_0(12X) &\equiv b_0(m_1^2, m_2^2, q_X^2) = \int_0^1 dx \log(\Delta(m_1^2, m_2^2, q_X^2)/M^2), \\ b_1(12X) &\equiv b_1(m_1^2, m_2^2, q_X^2) = \int_0^1 dx x \log(\Delta(m_1^2, m_2^2, q_X^2)/M^2), \\ b_2(12X) &\equiv b_2(m_1^2, m_2^2, q_X^2) = \int_0^1 dx x(1-x) \log(\Delta(m_1^2, m_2^2, q_X^2)/M^2). \end{aligned} \quad (21.148)$$

The abbreviated notation will prove useful below. In (21.148), X labels a momentum scale; we will need $q_X = 0, m_W, m_Z$. Note that for equal masses,

$$b_1(11X) = \frac{1}{2}b_0(11X). \quad (21.149)$$

With this notation,

$$\begin{aligned} \Pi_{LL}(q_X^2) &= -\frac{4}{(4\pi)^2} \left[\left(\frac{1}{6}q_X^2 - \frac{1}{4}(m_1^2 + m_2^2) \right) E - q_X^2 b_2(12X) \right. \\ &\quad \left. + \frac{1}{2}(m_2^2 b_1(12X) + m_1^2 b_1(21X)) \right] \end{aligned} \quad (21.150)$$

and

$$\Pi_{LR}(q_X^2) = -\frac{2}{(4\pi)^2} [m_1 m_2 E - m_1 m_2 b_0(12X)]. \quad (21.151)$$

We can now reconstruct all of the specific vacuum polarization amplitudes that appear in Eq. (21.135) in terms of divergences proportional to E and finite parts proportional to the b_i . The simplest is the expectation value of

electromagnetic currents, which is given in our present notation by

$$\begin{aligned}\Pi_{QQ}(q_X^2) = -3 \cdot \frac{8}{(4\pi)^2} & \left[\left(\frac{2}{3}\right)^2 \left(\frac{1}{6}q_X^2 E - q_X^2 b_2(ttX)\right) \right. \\ & \left. + \left(\frac{1}{3}\right)^2 \left(\frac{1}{6}q_X^2 E - q_X^2 b_2(bbX)\right) \right].\end{aligned}\quad (21.152)$$

The prefactor 3 is the trace over colors. As we expect from QED, (21.152) contains a divergence only in a term proportional to q_X^2 . The divergent parts of the other amplitudes are

$$\begin{aligned}\Pi_{33}(q_X^2) &= -\frac{12}{(4\pi)^2} \cdot \frac{1}{2} \left[\frac{1}{6}q_X^2 - \frac{1}{4}(m_t^2 + m_b^2) \right] E + \dots, \\ \Pi_{11}(q_X^2) &= -\frac{12}{(4\pi)^2} \cdot \frac{1}{2} \left[\frac{1}{6}q_X^2 - \frac{1}{4}(m_t^2 + m_b^2) \right] E + \dots, \\ \Pi_{3Q}(q_X^2) &= -\frac{12}{(4\pi)^2} \cdot \frac{1}{2} \left[\frac{1}{6}q_X^2 \right] E + \dots.\end{aligned}\quad (21.153)$$

These divergences indeed follow the pattern claimed in Eq. (21.133), and thus the predictions of the weak interaction gauge theory given in (21.135) are free of ultraviolet divergences.

The Effect of m_t

Using the notation we have developed, we can write the finite parts of the relations (21.135) in a compact form. The first relation becomes

$$\begin{aligned}s_*^2 - \sin^2 \theta_0 &= \frac{3\alpha}{\pi(\cos^2 \theta_w - \sin^2 \theta_w)} \left\{ \left(\frac{1}{4} - \frac{1}{3}\right) b_2(ttZ) + \left(\frac{1}{4} - \frac{1}{6}\right) b_2(bbZ) \right. \\ &\quad - \frac{1}{4} \left(\frac{m_t^2}{m_Z^2} [b_1(ttZ) - b_1(bt0)] + \frac{m_b^2}{m_Z^2} [b_1(bbZ) - b_1(tb0)] \right) \\ &\quad + 2 \sin^2 \theta_w \cos^2 \theta_w \left(\frac{4}{9} [b_2(ttZ) - b_2(tt0) - m_Z^2 b'_2(tt0)] \right. \\ &\quad \left. \left. + \frac{1}{9} [b_2(bbZ) - b_2(bb0) - m_Z^2 b'_2(bb0)] \right) \right\}.\end{aligned}\quad (21.154)$$

Similarly, the second relation becomes

$$\begin{aligned}s_W^2 - s_*^2 &= \frac{3\alpha}{\pi \sin^2 \theta_w} \left\{ \left(\frac{1}{4} - \frac{1}{3} \sin^2 \theta_w\right) b_2(ttZ) + \left(\frac{1}{4} - \frac{1}{6} \sin^2 \theta_w\right) b_2(bbZ) \right. \\ &\quad - \frac{1}{4} \cos^2 \theta_w b_2(tbW) \\ &\quad \left. - \frac{1}{4} \left(\frac{m_t^2}{m_Z^2} [b_1(ttZ) - b_1(btW)] + \frac{m_b^2}{m_Z^2} [b_1(bbZ) - b_1(tbW)] \right) \right\}.\end{aligned}\quad (21.155)$$

Though it is now straightforward to work out the complete expressions for the relations (21.154) and (21.155), we will content ourselves here with identifying the most important term in the limit in which the t quark mass becomes large. Notice that, in each of these expressions, there are terms with

coefficients proportional to m_t^2/m_Z^2 . These are easiest to understand within the simpler combination of vacuum polarization amplitudes

$$\begin{aligned}
\Pi_{11}(0) - \Pi_{33}(0) &= \frac{4}{(4\pi)^2} \frac{1}{4} \left[m_t^2 (b_1(tt0) - b_1(bt0)) + m_b^2 (b_1(bb0) - b_1(tb0)) \right] \\
&= \frac{3}{16\pi^2} \int_0^1 dx \left\{ xm_t^2 \log \frac{m_t^2}{M^2} + (1-x)m_b^2 \log \frac{m_b^2}{M^2} \right. \\
&\quad \left. - (xm_t^2 + (1-x)m_b^2) \log \frac{xm_t^2 + (1-x)m_b^2}{M^2} \right\} \\
&= -\frac{3}{16\pi^2} \int_0^1 dx \left\{ xm_t^2 \log \frac{xm_t^2 + (1-x)m_b^2}{m_t^2} + \mathcal{O}(m_b^2) \right\} \\
&= \frac{3}{16\pi^2} \cdot \frac{1}{4} m_t^2 + \mathcal{O}(m_b^2) \tag{21.156}
\end{aligned}$$

for $m_t \gg m_b$. If m_t is also much greater than m_Z , one can find a contribution proportional to m_t^2/m_Z^2 in each of the relations (21.154), (21.155) by replacing the argument $q_X^2 = m_Z^2$ with $q_X^2 = 0$, using (21.156), and ignoring all other contributions. One can show, by detailed examination of (21.154) and (21.155), that this procedure gives the complete leading term in m_t . The result is

$$\begin{aligned}
s_*^2 - \sin^2 \theta_0 &= -\frac{3\alpha}{16\pi(\cos^2 \theta_w - \sin^2 \theta_w)} \frac{m_t^2}{m_Z^2} + \dots, \\
s_W^2 - s_*^2 &= -\frac{3\alpha}{16\pi \sin^2 \theta_w} \frac{m_t^2}{m_Z^2} + \dots, \tag{21.157}
\end{aligned}$$

where the omitted terms are of order α with no enhancement.

The enhancement factor m_t^2/m_Z^2 is exactly the one that we found in our study of top quark decay in Section 21.2. It reflects the fact that some electroweak couplings of the top quark are effectively proportional to λ_t , the top quark coupling to the Higgs sector, instead of simply to the weak interaction coupling g .

The complete numerical evaluation of the formulae for s_*^2 and s_W^2 is shown in Fig. 21.14. To compare the results of this section to experiment, we have included, in addition to the top quark effect, the m_t -independent one-loop corrections from loops containing W and Z bosons and light quarks and leptons. In the figure, the predictions are compared to the value of s_*^2 obtained from the measurement of the Z^0 polarization and forward-backward asymmetries and the value of s_W^2 obtained from measurement of the W boson mass.

According to the figure, the weak interaction gauge theory requires the top quark mass radiative correction (or a similar radiative correction from some other heavy particle) for its consistency with experiment. The top quark is predicted to have a mass approximately equal to 170 GeV. A recent analysis

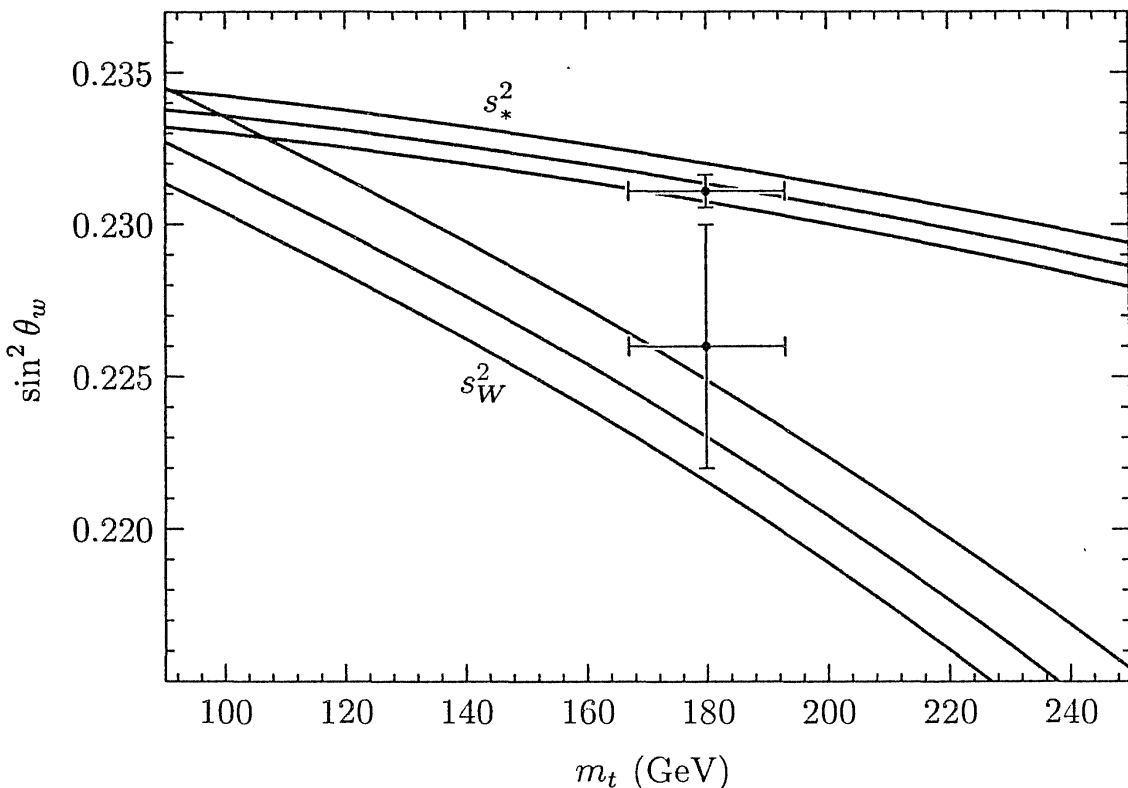


Figure 21.14. Dependence of s_*^2 and s_W^2 on the top quark mass, for fixed α , G_F , m_Z . The three curves in each group correspond to three different values of the Higgs boson mass: 100, 300, 1000 GeV from bottom to top. The curves are compared to values of s_*^2 and s_W^2 , taken from the article of Langacker and Erler quoted in Table 20.1, and the CDF/D0 value of the top quark mass given in Eq. (21.159).

of all neutral current weak interaction data has given the prediction[†]

$$m_t = 169 \pm 24 \text{ GeV.} \quad (21.158)$$

Just as this book was being completed, the CDF and D0 experiments at Fermilab announced the observation of the production of top quark pairs in proton-antiproton scattering. From kinematic fits to events believed to contain top quarks, these experiments reported[‡]

$$m_t = 180 \pm 13 \text{ GeV.} \quad (21.159)$$

The discovery of the top quark in just the range required by precision electroweak measurements is quite remarkable. We can only conclude that, in the domain of weak interactions as well as those of electromagnetic, strong, and scalar interactions that we have studied earlier, the fluctuations predicted by quantum field theory make their imprint on the phenomena of Nature.

[†]P. Langacker and J. Erler, in *Review of Particle Properties*, *Phys. Rev. D* **50**, 1304 (1994).

[‡]F. Abe, et. al., *Phys. Rev. Lett.* **74**, 2626 (1995); S. Abachi, et. al., *Phys. Rev. Lett.* **74**, 2632 (1995).

Problems

21.1 Weak-interaction contributions to the muon $g - 2$. The GWS model of the weak interactions leads to two new contributions to the anomalous magnetic moments of the leptons. Because these contributions are proportional to $G_F m_\ell^2$, they are extremely small for the electron, but for the muon they might possibly be observable. Both contributions are larger than the contribution of the Higgs boson discussed in Problem 6.3.

- (a) Consider first the contribution to the muon electromagnetic vertex function that involves a W -neutrino loop diagram. In the R_ξ gauges, this diagram is accompanied by diagrams in which W propagators are replaced by propagators for Goldstone bosons. Compute the sum of these diagrams in the Feynman-'t Hooft gauge and show that, in the limit $m_W \gg m_\mu$, they contribute the following term to the anomalous magnetic moment of the muon:

$$a_\mu(\nu) = \frac{G_F m_\mu^2}{8\pi^2 \sqrt{2}} \cdot \frac{10}{3}.$$

- (b) Repeat the calculation of part (a) in a general R_ξ gauge. Show explicitly that the result of part (a) is independent of ξ .
- (c) A second new contribution is that from a Z -muon loop diagram and the corresponding diagram with the Z replaced by a Goldstone boson. Show that these diagrams contribute

$$a_\mu(Z) = -\frac{G_F m_\mu^2}{8\pi^2 \sqrt{2}} \cdot \left(\frac{4}{3} + \frac{8}{3} \sin^2 \theta_w - \frac{16}{3} \sin^4 \theta_w \right).$$

21.2 Complete analysis of $e^+ e^- \rightarrow W^+ W^-$.

- (a) Using explicit polarization vectors, work out the amplitudes for $e^+ e^- \rightarrow W^+ W^-$ from left- and right-handed electrons to states in which the W^+ and W^- have definite helicity. For the cases in which both W bosons have longitudinal polarization, verify that Eq. (21.99) gives the correct high-energy limit for right-handed electrons, and verify the complete expression (21.108) for left-handed electrons. For the cases in which one W is longitudinally polarized and the second is transversely polarized, show that the individual diagrams give contributions to the amplitudes that grow like \sqrt{s} , but that the complete amplitudes fall as $1/\sqrt{s}$.
- (b) Show that the contributions to $e_L^- e_R^+ \rightarrow W^- W^+$ found in part (a) reproduce Fig. 21.10, and that the differential cross section for $e_R^- e_L^+ \rightarrow W^- W^+$ is about 30 times smaller. How many of the qualitative features of the figure can you understand physically?

21.3 Cross section for $d\bar{u} \rightarrow W^- \gamma$.

Compute the amplitudes for $d\bar{u} \rightarrow W^- \gamma$ for the various possible initial and final helicities. Ignore the quark masses. In this approximation, only the annihilation amplitude from $d_L \bar{u}_R$ is nonzero. Show that the scattering amplitudes for all final helicity combinations vanish at $\cos \theta = -1/3$, where θ is the scattering angle in the center-of-mass system. Compute the differential cross section as a function of $\cos \theta$.

21.4 Dependence of radiative corrections on the Higgs boson mass.

- (a) Consider the contributions to weak-interaction radiative corrections involving the physical Higgs boson h^0 of the GWS model. The couplings of the h^0 were discussed near the end of Section 20.2. Show that, if we ignore terms proportional to the masses of light fermions, the Higgs boson contributes one-loop corrections to the processes considered in Section 21.3 only through vacuum polarization diagrams. It follows that the contributions to vacuum polarization amplitudes that depend on the Higgs boson mass are gauge invariant.
- (b) Draw the vacuum polarization diagrams in Feynman-'t Hooft gauge that involve the Higgs boson, and compute the dependence of the various vacuum polarization amplitudes on the Higgs boson mass m_h .
- (c) Show that, for $m_h \gg m_W$, the natural relations discussed in Section 21.3 receive corrections

$$s_*^2 - s_0^2 = \frac{\alpha}{\cos^2 \theta_w - \sin^2 \theta_w} \frac{(1 + 9 \sin^2 \theta_w)}{48\pi} \log \frac{m_h^2}{m_W^2},$$

$$s_W^2 - s_*^2 = \alpha \frac{5}{24\pi} \log \frac{m_h^2}{m_W^2}.$$

The effect of varying m_h is displayed in Fig. 21.14 and is included as a theoretical uncertainty in the prediction (21.158). More accurate experiments might allow one to predict m_h from its effect on electroweak radiative corrections.

Decays of the Higgs Boson

At the end of Section 20.2, we discussed the mystery of the origin of spontaneous symmetry breaking in the weak interactions. The simplest hypothesis is that the $SU(2) \times U(1)$ gauge symmetry of the weak interactions is broken by the expectation value of a two-component scalar field ϕ . However, since we have almost no experimental information about the mechanism of this symmetry breaking, many other possibilities can be suggested.

Eventually, this problem should be resolved by experimental observation of the particles associated with the symmetry breaking. To form incisive experimental tests, we should compute the properties expected for these particles. We saw in Section 20.2 that, if the symmetry is indeed broken by a single scalar field ϕ , the symmetry-breaking sector contributes only one new particle, a scalar h^0 called the Higgs boson. The mass m_h of this particle is unknown. However, the couplings of the h^0 to known fermions and bosons are completely determined by the masses of those particles and the weak interaction coupling constants. Thus, it is possible to compute the amplitudes for production and decay of the h^0 in some detail. More complicated models of $SU(2) \times U(1)$ symmetry breaking typically contain one or more particles that share some properties with the h^0 . Thus, this study is a useful starting point for the more general analysis of experimental tests of these models.

In this Final Project you will compute the amplitudes for the Higgs boson h^0 to decay to pairs of quarks, leptons, and gauge bosons. The computations beautifully illustrate the working of perturbation theory for non-Abelian gauge fields. Those decays of the Higgs boson that involve quarks and gluons bring in aspects of QCD. Thus, this exercise reviews all of the important technical methods of Part III. Except for a question raised at the end of part (a), the problem relies only on material from unstarred sections of Part III. The material in Chapter 20 plays an essential role. Material from Chapter 21 enters the analysis only in parts (b) and (f), and the other parts of the problem (except for the final summary in part (h)) do not rely on these. If you have studied Section 19.5, you will have some additional insight into the results of parts (c) and (f), but this insight is not necessary to work the problem.

Consider, then, the minimal form of the Glashow-Weinberg-Salam electroweak theory with one Higgs scalar field ϕ . The physical Higgs boson h^0 of

this theory was discussed in Section 20.2, and we listed there the couplings of this particle to quarks, leptons, and gauge bosons. You can now use that information to compute the amplitudes for the various possible decays of the h^0 as a function of its mass m_h . You will discover that the decay pattern has a complicated dependence on the mass of the Higgs boson, with different decay modes dominating in different mass ranges. The dependences of the various decay rates on m_h illustrate many aspects of the physics of gauge theories that we have discussed in Part III.

In working this exercise, you should consider m_h as a free parameter. For the other parameters of weak-interaction theory, you might use the following values: $m_b = 5$ GeV, $m_t = 175$ GeV, $m_W = 80$ GeV, $m_Z = 91$ GeV, $\sin^2 \theta_w = 0.23$, $\alpha_s(m_Z) = 0.12$.

- (a) Compute first the rate for $h^0 \rightarrow f\bar{f}$, where f is a quark or lepton of the standard model. After a completely trivial computation, you should find

$$\Gamma(h^0 \rightarrow f\bar{f}) = \left(\frac{\alpha m_h}{8 \sin^2 \theta_w} \right) \cdot \frac{m_f^2}{m_W^2} \left(1 - \frac{4m_f^2}{m_h^2} \right)^{3/2} \cdot N_c(f),$$

where $N_c(f) = 1$ for leptons, 3 for quarks. If you have studied Chapter 18, you might improve this result for the case in which the fermion f is a quark, by computing the leading-log QCD corrections for the case $m_h \gg m_q$. Remember that the quark mass m_q is determined at the quark threshold $M^2 \sim m_q^2$.

- (b) If $m_h > 2m_W$, the Higgs boson can decay to W^+W^- ; if it is just a bit heavier, it can also decay to Z^0Z^0 . Compute the decay widths to these final states. You can check your result in the following way: If $m_h \gg m_W$, the dominant contribution to the decay comes from production of longitudinally polarized W or Z bosons, and this contribution can be estimated as follows:

$$\Gamma(h^0 \rightarrow W^+W^-) \approx \Gamma(h^0 \rightarrow \phi^+\phi^-), \quad \Gamma(h^0 \rightarrow Z^0Z^0) \approx \Gamma(h^0 \rightarrow \phi^3\phi^3),$$

where ϕ^\pm, ϕ^3 are the Goldstone bosons of the Higgs sector and the quantities on the right-hand sides of these relations are computed in the *un-gauged* Higgs theory. Explain why this statement should be true, and verify it explicitly.

- (c) The third important decay mode of the Higgs is the decay to 2 gluons. The amplitude for this decay is generated by diagrams involving quark loops. Compute these diagrams, using dimensional regularization. The diagrams will be finite, but nevertheless there is a subtle contribution which apparently depends on the regulator. Check that you have computed the amplitude correctly by verifying that it is gauge invariant. Then square the amplitude and construct the decay rate. You should find

$$\Gamma(h^0 \rightarrow 2g) = \left(\frac{\alpha m_h}{8 \sin^2 \theta_w} \right) \cdot \frac{m_h^2}{m_W^2} \cdot \frac{\alpha_s^2}{9\pi^2} \cdot \left| \sum_q I\left(\frac{m_h^2}{m_q^2}\right) \right|^2,$$

where the sum runs over all quark species and $I(m_h^2/m_q^2)$ is a form factor with the property that $I(x) \rightarrow 1$ as $x \rightarrow 0$ and $I(x) \rightarrow 0$ as $x \rightarrow \infty$. This property implies that the dominant contribution to the decay rate comes from very heavy quarks. You need not evaluate $I(x)$ explicitly at this stage; just leave it in the form of a Feynman parameter integral.

- (d) The existence of the process $h^0 \rightarrow 2g$ implies the existence of the inverse process $g + g \rightarrow h^0$, which is a mechanism for production of Higgs bosons in proton-proton collisions. Using the parton model, derive a relation between the partial width $\Gamma(h^0 \rightarrow 2g)$ and the total cross section for $pp \rightarrow h^0 + X$. Compute this cross section numerically (in nanobarns) for a 30 GeV Higgs for pp collisions of center of mass energy 1–40 TeV. (1 TeV = 10^3 GeV.) For the purposes of this problem set (though this is not actually a good approximation) you may ignore the Q^2 dependence of the gluon distribution function and take simply

$$f_g(x) = 8 \cdot \frac{1}{x} (1-x)^7.$$

You may also set $I(m_h^2/m_t^2) = 1$; this is correct to about 10%.

- (e) The final decay mode that you should consider is $h^0 \rightarrow 2\gamma$. Consider first the contribution from the loop diagrams involving quarks and leptons. Show that the result is simply expressed in terms of the form factor $I(m_h^2/m^2)$ that you derived in part (c).
- (f) Next, compute the contribution to this decay amplitude from the loop diagram involving W bosons, and the various diagrams one must add to this to obtain a gauge-invariant result. It is easiest to work in Feynman-‘t Hooft gauge. Add this contribution to that of very heavy quarks and leptons, each with electric charge Q_f . Your result should reduce to the following expression in the limit $m_h \ll m_W$:

$$\Gamma(h^0 \rightarrow 2\gamma) = \left(\frac{\alpha m_h}{8 \sin^2 \theta_w} \right) \cdot \frac{m_h^2}{m_W^2} \cdot \frac{\alpha^2}{18\pi^2} \cdot \left| \sum_f Q_f^2 N_c(f) - \frac{21}{4} \right|^2.$$

- (g) Now work out the detailed behavior of the form factor $I(x)$ defined in part (c). Reduce your expression from part (c) to a one-parameter integral, then evaluate this integral numerically. Plot $I(m_h^2/m_t^2)$ over the range 50 GeV $< m_h <$ 500 GeV, and compute the decay width $\Gamma(h^0 \rightarrow 2g)$ numerically (in keV) over this range. The computation of part (f) introduces an addition form factor; compute this function in the same way.
- (h) Finally, put together all the pieces. Find the branching fraction of the h^0 into each of its five major decay modes $b\bar{b}$, $t\bar{t}$, gg , W^+W^- , Z^0Z^0 , for Higgs bosons of mass 50 GeV – 500 GeV.

Epilogue

Quantum Field Theory at the Frontier

In this textbook we have surveyed the most important ideas of quantum field theory. Working from the basic concepts that come from fusing relativity, quantum mechanics, and fields, we have built an elaborate structure, which includes such remarkable elements as coupling constant renormalization and non-Abelian gauge fields. We have seen at many points that the strange and abstract elements of this structure actually intersect with observation and even produce explanations for unexpected aspects of the behavior of elementary particles.

In the course of our study, we have arrived at a complete theory of the strong, weak, and electromagnetic interactions of elementary particles. Each element of this theory has been described as a quantum field theory, and these quantum field theories have turned out to have very similar structure as gauge theories coupled to fermions. At various points in our discussion, we have noted that these theories have passed stringent quantitative experimental tests. We have not had space to describe the wide variety of experiments that contribute to our faith in these theories, but today almost all particle physicists consider this $SU(3) \times SU(2) \times U(1)$ gauge theory as established. In fact, most of these people refer to this theory condescendingly as ‘the standard model’.

Though the best data to support the standard model have come from experiments of the past five years, the ideas behind it are much older. Most of the theoretical developments described in this book were concluded in the 1970s, a generation removed from the current frontier of physics. But this does not mean that quantum field theory is irrelevant to that frontier, any more than quantum mechanics and electrodynamics have lost their relevance after many years of exploration. On the contrary, the theory of elementary particles—like other areas of physics that depend on quantum fluctuations in continua—still holds deep mysteries, and quantum field theory remains the principal tool for exploration of these questions.

In this final chapter, we will flash forward to the present day and discuss the relevance of quantum field theory to current questions in the physics of the fundamental interactions. We will present what are, in our view, the outstanding unsolved problems of elementary particle physics and describe how quantum field theory is being used to confront these problems. Many of

these applications involve aspects of quantum field theory that are beyond the scope of this book. These include the use of quantum field theory in the regime beyond the reach of perturbation theory and the use of quantum field theory to explore the special properties of theories with higher spin and local symmetry. In these areas our discussion will be mainly qualitative, but we will give references that provide points of entry into each of these subjects.

It should be obvious that our discussion in this final chapter will express our personal opinions and by no means represents the consensus of experts in quantum field theory. In addition, any collection of ‘current problems’ in a rapidly developing area of research should quickly become dated. In fact, we hope the readers of this book will quickly make this chapter obsolete by solving the problems that we highlight here.

22.1 Strong Strong Interactions

One paradoxical aspect of our discussion of the strong interactions is that all of our concrete results were obtained by assuming that these interactions are weak. At large momentum transfer, we argued, this assumption is actually valid due to asymptotic freedom. Still, it is uncomfortable that we have left the most obvious questions about strongly interacting particles—for example, their masses and low-energy interactions—in a mysterious regime excluded from our analysis.

To work with QCD in the region where the strong interactions are strong, we need to answer three questions: First, how do we describe the forces that bind quarks together into hadrons? Second, what is an appropriate description of the quark-antiquark and three-quark systems bound by those forces? And finally, how do we compute scattering amplitudes and matrix elements of currents using these bound states?

At this moment, there is no derivation of the complete force between quarks from the QCD Lagrangian. Explicit calculations can be done only in the limits of weak and strong coupling. In the weak-coupling limit, the result is a Coulomb potential with an asymptotically free coupling constant. The strong coupling limit, on the other hand, gives a linear potential which confines color in the way that we described, but did not derive, at the end of Section 17.1. The derivation of this result is quite unusual and brings in a new set of mathematical methods.

So far in this book, we have not discussed a strong coupling approximation to a quantum field theory. There is a simple reason for this: In a quantum field theory in which the coupling g^2 is very large, the elementary particles or their bound states typically acquire masses that grow with g^2 . For $g^2 \rightarrow \infty$, these masses become comparable to the cutoff Λ and the field theory ceases to have a local continuum description.

Wilson proposed to solve this problem in a radical way, by replacing spacetime with a lattice of discretely spaced points. Such a lattice is easiest

to visualize in Euclidean spacetime, and so we can use a functional integral over fields on a lattice to approximate Euclidean Green's functions. Such a theory can have a well-defined strong coupling limit. A theory of this type is very similar to a lattice model of a magnetic system.

In fact, we can understand this construction of a quantum field theory by using the concepts of Chapters 13. A lattice theory with fluctuating spin variables at each lattice site is described in the large by a quantum field theory of scalar fields with the symmetry of the underlying spin variables. Typically, the strong-coupling limit of the quantum field theory corresponds to the high-temperature limit of the magnet, in which the correlation length is much smaller than the lattice spacing. Decreasing the coupling constant corresponds to decreasing the temperature. Eventually, the coupling constant comes close to a fixed point of the renormalization group, and one can use this fixed point to define a limit of the lattice functional integral in which the lattice spacing is taken to zero.

To build a lattice model of the strong interactions, one needs to find a set of variables on the discrete lattice that correspond in the large to non-Abelian gauge fields. Wilson proposed that the fundamental variables for such a theory should be the line elements from one lattice vertex v_1 to a neighboring vertex v_2 ,

$$U(v_2, v_1) = P \exp \left[ig \int dx^\mu A_\mu^a t^a \right]. \quad (22.1)$$

To construct the lattice gauge theory with gauge group G , one should integrate over a finite group transformation U for each link of the lattice. Taking a product of these U matrices around a closed path, one can construct gauge-invariant observables, just as we did in Section 15.3. An appropriate Lagrangian can also be constructed as a sum of gauge-invariant products of the U matrices about elementary closed loops of the lattice.*

In a spin system, the defining property of the high-temperature phase is the exponential decay of correlations

$$\langle \vec{s}(0) \cdot \vec{s}(x) \rangle \sim \exp[-|x|/\xi] \quad (22.2)$$

as $|x| \rightarrow \infty$. The analogous property of the gauge-invariant correlation function of U matrices around a closed path P is

$$\left\langle \prod_P U \right\rangle \sim \exp[-A/\xi^2], \quad (22.3)$$

where A is the area spanned by the path. This behavior is in fact seen explicitly in the expansion of Wilson's lattice gauge theory for strong coupling. A pair of color sources that stand a distance R apart for a Euclidean time T are represented by a large rectangular loop of width R and length T . For such a

*This construction was introduced by K. Wilson, *Phys. Rev. D* 10, 2445 (1974). The construction is described pedagogically in M. Creutz, *Quarks, Gluons, and Lattices* (Cambridge University Press, Cambridge, 1983).

loop, we can compare the result (22.3) to the expression for the energy of an excited state in Euclidean time,

$$\langle \exp[-H_E T] \rangle \sim \exp[-RT/\xi^2]. \quad (22.4)$$

Then we see that static sources of gauge charge, in the strong-coupling limit, are attracted to one another by a potential energy

$$V(R) \sim R/\xi^2 \quad (22.5)$$

at sufficiently large R . Similarly, when one introduces dynamical quarks into a lattice gauge theory and studies their properties in the strong-coupling limit, configurations with large separation of color sources are suppressed in the Euclidean functional integral by factors of the form of (22.3). The strong-coupling limit then predicts the permanent confinement of quarks into color-singlet bound states.

The argument we have just given applies equally well to gauge theories based on Abelian or non-Abelian symmetry groups. But non-Abelian gauge theories have the important additional property of asymptotic freedom. In this context, that implies that a theory with weak coupling at short distances flows to a theory with strong coupling at large distances. If we imagine integrating out short-distance degrees of freedom as we described in Section 12.1, and if there is no zero of the β function or other barrier to the renormalization group flow, we should eventually arrive at an effective theory for which the strong-coupling expansion is a good approximation. Thus, in the particular case of non-Abelian gauge theories, asymptotic freedom allows us to connect a short-distance picture based on free quarks and gluons to a large-distance picture based on color confinement.

It would be wonderful if the strong-coupling picture that we have described led to mathematical equations in continuum spacetime describing the motion of permanently confined quarks and antiquarks. Many authors have tried to write such equations by imagining the area suppression of the Wilson loop correlation function (22.3) to result from a physical surface that spans the loop. For the large rectangular loop associated with color sources, this surface can be interpreted physically as the lines of color electric flux that run from one source to the other (as in Fig. 17.1), swept out through Euclidean time. At one moment of Euclidean time, this surface can be idealized as an abstract one-dimensional excitation, often called a *string*. Unfortunately, the quantum properties of an idealized string turn out to be very complicated, since each small element of the string must be considered as an independent quantum degree of freedom. The only systems of string equations that have actually been solved have bizarre features, including unwanted massless particles. Up to now, no one has succeeded in writing an equation for the quark-confining string that is useful for quantitative calculations of quark bound states.[†]

[†]For one approach to color confinement from a picture involving Wilson loops and strings, see A. A. Migdal, *Phys. Repts.* **102**, 199 (1983).

However, the lattice regularization of a non-Abelian gauge theory suggests another approach to quantitative calculations in strong-interaction theory. By approximating QCD by a lattice gauge theory with a nonzero lattice spacing and a finite spacetime volume, we reduce the functional integral to a finite number of bounded integrations, that is, an integral over $SU(3)$ group matrices for each of the finite number of links in the lattice. A lattice of size, for example, 20^4 allows the lattice spacing to be smaller than the size of a hadron while the full size of the lattice is much larger than a hadronic radius. Then one can compute correlation functions by evaluating the integrals numerically, by the Monte Carlo method. Since the functional integral with a finite lattice spacing is related to the original functional integral with zero lattice spacing by integrating out short-distance degrees of freedom, the lattice approximation can be systematically improved by computing the short-distance effects perturbatively, using asymptotic freedom to justify a weak-coupling analysis.[‡]

This numerical method has now become the principal theoretical tool for quantitative calculations in hadron physics. This method currently gives the masses of the low-lying mesons and baryons to accuracies of 10–20%; it also allows the calculation of weak interaction matrix elements of hadrons at the 25% level. As computers become more powerful, this numerical method can be pushed to higher accuracy.

Eventually, it will be interesting to ask whether these nonperturbative numerical calculations are consistent with our precision knowledge of the perturbative region of QCD. At the time of this writing, the first such comparison has been made: We have listed in Table 17.1 a value of α_s from ψ and Υ spectroscopy. In this calculation, the experimentally determined masses of $\bar{c}c$ and $\bar{b}b$ bound states are compared to values computed numerically with lattice regularization. The comparison of these values gives the required bare coupling constant of the lattice theory, which can be converted to a value of $\alpha_s(m_Z)$ in the convention of the table. The resulting estimate for $\alpha_s(m_Z)$ does agree reasonably well with purely perturbative determinations.

What is the future of nonperturbative calculations in hadron physics? On the one hand, we expect to see further development of numerical lattice methods. These methods have hardly begun to address problems of hadron-hadron scattering and multiparticle matrix elements, and this seems an important direction for the future. In addition, these methods should eventually supply an engineering understanding of hadrons at the percent level or better. On the other hand, we hope also to see a quantitative continuum approach to hadron structure, in which dynamical quarks interact with some appropriate type of string degrees of freedom.

[‡]For an introduction to numerical lattice gauge theory, see *From Actions to Answers*, T. DeGrand and D. Toussaint, eds. (World Scientific, Singapore, 1990).

22.2 Grand Unification and its Paradoxes

If we put aside our questions about the low-energy, nonperturbative behavior of QCD, the $SU(3) \times SU(2) \times U(1)$ gauge theory gives an apparently complete description of elementary particle interactions at those energies that we have probed experimentally. But what happens beyond our current reach? Does this theory need modification, or could it continue to be valid at much higher energies?

The $SU(3) \times SU(2) \times U(1)$ gauge theory contains three independent gauge coupling constants, and the observed values of these couplings are larger for the larger components of the gauge group. This pattern can be explained by a bold hypothesis about the behavior of the gauge couplings at very high energy. If at some very large energy scale, these three couplings were equal, the values of the $SU(3)$ and $SU(2)$ couplings would increase at smaller momentum scales due to their asymptotically free renormalization group equations, while the value of the $U(1)$ coupling would decrease, resulting in the observed pattern of couplings at low energies. An even bolder hypothesis would be that the three gauge symmetries are subgroups of a single large symmetry group, which is spontaneously broken at very high energy scales. The simplest choice for this larger symmetry is $SU(5)$. In that theory, the coupling constants of $SU(3) \times SU(2) \times U(1)$ have the following relation to the underlying $SU(5)$ coupling at the scale of $SU(5)$ breaking:

$$g_5 = g_3 = g = \sqrt{\frac{5}{3}} g'. \quad (22.6)$$

The idea that the $SU(3) \times SU(2) \times U(1)$ gauge group is embedded in a larger simple group is known as *grand unification*; the particular choice of $SU(5)$ as the unifying group is due to Georgi and Glashow.* The observed quarks and leptons can be seen to fit neatly into an anomaly-free chiral representation of $SU(5)$; this embedding leads to a natural explanation of the fractional charges of quarks.[†]

Within this framework, we can extrapolate the values of the three coupling constants from the energy scale of m_Z upward. The result of this extrapolation is shown as the solid lines in Fig. 22.1. The coupling constants do come close together at very high energies, though they do not actually meet. The dashed lines in the figure show the evolution with a modified set of renormalization group equations, to be explained in Section 22.4; with this choice, the three couplings meet accurately within their current uncertainties. In any event, the evolution of coupling constants occurs on a logarithmic scale in energy, so grand unification cannot be achieved without assuming an enormous value—of order 10^{16} GeV—for the symmetry-breaking scale.

*H. Georgi and S. L. Glashow, *Phys. Rev. Lett.*, **32**, 438 (1974). The remarkable hubris of this paper makes it required reading for every student.

[†]For a pedagogical introduction to grand unification, see Ross (1984).

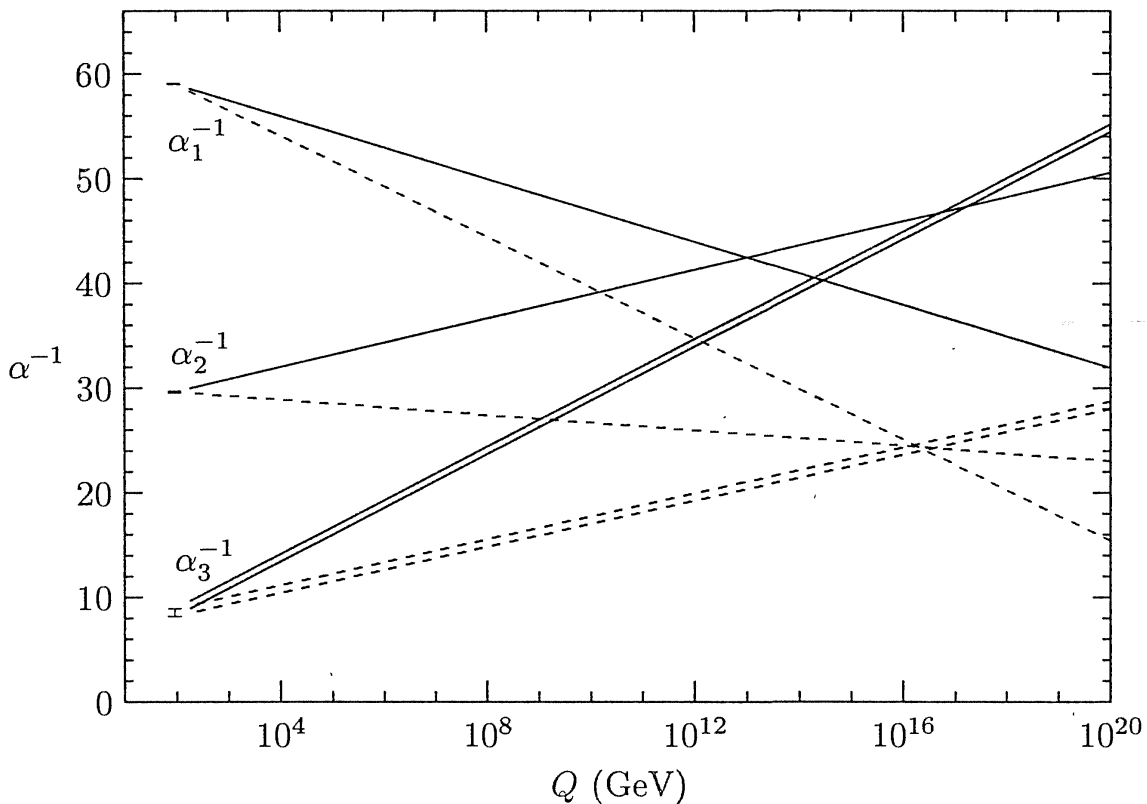


Figure 22.1. Extrapolation in energy of the coupling constants of the $SU(3) \times SU(2) \times U(1)$ gauge model, g_3 , g , and $\sqrt{5/3}g'$. The solid lines are plotted using the β functions corresponding to the known set of elementary particles; the dashed lines are plotted using the β functions corresponding to a supersymmetric multiplet of particles.

The idea of a grand unification at such enormous energies raises many difficult questions, but it also suggests a wonderful opportunity. There is another enormous energy scale in quantum field theory, the scale at which the gravitational attraction of elementary particles becomes comparable to their strong, weak, and electromagnetic interactions. Conventionally, one defines the *Planck scale* as the energy for which the gravitational interaction of particles becomes of order 1:

$$m_{\text{Planck}} = (G_N/\hbar c)^{-1/2} \sim 10^{19} \text{ GeV.} \quad (22.7)$$

However, already at energies of order 10^{18} GeV, the gravitational attraction of particles is comparable to the gauge force due to the vector bosons of a grand unified theory. Though this scale is still slightly higher than the scale at which the standard model coupling constants meet, it is not unreasonable to hope that grand unification is somehow related to the unification of gravity with the forces of elementary particle physics.

On the other hand, the introduction of this large scale into physics leads to a number of conceptual problems. The first of these problems, which one meets immediately upon suggesting this extension of the standard model, is the Higgs boson mass. In our discussion at the end of Section 20.2, we came to a somewhat ambiguous conclusion about the nature of the Higgs boson. As



a part of the gauge theory of weak interactions, we need some new sector that will cause the spontaneous breaking of $SU(2) \times U(1)$. This might be supplied by the vacuum expectation value of a scalar field, or by the more complicated dynamics of a new sector of particles. At this moment, we do not know which hypothesis is to be preferred.

If $SU(2) \times U(1)$ is broken by the vacuum expectation value of an elementary scalar field, that scalar field should be part of the grand unification. This leads to a serious conceptual problem. In order to produce a vacuum expectation value of the right size to give the observed W and Z boson masses, the Higgs scalar field must obtain a negative mass term, of the size

$$-\mu^2 \sim -(100 \text{ GeV})^2. \quad (22.8)$$

Unfortunately, the $(\text{mass})^2$ of a scalar field receives additive renormalizations. In a theory with cutoff scale Λ , μ^2 can be much smaller than Λ^2 only if the bare mass of the scalar field is of order $-\Lambda^2$, and this value is canceled down to $-\mu^2$ by radiative corrections. If we envision that our theory of Nature contains the very large scales of grand unification, we must take seriously the idea that the appropriate value to take for Λ in this discussion is 10^{16} GeV or larger. This seems to require dramatic and even bizarre cancellations in the renormalized value of μ^2 .

We met a situation of this type in the theory of phase transitions. At zero temperature, a ferromagnet typically has a spin expectation value of the order of the underlying atomic parameters. As the temperature is raised, or as some other variable in the system is changed, the magnetization decreases. Finally, by fine adjustment of the temperature, we can arrive at a situation where the system approaches a critical point. In the very near vicinity of this point, the expectation value of the spin field is much smaller than the value predicted from atomic parameters, and the system is described by an approximately massless continuum scalar field theory.

In statistical mechanics, this picture of the light scalar field makes sense because there is an experimenter sensitively adjusting a dial. In the theory of weak interactions, there is no one obviously making a fine adjustment that gives the $(\text{mass})^2$ of the Higgs boson a value 28 orders of magnitude or more below its natural value. Thus, it is a mystery why the Higgs boson mass should be so small compared to the grand unification scale. Particle physicists refer to this question as the *gauge hierarchy problem*.

How can one naturally arrange a Higgs field mass term to be so much smaller than the underlying mass scale of the fundamental interactions? One possible strategy would be to arrange for a symmetry of the fundamental Lagrangian that forbids the Higgs boson mass term and that is very weakly broken. This idea turns out to be very difficult to implement. To build a theory of this type, one would need to create a scalar field theory in which additive radiative corrections to the Higgs boson mass must cancel to any foreseeable

order in perturbation theory. But the Higgs mass term is very simple in form,

$$\Delta\mathcal{L} = \mu^2 |\phi|^2, \quad (22.9)$$

and it is hard to imagine any principle that would keep this term from being generated by radiative corrections. There is one proposal for a symmetry with this property, but it requires the introduction of a profound principle called *supersymmetry* that entails deep modifications of fundamental physics. In particular, it requires a large number of new elementary particles, some of which should have masses below 1000 GeV, within the reach of the next generation of accelerators. We will discuss this possibility further in Section 22.4.

In this discussion, the problem of the Higgs mass stemmed from the hypothesis that the Higgs boson was an elementary particle. An alternative viewpoint, already suggested at the end of Section 20.2, is that the Higgs boson is a composite state bound by a new set of interactions. This idea also leads to observable experimental consequences, since the mass scale of these new interactions must be close to the weak interaction mass scale. In the simplest theories of this type, the symmetry breaking of the Higgs sector is modeled on the dynamical chiral symmetry breaking of the strong interactions, which we discussed in Section 19.3. The new strong interactions required by the theory lead to a spectrum of new particles with masses of about 1000 GeV.[‡] Thus, the two conflicting hypotheses on the nature of the sector that breaks $SU(2) \times U(1)$ both lead to new phenomena observable at future accelerators, and possibly even at present ones.

Just as these two different theories of the Higgs sector present completely different answers to the question of why the weak-interaction symmetry $SU(2) \times U(1)$ should be spontaneously broken, they also imply completely different answers to the question of the origin of the quark and lepton masses. In a model in which the Higgs field is elementary, the quark and lepton masses are derived from the renormalizable couplings of fermions to the Higgs field. These couplings would presumably be part of the grand unification and could be predicted only by theories that made explicit reference to the grand unification scale. In principle, the knowledge of these couplings could give us clues as to the details of the grand unification. Even if the Higgs field is composite, we cannot avoid the fact that the generation of masses for the quarks and leptons requires the breaking of $SU(2) \times U(1)$. Thus, these mass terms must arise from couplings of the quarks and leptons to the Higgs sector of interactions. In this class of models, the interactions leading to the quark and lepton masses must arise at energies close to the scale of the Higgs sector strong interaction and may eventually be observable experimentally.

From either viewpoint, it is still mysterious why the spectrum of quarks

[‡]The properties of these models of the Higgs sector, known to specialists as *technicolor* models, are described in R. Kaul, *Rev. Mod. Phys.* **55**, 449 (1983) and K. D. Lane, in *The Building Blocks of Creation*, S. Raby, ed. (World Scientific, 1993).

and leptons covers 5 orders of magnitude, from the electron at 0.5 MeV to the top quark at 175 GeV. It is also not understood what gives rise to the pattern of quark mixings encoded in the CKM matrix and the magnitude of CP violation. Even with detailed confirmation of the standard model, these questions seem today very far from solution.

The enormous mass scale of grand unification can also enter one more physical quantity, one that poses an even greater paradox than that of the Higgs boson mass. When we first quantized a field in Section 2.3, we discovered that the energy density of the vacuum in free scalar field theory received an infinite positive contribution from the zero-point energies of the various modes of oscillation. With a cutoff scale Λ , this zero-point energy is given roughly by

$$\langle 0 | H | 0 \rangle \sim \Lambda^4. \quad (22.10)$$

At many other points in our discussion, we found similarly large contributions to the vacuum energy. The filling of the Dirac sea in the quantization of the free fermion theory led to a downward shift in the vacuum energy with a similar ultraviolet divergence. Spontaneous symmetry breaking gives a finite but still possibly large shift in the vacuum energy density,

$$\Delta \langle 0 | H | 0 \rangle \sim -cv^4, \quad (22.11)$$

with dimensionless c , for a field vacuum expectation value v . The spontaneous breaking of the weak interaction $SU(2) \times U(1)$ symmetry and of the strong interaction chiral symmetry both would be expected to shift the vacuum energy density in this way.

In elementary particle physics experiments, this shift of the vacuum energy is unobservable. Experimentally measured particle masses, for example, are energy differences between the vacuum and certain excited states of H , and the absolute vacuum energy cancels out in the calculation of these differences. However, there is a way that the absolute vacuum energy could potentially be observed, through the coupling of the vacuum energy to gravity. According to Einstein, the energy-momentum tensor of matter $\Theta^{\mu\nu}$ is the source of the gravitational field. A vacuum energy density $\langle 0 | H | 0 \rangle = \lambda$ contributes to this source a term

$$\Theta^{\mu\nu} = N(\Theta^{\mu\nu}) + \lambda g^{\mu\nu}, \quad (22.12)$$

where the first term on the right is subtracted to have zero vacuum expectation value. The vacuum energy term has the form of Einstein's cosmological constant and thus potentially affects the expansion of the universe.

In fact, measurements of the cosmological expansion exclude a large cosmological constant. The current limit is

$$\lambda < 10^{-29} \text{ g/cm}^3 \sim (10^{-11} \text{ GeV})^4. \quad (22.13)$$

We have no understanding of why λ is so much smaller than the vacuum energy shifts generated in the known phase transitions of particle physics, and so much again smaller than the underlying field zero-point energies. The

discrepancy in λ between the experimental bound (22.13) and naive intuition is 120 orders of magnitude! The solution to this problem may come from one of many sources. It may be that the formalism of the quantum field theory of gravity requires that the vacuum energy be subtracted from the energy-momentum tensor that appears in Einstein's equations of gravity. It may be that there is a new physical mechanism coming from particle physics or from gravity itself that sets the total vacuum energy to zero. Or it may be that the overall scale of energy-momentum is genuinely ambiguous and is set by a cosmological boundary condition. At this moment, all of these possibilities are just guesses. All we know for certain is that the unification of quantum field theory and gravity cannot be straightforward, that there is some important concept still missing from our current understanding.*

22.3 Exact Solutions in Quantum Field Theory

From the idea of grand unification, with its great promise and mystery, we turn to the study of model quantum field theories that are so simple that they can be solved exactly. Throughout this book, we have stressed the intrinsic complexity of quantum field theory and the importance of using perturbation theory as a replacement for exact knowledge. But there are a variety of quantum field theories for which exact solutions are known. In this section, we will describe some of these and review the insights we have gained from them.

In searching for exact solutions to quantum field theory models, there is no reason to restrict our attention to four-dimensional spacetime. In fact, we have seen examples of two-dimensional theories with similar complexity of renormalization and short-distance behavior. At the same time, these theories occupy a one-dimensional space, and their degrees of freedom can be visualized as links in a chain. This allows some powerful simplifications.

In our discussion of the axial anomaly in two dimensions in Section 19.1, we showed that the photon of two-dimensional massless QED becomes a massive boson. More detailed examination of this theory shows that this boson is a noninteracting particle. The theory is originally formulated in terms of fermions, interacting through Coulomb forces. However, it is possible to exactly rewrite the theory as a theory of a scalar field that creates and destroys fermion-antifermion pairs. Heuristically, a particle and an antiparticle moving down the light-cone in one-dimensional space do not separate and therefore comprise one bosonic degree of freedom. In a wide class of models, the bosonic theories rewritten in this way are free-field theories. A remarkable model of this type is the *Thirring model*,

$$\mathcal{L} = \bar{\psi} i \partial \psi - \frac{g}{2} \bar{\psi} \gamma^\mu \psi \bar{\psi} \gamma_\mu \psi, \quad (22.14)$$

*The cosmological constant problem and a variety of unsuccessful solutions are reviewed in S. Weinberg, *Rev. Mod. Phys.* **61**, 1 (1989).

in two dimensions. In this model, the replacement of the fermion field by a boson field leads to a free field theory. Using this field theory, one can compute correlation functions of fermion bilinears explicitly and show directly that these operators have anomalous dimensions. In renormalization-group language, the model contains a line of fixed points parametrized by the coupling constant g .[†]

A more general class of two-dimensional models can be solved by visualizing them in a Hamiltonian picture as a one-dimensional chain of coupled field operators. The prototype of this method is a problem in the statistical mechanics of magnets, the one-dimensional chain of coupled spins. Consider a long chain of N discrete sites, with a spin-1/2 system at each site. The Pauli sigma matrices σ_i act on the two-dimensional Hilbert space at the site i . The Hamiltonian for the spin chain is then

$$H = \sum_i (-J \sigma_i \cdot \sigma_{i+1}). \quad (22.15)$$

Since

$$\sigma_i \cdot \sigma_{i+1} = 2(\sigma_i^+ \sigma_{i+1}^- + \sigma_i^- \sigma_{i+1}^+) + \sigma_i^3 \sigma_{i+1}^3, \quad (22.16)$$

this Hamiltonian conserves the number of up spins. The state with all spins down is an eigenstate of the Hamiltonian, and the states with one spin up in a state of definite momentum are also eigenstates. In 1934, Bethe analyzed the problem of two spins up and computed their S -matrix. He then discovered an amazing fact, that by multiplying the S -matrices for the two-spin problem, he could find the exact eigenstates of the Hamiltonian for any number of spins up. By considering $N/2$ spins up, he found the ground state of the system. This technique, now known as *Bethe's ansatz*, has been used to solve a wide variety of one-dimensional problems in condensed matter physics and quantum field theory. For example, this technique has been used by Andrei and Lowenstein to solve the Gross-Neveu model presented in Problem 11.3 and to demonstrate that the spectrum of this model has the properties expected from asymptotic freedom.[‡]

Even where it is not possible to solve a model for all values of its parameters, it is sometimes possible to find exact information about two-dimensional models at points where they contain massless fields. It is well known that a variety of classical two-dimensional partial differential equations can be solved by exploiting techniques of complex variables. For example, the two-dimensional Laplace equation $\nabla^2 \phi = 0$ is invariant to conformal mappings $z \rightarrow w(z)$,

[†]For an introduction to these models, see S. Coleman, *Phys. Rev.* **D11**, 2088 (1975), *Ann. Phys.* **101**, 239 (1976).

[‡]For an introduction to Bethe's ansatz and its generalizations, see N. Andrei, K. Furuya, and J. H. Lowenstein, *Rev. Mod. Phys.* **55**, 331 (1983), L. D. Faddeev, in *Recent Advances in Field Theory and Statistical Mechanics*, J. B. Zuber and R. Stora, eds. (North-Holland, Amsterdam, 1984), and R. J. Baxter, *Exactly Solved Models in Statistical Mechanics* (Academic Press, London, 1982).

where $z = x + iy$. Two-dimensional quantum field theories with massless particles often have this conformal symmetry at the classical level, though generically it is anomalous. In special systems, however, these anomalies vanish and the quantum theory is invariant to conformal mapping. These theories typically contain operators with anomalous dimensions, indicating that each such theory is a new, nontrivial fixed point of the renormalization group. The conformal symmetry of the theory can be used to compute these anomalous dimensions.

As an example of this class of theories, consider the two-dimensional nonlinear sigma model in which the basic field is not a unit vector, as we discussed in Section 13.3, but rather a unitary matrix of a Lie group G . The Lagrangian of this theory is

$$\mathcal{L} = \frac{1}{4g^2} \int d^2x \operatorname{tr}[\partial_\mu U^\dagger \partial^\mu U]. \quad (22.17)$$

Like the theory of Section 13.3, this model is asymptotically free. However, Witten has shown that, by adding to this Lagrangian a particular perturbation of a rather complicated form first written by Wess and Zumino, one can find a fixed point of the renormalization group with manifest $G \times G$ global symmetry. This theory is conformally invariant, and all operator correlation functions can be computed using the conformal symmetry.*

One result of the nonperturbative exploration of quantum field theory was the realization that field theories can contain particle states that are not simply related to the quanta of the original fields. In the weak-coupling limit of a quantum field theory, such new states can appear as new solutions of the classical field equations. Consider, for example, ϕ^4 theory in two dimensions in the broken-symmetry phase. The equation of motion is

$$\frac{\partial^2}{\partial t^2}\phi - \frac{\partial^2}{\partial x^2}\phi - \mu^2\phi + \lambda\phi^3 = 0. \quad (22.18)$$

Treating this equation as a classical partial differential equation, we can find the time-independent solution

$$\phi(x) = \frac{\mu}{\sqrt{\lambda}} \tanh \frac{x\mu}{\sqrt{2}}. \quad (22.19)$$

This is a field configuration that begins in one well of the potential at $x = -\infty$ and crosses over to the other well as $x \rightarrow +\infty$. This solution has an energy of order μ/λ , larger by a factor of $1/\lambda$ than the mass of a ϕ quantum. Since the original equation (22.18) was Lorentz-covariant, the boosts of this solution must also be solutions to the classical partial differential equation. It is natural to suggest that, in the ϕ^4 quantum field theory, these solutions form a new set of massive particles. Such solutions, and the particles corresponding to

*For an introduction to conformally invariant two-dimensional quantum field theories, see P. Ginsparg, in *Fields, Strings, Critical Phenomena*, E. Brezin and J. Zinn-Justin, eds. (North-Holland, Amsterdam, 1989).

them, are often called *solitons*, borrowing a more specialized term from the literature on two-dimensional partial differential equations.[†]

Many examples are now known of particles that are associated in this way with classical solutions of a quantum field theory. In theories with spontaneously broken symmetry, the appearance of such particles is often related to the topology of the set of vacuum states; the ϕ^4 theory above gives a simple example of this relation. These examples are not limited to two dimensions but can also occur in theories that are potentially realistic. Such solutions can have magical properties. One interesting example is found in the $SU(2)$ gauge theory with a Higgs scalar field in the vector representation, the Georgi-Glashow model considered in Section 20.1. 't Hooft and Polyakov showed that this theory has a classical solution in which the Higgs field ϕ_a has the form

$$\phi_a(\mathbf{x}) = f(|\mathbf{x}|)x_a. \quad (22.20)$$

They showed that, when the gauge theory is interpreted as a unified model of weak and electromagnetic interactions, this solution is a magnetic monopole! In addition, particles that arise as heavy classical states in the weak coupling limit can have a more intricate relation to the dynamics of the theory when the coupling is increased. For example, in theories of the type of two-dimensional QED or the Thirring model in which fermions can be replaced by bosons, a weak-coupling limit is obtained by adding to the theory a large fermion mass. Then the original fermions are recovered from the bosonic representation of the theory as classical solutions very similar to that given in (22.19).

In some theories, one can find classical solutions of the Euclidean field equations. These solutions, called *instantons*, are localized in Euclidean time as well as in space. Thus, they are interpreted as quantum processes that modify the effective Hamiltonian of a quantum field theory. The most famous example of an instanton is found in four-dimensional non-Abelian gauge theories. It was shown by 't Hooft that this field configuration leads to a quantum process that violates the conservation of the $U(1)$ axial current in QCD. We have explained in Section 19.3 that this violation of current conservation is exactly what is needed to explain the spectrum of light mesons in QCD.

There is probably much more to be learned, especially about the strong-coupling behavior of gauge theories, by deeper analysis of the classical solutions to the field equations, and of the interrelations of the many exactly or partially solvable two-dimensional field theories.

[†]For an introduction to the use of solutions of the classical field equations in the analysis of problems in field theory, see S. Coleman (1985), Chaps. 6 and 7, and R. Rajaraman, *Solitons and Instantons* (North-Holland, Amsterdam, 1982).

22.4 Supersymmetry

Among the properties that a quantum field theory might possess to make it more beautiful or more mathematically tractable, there is one higher symmetry with particularly far-reaching implications. This is a symmetry that relates fermions and bosons, known (without hyperbole) as *supersymmetry*. In this section, we will introduce some of the purely mathematical consequences of supersymmetry, and then discuss the question of whether the true field equations of Nature could be supersymmetric.

A generator of supersymmetry is an operator that commutes with the Hamiltonian and converts bosonic into fermionic states. Such an operator must carry half-integer spin, in the simplest case spin 1/2. Let Q_α , with $\alpha = 1, 2$, be the left-handed spinor components of this operator. Their Hermitian conjugates, Q_β^\dagger , form a right-handed spinor. The anticommutator $\{Q_\alpha, Q_\beta^\dagger\}$ is a 2×2 matrix with positive diagonal elements; thus it cannot vanish. This matrix commutes with H but transforms nontrivially under Lorentz transformations. A Lorentz-covariant expression for this anticommutator is

$$\{Q_\alpha, Q_\beta^\dagger\} = 2\sigma_{\alpha\beta}^\mu P^\mu, \quad (22.21)$$

where P^μ is a conserved vector quantity. Such quantities are severely restricted; a theorem of Coleman and Mandula states that, if a quantum field theory in more than two dimensions has a second conserved vector quantity in addition to the energy-momentum 4-vector, the S -matrix equals 1 and no scattering is allowed. Thus the only possible choice for P^μ in Eq. (22.21) is the total energy-momentum. The Coleman-Mandula theorem also rules out any higher-spin conservation laws. This eliminates the possibility that a supersymmetry generator could have spin 3/2 or higher. The most general possibility is a collection of spin-1/2 operators with the anticommutation relations

$$\{Q_\alpha^i, Q_\beta^{j\dagger}\} = 2\delta^{ij}\sigma_{\alpha\beta}^\mu P^\mu, \quad (22.22)$$

with $i, j = 1, \dots, N$. In the following discussion, we will mainly consider only the simplest case, $N = 1$.[‡]

The algebra (22.22) of conserved quantities has profound consequences for the theory. Since the right-hand side of (22.22) is the total energy-momentum, it involves every field in the theory. To reproduce this algebra, the left-hand side must also involve every field. The representations of this algebra pair every bosonic state with a fermionic state at the same energy, and vice versa. If supersymmetry is an exact symmetry of the quantum field theory, it must act on every sector of the theory. In a realistic model, even the gravitational field must have a fermionic partner. This means that Einstein's equations of gravity must be generalized to a new set of geometrical equations that involve a fermionic (spin-3/2) field.

[‡]An excellent introduction to the formalism of supersymmetry is J. Wess and J. Bagger, *Supersymmetry and Supergravity* (Princeton University Press, 1983).

The first consequences of making a quantum field theory supersymmetric are easy to understand. For every (complex) scalar field, one must introduce a chiral fermion field. The self-interactions of the bosonic fields are related to the interactions of these fields with the fermions; for example, a possible interaction Lagrangian with coupling constant λ is

$$\Delta\mathcal{L} = -\lambda^2|\phi|^2 - \frac{1}{2}\lambda\psi^T\sigma^2\psi. \quad (22.23)$$

We have written a more general supersymmetric Lagrangian in Problem 3.5. Similarly, for every gauge field, one must introduce a chiral fermion in the adjoint representation of the gauge group. This fermion, called the *gaugino*, mediates interactions of the scalar fields with their fermionic partners whose strength is given by the gauge coupling g .

The special relation between the bosonic and fermionic interactions leads to great simplifications in the renormalization of supersymmetric theories. Some of these simplifications can be anticipated. Since supersymmetry requires that each scalar particle have a fermionic partner of the same mass, these particles must have the same mass renormalization. But we have seen that the fermion mass is multiplicatively renormalized and thus is only logarithmically divergent, while a scalar mass term is additively renormalized and thus can be quadratically divergent. Supersymmetry must imply that the quadratic divergences of scalar mass terms automatically vanish. In fact, these cancellations occur in every order of perturbation theory, with loop diagrams involving bosons canceling against diagrams with virtual fermions. To see another simplification required by supersymmetry, take the vacuum expectation value of the anticommutation relation (22.21). The vacuum state has zero momentum: $P^i|0\rangle = 0$. If the vacuum state is supersymmetric, $Q_\alpha|0\rangle = Q_\beta^\dagger|0\rangle = 0$. Then Eq. (22.21) implies

$$\langle 0|H|0\rangle = 0. \quad (22.24)$$

We have noted already that bosonic fields give positive contributions to the vacuum energy through their zero-point energy, and fermionic fields give negative contributions. We now see that, in a supersymmetric model, these contributions cancel exactly, not only at the leading order but to all orders in perturbation theory.

Deeper examination of supersymmetric theories leads to additional, and quite unexpected, cancellations in renormalization theory. For example, one can show that the coupling constants in scalar-fermion self-interactions, such as λ in (22.23), are renormalized only through field strength renormalizations. Thus the relative size of two different scalar interactions remains unchanged. If a particular type of renormalizable interaction is omitted, it cannot be generated by renormalization, in contrast to the case in ordinary field theory. The simplest supersymmetry does not constrain the renormalization of gauge couplings, but higher supersymmetries can have a profound effect: In $N = 2$ supersymmetric models, the β function vanishes if the leading-order term is

arranged to be zero. In $N = 4$ supersymmetric models, this cancellation is automatic and $\beta(g) = 0$ exactly. These models give examples of four-dimensional quantum field theories with no ultraviolet divergences.*

Supersymmetry thus endows a quantum field theory with remarkable, even magical properties. But is it possible that the true equations of Nature could possess such a high degree of symmetry? Since we are certain that there is no charged boson with the same mass as the electron, we know that supersymmetry cannot be an exact symmetry of Nature. But it is tempting to guess that it might be a spontaneously broken symmetry of the underlying equations.

In fact, this conjecture has fruitful consequences for the grand unified theories that we discussed in Section 22.2. The problem of the Higgs boson mass that we highlighted in that section has an elegant solution in supersymmetry models. In a supersymmetric version of the standard model, the Higgs field is one of a large number of scalar fields with various $SU(3) \times SU(2) \times U(1)$ quantum numbers. For all of these scalar fields, the mass terms get only a logarithmic multiplicative renormalization. If supersymmetry were broken in such a way as to give mass differences of a few hundred GeV between the observed fermionic quarks and leptons and their scalar partners, one would also find a Higgs boson (mass)² of the correct size. There are good reasons, which follow from more detailed properties of the theory, why it is the Higgs field, rather than some other scalar field, that obtains a vacuum expectation value.[†]

If this set of ideas is correct, the scalar partners of quarks and leptons would be light enough to be discovered experimentally in the near future. In that case, these scalar particles and the fermionic partners of gauge bosons would affect the renormalization of coupling constants between present energies and the grand unification scale. This might potentially disturb the prospects for grand unification, but, instead, it improves them: the dashed lines of Fig. 22.1, with a more impressive meeting of the three coupling constants, were generated by replacing the conventional β functions with ones including the supersymmetric partners.

The last of the problems discussed in Section 22.2 is also ameliorated by the introduction of supersymmetry. In a grand unified theory with broken supersymmetry, those momentum scales that are much larger than the mass differences of supersymmetry partners give no contribution to the vacuum energy. Thus the natural size of the cosmological constant in these theories is $\lambda \sim (100 \text{ GeV})^4$. This reduces the cosmological constant problem to a discrepancy of 50 orders of magnitude—but this is not nearly enough.

*Supersymmetric models with vanishing β function are reviewed by P. West, in *Shelter Island II*, R. Jackiw, N. N. Khuri, S. Weinberg, and E. Witten, eds. (MIT Press, Cambridge, 1985).

†Supersymmetric models of quarks and leptons, and their observable consequences, are reviewed in H. P. Nilles, *Phys. Repts.* **110**, 1 (1984), and in H. E. Haber and G. L. Kane, *Phys. Repts.* **117**, 75 (1985).

It is an exciting prospect that supersymmetric partners of the particles of the standard model might soon be seen in experiments. What we anticipate, in any event, is that the experiments of the next generation will make a definite choice between this hypothesis for the nature of the Higgs sector and the other possibilities discussed in Section 22.2. Either way, we will have advanced our knowledge one step toward the truly fundamental equations.

22.5 Toward an Ultimate Theory of Nature

What are these fundamental equations? Do they involve quantum field theory, or some very different organizing principle? Any answer to this question must be completely speculative. Nevertheless, there are some principles, and an example, that can guide this search.

For all the attention we have given in this book to the basic interactions of particle physics, we have given very little attention to gravity. In part, this is because the quantum theory of gravity has no known observational consequences. But it is also true that the quantum theory of gravity is still ill-formed and uncertain. If gravity is treated as a weak-coupling field theory with Feynman diagrams, one quickly finds that the divergences of these diagrams render the theory nonrenormalizable. This is no surprise, because gravity is a theory in which the coupling constant has inverse mass dimensions, with the mass scale m_{Planck} given by (22.7). In our general philosophy of renormalization, all of the complexity of this theory should be concentrated at the scale m_{Planck} .

At the scale where quantum fluctuations of the gravitational field are important, we must expect profound changes in physics. If these changes occur within the context of quantum field theory, they will at the least entail fluctuating spacetime geometry and topology. But it seems equally probable that quantum field theory will actually break down at this scale, with continuous spacetime replaced by a new discrete or nonlocal geometry.

One particular model for the behavior of spacetime at very small distances is *string theory*, the dynamics of abstract one-dimensional extended objects. In Section 22.1, we mentioned that such objects seemed to occur naturally in attempts to describe quark confinement in QCD, but that the detailed properties of these objects made them unsuitable for strong interaction phenomenology. Among the disappointing properties of these systems were the appearance of massless spin-2 states of the string, and a constraint that the dimension of spacetime must be increased unless the spectrum of the theory contained many massless spin-1 states. In 1974, Scherk and Schwarz made the remarkable suggestion that string theory was a correct mathematical description of a different problem, the unification of elementary particle interactions with gravity. They interpreted the spin-2 quantum as the graviton and the spin-1 quanta as gauge bosons of a gauge theory.[†] A decade later,

[†]J. Scherk and J. H. Schwarz, *Nucl. Phys.* **B81**, 118 (1974).

Green and Schwarz put this conjecture on a firmer footing by showing that a particular string theory could be interpreted as a grand unified theory in ten spacetime dimensions, with all gravitational and gauge Ward identities automatically satisfied and all anomalies automatically canceling. Since that time, many other solutions to the constraint equations of string theory have been found, some of which correspond to unified models of gauge interactions and gravity in four dimensions. These models can naturally incorporate supersymmetry and, under that condition, give ultraviolet-finite results for all scattering amplitudes, including those of gravitons.*

String theories solve the ultraviolet divergence problems of quantum field theory by rejecting the idea that elementary particles are pointlike objects with contact interactions. Rather, in string theory, quarks, leptons, gauge bosons, and gravitons are extended loops of string excitation which thus interact nonlocally. Since particles cannot be definitely localized, spacetime itself takes on a nonlocal character. In some sense, distances much less than the Planck length $1/m_{\text{Planck}}$ do not exist in the string description of gravity. As yet, it is not clear how to understand intuitively the sort of geometry that string theory requires. This mathematical problem is now being actively investigated.

If indeed the truly fundamental geometry of Nature is nonlocal, discrete, or discontinuous in some other way, then the grand program for the fundamental interactions that we have set forth in this book must be altered in an essential way. The most elementary equations of Nature will not be gauge-invariant quantum field theories, but instead theories built from very different elements. Even the principles of model construction will be different from those based on gauge and Lorentz invariance that we have discussed here.

On the other hand, quantum field theory will still play an essential role in the interpretation of this structure. All of the processes we now observe, even the elementary particle processes at the highest energies currently accessible, occur over distances 15 orders of magnitude larger than the sizes of the strings or other fluctuating structures that appear in the underlying equations. The relation of experimental observations to these fundamental structures is thus very similar to the relation of macroscopic observations to the underlying atomic structure of matter. In the study of matter, we use a classical, Newtonian description of atoms to bridge this gap and to relate the properties of gases, liquids, and solids to underlying atomic properties. We might say that the quantum theory of atoms gives rise to a set of effective Newtonian equations that is extremely powerful in the macroscopic domain. Especially in the theory of gases, this Newtonian description was also used as a tool to realize the existence of atoms and to derive their properties.

*A technical introduction to string theory and its use in building unified models has been given by M. B. Green, J. H. Schwarz, and E. Witten, *Superstring Theory*, 2 vols. (Cambridge University Press, 1987).

Similarly, whatever the nature of Planck-scale physics, it leads to some effective continuum quantum field theory. This quantum field theory might well be an accurate approximation to the underlying physics already at distances of 100 Planck lengths, corresponding to momenta of 10^{17} GeV. From here to the scale of weak interactions, and from there up to the wavelength of light, and from there to the size of the universe, quantum field theory can be treated as the basic framework for the equations of physics. By recognizing the symmetries of the particular set of field equations that Nature has provided us, we can learn to compute all of the details of physical processes over this whole enormous domain. And, by contemplating the origin of these symmetries, perhaps we will also be able to see through to the next level and unlock the true structure of spacetime.

Appendix

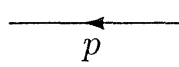
Reference Formulae

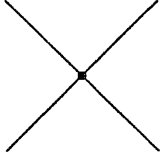
This Appendix collects together some of the formulae that are most commonly used in Feynman diagram calculations.

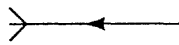
A.1 Feynman Rules

In all theories it is understood that momentum is conserved at each vertex, and that undetermined loop momenta are integrated over: $\int d^4p/(2\pi)^4$. Fermion (including ghost) loops receive an additional factor of (-1) , as explained on page 120. Finally, each diagram can potentially have a symmetry factor, as explained on page 93.

$$\phi^4 \text{ theory: } \mathcal{L} = \frac{1}{2}(\partial_\mu\phi)^2 - \frac{1}{2}m^2\phi^2 - \frac{\lambda^4}{4!}\phi^4$$

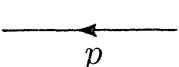
Scalar propagator:  $= \frac{i}{p^2 - m^2 + i\epsilon}$ (A.1)

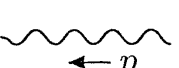
ϕ^4 vertex:  $= -i\lambda$ (A.2)

External scalar:  $= 1$ (A.3)

(Counterterm vertices for loop calculations are given on page 325.)

Quantum Electrodynamics: $\mathcal{L} = \bar{\psi}(i\partial - m)\psi - \frac{1}{4}(F_{\mu\nu})^2 - e\bar{\psi}\gamma^\mu\psi A_\mu$

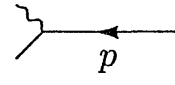
Dirac propagator:  $= \frac{i(\not{p} + m)}{p^2 - m^2 + i\epsilon}$ (A.4)

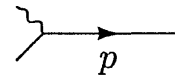
Photon propagator:  $= \frac{-ig_{\mu\nu}}{p^2 + i\epsilon}$ (A.5)

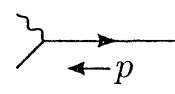
(Feynman gauge; see page 297 for generalized Lorentz gauge.)

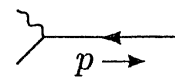
QED vertex:  $= iQe\gamma^\mu$ (A.6)

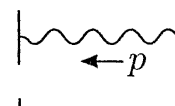
$(Q = -1$ for an electron)

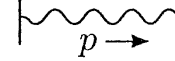
External fermions:  $= u^s(p)$ (initial) (A.7)

 $= \bar{u}^s(p)$ (final)

External antifermions:  $= \bar{v}^s(p)$ (initial) (A.8)

 $= v^s(p)$ (final)

External photons:  $= \epsilon_\mu(p)$ (initial) (A.9)

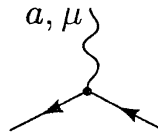
 $= \epsilon_\mu^*(p)$ (final)

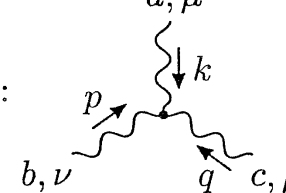
(Counterterm vertices for loop calculations are given on page 332.)

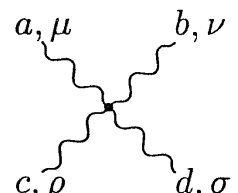
Non-Abelian Gauge Theory:

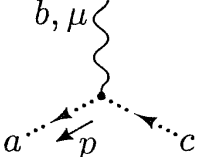
$$\mathcal{L} = \bar{\psi}(i\partial^\mu - m)\psi - \frac{1}{4}(\partial_\mu A_\nu^a - \partial_\nu A_\mu^b)^2 + gA_\mu^a\bar{\psi}\gamma^\mu\psi - gf^{abc}(\partial_\mu A_\nu^a)A^{\mu b}A^{\nu c} - g^2(f^{eab}A_\mu^aA_\nu^b)(f^{ecd}A^{\mu c}A^{\nu d})$$

The fermion and gauge boson propagators are the same as in QED, times an identity matrix in the gauge group space. Similarly, the polarization of external particles is treated the same as in QED, but each external particle also has an orientation in the group space.

Fermion vertex:  $= ig\gamma^\mu t^a$ (A.10)

3-boson vertex:  $= gf^{abc}[g^{\mu\nu}(k-p)^\rho + g^{\nu\rho}(p-q)^\mu + g^{\rho\mu}(q-k)^\nu]$ (A.11)

4-boson vertex:  $= -ig^2[f^{abe}f^{cde}(g^{\mu\rho}g^{\nu\sigma} - g^{\mu\sigma}g^{\nu\rho}) + f^{ace}f^{bde}(g^{\mu\nu}g^{\rho\sigma} - g^{\mu\sigma}g^{\nu\rho}) + f^{ade}f^{bce}(g^{\mu\nu}g^{\rho\sigma} - g^{\mu\rho}g^{\nu\sigma})]$ (A.12)

Ghost vertex:  $= gf^{abc} p^\mu$ (A.13)

Ghost propagator: $a \cdots \cdots \xleftarrow[p]{p^2 + i\epsilon} b = \frac{i\delta^{ab}}{p^2 + i\epsilon}$ (A.14)

(Counterterm vertices for loop calculations are given on pages 528 and 532.)

Other theories. Feynman rules for other theories can be found on the following pages:

Yukawa theory	page 118
Scalar QED	page 312
Linear sigma model	page 353
Electroweak theory	pages 716, 743, 753

A.2 Polarizations of External Particles

The spinors $u^s(p)$ and $v^s(p)$ obey the Dirac equation in the form

$$0 = (\not{p} - m)u^s(p) = \bar{u}^s(p)(\not{p} - m) \\ = (\not{p} + m)v^s(p) = \bar{v}^s(p)(\not{p} + m), \quad (\text{A.15})$$

where $\not{p} = \gamma^\mu p_\mu$. The Dirac matrices obey the anticommutation relations

$$\{\gamma^\mu, \gamma^\nu\} = 2g^{\mu\nu}. \quad (\text{A.16})$$

We use a chiral basis,

$$\gamma^\mu = \begin{pmatrix} 0 & \sigma^\mu \\ \bar{\sigma}^\mu & 0 \end{pmatrix}, \quad \gamma^5 = \begin{pmatrix} -1 & 0 \\ 0 & 1 \end{pmatrix}, \quad (\text{A.17})$$

where

$$\sigma^\mu = (1, \boldsymbol{\sigma}), \quad \bar{\sigma}^\mu = (1, -\boldsymbol{\sigma}). \quad (\text{A.18})$$

In this basis the normalized Dirac spinors can be written

$$u^s(p) = \begin{pmatrix} \sqrt{p \cdot \sigma} \xi^s \\ \sqrt{p \cdot \bar{\sigma}} \xi^s \end{pmatrix}, \quad v^s(p) = \begin{pmatrix} \sqrt{p \cdot \sigma} \eta^s \\ -\sqrt{p \cdot \bar{\sigma}} \eta^s \end{pmatrix}, \quad (\text{A.19})$$

where ξ and η are two-component spinors normalized to unity. In the high-energy limit these expressions simplify to

$$u(p) \approx \sqrt{2E} \begin{pmatrix} \frac{1}{2}(1 - \hat{p} \cdot \boldsymbol{\sigma}) \xi^s \\ \frac{1}{2}(1 + \hat{p} \cdot \boldsymbol{\sigma}) \xi^s \end{pmatrix}, \quad v(p) \approx \sqrt{2E} \begin{pmatrix} \frac{1}{2}(1 - \hat{p} \cdot \boldsymbol{\sigma}) \eta^s \\ -\frac{1}{2}(1 + \hat{p} \cdot \boldsymbol{\sigma}) \eta^s \end{pmatrix}. \quad (\text{A.20})$$

Using the standard basis for the Pauli matrices,

$$\sigma^1 = \begin{pmatrix} 0 & 1 \\ 1 & 0 \end{pmatrix}, \quad \sigma^2 = \begin{pmatrix} 0 & -i \\ i & 0 \end{pmatrix}, \quad \sigma^3 = \begin{pmatrix} 1 & 0 \\ 0 & -1 \end{pmatrix}, \quad (\text{A.21})$$

we have, for example, $\xi^s = \begin{pmatrix} 1 \\ 0 \end{pmatrix}$ for spin up in the z direction, and $\xi^s = \begin{pmatrix} 0 \\ 1 \end{pmatrix}$ for spin down in the z direction. For antifermions the physical spin is opposite to that of the spinor: $\eta^s = \begin{pmatrix} 1 \\ 0 \end{pmatrix}$ corresponds to spin *down* in the z direction, and so on.

In computing unpolarized cross sections one encounters the polarization sums

$$\sum_s u^s(p) \bar{u}^s(p) = \not{p} + m, \quad \sum_s v^s(p) \bar{v}^s(p) = \not{p} - m. \quad (\text{A.22})$$

For polarized cross sections one can either resort to the explicit formulae (A.19) or insert the projection matrices

$$\left(\frac{1 + \gamma^5}{2} \right), \quad \left(\frac{1 - \gamma^5}{2} \right), \quad (\text{A.23})$$

which project onto right- and left-handed spinors, respectively. Again, for antifermions, the helicity of the spinor is opposite to the physical helicity of the particle.

Many other identities involving Dirac spinors and matrices can be found in Chapter 3.

Polarization vectors for photons and other gauge bosons are conventionally normalized to unity. For massless bosons the polarization must be transverse:

$$\epsilon^\mu = (0, \epsilon), \quad \text{where } \mathbf{p} \cdot \epsilon = 0. \quad (\text{A.24})$$

If \mathbf{p} is in the $+z$ direction, the polarization vectors are

$$\epsilon^\mu = \frac{1}{\sqrt{2}}(0, 1, i, 0), \quad \epsilon^\mu = \frac{1}{\sqrt{2}}(0, 1, -i, 0), \quad (\text{A.25})$$

for right- and left-handed helicities, respectively.

In computing unpolarized cross sections involving photons, one can replace

$$\sum_{\text{polarizations}} \epsilon_\mu^* \epsilon_\nu \longrightarrow -g_{\mu\nu}, \quad (\text{A.26})$$

by virtue of the Ward identity. In the case of massless non-Abelian gauge bosons, one must also sum over the emission of ghosts, as discussed in Section 16.3. In the massive case, one must in addition include the emission of Goldstone bosons, as discussed in Section 21.1.

A.3 Numerator Algebra

Traces of γ matrices can be evaluated as follows:

$$\begin{aligned}
 \text{tr}(1) &= 4 \\
 \text{tr}(\text{any odd } \# \text{ of } \gamma\text{'s}) &= 0 \\
 \text{tr}(\gamma^\mu \gamma^\nu) &= 4g^{\mu\nu} \\
 \text{tr}(\gamma^\mu \gamma^\nu \gamma^\rho \gamma^\sigma) &= 4(g^{\mu\nu} g^{\rho\sigma} - g^{\mu\rho} g^{\nu\sigma} + g^{\mu\sigma} g^{\nu\rho}) \quad (\text{A.27}) \\
 \text{tr}(\gamma^5) &= 0 \\
 \text{tr}(\gamma^\mu \gamma^\nu \gamma^5) &= 0 \\
 \text{tr}(\gamma^\mu \gamma^\nu \gamma^\rho \gamma^\sigma \gamma^5) &= -4i\epsilon^{\mu\nu\rho\sigma}
 \end{aligned}$$

Another identity allows one to reverse the order of γ matrices inside a trace:

$$\text{tr}(\gamma^\mu \gamma^\nu \gamma^\rho \gamma^\sigma \dots) = \text{tr}(\dots \gamma^\sigma \gamma^\rho \gamma^\nu \gamma^\mu). \quad (\text{A.28})$$

Contractions of γ matrices with each other simplify to:

$$\begin{aligned}
 \gamma^\mu \gamma_\mu &= 4 \\
 \gamma^\mu \gamma^\nu \gamma_\mu &= -2\gamma^\nu \\
 \gamma^\mu \gamma^\nu \gamma^\rho \gamma_\mu &= 4g^{\nu\rho} \\
 \gamma^\mu \gamma^\nu \gamma^\rho \gamma^\sigma \gamma_\mu &= -2\gamma^\sigma \gamma^\rho \gamma^\nu
 \end{aligned} \quad (\text{A.29})$$

(These identities apply in four dimensions only; see the following section.) Contractions of the ϵ symbol can also be simplified:

$$\begin{aligned}
 \epsilon^{\alpha\beta\gamma\delta} \epsilon_{\alpha\beta\gamma\delta} &= -24 \\
 \epsilon^{\alpha\beta\gamma\mu} \epsilon_{\alpha\beta\gamma\nu} &= -6\delta^\mu_\nu \\
 \epsilon^{\alpha\beta\mu\nu} \epsilon_{\alpha\beta\rho\sigma} &= -2(\delta^\mu_\rho \delta^\nu_\sigma - \delta^\mu_\sigma \delta^\nu_\rho)
 \end{aligned} \quad (\text{A.30})$$

In some calculations, it is useful to rearrange products of fermion bilinears by means of *Fierz identities*. Let u_1, \dots, u_4 be Dirac spinors, and let $u_{iL} = \frac{1}{2}(1 - \gamma^5)u_i$ be the left-handed projection. Then the most important Fierz rearrangement formula is

$$(\bar{u}_{1L} \gamma^\mu u_{2L})(\bar{u}_{3L} \gamma_\mu u_{4L}) = -(\bar{u}_{1L} \gamma^\mu u_{4L})(\bar{u}_{3L} \gamma_\mu u_{2L}). \quad (\text{A.31})$$

Additional formulae can be generated by the use of the following identities for the 2×2 blocks of Dirac matrices:

$$(\sigma^\mu)_{\alpha\beta} (\sigma_\mu)_{\gamma\delta} = 2\epsilon_{\alpha\gamma} \epsilon_{\beta\delta}; \quad (\bar{\sigma}^\mu)_{\alpha\beta} (\bar{\sigma}_\mu)_{\gamma\delta} = 2\epsilon_{\alpha\gamma} \epsilon_{\beta\delta}. \quad (\text{A.32})$$

In non-Abelian gauge theories, the Feynman rules involve gauge group matrices t^a that form a representation r of a Lie algebra G . The symbol G also denotes the adjoint representation of the algebra. The matrices t^a obey

$$[t^a, t^b] = if^{abc}t^c, \quad (\text{A.33})$$

where the structure constants f^{abc} are totally antisymmetric. The invariants $C(r)$ and $C_2(r)$ of the representation r are defined by

$$\text{tr}[t^a t^b] = C(r) \delta^{ab}, \quad t^a t^a = C_2(r) \cdot 1. \quad (\text{A.34})$$

These are related by

$$C(r) = \frac{d(r)}{d(G)} C_2(r), \quad (\text{A.35})$$

where $d(r)$ is the dimension of the representation. Traces and contractions of the t^a can be evaluated using the above identities and their consequences:

$$\begin{aligned} t^a t^b t^a &= [C_2(r) - \frac{1}{2} C_2(G)] t^b \\ f^{acd} f^{bcd} &= C_2(G) \delta^{ab} \\ f^{abc} t^b t^c &= \frac{1}{2} i C_2(G) t^a \end{aligned} \quad (\text{A.36})$$

For $SU(N)$ groups, the fundamental representation is denoted by N , and we have

$$C(N) = \frac{1}{2}, \quad C_2(N) = \frac{N^2 - 1}{2N}, \quad C(G) = C_2(G) = N. \quad (\text{A.37})$$

The following relation, satisfied by the matrices of the fundamental representation of $SU(N)$, is also very helpful:

$$(t^a)_{ij} (t^a)_{kl} = \frac{1}{2} \left(\delta_{il} \delta_{kj} - \frac{1}{N} \delta_{ij} \delta_{kl} \right). \quad (\text{A.38})$$

A.4 Loop Integrals and Dimensional Regularization

To combine propagator denominators, introduce integrals over Feynman parameters:

$$\frac{1}{A_1 A_2 \cdots A_n} = \int_0^1 dx_1 \cdots dx_n \delta(\sum x_i - 1) \frac{(n-1)!}{[x_1 A_1 + x_2 A_2 + \cdots + x_n A_n]^n} \quad (\text{A.39})$$

In the case of only two denominator factors, this formula reduces to

$$\frac{1}{AB} = \int_0^1 dx \frac{1}{[xA + (1-x)B]^2}. \quad (\text{A.40})$$

A more general formula in which the A_i are raised to arbitrary powers is given in Eq. (6.42).

Once this is done, the bracketed quantity in the denominator will be a quadratic function of the integration variables p_i^μ . Next, complete the square and shift the integration variables to absorb the terms linear in p_i^μ . For a one-loop integral, there is a single integration momentum p^μ , which is shifted to a momentum variable ℓ^μ . After this shift, the denominator takes the form

$(\ell^2 - \Delta)^n$. In the numerator, terms with an odd number of powers of ℓ vanish by symmetric integration. Symmetry also allows one to replace

$$\ell^\mu \ell^\nu \rightarrow \frac{1}{d} \ell^2 g^{\mu\nu}, \quad (\text{A.41})$$

$$\ell^\mu \ell^\nu \ell^\rho \ell^\sigma \rightarrow \frac{1}{d(d+2)} (\ell^2)^2 (g^{\mu\nu} g^{\rho\sigma} + g^{\mu\rho} g^{\nu\sigma} + g^{\mu\sigma} g^{\nu\rho}). \quad (\text{A.42})$$

(Here d is the spacetime dimension.) The integral is most conveniently evaluated after Wick-rotating to Euclidean space, with the substitution

$$\ell^0 = i\ell_E^0, \quad \ell^2 = -\ell_E^2. \quad (\text{A.43})$$

Alternatively, one can use the following table of d -dimensional integrals in Minkowski space:

$$\int \frac{d^d \ell}{(2\pi)^d} \frac{1}{(\ell^2 - \Delta)^n} = \frac{(-1)^n i}{(4\pi)^{d/2}} \frac{\Gamma(n - \frac{d}{2})}{\Gamma(n)} \left(\frac{1}{\Delta}\right)^{n - \frac{d}{2}} \quad (\text{A.44})$$

$$\int \frac{d^d \ell}{(2\pi)^d} \frac{\ell^2}{(\ell^2 - \Delta)^n} = \frac{(-1)^{n-1} i}{(4\pi)^{d/2}} \frac{d}{2} \frac{\Gamma(n - \frac{d}{2} - 1)}{\Gamma(n)} \left(\frac{1}{\Delta}\right)^{n - \frac{d}{2} - 1} \quad (\text{A.45})$$

$$\int \frac{d^d \ell}{(2\pi)^d} \frac{\ell^\mu \ell^\nu}{(\ell^2 - \Delta)^n} = \frac{(-1)^{n-1} i}{(4\pi)^{d/2}} \frac{g^{\mu\nu}}{2} \frac{\Gamma(n - \frac{d}{2} - 1)}{\Gamma(n)} \left(\frac{1}{\Delta}\right)^{n - \frac{d}{2} - 1} \quad (\text{A.46})$$

$$\int \frac{d^d \ell}{(2\pi)^d} \frac{(\ell^2)^2}{(\ell^2 - \Delta)^n} = \frac{(-1)^n i}{(4\pi)^{d/2}} \frac{d(d+2)}{4} \frac{\Gamma(n - \frac{d}{2} - 1)}{\Gamma(n)} \left(\frac{1}{\Delta}\right)^{n - \frac{d}{2} - 2} \quad (\text{A.47})$$

$$\begin{aligned} \int \frac{d^d \ell}{(2\pi)^d} \frac{\ell^\mu \ell^\nu \ell^\rho \ell^\sigma}{(\ell^2 - \Delta)^n} &= \frac{(-1)^n i}{(4\pi)^{d/2}} \frac{\Gamma(n - \frac{d}{2} - 2)}{\Gamma(n)} \left(\frac{1}{\Delta}\right)^{n - \frac{d}{2} - 2} \\ &\times \frac{1}{4} (g^{\mu\nu} g^{\rho\sigma} + g^{\mu\rho} g^{\nu\sigma} + g^{\mu\sigma} g^{\nu\rho}) \end{aligned} \quad (\text{A.48})$$

If the integral converges, one can set $d = 4$ from the start. If the integral diverges, the behavior near $d = 4$ can be extracted by expanding

$$\left(\frac{1}{\Delta}\right)^{2 - \frac{d}{2}} = 1 - (2 - \frac{d}{2}) \log \Delta + \dots \quad (\text{A.49})$$

One also needs the expansion of $\Gamma(x)$ near its poles:

$$\Gamma(x) = \frac{1}{x} - \gamma + \mathcal{O}(x) \quad (\text{A.50})$$

near $x = 0$, and

$$\Gamma(x) = \frac{(-1)^n}{n!(x+n)} - \gamma + 1 + \dots + \frac{1}{n} + \mathcal{O}(x+n) \quad (\text{A.51})$$

near $x = -n$. Here γ is the Euler-Mascheroni constant, $\gamma \approx 0.5772$. The following combination of terms often appears in calculations:

$$\frac{\Gamma(2-\frac{d}{2})}{(4\pi)^{d/2}} \left(\frac{1}{\Delta}\right)^{2-\frac{d}{2}} = \frac{2}{\epsilon} - (\log \Delta + \gamma - \log(4\pi)) + \mathcal{O}(\epsilon), \quad (\text{A.52})$$

with $\epsilon = 4 - d$.

Notice that Δ is positive if it is a combination of masses and *spacelike* momentum invariants. If Δ contains timelike momenta, it may become negative. Then these integrals acquire imaginary parts, which give the discontinuities of S -matrix elements. To compute the S -matrix in a physical region, choose the correct branch of the function by the prescription

$$\left(\frac{1}{\Delta}\right)^{n-\frac{d}{2}} \rightarrow \left(\frac{1}{\Delta - i\epsilon}\right)^{n-\frac{d}{2}}, \quad (\text{A.53})$$

where $-i\epsilon$ (not to be confused with ϵ in the previous paragraph!) gives a tiny negative imaginary part.

Traces in Eq. (A.27) that do not involve γ^5 are independent of dimensionality. However, since

$$g^{\mu\nu} g_{\mu\nu} = \delta^\mu_\mu = d \quad (\text{A.54})$$

in d dimensions, the contraction identities (A.29) are modified:

$$\begin{aligned} \gamma^\mu \gamma_\mu &= d \\ \gamma^\mu \gamma^\nu \gamma_\mu &= -(d-2)\gamma^\nu \\ \gamma^\mu \gamma^\nu \gamma^\rho \gamma_\mu &= 4g^{\nu\rho} - (4-d)\gamma^\nu \gamma^\rho \\ \gamma^\mu \gamma^\nu \gamma^\rho \gamma^\sigma \gamma_\mu &= -2\gamma^\sigma \gamma^\rho \gamma^\nu + (4-d)\gamma^\nu \gamma^\rho \gamma^\sigma \end{aligned} \quad (\text{A.55})$$

A.5 Cross Sections and Decay Rates

Once the squared matrix element for a scattering process is known, the differential cross section is given by

$$\begin{aligned} d\sigma &= \frac{1}{2E_A 2E_B |v_A - v_B|} \left(\prod_f \frac{d^3 p_f}{(2\pi)^3} \frac{1}{2E_f} \right) \\ &\quad \times |\mathcal{M}(p_A, p_B \rightarrow \{p_f\})|^2 (2\pi)^4 \delta^{(4)}(p_A + p_B - \sum p_f). \end{aligned} \quad (\text{A.56})$$

The differential decay rate of an unstable particle to a given final state is

$$d\Gamma = \frac{1}{2m_A} \left(\prod_f \frac{d^3 p_f}{(2\pi)^3} \frac{1}{2E_f} \right) |\mathcal{M}(m_A \rightarrow \{p_f\})|^2 (2\pi)^4 \delta^{(4)}(p_A - \sum p_f). \quad (\text{A.57})$$

For the special case of a two-particle final state, the Lorentz-invariant phase space takes the simple form

$$\left(\prod_f \int \frac{d^3 p_f}{(2\pi)^3} \frac{1}{2E_f} \right) (2\pi)^4 \delta^{(4)}(\sum p_i - \sum p_f) = \int \frac{d\Omega_{\text{cm}}}{4\pi} \frac{1}{8\pi} \left(\frac{2|\mathbf{p}|}{E_{\text{cm}}} \right), \quad (\text{A.58})$$

where $|\mathbf{p}|$ is the magnitude of the 3-momentum of either particle in the center-of-mass frame.

A.6 Physical Constants and Conversion Factors

Precisely known physical constants:

$$\begin{aligned} c &= 2.998 \times 10^{10} \text{ cm/s} \\ \hbar &= 6.582 \times 10^{-22} \text{ MeV s} \\ e &= -1.602 \times 10^{-19} \text{ C} \\ \alpha &= \frac{e^2}{4\pi\hbar c} = \frac{1}{137.04} = 0.00730 \\ \frac{G_F}{(\hbar c)^3} &= 1.166 \times 10^{-5} \text{ GeV}^{-2} \end{aligned}$$

The values of the strong and weak interaction coupling constants depend on the conventions used to define them, as explained in Sections 17.6 and 21.3. For the purpose of estimation, however, one can use the following values:

$$\begin{aligned} \alpha_s(10 \text{ GeV}) &= 0.18 \\ \alpha_s(m_Z) &= 0.12 \\ \sin^2 \theta_w &= 0.23 \end{aligned}$$

Particle masses (times c^2):

$$\begin{array}{ll} e : & 0.5110 \text{ MeV} \\ \mu : & 105.6 \text{ MeV} \\ \tau : & 1784 \text{ MeV} \\ W^\pm : & 80.2 \text{ GeV} \\ Z^0 : & 91.19 \text{ GeV} \end{array} \quad \begin{array}{ll} p : & 938.3 \text{ MeV} \\ n : & 939.6 \text{ MeV} \\ \pi^\pm : & 139.6 \text{ MeV} \\ \pi^0 : & 135.0 \text{ MeV} \end{array}$$

Useful combinations:

$$\begin{aligned} \text{Bohr radius: } a_0 &= \frac{\hbar}{\alpha m_e c} = 5.292 \times 10^{-9} \text{ cm} \\ \text{electron Compton wavelength: } \lambda &= \frac{\hbar}{m_e c} = 3.862 \times 10^{-11} \text{ cm} \\ \text{classical electron radius: } r_e &= \frac{\alpha \hbar}{m_e c} = 2.818 \times 10^{-13} \text{ cm} \\ \text{Thomson cross section: } \sigma_T &= \frac{8\pi r_e^2}{3} = 0.6652 \text{ barn} \\ \text{annihilation cross section: } 1 \text{ R} &= \frac{4\pi\alpha^2}{3E_{\text{cm}}^2} = \frac{86.8 \text{ nbarn}}{(E_{\text{cm}} \text{ in GeV})^2} \end{aligned}$$

Conversion factors:

$$\begin{aligned}(1 \text{ GeV})/c^2 &= 1.783 \times 10^{-24} \text{ g} \\ (1 \text{ GeV})^{-1}(\hbar c) &= 0.1973 \times 10^{-13} \text{ cm} = 0.1973 \text{ fm}; \\ (1 \text{ GeV})^{-2}(\hbar c)^2 &= 0.3894 \times 10^{-27} \text{ cm}^2 = 0.3894 \text{ mbarn} \\ 1 \text{ barn} &= 10^{-24} \text{ cm}^2 \\ (1 \text{ volt/meter})(e\hbar c) &= 1.973 \times 10^{-25} \text{ GeV}^2 \\ (1 \text{ tesla})(e\hbar c^2) &= 5.916 \times 10^{-17} \text{ GeV}^2\end{aligned}$$

A complete, up-to-date tabulation of the fundamental constants and the properties of elementary particles is given in the *Review of Particle Properties*, which can be found in a recent issue of either *Physical Review D* or *Physics Letters B*. The most recent *Review* as of this writing is published in *Physical Review D50*, 1173 (1994).

Bibliography

Mathematical Background and Reference

- Cahn, Robert N., *Semi-Simple Lie Algebras and Their Representations*, Benjamin/Cummings, Menlo Park, California, 1984. Written by a physicist, for physicists.
- Carrier, George F., Krook, Max, and Pearson, Carl E., *Functions of a Complex Variable*, McGraw-Hill, New York, 1966. An excellent practical introduction to methods of complex variables and contour integration.
- Gradshteyn, I. S. and Ryzhik, I. M., *Table of Integrals, Series, and Products* (trans. and ed. by Alan Jeffrey), Academic Press, Orlando, Florida, 1980.

Physics Background

- Baym, Gordon, *Lectures on Quantum Mechanics*, Benjamin/Cummings, Menlo Park, California, 1969. A concise, informal text that is especially rich in nontrivial applications.
- Fetter, Alexander L. and Walecka, John Dirk, *Theoretical Mechanics of Particles and Continua*, McGraw-Hill, New York, 1980. Includes several chapters on continuum mechanics and useful appendices of mathematical reference material.
- Feynman, Richard P., *QED: The Strange Theory of Light and Matter*, Princeton University Press, Princeton, New Jersey, 1985. A transcription of four lectures given to a general audience, presenting Feynman's approach to quantum mechanics, including Feynman diagrams. Highly recommended.
- Feynman, Richard P. and Hibbs, A. R., *Quantum Mechanics and Path Integrals*, McGraw-Hill, New York, 1965. An introduction to the use of path integrals in nonrelativistic quantum mechanics.
- Goldstein, Herbert, *Classical Mechanics* (second edition), Addison-Wesley, Reading, Massachusetts, 1980. Chapter 12 introduces classical relativistic field theory.
- Jackson, J. D., *Classical Electrodynamics* (second edition), Wiley, New York, 1975.

- Landau, L. D. and Lifshitz, E. M., *The Classical Theory of Fields* (fourth revised English edition, trans. Morton Hamermesh), Pergamon, Oxford, 1975. Contains a succinct development of electromagnetic theory from the Lagrangian viewpoint.
- Landau, L. D. and Lifshitz, E. M., *Statistical Physics* (third edition, Part 1, trans. J. B. Sykes and M. J. Kearsley), Pergamon Press, 1980. An insightful if concise textbook of statistical mechanics, containing the original pedagogical exposition of Landau's theory of phase transitions.
- Reichl, L. E., *A Modern Course in Statistical Physics*, University of Texas Press, Austin, 1980. A complete textbook of statistical mechanics.
- Schiff, Leonard I., *Quantum Mechanics* (third edition), McGraw-Hill, New York, 1968.
- Shankar, Ramamurti, *Principles of Quantum Mechanics*, Plenum, New York, 1980. A very clear presentation of the basic theory.
- Taylor, Edwin F. and Wheeler, John Archibald, *Spacetime Physics* (second edition), Freeman, New York, 1992. An elementary but insightful introduction to special relativity.
- Taylor, John R., *Scattering Theory*, Robert E. Krieger, Malabar, Florida, 1983 (reprint of original edition published by Wiley, New York, 1972). A very clear development of scattering theory for nonrelativistic quantum mechanics.

Relativistic Quantum Mechanics and Field Theory

- Bailin, D. and Love, A., *Introduction to Gauge Field Theory*, Adam Hilger, Bristol, 1986. Develops the theory entirely from the path integral viewpoint.
- Balian, Roger and Zinn-Justin, Jean (eds.), *Methods in Field Theory*, North-Holland, Amsterdam, 1976. Proceedings of the 1975 Les Houches Summer School in Theoretical Physics, including lectures on functional methods, renormalization, and gauge theories.
- Berestetskii, V. B., Lifshitz, E. M., and Pitaevskii, L. P., *Quantum Electrodynamics* (second edition, trans. J. B. Sykes and J. S. Bell), Pergamon, Oxford, 1982. An excellent reference for QED applications.
- Bjorken, James D. and Drell, Sidney D., *Relativistic Quantum Mechanics*, McGraw-Hill, New York, 1964. Develops Feynman diagrams using intuitive arguments, without using fields.
- Bjorken, James D. and Drell, Sidney D., *Relativistic Quantum Fields*, McGraw-Hill, New York, 1965. Redevelops Feynman diagrams from the field viewpoint, using canonical quantization.
- Brown, Lowell S., *Quantum Field Theory*, Cambridge University Press, New York, 1992. A careful treatment of the foundations of quantum field theory and its application to scattering processes.

- Coleman, Sidney, *Aspects of Symmetry*, Cambridge University Press, Cambridge, 1985. Informal lectures on a number of topics involving gauge theories and symmetry, given between 1966 and 1979.
- Collins, John, *Renormalization*, Cambridge University Press, Cambridge, 1984. A careful development of the technical machinery needed for all-orders proofs of renormalizability, operator product expansion, and factorization theorems.
- Deser, Stanley, Grisaru, Marc, and Pendleton, Hugh, *Lectures on Elementary Particles and Quantum Field Theory*, MIT Press, Cambridge, 1970, vol. 1. Four extremely useful summer school lectures.
- Gross, Franz, *Relativistic Quantum Mechanics and Field Theory*, Wiley, New York, 1993. Includes a number of topics in "advanced quantum mechanics", and an introductory chapter on bound states.
- Itzykson, Claude and Zuber, Jean-Bernard, *Quantum Field Theory*, McGraw-Hill, New York, 1980. A comprehensive textbook.
- Jauch, J. M. and Rohrlich, F., *The Theory of Photons and Electrons* (second edition), Springer-Verlag, Berlin, 1976. An authoritative monograph on QED.
- Kaku, Michio, *Quantum Field Theory: A Modern Introduction*, Oxford University Press, New York, 1993. Contains brief introductory chapters on a number of advanced topics.
- Kinoshita, T., ed., *Quantum Electrodynamics*, World Scientific, Singapore, 1990. A collection of review articles on precision tests of QED.
- Mandl, F. and Shaw, G., *Quantum Field Theory*, Wiley, New York, 1984. The easiest book on field theory; introduces QED and some electroweak theory using canonical quantization.
- Ramond, Pierre, *Field Theory: A Modern Primer* (second edition), Addison-Wesley, Redwood City, California, 1989. Contains very nice treatments of the Lorentz group, path integrals, ϕ^4 theory, and quantization of gauge theories.
- Ryder, Lewis H., *Quantum Field Theory*, Cambridge University Press, Cambridge, 1985. A concise treatment of the more formal aspects of the subject.
- Sakurai, J. J., *Advanced Quantum Mechanics*, Addison-Wesley, Reading, 1967. Develops Feynman diagrams without using fields.
- Schweber, Silvan S., *QED and the Men Who Made It: Dyson, Feynman, Schwinger, and Tomonaga*, Princeton University Press, Princeton, 1994. An excellent history of the subject up to about 1950.
- Schwinger, Julian (ed.), *Selected Papers on Quantum Electrodynamics*, Dover, New York, 1958. Reprints of important papers written between 1927 and 1953.
- Sterman, George, *Introduction to Quantum Field Theory*, Cambridge University Press, Cambridge, 1993. An introductory textbook with special emphasis on the essentials of perturbative QCD.

Elementary Particle Physics

- Aitchison, Ian J. R. and Hey, Anthony J. G., *Gauge Theories in Particle Physics* (second edition), Adam Hilger, Bristol, 1989. An elementary introduction to gauge theories, concentrating mostly on tree-level processes.
- Barger, Vernon and Phillips, Roger J. N., *Collider Physics*, Addison-Wesley, Menlo Park, California, 1987. Basic discussion of the application of QCD to high-energy collider phenomenology.
- Cahn, Robert N. and Goldhaber, Gerson, *The Experimental Foundations of Particle Physics*, Cambridge University Press, Cambridge, 1989. Reprints of many original papers, supplemented by introductory overviews, additional references, and exercises. Highly recommended.
- Cheng, Ta-Pei and Li, Ling-Fong, *Gauge Theory of Elementary Particle Physics*, Oxford University Press, New York, 1984. An advanced, authoritative monograph.
- Commins, Eugene D. and Bucksbaum, Philip H., *Weak Interactions of Leptons and Quarks*, Cambridge University Press, Cambridge, 1983. A thorough review of both theory and experiment.
- Field, Richard D., *Applications of Perturbative QCD*, Benjamin/Cummings, Menlo Park, 1989. A useful description of the techniques needed for QCD calculations beyond the leading order.
- Georgi, Howard, *Weak Interactions and Modern Particle Theory*, Benjamin/Cummings, Menlo Park, California, 1984. Advanced, insightful treatment of selected topics.
- Griffiths, David, *Introduction to Elementary Particles*, Wiley, New York, 1987. A good undergraduate-level survey.
- Halzen, Francis and Martin, Alan D., *Quarks and Leptons: An Introductory Course in Modern Particle Physics*, Wiley, New York, 1984. Uses Feynman diagrams throughout, and concentrates on gauge theories.
- Perkins, Donald H., *Introduction to High Energy Physics* (third edition), Addison-Wesley, Menlo Park, California, 1987. A good introduction to phenomena, with relatively little emphasis on Feynman diagrams and gauge theories.
- Ross, Graham G., *Grand Unified Theories*, Benjamin/Cummings, Menlo Park, California, 1984. A clear introduction to gauge theories that unify the interactions of particle physics.
- Quigg, Chris, *Gauge Theories of the Strong, Weak, and Electromagnetic Interactions*, Benjamin/Cummings, Menlo Park, California, 1983. A very nice overview of gauge theories and their experimental tests.
- Taylor, J. C., *Gauge Theories of Weak Interactions*, Cambridge University Press, Cambridge, 1976. A concise treatment of the standard model and related theoretical issues.

Condensed Matter Physics

- Abrikosov, A. A., Gorkov, L. P., and Dzyaloshinskii, I. E., *Quantum Field Theoretical Methods in Statistical Physics* (second edition), Pergamon, Oxford, 1965. A classic, but very terse, exposition of the application of Feynman diagrams to condensed matter problems.
- Anderson, P. W., *Basic Notions of Condensed Matter Physics*, Benjamin/Cummings, Menlo Park, California, 1984. An informal overview of the concepts of broken symmetry and renormalization as applied to condensed matter systems.
- Fetter, Alexander L. and Walecka, John Dirk, *Quantum Theory of Many-Particle Systems*, McGraw-Hill, New York, 1971. A straightforward introduction to the use of Feynman diagrams in nuclear and condensed matter physics.
- Ma, Shang-Keng, *Modern Theory of Critical Phenomena*, Benjamin/Cummings, 1976. An introduction to the use of renormalization group methods in the theory of critical phenomena.
- Mattuck, Richard D., *A Guide to Feynman Diagrams in the Many-Body Problem*, McGraw-Hill, New York, 1967. A clear and easy introduction to the use of Feynman diagrams in solid state physics.
- Parisi, Giorgio, *Statistical Field Theory*, Benjamin/Cummings, 1988. Far-ranging applications of ideas from quantum field theory to problems in statistical mechanics.
- Stanley, H. Eugene, *Introduction to Phase Transitions and Critical Phenomena*, Oxford University Press, Oxford, 1971.
- J. Zinn-Justin, *Quantum Field Theory and Critical Phenomena* (second edition), Oxford University Press, Oxford, 1993. A treatise on the application of renormalization theory to the study of critical phenomena.

Corrections to This Book

A list of misprints and corrections to this book is posted on the World-Wide Web at the URL '<http://www.slac.stanford.edu/~mpeskin/QFT.html>', or can be obtained by writing to the authors. We would be grateful if you would report additional errors in the book, or send other comments, to mpeskin@slac.stanford.edu or to dschroeder@cc.weber.edu.

Index

- A_{LR}^f (polarization asymmetry at Z^0), 710–712, 728, 760–763, 771–772
 Abelian group, 487, 496
 Abelian Higgs model, 690–692, 732–739
 Accelerated track, xiv
 Acknowledgments, xvii
 Action, 15, 277
 Active transformations, 35–37
Ad hoc subtraction, 195, 221–222, 230
 Adjoint representation, 499, 501–502
 Adler-Bell-Jackiw anomaly, 661–667, 672–676, 686, 688, 705–707
 operator equation, 661
 ALEPH experiment, 711
 Alloys, binary, 267–268, 272, 437
 α (critical exponent), 441, 446–447
 α (fine-structure constant), xxi, 125, 809
 measurements of, 197–198
 radiative corrections to, 252–257, 335, 424, 762–764
 α_* ($\alpha(m_Z)$), 759
 α_s , 260–262, 550, 573, 712
 measurements of, 593–595
 running of, 551–553, 594–595
 α^i (Dirac matrices), 52
 Altarelli-Parisi equations, xvi, 590–593, 597–598, 644–647, 649
 splitting functions for QED, 587
 splitting functions for QCD, 590
 initial conditions, 587, 591
 Ambiguity in choice of momentum scale, 552, 573
 Amplitude, in quantum mechanics, 276
 Amplitude (\mathcal{M}), see Scattering amplitude
 Amputated diagrams, 109, 113–114, 175, 227–229, 331
 Analogies to statistical mechanics, 266–275, 292–294, 364, 367 (table), 395, 440–442, 788
 Analytic continuation to Euclidean space, 293
 Analytic properties of amplitudes, 211–237, 252–253, 619–621, 633, 808
 Angular momentum, 6–7, 38–39, 60, 144, 147
 Annihilation, see e^+e^- annihilation, Cross section
 Annihilation operators, 26, 58, 123
 Anomalous dimensions, 427, 447, 613–615, see also γ
 Anomalous magnetic moment, 188, 210
 of electron, 196–198
 of muon, 197–198, 773
 Anomaly, see Axial vector anomaly, Adler-Bell-Jackiw anomaly, Trace anomaly
 Anomaly cancellation, 705–707, 799
 Anomaly coefficient, 680–681, 687–688
 Anomaly-free theories, 679–681, 786
 Anticommutation relations, Dirac, 40, 56
 Anticommuting numbers, 73, 298–302, 518
 Antifermions, 59, 61, 804
 Antiferromagnets, 449–450
 Antilinear operator, 67
 Antiparticles, 4, 14, 29
 Antiquarks, see Quarks, Parton distribution functions
 Antiscreening, 542–543

- Antiunitary operator, 67
- Area of d -dimensional unit sphere, 249
- Arnowitt-Fickler gauge, 544
- Arrogance, 81
- Arrows, in diagrams, 5, 118–119
- Asterisk in Contents, xiv
- Asymmetries at Z resonance, see A_{LR}^f
- Asymptotic behavior of amplitudes, 265, 341, 344–345, 418–421
- Asymptotic freedom, 425–427, 505
- in Gross-Neveu model, 438
 - in nonlinear sigma model, 458–461
 - in QCD, 140, 479–480, 551–554, 627, 782, 784
 - in gauge theories, 531–543
 - intuitive explanations, 460, 541–543
 - price of, 543
 - see also α_s , β
- Asymptotic states, 102–104, 108–109, 223–226, 298
- classification by BRST operator, 519–520
- Asymptotic symmetry, 438
- Atomic energy levels,
- effects of QED, 197–198, 253
 - effects of weak interaction, 709, 712
- Atomic scale, 266–267, 272, 395, 402
- Attractive forces, 122–125
- Auxiliary field, 74, 517
- Averaging over short-wavelength fluctuations, 460–461
- Awkward phases and overlap factors, 108–109, 284
- Axial vector anomaly,
- in 2 dimensions, 651–658
 - in 4 dimensions, 661–667, 672–676, 686, 688, 705–707
 - in d dimensions, 667
- Axial vector currents, 50–51, 651–667, 705–707
- of QCD, 668–676, 794
- Axion, 210, 726
- Background field perturbation theory, 533–535, 685
- Background gauge fields, 304–305, 533–540, 653–667, 684–685, see also Classical source, Effective action
- Backward polarization, 511
- Bacteria, 418–420, 433–434
- Bar notation, 43, 44, 132
- Bare coupling constants, 247, 252, 258, 334–335, 410, 425
- Bare Green's functions, 410
- perturbation theory with, 323, 326, 353, 416–417
- Bare mass, 214
- Barn (cross section unit), 810
- Baryon number current, 668
- Baryon number, nonconservation of, 647
- Baryons, 473, 546–547
- Beams of particles, 99–100, 151
- Bessel functions, 34
- β (Callan-Symanzik function), 410–417, 420, 424–428, 684–685
- sign of, 424–426
 - zero of, 425, see also Fixed point
 - in d dimensions, 435, 449
 - dependence on conventions, 427–428
 - for ϕ^4 theory, 413
 - for linear sigma model, 448
 - for nonlinear sigma model, 457, 464
 - for Gross-Neveu model, 438
 - for Yukawa theory, 438
 - for scalar QED, 470
 - for non-Abelian gauge theories, 531, 544
- in supersymmetric models, 787, 796–797
- see also Asymptotic freedom
- β (critical exponent), 274, 441, 446–447
- $B(\alpha, \beta)$ (Beta function), 250
- beta-brass, 449–450
- beta decay, 671, 709
- Bethe's ansatz, 792
- Bhabha scattering ($e^+e^- \rightarrow e^+e^-$), 10, 152–153, 157, 170, 171, 235–236, 253, 256
- Bianchi identity, 500
- Bifurcation, at critical point, 269
- Bilinears of Dirac fields, 49–52, 71
- Binary alloys, 267–268, 272, 437
- Binary fluids, 449–450
- Bjorken, J. D., 476
- Bjorken scaling, 478–480, 558, 635
- violation of, 480, 545, 562, 574, 588, 593–594, 635

- Bloch, F., 202
 Bogoliubov, N. N., 337–338
 Bohr radius, 809
 Boldface type, xix
 Bookkeeping, alternative methods, 326
 Boosts, 40–41, 71–72
 Born approximation, 121
 Bose-Einstein statistics, 22
 Bound states, 76, 140–141, 148–153, 213
 production amplitude for, 149–150
 Boundary conditions, Feynman, 95
 BPHZ (Bogoliubov-Parasiuk-Hepp-Zimmermann) theorem, 338, 384, 386
 Branch cut singularities, 215–216, 230,
 see also Analytic properties of amplitudes
 Breit-Wigner formula, 101, 237, 728
 Bremsstrahlung, 11, 175–184, 208, 580–584
 classical theory, 177–182
 Broad resonances, 237
 BRST (Becchi-Rouet-Stora-Tyutin) symmetry, 517–521, 734
- C* (charge conjugation), 64, 70–71, 75–76, 135, 318, 720–727
 $C(r)$ (invariant of Lie algebra representation), 498, 500–502, 504, 806
 $C_2(r)$ (quadratic Casimir operator), 500–502, 504, 806
 Cabibbo angle, 605, 714, 724, see also CKM matrix
 Cactus diagram, 92
 Callan, C., 411, 418
 Callan-Gross relation, 558, 626, 632
 Callan-Symanzik equation, 410–414, 418–423, 452, 464
 solution of, 418–423
 with local operators, 430, 433–434, 613–614
 for 1PI Green's functions, 444
 for effective action, 445
 for electromagnetic potential, 423
 for annihilation cross-section, 551–552
 for operator product coefficients, 613–614
 Callan-Symanzik functions, see β , γ
 Cancellations, see Unphysical degrees of freedom
 Cartan, E., 496
 Casimir operator, see $C_2(r)$
 Causality, 13–15, 27–29, 54
 CDF experiment, 573, 772
 CDHS experiment, 561
 Center-of-mass frame, 4, see also Kinematics
 Center-of-mass coordinate, 148
 Channels, 157
 Characteristics, method of, 418
 Charge conjugation, see *C*
 Charge, conserved, 18
 of a Dirac particle, 62
 see also Coupling constants, Current
 Charged-current weak interactions, 709
 Cheats, in Part I, 211
 Chiral fermions, 267, 676–768
 Chiral gauge theories, 676–682
 Chiral representation of γ^μ , 41
 Chiral symmetry, 51, 319
 in functional formalism, 664–667
 breaking of, 669–671, 719, 789
 see also Axial vector currents, Axial vector anomaly
 CKM (Cabibbo-Kobayashi-Maskawa) matrix, 714, 723, 730, 790
 phase, 724–726
 Classical electromagnetism, 33, 221, see also Bremsstrahlung
 Classical electron radius, 809
 Classical field theory, 15–19, 266, 682–683
 Classical field (of the effective potential formalism), 366–367, see also Background field, Effective action
 Classical groups, 496
 Classical path, 276
 Classical solutions, nontrivial, 793–794
 Classical source, 32–33, 126–127, 290–292, 365–367
 Clebsch-Gordan coefficients, 7, 145
 Clusters of spins, 267–268
 Coleman, S., 418
 Coleman-Mandula theorem, 795
 Coleman-Weinberg model, 469–470

- Collinear emission
 of photons, 173–174, 181–184, 209–
 210, 574–587, 710–711
 of e^+e^- pairs, 584–586
 of gluons, 550, 553–554, 574–575,
 587–588
- Color (of quarks), 139–140, 546–548
 confinement of, 547–548, 782, 784
 factor of 3, 140, 259, 548–549, 564,
 589, 674, 770
 see also Group theory relations
- Combining denominators, see Feynman
 parameters
- Commutation relations, for fields, 19–20,
 52, see also Lie algebras
- Commutator of covariant derivatives,
 485, 488
- Commutator of field operators, 28
- Comparator, 482–484, 487, see also
 Wilson line
- Completeness relation for states, 23, 212
- Completeness relations for spinors,
 48–49
- Complex conjugation, of fermion bilin-
 ears, 132
- Complex scalar field, 18, 29, 33–34,
 75–76, 312
- Compton formula, 162–163
- Compton scattering ($e^-\gamma \rightarrow e^-\gamma$), 11,
 158–167, 623
- Compton wavelength, xix, 122, 294, 809
- Condensate of $q\bar{q}$ pairs, 669
- Condensed matter physics, xiv, 266–274,
 792
- Conformally invariant theories, 792–793
- Conjugate representation, 498
- Connected correlation function, 380
- Connected diagrams, 109, 111–114
- Connection, 483, 487
- Conservation laws, 17–18, 34, 306,
 308–310
 for Dirac vector current, 51, 160, 244,
 311
 see also Angular momentum, Axial
 vector currents, Current, Energy-
 momentum tensor
- Constituents of the proton, see Parton
 model
- Contact terms, 307–312
- Continuous symmetry groups, see
 Groups, continuous
- Contractions, 89, 116, 118
 counting of equivalent, 92–93
 for external states, 110, 117
 in functional formalism, 288
- Conversion factors, 809–810
- Convexity of effective potential, 368–369
- Correction-to-scaling exponent, 466
- Corrections to this book, 815
- Correlation functions, 82
 perturbation expansion for, 87
 Feynman rules for, 94–95
 analytic structure of, 211–230
 relation to S -matrix, 227–229
 of Dirac fields, 115, 302
 of spin field, 272–273, 293, 389, 395,
 440–442
 functional computation, 283–284, 302
 of non-gauge-invariant operators,
 296–298
 scaling of, 406
 defined at scale M , 408
 bare vs. renormalized, 410
 see also Asymptotic behavior of
 amplitudes
- Correlation length, 272–273, 294, 436,
 440–441, 783
- Cosmological constant, 790–791, 797
- Coulomb gauge, 79, 541
- Coulomb potential, xxi, 125, 179, 503,
 542, 782
 radiative corrections to, 253–255, 423,
 762
- Coulomb scattering, 129–130, 155,
 169–170
- Counterterms, 324–326
 for ϕ^4 theory, 324–329, 408–409
 for Yukawa theory, 329–330, 409
 for QED, 331–334
 for linear sigma model, 353–354
 constrained by symmetry, 353–363,
 383–386, 738
- for $J(x)$, 370
- for computation of effective action,
 370–372
 relation to β and γ , 412–416
 for local operators, 429–432

- Counterterms, cont.
- for non-Abelian gauge theory, 527–533, 544
 - for GWS theory, 758
 - see also β , γ
- Counting, see Color, Contractions, Identical particles
- Coupling constants, 77–80
- dimensions of, 80, 322
 - bare vs. renormalized, 246–247, 252, 258, 334–335, 410, 425
 - effective or scale-dependent, 247, 255–257, see also Running coupling constant
 - equality of (in gauge theories), 508–510
 - in GWS theory, 701–703, 713–716
 - extrapolation to GUT scale, 786–787, 797
 - see also α , α_s , $\sin^2 \theta_w$
- Coupling to EM field, 78
- Covariant derivative, 78, 483, 485, 487–488, 490, 499
- in GWS theory, 703
- CP invariance, 64–65, 596, 721–726, 790
- CP^N model, 466–468
- CPT invariance, 64, 71, 76
- Creation and annihilation operators, 26, 58, 123
- Critical exponents, 272–274, 435–438, 440–451, 462, 466
- definitions, 441
 - relations among, 447
 - measurements of, 437, 449–451
- Critical point, 267, 269–274, 395, 406, 436, 440, 461, 465, 788
- Cross section, 4, 99–107, 237, 808
- relation to S -matrix, 106–107
 - Rutherford, 130
 - Thomson, 163, 809
 - for linear sigma model, 128
 - for Coulomb scattering, 130, 154, 169
 - for $e^+e^- \rightarrow \mu^+\mu^-$, 136, 143, 809
 - for $e^+e^- \rightarrow$ hadrons, 140, 262, 552
 - for bound state production, 151
 - for Compton scattering, 163
 - for $e^+e^- \rightarrow \gamma\gamma$, 168
 - for Bhabha scattering, 170
 - for ep elastic scattering, 208
- Cross section, cont.
- for $e^+e^- \rightarrow \bar{q}qg$, 261, 553
 - for deep inelastic scattering, 558
 - for deep inelastic ν , $\bar{\nu}$ scattering, 561
 - for Drell-Yan process, 566, 568
 - for parton-parton reactions, 568
 - for elementary QCD processes, 569–572
 - for $e^+e^- \rightarrow W^+W^-$, 757, 773
 - for $d\bar{u} \rightarrow W^-\gamma$, 773
- Crossing symmetry, 155, 168, 230
- CTEQ collaboration, 563, 573, 590, 643
- Current, conserved, 18, 244
- electromagnetic, xxi
 - of charged scalar field, 18
 - of classical point particle, 177
 - of Dirac fields, 50–51
 - for rotations, 60
 - normalization of, 430
 - of fermions in non-Abelian gauge theory, 491, 533
 - of fermions in GWS theory, 705
 - see also Axial vector current, Conservation laws. Noether's theorem, Ward identity
- Custodial $SU(2)$ symmetry, 719
- Cutkosky rules, 233–236, 515
- Cutoff, ultraviolet, 80, 266–268, 394–406, 409, 464–465, 788–790
- momentum, as a regulator, 257, 394–395, 458–461, 662
- Cutting rules, see Cutkosky rules
- D (degree of divergence), 316
- \mathcal{D} (measure of functional integral), 276
- D0 experiment, 772
- D_F , see Feynman propagator
- de Broglie wavelength, 103, 277
- Decay rate of a particle, 101, 107–108, 127, 151, 237, 808
- Decomposition of group representations, 501–502
- Deep inelastic scattering, 475–480, 547, 555–563, 591–592, 621–647
- from a photon, 649
 - neutral-current, 709, 712, 729
 - neutrino, 559–561, 593–594, 606, 634–635, 709, 712

- Definition of a quantum field theory, 283
 Definition of a theory at scale M , 408
 Definition of physical parameters, 325
 Degree of divergence, see D
 DELCO experiment, 138
 Delicate adjustments, 406, 788
 DELPHI experiment, 711
 δ (critical exponent), 441, 446–447
 δ function, xx–xxi
 functional, 295
 in parton splitting functions, 580–581
 $\delta_Z, \delta_m, \delta_1$, etc., see Counterterms
 $\Delta I = 1/2$ rule, 611–612
 Δ^{++} baryon, 546
 Democracy, functional, 276
 Derivative interactions, 80, 312, 399
 Detector sensitivity, 200–202, 207–208
 Determinant, see Functional determinant
 Dielectric property of vacuum, 255, 541
 Differential cross section, see Cross section
 Dilatation current, 683
 Dimensional analysis of renormalizability, 80, 322, 402
 Dimensional regularization, 248–251, 257, 333, 409, 524, 662, 681, 684, 767, 807–808
 Dimension of space, effect on scalar field theory, 465–466
 Dirac, P. A. M., 40
 Dirac algebra, see γ^μ
 Dirac equation, 3, 13, 35, 40–44, 803
 solutions of, 45–48
 see also γ^μ
 Dirac field, 42–75
 bilinears of, 49–52
 quantized, 58
 see also Feynman rules
 Dirac Hamiltonian, 52
 Dirac hole theory, 61, 658–659, 790
 Dirac matrices, see γ^μ
 Dirac representation, 40–41
 reducibility of, 41–50
 Dirac spinors, 41, 803
 Disclaimers, xv–xvi
 Disconnected diagrams, 96, see also Connected diagrams, Exponentiation
 Discontinuities, see Analytic properties of amplitudes
 Discrete symmetry, 348, see also C, P, T
 Disorder, 460–461
 Dispersion relations, 619–621, 632–634
 Displacive phase transitions, 469
 Distribution functions, see Parton distribution functions
 Distributions, xx–xxi
 $1/(1-x)_+$, 581
 Divergence-free theories, 321, 797
 Divergences, see Infrared divergences, Ultraviolet divergences
 Domains in a ferromagnet, 267
 Double logarithm, see Sudakov double logarithm, Two-loop diagrams
 Double-slit experiment, 276–277
 Double-well potential, 271, 349
 Drell-Yan process, 564–568
 Duality, particle-wave, 26
 Dyson, F., 82

 e (electron charge), xxi
 in GWS theory, 702
 e^+e^- annihilation
 to muons or τ leptons, 4, 131–153, 171
 to hadrons, 139–141, 259–262, 474, 548–554, 615–621, 710–711, 728–729
 to scalars, 312, 750–754
 to W^+W^- , 750–757, 773
 E_6, E_7, E_8 (Lie algebras), 497, 681
 $E[J]$ (vacuum energy), 365–367
 Eating, of Goldstone boson, 692, 744
 Effective action, 364–391, 443–444, 533, 535–537, 720
 computation of, 370–379
 as generating functional, 379–383
 Callan-Symanzik equation for, 444
 Effective coupling constant, see Running coupling constant
 Effective field theory, 266, 800
 Effective Lagrangian, 396–403
 for W exchange, 559, 605
 Effective mass, 403, 600–603, 669–670
 Effective potential, 367–369, 375, 384, 391, 443–445
 for $O(N)$ ϕ^4 theory, 376–379, 451–453
 for Coleman-Weinberg model, 469–470

- Electric dipole moment of neutron, 726
 Electromagnetic current, 18, 50–51, 705
 Electromagnetic field, 78–79
 quantization of, 79, 123, 124, 294–298
 in GWS theory, 701–702
 Electromagnetic field tensor, 33, 78, 484–485, 492
 Electromagnetic potential, see Coulomb potential
 Electromagnetism, xxi, 33, 64, 473, see also QED
 Electron, 4, 124
 structure of, 575–587
 see also Cross sections, e^+e^- annihilation, $\Sigma(p)$
 Electroweak theory, see GWS theory
 Energy functional, 365–367, 370, 372, 379–380
 Energy, in EM field, 179
 Energy, infinite, 21
 Energy, negative, 26, 54
 Energy-momentum fractions, see Parton distribution functions
 Energy-momentum tensor, 19, 310, 430, 682–685, 790–791
 symmetric, 642
 for electromagnetic field, 33, 683–685
 for QCD, 630, 642, 685
 Enhancements, see Logarithmic enhancements
 $\epsilon(4-d)$, 250, 377, 449
 ϵ expansion, 436, 449
 $\epsilon^{\mu\nu\rho\sigma}$, xx
 contraction identities, 134, 805
 Equal-time commutation relations, 20
 Equality of coupling constants, 514, 531
 Equation of motion, 16, 25
 for Green's functions, 306–312
 for gauge field, 500
 Equivalence theorem, Goldstone boson, 743–758
 Equivalent photon approximation, 209–210, 579
 Estimation of divergent part of a diagram, 529
 η (critical exponent), 273–274, 441, 443, 447, 466
 Euclidean space, 293, 394–395, 439, 807
 4-momentum in, 193
 Euler-Lagrange equation, 16, 308
 Event shapes, 593–594
 Evolution equations, see Altarelli-Parisi equations
 Evolution of parameters, see Running coupling constant, Callan-Symanzik equation
 Evolution of parton distributions, 574–593, 644–647
 Exactly solvable field theories, 81, 405, 791–794
 for large N , 463–465, 467
 Exotic contributions to anomalous magnetic moments, 210
 Experimental tests of quantum field theory, see Critical exponents, QED, QCD, GWS theory
 Exponentiation, 126, 207
 of disconnected diagrams, 96–98, 113, 399
 Extended supersymmetry, 425, 796–797
 External field, 185, 292, 304
 Feynman rule for, 129
 External leg corrections, 113, 175, 195
 External lines, see Feynman rules
 External source, see Classical source
 Extreme limit $q^2 \rightarrow \infty$, 642–643
- $f_e(x)$ (distribution function of electron in electron), 580–581, 583
 $f_f(x)$ (distribution function), 477, 556
 $f_\gamma(x)$ (distribution function of photon in electron), 579, 583
 $f^+(x)$ (distribution function), 632
 $f^-(x)$ (distribution function), 635
 f^{abc} (structure constants), 490, 495, 498–499, 806
 f_π (pion decay constant), 670–676, 687
 $F_1(q^2)$ (form factor), 186, 196, 230, 260, 334
 infrared divergence, 199–200
 $F_2(q^2)$ (form factor), 186, 196
 F_4 (exceptional Lie algebra), 497
 F^a_k (matrix connecting currents to Goldstone bosons), 698–700, 718, 739–742
 of $SU(3)$, 502
 see also Lie algebra

- $F_{\mu\nu}$ (field tensor)
 electromagnetic, 33, 78, 484–485, 492
 non-Abelian, 488–489, 494
- Faddeev-Popov Lagrangian, 514, 517
- Faddeev-Popov method, 295–298, 512–515, 533–534, 731–734, 741, see also Ghosts
- Fermi constant, see G_F
- Fermi-Dirac statistics, 57, 120, 313, 546–547
- Fermion couplings, in GWS theory, 703–705
- Fermion loops, 120, 801
- Fermion masses, 723
 in GWS theory, 704, 713–715
- Fermion minus signs, 116, 119–120
- Fermion number nonconservation, 657–659, 686–687
- Fermion self-energy, see $\Sigma(p)$
- Fermion-antifermion annihilation, see e^+e^- annihilation, Cross section
- Fermion-fermion scattering
 nonrelativistic, 121–123, 125–126
 in broken gauge theory, 735–737
- Fermions and antifermions, 59
 Feynman rules for, 115–120
- Ferromagnets, see Magnets
- Feynman, R. P., 82, 275, 476
- Feynman boundary conditions, 31, 95, 287–288
- Feynman diagrams, 3, 5, 211
 for correlation functions, 90–99
 for scattering amplitudes, 109–115
 general procedure for evaluating, 138
 relation to S -matrix, 229
 optical theorem for, 232–236
 for computing functional determinants, 304–305
 for computation of V_{eff} , 375
 see also Feynman rules, Perturbation theory
- Feynman gauge, 297, 416, see also Feynman-’t Hooft gauge
- Feynman parameters, 189–190, 342, 806
- Feynman prescription, see Feynman boundary conditions
- Feynman propagator, 31, 63, 213, 287–288, 293, 302
- Feynman rules, 5, 8, 94–95, 114–115, 801–803
 position-space, 94, 114
 momentum-space, 95, 115
 symmetry factors, 93, 118
 for correlation functions, 94–95
 for scattering amplitudes, 114–115
 for interaction with an external field, 129, 304
 for counterterms, 325, 331–332, 528
 functional derivation of, 284–289
 for ϕ^4 theory, 94–95, 114–115, 325, 801
 for Yukawa theory, 118
 for QED, 123, 303, 331–332, 801–802
 for scalar QED, 312
 for linear sigma model, 353–354
 for nonlinear sigma model, 455–456
 for non-Abelian gauge theory, 506–508, 514–515, 528, 802–803
 for scalar non-Abelian gauge theory, 544
 for Abelian Higgs model, 734–735
 for broken gauge theory, 742
 for GWS theory, 716, 743, 752–753
- Feynman-’t Hooft gauge, 513, 535, 640, 732, 737–738, 746, 749–750
- Fictitious heavy photons, see Pauli–Villars regularization
- Field operator, 20
 interpretation of, 24, 26
- Field rescaling, see Field-strength renormalization
- Field tensor, see $F_{\mu\nu}$
- Field-strength renormalization, 211–230, 408–410, 417, 421–422
 for electron (Z_2), 216, 220–221, 330–335
 for photon (Z_3), 246
 for ϕ^4 theory, 328–329, 345
 for Yukawa scalar, 330
 for non-Abelian gauge theory, 531–533
 for local operators ($Z_{\mathcal{O}}$), 429–432
 see also Counterterms
- Fierz transformations, 51–52, 75, 170, 607–609, 805
- Fine-structure constant, see α
- Finite quantum field theories, 425

- First-order phase transition, 269–270
- Fixed point (of renormalization group), 401–405, 424–426, 791–793
- free-field, 401–403, 407
 - and critical exponents, 443
 - Wilson-Fisher, 405, 435, 439, 441, 445, 448–449, 454, 461–462, 466
 - effect on operator product expansion, 614
 - see also Renormalization group, Running coupling constant
- Flavor (of quarks), 139, 259, 546
- Flavor mixing, 714–715
- Flavor symmetry, 670–671
- Flavor-changing neutral currents, 725
- Flipped spinor, 68
- Flow of coupling constant, 420
- Flow of Lagrangian, 401
- Fluctuations, 294, 393–394, see also Correlation length
- Fluids, 266, 437, 439
- Forces of Nature, symmetries of, 64, 719–727
- Form factors
- for QED current, 184–188, 208–209, 229
 - for axial vector current, 671–672
 - for deep inelastic scattering, 625, 647–648
- Forward Compton amplitude, 623–627
- Forward polarization, 511
- Forward scattering amplitude, 230–232
- Forward-backward asymmetry, 711–712
- 4π , factors of, xxi
- Four-gauge-boson vertex, 507
- Four-momentum, xix, 212–213
- Four-photon amplitude, QED, 320, 344
- Four-point function, see Correlation functions, Asymptotic behavior of amplitudes
- Four-vectors, xix
- built out of spinors, 72
- Fourier transforms, xx–xxi
- Fourth neutrino species, 729
- Fractional charges, 546, 786
- Free energy, 364–367, see also Gibbs free energy
- Free field theory, 19–29, 404, 458
- Free-field fixed point, 439, 441
- Frequency, positive/negative, 26, 45, 48
- Fujikawa’s derivation of axial vector anomaly, 664–667
- Functional, 276
- Functional delta function, 295
- Functional derivative, 276, 289–290
- Functional determinant, 287, 295, 304–305, 313, 371–375, 391, 512–514, 517, 535–540
- from Gaussian integration, 301
 - methods for evaluating, 304, 374
- Functional integral, 275–314, 394–400, 458, 503, 512–514, 534
- methods for evaluating, 284–288, 299–301, 370–373
 - momentum slicing, 395–399
 - chiral transformation of, 664–667
 - lattice definition, 783–785
- Functional quantization
- of scalar fields, 282–292
 - of spinor fields, 298–303
 - of gauge fields, 294–298, 512–515, 733–734, 741–743
- Fundamental constants, 809–810
- Fundamental representation, 499, 501
- Furry’s theorem, 318
- g (Landé g -factor), 188, see Anomalous magnetic moment
- G_2 (exceptional Lie algebra), 497
- G_F (Fermi constant), 559, 708, 760–763, 809
- γ (Callan-Symanzik function), 410–417, 427
- for operators, 428–435, 604, 612–615
 - matrix, 430, 610–611, 615
 - for ϕ^4 theory, 413, 466
 - for linear sigma model, 448
 - for nonlinear sigma model, 457, 464
 - for QED, 416
 - for ϕ^2 , 432, 448
 - for currents, 432, 602
 - for $\bar{q}q$, 601
 - for nonleptonic weak interactions, 611
 - for twist-2 operators, 636, 640
 - for proton decay operator, 647
- γ (critical exponent), 441, 447

- γ (Euler-Mascheroni constant), 250, 377
- γ^μ (Dirac matrices), 8, 40–41, 803
- traces of, 132–135, 805
 - contraction identities, 135, 805
 - contraction identities in d dimensions, 251, 808
 - in two dimensions, 652
 - in d dimensions, 251
 - see also Fierz identities
- γ^5 (chirality matrix), 50
- traces including, 134, 805
 - in d dimensions, 662, 667, 681–682, 767
 - see also Axial vector anomaly
- $\Gamma(x)$ (Gamma function), 250, 807
- $\Gamma[\phi_{\text{cl}}]$ (effective action), 366–367
- Gauge boson mass, see Higgs mechanism
- Gauge dependence, 416, 526, 601
- Gauge field, 79, 295, 481–491, see also Gauge invariance, Photon, $\Pi^{\mu\nu}(q)$
- Gauge hierarchy problem, 788
- Gauge invariance, 78–79, 244, 295, 481–494, 533, 689–777
- of S -matrix, 298
 - and axial current conservation, 651, 658
- Gauge transformation, 78, 482–491
- Gauge-covariant derivative, see Covariant derivative
- Gauge-dependent mass, 734
- Gauge-fixing function, 295–296, 733, 741, see also Faddeev-Popov method
- Gaugino, 796
- Gauss's law, for non-Abelian gauge theory, 542
- Gaussian integrals, infinite-dimensional, 279, 285, 300–301, see also Functional integration
- Gell-Mann, M., 545–546
- Generalized couplings, 433–435, 442
- Generating functional, 379–383
- of Green's functions, 290–292, 302
 - of connected correlation functions, 380
 - of 1PI correlation functions, 383
- Generations of quarks and leptons, 707, 714–715, 721
- Generators of a Lie algebra, 38, 490, 495
- of Lorentz transformations, 71–72
 - see also Lie algebra
- Geometric series, in self-energy diagrams, 220, 228
- Geometry, discrete or nonlocal, 798–800
- Georgi-Glashow model, 696, 794
- Ghosts, 514–521
- interpretation of, 515–517
 - in Abelian Higgs model, 734
 - in non-Abelian Higgs theories, 742–743
 - see also BRST symmetry, Faddeev-Popov method, Feynman rules
- Gibbs free energy, 269–271, 293, 364–367, 443, 445–446
- Callan-Symanzik equation for, 445
- Glashow, S., 700
- Glashow-Weinberg-Salam theory, see GWS theory
- Global aspect of nonconservation of axial current, 657–659
- Global properties of Lie groups, 496
- Gluons, 127, 259, 476, 480, 547
- polarization sums, 571
 - spin of, 596
 - see also Cross sections, Parton distribution functions, Twist-2 operators
- God-given units, xix
- Goldberger-Trieman relation, 672
- Goldstone boson, 267, 351–352, 455, 460, 690–700, 672, 718, 731–732, 741–743, see also Higgs mechanism
- Goldstone boson equivalence theorem, 743–758
- Goldstone's theorem, 351–352, 363, 388, 669–670, 699
- Gordon identity, 72, 186, 192
- Graininess of spacetime, 402
- Grand unification, 681, 786–791, 799
- scale of, 786–787, 797
- Grassmann numbers, 73, 298–302, 518
- Gravitational anomaly, 681, 706–707
- Graviton, 126, 798–799
- Gravity, 64, 402, 683, 787–791, 795–800
- Greek indices, xix
- Green's function
- retarded, 30, 32, 62–63
 - Feynman, 31, 63
 - for Klein-Gordon equation, 30–32, 503
 - for Dirac equation, 62–63
 - for interacting fields, 82, 406–422
 - see also Correlation functions

- Greenberg, O., 546
- Gribov-Lipatov equations, xvi, 586–587,
see also Altarelli-Parisi equations
- Gross, D. J., 479, 531
- Gross-Neveu model, 390–391, 438, 792
- Ground state, 20–22, 82, 86, see also
Vacuum
- Group theory relations, 495–502, 805–
806
- use in diagram computations, 523,
529–530, 569–572
- Groups, continuous, 38, 486, 495
- GUT, see Grand unification
- GWS (Glashow-Weinberg-Salam) theory
of weak interactions, 474, 677, 689,
700–719, 740, 742–743, 747–775
- experimental tests of, 707–713, 771–
772
- stripped-down version, 735
- symmetries of, 64, 719–727
- see also W , Z , Higgs boson, Fermion
masses, Gauge boson masses
- Hadron-hadron collisions, 563–573, 785
- Hadrons, 473, 546–547, 552, 782
- Hall effect, quantum, 197–198
- Hamiltonian, 16, 19
- Dirac, 58
- abandoning of, 283
- see also Analogies to statistical me-
chanics
- Han, M., 546
- Harmonic oscillator, 20, 313
- \hbar , as unit of action, 277
- h.c. (Hermitian conjugate), xx
- Heaviside step function, xx
- Heaviside-Lorentz units, xxi
- Heavy quarks
- as constituents of proton, 559, 643
- photoproduction of, 597
- radiative corrections from, 688, 760–
772
- Heisenberg equation of motion, 25
- Heisenberg picture, 20, 25, 283
- Helicity, 47
- projection operators, 142
- dependence of $\mu^+\mu^-$ production,
141–146
- Helicity conservation, 142, 166
- Helium, superfluid, 267, 437
- Helmholtz free energy, 364–367
- Hepp, K., 337–338
- Hidden symmetry, 347
- Hierarchy problem, 788
- Higgs boson, 210, 715–717, 740, 743
- mass, 716
- couplings to fermions, 721
- decays of, 775–777
- production in hadron collisions, 777
- effect on radiative corrections, 712,
772, 774
- origin of, 787–789
- Higgs field, 734
- vacuum expectation value, 701, 719
- in model with two doublets, 729–730
- in supersymmetric models, 797
- Higgs mechanism, 470, 690–700, 744–747
- gauge boson masses from, 693, 700
- vacuum polarization and, 691, 698–700
- see also Gauge invariance, Unphysical
degrees of freedom
- Higgs sector, 717–719, 726, 760, 789, 798
- symmetries of, 721
- High-momentum degrees of freedom,
393–406
- History of quantum field theory, xv
- Holes as antiparticles, 61, 658
- Horrible products of bilinears, 52
- HRS experiment, 169, 256
- Hydrodynamic-bacteriological analogy,
418–420
- Hydrogen, see Atomic energy levels
- Hydrogen maser, 197
- Hyperboloid of 4-momentum vectors, 24
- Hyperboloids in energy-momentum
space, 212–213
- Hyperfine splitting, 197–198
- $i\epsilon$ in functional integrals, 286
- Identical particles, 22, 108
- Imaginary part of scattering amplitude,
230–237, 253, see also Analytic
properties of amplitudes
- Impact parameter, 103
- Improper Lorentz transformation, 64

- In states, see Asymptotic states
 Inconsistencies, in vector field theories, 81, 508–511, 757–758
 Infinitesimal group element, 495
 Infinities, see Infrared divergences, Ultraviolet divergences
 Infrared divergences, 55, 176, 184, 195, 260–262, 550, 553, 574
 of electron vertex function, 199–202
 of electron self-energy, 217
 interpretation of, 202–208
 regulator for, 195, 207, 217, 361
 Infrared-stable fixed point, 427, 435
 Initial conditions, see Altarelli-Parisi equations
 Instantons, 794
 Integrals
 in d dimensions, 249–250, 807
 over anticommuting numbers, 299–301
 Interaction picture, 6, 83–87
 Interactions among vector fields, 489, 491
 Interactions found in Nature, 79, 473
 Interactions, effect on single-particle states, 109
 Interchange identities, see Fierz transformations
 Interference phenomena, in condensed-matter systems, 197–198
 Internal lines, 5, 8
 Interpolation of V_{eff} , 368–369
 Interpretation of field operator, 24, 26
 Invariant mass distribution for jet production, 572–573
 Invariant matrix element (\mathcal{M}), see S -matrix, scattering amplitude
 Inverse Compton scattering, 167
 Inverse propagator, 381, 383
 Invisible decays of Z boson, 728–729
 Irreducible representation, 498, 501–502
 Irrelevant operators, 402, 407, 443, 451, 485
 Isospin singlet axial current, 673–674
 Isospin, 127, 486, 546, 611, 668, 670, 719
 Isotriplet currents, 668
 Isotropic magnets, 437
 ITEP sum rules, 620–621
 $J(x)$ (source term in \mathcal{L}), 290
 J/ψ particle, 141, 152, 593–594
 Jackiw, R., 370
 Jacobi identity, 495–496, 499, 597
 Jets of hadrons, 140, 261, 476, 553–554
 in hadron collisions, 568–573
 Jona-Lasinio, G., 668
 Josephson effect, 197–198

 K meson, 259, 612, 725
 Källén-Lehmann spectral representation, 214, 619, see also Analytic properties of amplitudes
 Killing, W., 496
 Kinematics, 104
 for e^+e^- annihilation, 136
 for Compton scattering, 162–164
 for deep inelastic scattering, 476–477
 for hadron-hadron collisions, 565–568
 for collinear particle emission, 576–578
 for massive vector bosons, 745
 Klein-Gordon equation, 13, 17, 25
 Lorentz invariance of, 36
 complex, 18, 75–76
 see also Feynman rules, scalar field
 Klein-Gordon Lagrangian, 16
 Klein-Nishina formula, 163

 L subscript, 605
 L3 experiment, 711
 Lab frame, 162
 Ladder operators, 26, 58, 123
 Lagrange equation, 16
 Lagrangian, 15, 35
 fundamental significance, 283, 466, 798–800
 most general gauge-invariant, 485, 489, 720–722
 Klein-Gordon, 16
 Dirac, 43
 Maxwell, 37
 for ϕ^4 theory, 77
 for QED, 78, 483
 for scalar QED, 80
 for Yukawa theory, 79
 for linear sigma model, 349–350
 for nonlinear sigma model, 454–455
 for non-Abelian gauge theory, 489, 491

- Lagrangian, cont.
- for GWS theory, 704, 715–716, 720–724
 - see also Effective Lagrangian
- Lagrangian density, 15
- Lagrangians, space of, 401
- Lamb shift, 197–198, 253
- λ (coupling constant), 77
- λ (cosmological constant), 790
- λ_* (fixed point), 426
- λ_e (electron-Higgs coupling), 713
- Λ (ultraviolet cutoff), 80, 194
- Λ (QCD scale), 552
- Landé g -factor, see Anomalous magnetic moment
- Landau gauge, 297, 470, 529
- Landau theory of phase transitions, 269–272, 293, 436, 439, 447, 450
- Landau-Ginzburg free energy, 470
- Large-distance behavior of QCD, 548, 782–785
- Large- N limit, 463–465, 467
- Laser, polarized, 167
- Lattice gauge theory, 547–548, 782–785
- Lattice statistical mechanical models, 449–451
- Least action, principle of, 15
- Lee, B., 347
- Left-handed current, 51
- Left-handed particle, 6, 47
- Left-handed spinors, 44
- Left-handedness of W couplings, 559–560, 703
- Left-moving fermions, 652
- Legendre transform, 365–366, 370
- Lehmann, H., 222
- Lehmann spectral representation, 214
- Length contraction, 23
- Lepton number conservation, 727
- Lepton pair production in hadron collisions, 564–568
- Leptons, 473, 726–727
- Lie algebras, 38, 495–504
- classification of, 496
 - see also Group theory relations, Groups
- Lifetime, see Decay rate
- Light-cone, 14
- Lightlike polarization states, 511
- Linear sigma model, 127–128, 349–363, 373–379, 385–387, 389–390, see also Feynman rules
- Liquid crystals, 367
- Liquid-gas critical point, 449–450
- Liquid-gas transition, 267, 272–274
- Local conservation laws, 18
- Local divergence, 337
- Local phase rotation, see Gauge transformation
- Local symmetry, see Gauge invariance
- Locality of ultraviolet divergences, 386
- Logarithm of a dimensionful quantity, 251
- Logarithmic enhancements
- in Compton scattering, 164
 - in bremsstrahlung, 184, 200–202, 207–208
 - from multiloop diagrams, 341, 422, 551
 - in corrections to V_{eff} , 378–379, 451–453
 - from mass singularities, 574–575, 579
 - from QCD, 603–612, 647
- Long-range correlations, 395, 442, see also Correlation length
- Longitudinal fraction, 477, 555
- Longitudinal polarization, 161, 481
- of massive gauge boson, 692, 732, 743
 - see also Higgs mechanism, Goldstone boson equivalence theorem
- Longitudinal rapidity, 566
- Longitudinal W production, 754
- Loop diagrams, 12, 401, see also One-loop diagrams
- Loop integrals, evaluation of, 189–195, 806–808
- Loops of fermions, 120
- Lorentz algebra, 39
- Lorentz contraction, 23
- Lorentz gauge, 79, 123, 178, 295, 737, 745
- generalized, 296, 513
- Lorentz group, 7, 38, 71–72
- Lorentz invariance, 35, 186, 212
- of Dirac equation, 42
 - violation by gauge fixing, 544
- Lorentz transformations. 35–47
- of Dirac field, 42, 59

- Lorentz-invariant 3-momentum integral, 23
- Low-energy hadronic interactions, 782
- Lowering operators, 497
- LSZ (Lehmann-Symanzik-Zimmermann) reduction formula, 222–230
- $\bar{m}(Q)$ (running mass parameter), 600–603
- m_Z (Z boson mass), 593
- M (renormalization scale), 377–378, 407–408, 410–417
- $M^2(p)$ (scalar self-energy), 227–228, 236–237, 328–329
- two-loop contribution, 345
- in linear sigma model, 361–363
- sign convention for, 228
- \mathcal{M} (scattering amplitude), 104
- Magnetic field, 179, 269, 292, 293, 364–367
- Magnetic moment, see Anomalous magnetic moment
- Magnetic monopole, 794
- Magnetic susceptibility, 266, 441, 446–447
- Magnetization, 269, 364–367, 440, 441, 446, 788
- Magnets, 266–274, 293, 347, 364–367, 406, 439, 449–450, 783, 788, 792
- symmetry of, 437–438
- in $d > 4$, 404
- see also Analogies to statistical mechanics
- Majorana equation, 73
- Majorana fermions, 73–74
- Majorana mass term, 73, 678, 726–727
- Mandelstam variables, 156–158, 162, 170, 476
- at parton level, 557
- Marginal operators, 402, 407, 451, 454
- Mass(es)
- table of values, 809
 - bare vs. physical, 214
 - of an unstable particle, 237
 - relation to correlation length, 273
 - derived from effective action, 383
 - of σ , π fields, 348–352, 355, 363
 - of quarks, 599–603, 670–671
- Mass(es), cont.
- of top quark, 772
 - of π meson, 670
 - of nucleon, 672
 - of hadrons, 782, 785
 - of vector field, 81, 470, 484–485, 758
 - of photon in two dimensions, 653, 791
 - of W and Z bosons, 701, 703, 710, 712, 740, 762
 - of unphysical particles, 733–734
 - of fundamental fermions, 713–715, 723, 789–790
 - of neutrinos, 714–715, 726
 - of Higgs boson, 716
 - see also Higgs mechanism
- Mass matrix, in scalar field theory, 351–352
- in broken gauge theory, 693, 700
- Mass operator, 402, 406, 431–436, 442
- Mass renormalization, 220–221, 227–228, 328–333, 397, 408–409, 431–436
- in classical electrodynamics, 221
- in supersymmetric models, 796
- see also $M^2(p)$, $\Sigma(p)$, $\Pi^{\mu\nu}(q)$
- Mass scale, arbitrary, see Renormalization scale
- Mass shell, 33
- Mass singularities, 554, 574–575, 579, 587–588
- Massive gauge bosons, 689–777
- propagator for, 734
 - see also W boson, Z boson
- Massive vector boson, 173–174
- Massless particles, 128, 267–268, 350–352, 388, see also Goldstone boson
- Matrix element, see Scattering amplitude
- Maxwell construction, 368–369
- Maxwell's equations, xxi, 3, 33, 37, 78–79, 177, 474, 500
- Measure of functional integral, 276–279, 281–282, 285
- chiral transformation of, 664–667
- Measurement, 28
- Meissner effect, 692
- Mermin-Wagner theorem, 460–461
- Mesons, 546–549
- Metastable vacuum state, 368–369
- Metric tensor, xix

- Minimal coupling, 78, 473
 Minimal subtraction, see \overline{MS}
 Minimum of effective potential, 378–379
 Minus signs for fermions, 116, 119–120
 Miracle, 353–354
 Mixing
 of operators, 430, 610–612, 615
 of quark flavors, 605, 714–715, 722
 Model quantum field theories, 791–794
 Møller scattering (e^-e^- scattering), 157
 Moment sum rules, 634, 641–643
 Momentum, canonical, 16
 Momentum conservation in diagrams, 111
 Momentum cutoff, see Cutoff
 Momentum density, 16
 Momentum operator, xx, 19, 26, 58
 Momentum scale, for evaluating α_s , 552, 554, 568, 573
 Momentum sum rule for parton distributions, 563, 644
 Momentum transfer, in hadron collisions, 475
 Momentum-space Feynman rules, see Feynman rules
 Monte Carlo method, 785
 Mott formula, 169–170, 209
 \overline{MS} (modified minimal subtraction), 377, 391, 470, 593
 Multiloop diagrams, 335–345
 asymptotic behavior, 341, 344–345
 Multiparticle branch cut, see Analytic properties of amplitudes
 Multiple photon emission, 202–207, 582–584
 Multiplets of leptons and quarks, 707
 Muon, 4, 131, 335, 473. see also Anomalous magnetic moment
 Muon decay, 709, 727
 radiative corrections to, 760–761, 763
 Muon neutrinos, 559
 Muon-proton scattering, 555
 Muonium, hyperfine splitting, 197–198
 Mythology, xvi

 N (number of spin components), 437
 Nambu, Y., 546, 668

 Naturalness, see Delicate adjustments, Zeroth-order natural relations
 Ne'eman, Y., 546
 Negative degrees of freedom, 517, 520
 Negative energy, 13, 26, 54, 658, 790
 Negative frequency, 48
 Negative mass squared, 348
 Negative norm, 79, 124, 161, 481, see also BRST symmetry, Unphysical degrees of freedom
 Nested divergences, 335–338
 Neutral-current weak interactions, 709–712, 729
 Neutrinos, 473, 559–561, 704, 729
 mass, 714–715, 726
 number of, 729
 see also Deep inelastic scattering
 Neutron, 546, 562, 671
 Compton wavelength, 197–198
 electric dipole moment, 726
 Nilpotent operator, 519
 Noether's theorem, 17, 60, 308–310, 683, see also Current, Symmetry
 Non-Abelian gauge symmetry, see Gauge invariance
 Non-Abelian gauge theories, 81, 479–480, 486–491, 505–548, 692–700, 739–743
 Non-Abelian group, 487
 Noncompact group, 41
 Nonleptonic decay, 605
 Nonlinear sigma model, 454–467, 793, see also Asymptotic freedom, Feynman rules
 Nonlinear terms in Lagrangian, 77
 Nonlocal divergence, 337, 343–344
 Nonorthochronous transformation, 64
 Nonperturbative methods, 405, 782–785, 791–794
 Nonperturbative QCD, 612, 782–785
 Nonrelativistic bound states, 148
 Nonrelativistic expansion of spinors, 187
 Nonrelativistic quantum mechanics, 275–282
 Nonrenormalizable interactions, 321–322, 399, 434, 485
 Nonuniversal correction, 466
 Nordsieck, A., 202
 Norm, see Negative norm

- Normal order, 88, 116
 Normalization of distribution functions, 562–563
 Normalization of spinors, 45–48
 Normalization of states, 22, 149
 Notation, xix–xxi
 ν (critical exponent), 436–437, 440–441, 443, 447, 449, 462, 465
 ν (kinematic variable in deep inelastic scattering), 633
 Nuclear force, 122
 Nucleon, 79, 671–672
 Numerical computations of quarkonium spectra, 593–594
 Numerical lattice calculations, 785
- $O(2)$, 389, 438
 $O(3)$, 486, 496
 $O(4)$, 127, 719
 $O(N)$, 74, 349, 351, 454–455, 497
 $O(N)$ -symmetric ϕ^4 theory, see Linear sigma model
 Oblique corrections, 761
 Odd parity, 67
 ω (critical exponent), 466
 Ω (vacuum of interacting theory), 82, 86
 On-shell particle, 33
 One-loop corrections
 to electron scattering, 211
 in GWS theory, 758–772
 One-loop diagrams, computation of
 in QED, 189–196, 216–218, 247–252, 332–334
 in ϕ^4 theory, 326–330
 in linear sigma model, 356–363
 in non-Abelian gauge theories, 521–533
 1PI (one-particle-irreducible) diagrams, 219, 228, 245, 328, 331, 381–383, 408, see also Callan-Symanzik equation, Effective action
 One-particle states, Dirac, 59
 One-point amplitude
 in QED, 317–318, 344
 in linear sigma model, 355, 360–361
 OPAL experiment, 711
 OPE, see Operator product expansion
 Operator mixing, 430, 638, see also γ
 Operator product expansion, 612–649,
 see also Callan-Symanzik equation
 Operator rescaling, 429–432, see also γ
 Operators, relevant vs. irrelevant, 402, 407
 Optical theorem, 230–237, 257, 511–512, 515, 616, 622–623, see also Analytic properties of amplitudes
 Orbital angular momentum, 60–61
 Order parameter, 269, 273
 Orthochronous transformation, 64
 Orthogonal group, see $O(N)$
 Orthogonality of spinors, 48
 Oscillations in total cross section, 621
 Out states, see Asymptotic states
 Overlapping divergences, 335–338
- P (parity), 65–67, 71, 75–76, 185, 344–345, 485, 720–727
 in gauge theories, 676
 violation in weak interactions, 64, 709, 712
 Pair annihilation, see e^+e^- annihilation, Cross section
 Pair creation, 13
 Paradigm interactions, 77–79
 Paradigm reaction, 131
 Parasiuk, O., 337–338
 Parity-violating deep inelastic form factor, 647–649
 Partial-wave analysis, 750
 Particle-wave duality, 26
 Particles, as field excitations, 22
 Partition function, 292, 312–314, 364, 367
 Parton distribution functions, 477–478, 556, 562–563, 588–593, 621–622, 632, 634–635
 for proton, 562–563
 for neutron, 562
 for photon, 649
 antiquark component, 561, 562–563, 588
 gluon component, 562–563, 588, 777
 evolution of, 574–593, 644–647
 at small x , 597–598
 see also Altarelli-Parisi equations

- Parton model, 476–480, 547, 556–557, 597, 625–627, 648
- Path dependence of comparator, 491–494
- Path integral, 275–282, see also Functional integral
- Path ordering, 493, 504
- Pauli sigma matrices, xx, 34, 804
- Pauli, W., 58
- Pauli-Villars regularization, 194, 218, 248, 257, 662, 686, 688
- Periodic boundary conditions, 657–658, 687
- Perturbation theory, 5, 77, 82
in quantum mechanics, 5–6
for correlation functions, 87
validity of, 401, 405–406, 422, 425, 552, 554
- Phase, *CP*-violating, 724–726
- Phase diagram, for a ferromagnet, 270
- Phase invariance, local, 482
- Phase rotation, 78, 496
- Phase space, 106, 137
two-body, 808
three-body, 260–261
- Phase transitions, 268–274, 791, see also
Critical exponents, Critical point
- ϕ^4 theory, 77, 82–99, 109–115, 289, 323–329, 439–440
Feynman rules for, 94–95, 114–115, 325, 801
two-particle scattering in, 109–112
divergences of, 324
one-loop structure, 326–329
spontaneously broken, 348
renormalizaton group analysis, 394–406
existence of, 404
mass renormalization of, 409
limit $m_\sigma \rightarrow \infty$, 454–455
see also Linear sigma model
- ϕ^6 interaction, 398
- ϕ_{cl} (classical field), 366–367, 370
- Photon, 6, 78–79, 701–702
see also Bremsstrahlung, Compton scattering, Electromagnetic field, Feynman rules, $\Pi(q^2)$
- Photon distribution function, 579, 583
- Photon mass, 81, 653, 690–691
as infrared regulator, 195
induced by bad regulator, 248
- Photon polarization sums, 159–160
- Photon self-energy, see $\Pi^{\mu\nu}(q)$
- Photon sources, polarized, 167
- Photon structure functions, 649
- Photon-photon scattering, 210, 320, 344
- Photoproduction of heavy quarks, 597
- Physical charge and mass, 214, 246, 266, 331, 423
- Physical constants, 809–810
- Physical parameters of a quantum field theory, 325
- Physical pole in two-point function, 408
- π meson, 79, 122, 128, 259, 475, 669–676
as Goldstone boson, 669–671
coupling to nucleon, 672
decay of π^+ , 687
decay of π^0 , 674–676
 π^k (field of sigma model), 350
 π^k (Goldstone boson field), 698, 718
- \prod symbol, symbolic use of, 103, 278
- $\Pi(q^2)$ (QED vacuum polarization
amplitude), 176, 245–256, 331–333
contribution of scalars, 312
- $\Pi^{\mu\nu}(q)$ (gauge boson self-energy), 244–256, 320, 522–526
in two-dimensional QED, 653–655
in Higgs mechanism, 691, 693–694, 700
in GWS theory, 718, 761–771
sign convention for, 762
- Π_h (hadronic vacuum polarization), 616–620
- Pictures,
Heisenberg and Schrödinger, 20, 283
interaction, 83
- Pion decay constant, see f_π
- Pion, see π meson
- Planck scale, 787, 798–800
- Plane waves, xx
- Plane-wave solutions, Dirac, 45–48
- Poisson distribution, 127, 208
- Polarization asymmetry, see A_{LR}^f
- Polarization of fermions, 4, 141
sums over, 48–49, 575, 804

- Polarization of photons and vector bosons, 123, 145–146, 511, 748–749
 sums over, for photons, 159–160
 sums over, for gluons, 571
 sums over, for massive vector bosons, 260, 748–749
 of intermediate-state photons, 576
 of intermediate-state gluons, 589
 see also Longitudinal polarization, Timelike polarization, Unphysical degrees of freedom
- Polarized laser, 167
- Pole at $d = 2$, 251, 524–525
- Poles in dimensional regularization, 250
- Poles in two-point function, 215–216
- Politzer, H. D., 479, 531
- Polyakov, A. M., 458, 533
- Position-space Feynman rules, 94
- Positive frequency, 45, 48
- Positive norm, 124
- Positronium
 annihilation rates, 171–172, 197–198
 energy levels, 197–198
 selection rules for, 76
- Potential, double-well, 349
- Potential, electromagnetic, xxi
- Potential, for spontaneous symmetry breaking, 348–350
- Potential functions
 Yukawa, 121–123
 Coulomb, 125, 253–255
- Power laws, see Anomalous dimensions, Critical exponents
- Poynting vector, 33
- Predictions, unambiguous, 387
- Pressure, 292
- Price of asymptotic freedom, 543
- Principle of least action, 15
- Probability of scattering, 104–105
- Products of group representations, 501–502
- Projection
 onto helicity states, 142, 804
 onto transverse polarization states, 245
- Propagation amplitude, 13, 27, 34
- Propagator (Feynman), 92
 Klein-Gordon, 29–31
 Dirac, 62–63, 302, 506
- Propagator, cont.
 photon, 123–124, 294, 297
 non-Abelian gauge field, 506, 513
 ghost, 514–515
 massive gauge boson, 734, 742
 unphysical bosons, 735, 742
 in background field, 504
 see also Feynman rules
- Propagator, interaction picture, 84, see also Time-evolution operator
- Proper Lorentz transformation, 64
- Proton, 197, 486, 475, 546, 564, 588, 622
 form factors, 188, 208–209
 decay, 647
 see also Parton model, Parton distribution functions
- Pseudo-scalar, 50, 66, 71
- Pseudo-vector, 50, 66, 71
- Pseudoreal representation, 499
- Pseudoscalar operators, 720
- ψ particles, 593–594
- Q^2 (momentum transfer in deep inelastic scattering), 477, 555
- QCD (Quantum Chromodynamics), 139–140, 259–260, 545–649, 677–678
 use of perturbation theory in, 551–554
 elementary processes of, 568–572
 experimental tests of, 593–595
 chiral symmetries of, 667–676
 strong-coupling regime, 547–548, 782–785
 see also α_s , Parton model, Quarks, Strong interactions
- QED (Quantum Electrodynamics), 3, 78, 303, 482–486
 scope of, 3
 elementary processes of, 131–174
 radiative corrections in, 175–210, 216–222, 244–258
 scalar, 312
 precision tests, 196–198
 renormalization of, 318–320, 330–335, 344
 evolution equations for, 586–587
 in d dimensions, 320–321
 in two dimensions, 651–659, 791

- QED, cont.
- see also α , Cross section, Electromagnetic field, Gauge invariance, Photon
- Quadratic divergence in self-energy, 409, 525
- Quantization
- of Klein-Gordon field, 19–24
 - of Dirac field, 52–63
 - see also Functional quantization
- Quantization, second, 19
- Quantum Chromodynamics, see QCD
- Quantum Electrodynamics, see QED
- Quantum field theory, xi
- necessity for, 13
 - domain of, 798–800
- Quantum gravity, 402
- Quantum mechanics, xx, 275–282
- Quantum statistical mechanics, 312–314
- Quark-gluon scattering, 572–573
- Quark-quark potential, 782, 784
- Quark-quark reactions, 568–573, 573, 596
- Quarkonium, 152
- decays, 593–594
 - spectra, 593–594, 785
- Quarks, 127, 139–140, 473, 474, 476, 546–548, 559
- masses of, 599–603, 670–671
 - number of in proton, 635
 - production in e^+e^- annihilation, 139–140
 - weak interactions of, 428–429
- R (ratio of hadronic to leptonic cross sections), 141, 593–594, 622, see also e^+e^- annihilation
- R unit (annihilation cross section), 140, 809
- R_ξ gauges, 731–743
- Radiative corrections, 9, 175–176, 256
- see also QED, QCD, GWS theory
- Raising and lowering operators, 497
- Ralston, J., 597–598
- Ramsey, N., 197
- Range of Yukawa force, 122
- Rapidity, 46, 565
- Rapidity, longitudinal, 566
- Real representation, 498
- Rearrangement identities, see Fierz transformations
- Reducibility of Dirac representation, 50
- Reducible representation, 43, 498
- Redundancy, in functional integration over gauge fields, 295
- Regularization, 194–195
- effect on symmetries and conservation laws, 248–249, 257, 654–655, 662, 679, 682, 686
 - see also Cutoff, Dimensional regularization, Pauli-Villars regularization, Infrared divergences
- Relativistic invariance, 3, 35
- Relativistic quantum mechanics, 13
- Relativistic wave equations, 13
- Relativistically invariant phase space, 106
- Relativity, xix
- Relevant operators, 402, 407, 443
- Renormalizability, xv, 79–80, 265, 321–323, 407
- proof of, 417–418
 - of non-Abelian gauge theories, 521, 738
- Renormalizability gauges, 738
- Renormalization, 211–222, 244–256, 315–345
- and spontaneously broken symmetry, 347, 352–363, 383–388
 - of local operators, 428–432
 - beyond leading order, 335–345
- Renormalization conditions, 325, 527, 532
- for ϕ^4 theory, 325, 328, 408
 - for QED, 332
 - for linear sigma model, 355
 - for GWS theory, 711–712, 758–761
 - \overline{MS} , 377, 391, 470, 593
 - at spacelike p , 407–410
- Renormalization group, 401–406, 424–428, 432–435
- and critical exponents, 442–447
 - in QCD, 551–554, 599–615
- Renormalization group equation, 420, 424–426, 786
- see also Callan-Symanzik equation, Running coupling constant

- Renormalization group flow, 401–406, 417, 422, 466
- Renormalization group improvement of perturbation theory, 453, 470, 552
- Renormalization scale, 377–378, 407–417, 440, 551, 593, 599, 682
- Renormalized perturbation theory, 323–326, 330, 410
- for ϕ^4 theory, 323–330
 - for QED, 330–335
 - for non-Abelian gauge theories, 528, 531–533
- see also Counterterms
- Representations of Lie algebras, 497–502
- rotation group, 38, 72
 - Lorentz group, 39–41
 - $SU(3)$, 547
- Repulsive force, 125–126
- Rescaling, see Field strength renormalization, γ , Z
- Resolution of electron structure, 583
- Resolution of hadronic structure, 588, 647
- Resonances, 101, 151, 237
- in e^+e^- annihilation, 151, 621
- see also Breit-Wigner formula
- Retarded boundary conditions, 178
- Retarded Green's function, 30, 32, 62–63
- Right-handed current, 51
- Right-handed neutrino, 704, 715, 726
- Right-handed particle, 6, 47
- Right-handed spinors, 44
- Right-moving fermions, 652
- Roman indices, xix
- Rosenbluth formula, 208–209
- Rotation generators for fermions, 41, 60–61, 71–72
- Rotation group, 38–40, 72
- in N dimensions, see $O(N)$
- Running coupling constant, 255–257, 404–405, 420–422, 424–428
- in ϕ^4 theory, 422
 - in QED (α), 255–257, 424
 - in nonlinear sigma model, 458–461
 - in QCD (α_s), 551–553, 593–596
- see also Asymptotic freedom, β , Fixed point
- Running mass parameter, 600–604
- Rutherford scattering, 129–130, 155
- s (Mandelstam variable), 156
- \hat{s} , \hat{t} , \hat{u} (parton-level Mandelstam variables), 476, 557
- s quark, decay of, 606–612
- $s(x)$ (local spin density), 271
- s_*^2 (definition of $\sin^2 \theta_w$), 763–772, 774
- s_0^2 (definition of $\sin^2 \theta_w$), 759
- s_W^2 (definition of $\sin^2 \theta_w$), 712, 759–772, 774
- s -channel, 157
- S -matrix, 102–115
- relation to cross section, 106–107
 - in terms of Feynman diagrams, 114, 229, 324
 - relation to correlation functions, 227–229
 - in renormalized perturbation theory, 324
 - gauge invariance of, 297–298
 - see also Analytic properties of amplitudes, Unitarity
- S -wave, 147
- Salam, A., 700
- Scalar field, real, 15–33
- complex, 33–34
 - elementary, 406
- Scalar field theory, 321–322, 394–406, 432–468, see also ϕ^4 theory
- Scalar gluon (hypothetical), 596
- Scalar non-Abelian gauge theory, 544
- Scalar particle exchange, 121–123
- Scalar QED, 80, 312
- Scale invariance
- classical description, 682–683
 - anomalous breaking, 682–686
- Scale-dependent parameter, see Running coupling constant
- Scaling, see Bjorken scaling
- Scaling behavior in magnets, 436–437
- Scaling laws, in critical phenomena, 440
- Scaling of two-point function, anomalous, 427
- Scattering, see Cross sections, S -matrix
- Scattering amplitude (\mathcal{M}), 5, 104
- near resonance, 101
 - see also Analytic properties of amplitudes, S -matrix
- Scattering experiments, 99–100

- Schrödinger equation, 84, 149, 153, 279, 503–504
- Schrödinger picture, 20, 25, 283
- Schrödinger wavefunction, xx, 149
- Schur's lemma, 50
- Schwinger, J., 82, 189, 196, 492, 653
- Schwinger-Dyson equations, 308–312
- Screening, 255, 458, 541
- Second quantization, 19
- Second-order phase transition, 268–274
- Selection rules of positronium, 76
- Self-energy, see $M^2(p)$, $\Sigma(p)$, $\Pi^{\mu\nu}(q)$
- Semi-simple Lie algebra, 496
- Semileptonic decay, 605
- Shift of integration variable, 242, 299, 662
- Short distance scales, effect on theory, 393–406
- σ (cross section), 100
- σ (field of linear sigma model), 350
- σ matrices, see Pauli sigma matrices
- Sigma model, see Linear sigma model, Nonlinear sigma model
- σ^μ , $\bar{\sigma}^\mu$ (components of γ^μ), 44
- $\Sigma(p)$ (fermion self-energy), 216–222, 318–319, 331–333
- in non-Abelian gauge theory, 528–529
- sign convention for, 220
- Sign of mass shifts, see $M(p)$, $\Sigma(p)$, $\Pi^{\mu\nu}(q)$
- Simple harmonic oscillator, 20, 313
- Simple Lie algebra, 496
- $\sin^2 \theta_w$, 702, 705, 809
- definitions of, 711–712, 759–760
- measurements of, 711–713
- see also GWS theory
- Single-particle states, affected by interactions, 109
- Single-particle wave equations, 13, 35
- Singularities of Feynman diagrams, 211, 164–167, 407
- in QCD, 553–554, 574–575
- see also Analytic properties of amplitudes
- SLAC-MIT experiments, 475, 478
- Slash notation, 49
- $SO(4)$, 127
- $SO(10)$, 681
- $SO(N)$, 497, see also $O(N)$
- Soft photons, 176
- multiple, 202–207
- Solitons, 367, 793–794
- Sound waves, 266–267
- Source, see Classical source
- $Sp(N)$, 497
- Spacelike reference momenta, 407–408
- Spacetime dimension, effect on scalar field theory, 465–466
- Spacetime formulation of perturbation theory, 82
- Spacetime geometry and topology, 402, 798–800
- Spatially varying background field, 386–387
- Specific heat, 441, 446
- Spectator quarks, 555
- Spectral density function, 214
- Spectral representation of two-point function, 214, 619
- Spectroscopy of ψ , Υ , 593–594, 785
- Spectrum of hadrons, 545–547
- Spectrum of harmonic oscillator, 20
- Spectrum of Klein-Gordon theory, 22
- Speed of sound, 266
- Sphere in d dimensions, 193, 249
- Spin, 4, 38–40
- of Dirac particle, 60–61
- conservation of, 147
- in magnetic systems, 266–267
- of gluon, 596
- Spin and statistics, 52–58, 514, 546–547
- Spin chain, 792
- Spin correlation function, 272–273, 293, 442
- Spin density, 271, 389
- Spin field, 293, 395, 440
- Spin sums for fermions, 48–49
- Spin-3/2 field, 795
- Spin-wave theory, 389
- Spinor (of Dirac theory), 41–49
- for antifermions, 61
- high-energy limit, 46–47, 144
- nonrelativistic limit, 187
- two-component (Weyl), 43–44, 68
- Spinor (of $SU(2)$), 5, 45, 486, 501
- Spinor products, 72–73, 170–171, 174
- Splitting functions, see Altarelli-Parisi equations

- Spontaneous symmetry breaking, 128, 347–363, 368, 383–388, 454, 460, 469–470, 474, 689–777, 786, 793–794
 of chiral symmetry, 668–672
 of supersymmetry, 797
 and vacuum energy, 790
 nonperturbative mechanisms, 698–700
 see also Goldstone boson, GWS
 theory, Higgs mechanism
- Square bracket notation, 276 .
- Standard model, 781, see also GWS theory, QCD
- Stationary phase, method of, 14
- Statistical mechanics, 269–274, 440–451, 792–793
 quantum, 312–314
 see also Analogies to statistical mechanics, Critical exponents
- Statistics and spin, 22, 52–58
- Stokes's theorem, 492
- Stress-energy tensor, see Energy-Momentum tensor
- Strictly real representation, 499
- String theory, 798–799
- Strings, in describing strong interactions, 784–785
- Strong coupling regime, 405, 547–548, 552
- Strong CP problem, 726–727
- Strong interactions, 64, 127, 139–140, 259–260, 347, 473–480, 545–598, 667–676
 see also α_s , QCD
- Strongly coupled W bosons, 751
- Strongly interacting particles, 139–141
- Strongly ordered, 582–583
- Structure constants, see f^{abc}
- Structure functions, see Parton distribution functions
- Structure of the electron, 583
- $SU(2)$, 34, 486, 496, 502, see also Isospin
- $SU(2)$ gauge theory, 494, 542–543
 spontaneously broken, 694–696, 699–700
- $SU(2) \times SU(2)$, 127
- $SU(2) \times U(1)$ theory, see GWS theory
- $SU(3)$, 502
- $SU(3)$ broken gauge theory, 696–697
- $SU(3)$ color symmetry, 545, 547
 $SU(3)$ flavor symmetry, 546, 670–671
- $SU(3) \times SU(2) \times U(1)$ theory, 781
- $SU(5)$, 728, 786
- $SU(N)$, 496–497, 502, 504, 687–688
 group identities, 806
- Subdiagrams, divergent, 316, 335
- Subtraction of UV divergence, 195
- Sudakov double logarithm, 184, 200, 202, 207–208, 407
- Sudakov form factor, 207–208
- Sum over paths, 276
- Sum rules for distribution functions, 562–563
- Sum rules
 for parton distribution functions, 562–563, 590
 for distribution functions in QED, 587
 for $e^+e^- \rightarrow$ hadrons, 620–621
 for deep inelastic form factors, 634, 641–643
- Summation convention, xix
- Summation of logarithms, 452–453, 551, 575, 584–586, 635, see also Exponentiation, Mass singularities
- Sums over polarizations, see Polarization
- Super-renormalizable interactions, 321–322, 402
- Superconductivity, 470, 669, 692, 697
- Superficial degree of divergence, 316–323
- Superfluids, 267, 272, 437, 449–450
- Superposition principle in quantum mechanics, 94, 276
- Superpotential, 75
- Supersymmetry, 74, 789, 795–799
 extended, 425, 796–797
- Susceptibility, magnetic, 441, 446–447
- Symanzik, K., 222, 411
- symm lim, 655
- Symmetric integration tricks, 251, 807
- Symmetries, 17, 283, 306–312, 383, 800
 more fundamental than Lagrangian, 249, 466
 in presence of divergences, 248–249, 347, 352–363, 383–388, 651–686
 see also C , P , T , Gauge invariance, Noether's theorem, Lie algebras, Spontaneous symmetry breaking
- Symmetry current, see Current, Noether's theorem

- Symmetry factors, see Feynman rules
 Symmetry generators, see Lie algebras
 Symplectic transformations, 497
- t* (Mandelstam variable), 156
 t^a (group representation matrices), 490, 498
 identities for, 805–806
 T (time reversal), 64, 67–69, 71, 75–76, 485, 720–727
 T -matrix, 104, 109–112, 231
 T^a (group representation matrices on real vectors), 693
 T_C (critical temperature), 269–274
t-channel, 157
't Hooft, G., 248, 479, 531, 662
't Hooft-Veltman definition of γ^5 , 681
 Tables
 C, P, T transformations, 71
 attractive/repulsive forces, 126
 measurements of α , 198
 analogies between magnetic system and field theory, 367
 values of critical exponents, 450
 measurements of α_s , 594
 measurements of $\sin^2 \theta_w$, 712
 integrals in d dimensions, 807
 Tadpole diagrams, 373
 in QED, 317–318, 344
 in linear sigma model, 355
 in non-Abelian gauge theory, 522
 τ lepton, 137–138, 473
 decay, 594
 Technicolor, 719, 789
 Temperature, 267–274, 364, 441, 446–447, 461
 Tensor, 37
 Tensor, energy-momentum, see Energy-momentum tensor
 Tensor notation, xix–xx
 Tensor particle exchange, 126
 Tensors built from Dirac fields, 49–52
 Thermal fluctuations, 267
 Thermodynamics of early universe, 469
 θ function (step function), xx
 θ_0 (weak mixing angle), 759
 θ_c (Cabibbo angle), 714
- θ_w (weak mixing angle), 702, see also GWS theory, $\sin^2 \theta_w$
 Thirring model, 791–792, 794
 Thomson cross section, 163, 809
 Three-body phase space, 260–261
 Three-gauge-boson vertex, 507
 Three-jet events, 261
 Three-photon amplitude, QED, 318
 Three-point function, see Correlation functions
 Three-vectors, xix
 Threshold, 137–138, 146
 see also Analytic properties of amplitudes
 Threshold of photon detection, 200–202, 207–208
 Thresholds, effect on renormalization group, 553
 Tilde notation, xxi
 Time-dependent perturbation theory, 82
 Time-evolution operator, 84, 102, 275, 278–282
 Time-ordered product, 31, 63, 85, 115, 307
 Time reversal, see T
 Timelike polarization, 161, 481, 732, 737, 741, 746
 Tomonaga, S., 82
 Top quark, 546, 747
 decay of, 747–750
 radiative corrections from, 712, 770–772
 prediction of mass, 772
 Topology of vacuum states, 794
 Total cross section, for identical particles, 108
 tr (trace of matrix), 304
 Tr (trace of operator), 304
 Trace anomaly, 684–686, 688
 Trace of Dirac matrices, 132–135, 805
 Trajectory in space of Lagrangians, 401
 Transition energies in hydrogen, 197–198
 Translations, 18
 Transverse momentum, of pp collision products, 475
 Transverse polarization vectors, 124, 160, 804
 Tree-level processes, 175

- Triangle diagrams, 661–664, 679, 705–707, see also Adler-Bell-Jackiw anomaly
- Tube of gauge field, 548
- Tuning of parameters, 267
- Tunneling, 368–369
- Twist, 631
- Two-body phase space, 808
- Two-component magnet, 438
- Two-component spinors, 68
- Two-dimensional model theories, 390–391, 405, 454, 791–794
- Two-dimensional QED, 651–659
- Two-level system, in statistical mechanics, 313
- Two-loop diagrams, 336–345
- double logarithms in, 314, 344
 - and renormalization group relations, 595–596
- Two-point amplitude, 82, 214
- analytic structure, 211–222
 - scaling behavior, 418–421
 - see also $M^2(p)$, $\Sigma(p)$, $\Pi^{\mu\nu}(q)$
- Two-state model system, 57
- u* (Mandelstam variable), 156
- U* gauge, 691, 715, 723, 730, 738, 749
- $U(1)$, 496
- $U(1)$ charge, in GWS theory, 702–704
- $U(1)$ factors, and gravitational anomaly, 681
- $U(1)$ gauge theory, 482–486, 690–692, 732–734
- $U(1)$ symmetry, broken, 389
- $U(y, x)$ (comparator), 482–484, 487
- u*-channel, 157
- Uehling potential, 255
- Ultraviolet divergences, xii, 12, 80, 393
- in zero-point energy, 21
 - in QED, 176, 193–195, 220–221, 248, 251–252, 318–320
 - in scalar field theory, 321–322
 - in ϕ^4 theory, 324
 - in linear sigma model, 353–354
 - in GWS theory, 758, 764–765
 - effect upon shift of integration variable, 242
 - classification of, 315
- Ultraviolet divergences, cont.
- in subdiagrams, 316
 - overlapping, 336
 - local vs. nonlocal, 337, 343–344, 386
 - effect on symmetries, 347, 352–363, 383–388
 - in V_{eff} , 375
 - origin of, 265–266
 - viewpoint toward, 265–266
 - reinterpretation of, 398
- Ultraviolet-stable fixed point, 427, 461
- Unification of the fundamental interactions, 347, 497, 786–791
- with gravity, 787, 791, 798
- Unified electroweak model, of Georgi and Glashow, 696
- Unified electroweak theory, see GWS theory
- Unitarity gauge, see *U* gauge
- Unitarity of *S*-matrix, 231, 298, 520–521, 679, 746
- in broken gauge theories, 731, 738
 - limit on \mathcal{M} , 750–751
 - see also BRST symmetry
- Unitary implementation of Lorentz transformations, 59
- Unitary transformations, 496–497
- Units, xix, xxi
- Universality (in critical phenomena), 268, 272, 437, 447, 449, 466
- classes, 273–274
- Universality of coupling constants, 533, 717
- Unphysical degrees of freedom, 124, 505, 508–512, 517, 520, 738, 743
- cancellation of, 160–161, 298, 510, 520, 735–736
- Unsolved problems, 781–800
- Unstable particles, 236–237, see also Decay rate
- Υ particle, 141, 152, 593–594
- $V(x)$ (gauge transformation matrix), 486
- Vacuum (ground state), 21–22, 82, 86, 368–369, 383
- Vacuum bubble diagrams, 96–98, 113
- Vacuum energy, 21, 98, 317, 790–791, 796–797

- Vacuum expectation value, 348–350, 364, 372, see also Higgs field
- Vacuum polarization, see $\Pi(q^2)$, $\Pi^{\mu\nu}(q)$, Π_h
- Vector boson, 173–174, 757–758
see also Gauge field, Higgs mechanism, Photon, W , Z
- Vector, built from Dirac fields, 50
- Vector current, see Current
- Vector meson, 150–153
- Vector particle exchange, 125
- Vector potential, xxi, 483
- Veltman, M. J. G., 248, 662
- Vertex, see Feynman rules
- Vertex corrections, 175, 184–202, 529–530
- Violence
to discrete and flavor symmetries, 722
to gauge invariance, 656, 679
in high-energy behavior, 758
- Virtual particles, 5, 113, 393–406, 479
almost real, 155, 209–210, 575
 e^+e^- pairs, 245, 255
- Viscosity, 266
- Volume, transformation under boosts, 23
- W boson, 428–429, 474, 559–560, 696, 701
mass, 710, 712, 762–764, 771–772, 809
decays, 728
in QCD corrections, 609
production in hadron collisions, 593–594, 710
see also e^+e^- annihilation
- W_1 , W_2 (deep inelastic form factors), 625–634, 648–649
- W_3 (deep inelastic form factor), 648–649
- Ward identity, 160–161, 186, 192, 238, 242, 245–251, 257, 316, 334, 481, 505, 616, 625
trick for proving, 239
violation by bad regulator, 248, 654
in non-Abelian gauge theories, 508–511, 522, 679, 698, 705–706, 744
of GWS theory, 752
in string theory, 799
see also BRST symmetry, Unphysical degrees of freedom
- Ward-Takahashi identity, 238–244, 297
for arbitrary symmetry, 311
and counterterm relations, 243, 311–312, 334
- Wave equations, relativistic, 13, 35
- Wave-particle duality, 26
- Wavefunction of a bound state, 148–153
- Wavepackets, 102–103, 224–226
- Weak coupling regime, 548
- Weak interactions, 473–474, 700–719
at low energies, 428–429, 559–560, 605–606, 708–709
QCD enhancements to, 605–612
see also GWS theory
- Weak mixing angle, see $\sin^2 \theta_w$
- Weak-interaction gauge theory, see GWS theory
- Weinberg, S., 202, 700
- Weinberg's nose, 729
- Weiszacker-Williams distribution function, 174, 210, 579
- Wess-Zumino term, 793
- Weyl equations, 44
- Weyl ordering, 281
- Weyl representation, 41
- Weyl spinors, 43
- Wick rotation, 192–193, 292–293, 394, 807
- Wick's theorem, 88–90, 110, 115, 116, 288, 302
- Width of a resonance, see Breit-Wigner formula
- Width of Z resonance, see Z boson
- Wilczek, F., 479, 531
- Wilson, K., 266, 393–394, 533, 547, 613
- Wilson-Fisher fixed point, 405, 435, 439, 441, 445, 448–449, 454, 462, 466
- Wilson line, 491–494, 504, 655–657, 783
- Wilson loop, 492, 494, 503, 658, 783–784
- Wilson's approach to renormalization, 393–406
- Wonderful trick, 619
- x (kinematic variable in deep inelastic scattering), 477–478, 557
- ξ (correlation length), 272

- ξ (gauge parameter), 296–297, 505, 513, 526, 733
 dependence of results on, 297, 526, 734–739, 773
- ξ (longitudinal fraction of parton), 477, 555
- ξ (spinor), 45, 68, 803–804
- y (kinematic variable in deep inelastic scattering), 558, 561
- y (longitudinal rapidity), 566
- Y (rapidity), 565
- Y ($U(1)$ charge), 702–704
- Yang-Mills Lagrangian, 489, 506
- Yang-Mills theories, see Non-Abelian gauge theories
- Yennie gauge, 297
- Yukawa coupling constant, 79
- Yukawa potential, 121–123
- Yukawa theory, 79, 116–123, 257, 329–330
 Feynman rules for, 118
 renormalization of, 344–345
- Yukawa theory, cont.
 counterterms for, 408–409
 β functions of, 438
- Z^0 boson, 173, 474, 593, 701, 710–711
 decay of, 594, 710, 712, 728
 mass of, 593, 710, 712, 762–764
 see also A_{LR}^f
- Z (field-strength renormalization), 214
- Z_1 (QED vertex rescaling), 230, 331, 334–335
 relation to Z_2 , 243
- Z_2, Z_3 , see Field-strength renormalization
- $Z_{\mathcal{O}}$, 429–430
- $Z[J]$ (generating functional), 290–292, 302, 365, 367, 394
- Zero-point energy, 21, 790
- Zero-point function, in QED, 317
- Zeroth-order natural relations, 387, 389–390, 758, 774
 in GWS theory, 759–766
- Zimmermann, W., 222, 338
- Zweig, G., 545

